UNIVERSITEIT GENT

Plant Systems Biology

VIB

SBRC

Vrije Universiteit Brussel

Genetic screens to identify ROS signal transducers in *Arabidopsis thaliana*

Cezary Waszczak

Cezary Waszczak

Promoters:

Prof. Dr Frank Van Breusegem and Prof. Dr Joris Messens

Ghent, July 2014

Ghent University

Faculty of Sciences

Dept. of Plant Biotechnology and Bioinformatics

Vrije Universiteit Brussel

Faculty of Science and Bio-engineering Sciences

Dept. of Applied Biological Sciences

Genetic screens to identify ROS signal transducers
in *Arabidopsis thaliana*

Cezary Waszczak

Thesis submitted in partial fulfillment of requirements
for the degree of

Doctor (Ph. D.) in Sciences, Biotechnology   Doctor (Ph. D.) in Bio-engineering Sciences

Academic year: **2013-2014**

Promoter:

Prof. Dr Frank Van Breusegem

Faculty of Sciences, Department of Plant Biotechnology
and Bioinformatics, Ghent University, Belgium

VIB Department of Plant Systems Biology
Oxidative Stress Signaling Group
Technologiepark 927, 9052 Ghent, Belgium

Co-promoter:

Prof. Dr Joris Messens

Faculty of Science and Bio-engineering Sciences,
Department of Applied Biological Sciences,
Vrije Universiteit Brussel, Belgium

VIB Structural Biology Research Center
Oxidative Stress Signaling Group
Pleinlaan 2, 1050 Brussels, Belgium

EXAMINATION COMMISSION

Prof. Dr Ann Depicker (Chair)

Faculty of Sciences, Department of Plant Biotechnology and Bioinformatics, Ghent University, Belgium

Prof. Dr Frank Van Breusegem (Promoter)

Faculty of Sciences, Department of Plant Biotechnology and Bioinformatics, Ghent University, Belgium

Prof. Dr Joris Messens (Co-promoter)

Faculty of Science and Bio-engineering Sciences, Department of Applied Biological Sciences, Vrije Universiteit Brussel, Belgium

Prof. Dr Graham Noctor*

Institut de Biologie des Plantes, Université de Paris Sud, France

Prof. Dr Filip Rolland

Faculty of Sciences, Department of Biology, Katholieke Universiteit Leuven, Belgium

Prof. Dr Bart Devreese*

Faculty of Sciences, Department of Biochemistry and Microbiology, Ghent University, Belgium

Prof. Dr Geert De Jaeger

Faculty of Sciences, Department of Plant Biotechnology and Bioinformatics, Ghent University, Belgium

Prof. Dr Moritz Nowack*

Faculty of Sciences, Department of Plant Biotechnology and Bioinformatics, Ghent University, Belgium

Prof. Dr Henri De Greve

Faculty of Science and Bio-engineering Sciences, Department of Applied Biological Sciences, Vrije Universiteit Brussel, Belgium

Prof. Dr Jean-Pierre Hernalsteens

Faculty of Science and Bio-engineering Sciences, Department of Biology, Vrije Universiteit Brussel, Belgium

Dr Stijn Dhondt*

Faculty of Sciences, Department of Plant Biotechnology and Bioinformatics, Ghent University, Belgium

Dr Matthew Hannah

Bayer CropScience NV, Ghent, Belgium

* Member of the reading committee

TABLE OF CONTENTS

LIST OF ABBREVIATIONS

2-D	two-dimensional
35S	Cauliflower Mosaic Virus 35S promoter
μE	microEinstein (μmol photons $\cdot$ m^{-2} $\cdot$ s^{-1})
AMPSO	3-([1,1-Dimethyl-2-hydroxyethyl]amino)-2-hydroxypropanesulfonic acid
ANOVA	analysis of variance
attB	*E. coli* chromosome site-specific λ attachment (att) site
BC4	fourth filial generation after back-cross
BCAA	branched-chain amino acids
bHLH	basic helix-loop-helix
bp	base pair
CAPS	cleaved amplified polymorphic sequences
cDNA	complementary DNA
CDS	coding sequence
CoA	coenzyme A
Col-0	*Arabidopsis thaliana* Columbia-0 accession
Da	dalton
DAS	days after sowing
DNA	deoxyribonucleic acid
EMS	ethyl methanesulfonate
F1	first filial generation
F2	second filial generation
FC	fold change
Fm'	maximum fluorescence from light-adapted leaves
Fv'	variable fluorescence from light-adapted leaves
GEO	Gene Expression Omnibus
GFP	green fluorescent protein
GSH	reduced glutathione
GSSG	oxidized glutathione
kb	kilobase
kDa	kilodalton
LD	long day, 16 h light / 8 h dark
Mbp	megabase pair = million base pairs
mRNA	messenger RNA
MS	Murashige and Skoog basal salt mixture
MSTFA	N-Methyl-N-(trimethylsilyl) trifluoroacetamide
NASC	Nottingham Arabidopsis Stock Centre
OE	overexpressor
PCR	polymerase chain reaction
Pi	inorganic phosphate PO_4^{3-}
pK$_a$	acid dissociation constant (logarythmic scale)
ppm	parts per million
PSII	photosystem II
PTM	post-translational modification
PVDF	polyvinylidene difluoride

qRT-PCR   quantitative reverse transcriptase PCR
RNA   ribonucleic acid
RNAi   RNA interference
SA   salicylic acid
SALK   Salk Institute for Biological Studies
SDS   sodium dodecyl sulfate
SE   standard error
SNP   single-nucleotide polymorphism
T-DNA   transfer DNA
TAIR   The *Arabidopsis* Information Resource
TCA   tricarboxylic acid
Ws-0   *Arabidopsis thaliana* Wassilewskija-0 accession
WT   wild-type

SCOPE AND OBJECTIVES

In their natural environment plants are continuously confronted with a multitude of factors that can negatively affect their growth and development. Drought, fluctuating temperature, extreme light intensities, high salinity, air/soil pollution and pathogen attacks are commonly referred to as environmental stress conditions and are major factors limiting yield of crop species worldwide. To compensate for their sessile lifestyle, plants evolved sophisticated mechanisms for perception and transduction of external stimuli that result in enormous potential for acclimation towards these factors. Due to its economic significance, research towards understanding and improving plant stress resistance has become a major objective of plant biotechnology.

Most of suboptimal growth conditions disturb the equilibrium between production and scavenging of reactive oxygen species (ROS). Accumulation of these molecules serves as an early hallmark for stress conditions and is rapidly perceived and transduced at the cellular and whole organism level. Based on this information, plants are able to tune the gene expression pattern that ultimately leads to a finely tailored response. The main objective of this thesis was to identify proteins that are involved in ROS signaling pathways in plants. Efforts aiming at understanding these processes that were used throughout this work can be generally divided into forward (Chapter 2 & 3) and reverse (Chapter 4) approaches.

A recently emerging concept of redox signaling established a site-specific, covalent modification of proteins as a prominent molecular mechanism for transforming an oxidant signal into a biological response (reviewed in **Chapter 1**). The forward proteomics strategy described in **Chapter 2** aimed at identifying proteins that could be directly modified on a post-translational level by reactive oxygen species thus potentially serving as sensors of cellular redox status. We focused on hydrogen peroxide-dependent oxidation of cysteine thiols (-SH) that under oxidative stress conditions are oxidized to a sulfenic acid (-SOH). Our approach implemented a unique combination of in vivo Cys-SOH trapping with genetically encoded probe and tandem affinity purification. Additionally, we explored a possibility for adaptation of our strategy to field conditions.

In a forward genetic approach, described in C**hapter 3,** we focused on the discovery of genes modulating oxidative stress tolerance. For this, we made use of CATALASE2-deficient plants as a model system for non-invasive regulation of hydrogen peroxide level. An extensive screen for 2nd site mutations that revert the cell death phenotype exhibited by *cat2* mutant line under photorespiratory conditions was performed. Within this thesis, we identified the causative mutation of two mutant lines and aimed at revealing the molecular background of observed phenotypes.

Before the beginning of this Ph. D. project a significant progress has been made in understanding transcriptomic responses evoked by oxidative stress conditions. **Chapter 4** describes

the use of this knowledge in a reverse genetic approach focused at functional characterization of early hydrogen peroxide responsive genes. We aimed at identifying loss-of-function mutant lines that, upon exposure to oxidative stress-promoting conditions, exhibit phenotypical differences when compared to wild-type plants. This genetic screen was followed-up with a functional characterization of a single mutant line that exhibited the most prominent phenotype.

We believe that results presented in this thesis will contribute to a better understanding of mechanisms governing plant adaptation to stress conditions. In a long term, this knowledge will serve to enhance plant productivity for the benefit of society.

1

Oxidative post-translational modifications of cysteine residues in plant signal transduction

Cezary Waszczak, Silke Jacques, Joris Messens and Frank Van Breusegem

AUTHOR CONTRIBUTIONS

CW wrote the chapter with the help of SJ, JM and FVB

ABSTRACT

Reactive oxygen species (ROS) are unavoidably linked to aerobic metabolism. Hydrogen peroxide (H_2O_2), the two-electron reduction product of oxygen can reversibly as well as irreversibly modify proteins and other bio-molecules. Depending on concentration, these modifications can lead to oxidative damage or trigger signaling events through structural alterations of metabolic enzymes and protein redox sensors that act at initial stages of various signaling cascades. These modifications are largely related to oxidation of cysteine residues (R-SH) that via sulfenic acid intermediate (R-SOH) lead to further modifications affecting protein structure and function. The ability to cross membranes and multiple sites of generation make hydrogen peroxide a versatile signaling molecule able to interact with multiple signaling pathways. In this chapter we focus on oxidative modifications of proteins known to participate in signaling cascades initiated by plant stress hormones such as abscisic acid, ethylene, salicylic acid and jasmonates, as well as developmental cues. We discuss the functional consequences caused by the oxidation of these proteins and investigate the mechanistic aspects of these regulation. Finally, we provide a perspective for future directions of the plant redox signaling research.

INTRODUCTION

Being sessile organisms, plants need to adapt their developmental strategies towards challenging environmental conditions in order to ensure the production of numerous progeny. Such adaptations require mechanisms that are constantly monitoring, sensing and transducing the information about a diverse array of stimuli. Signaling via production of reactive oxygen species (ROS) such as hydrogen peroxide (H_2O_2), superoxide anion ($O_2^{\cdot-}$) or hydroxyl radical ($OH^\cdot$) as well as reactive nitrogen species (RNS) very often serves as an initial step towards efficient adaptation of transcriptomic response both at the cellular and whole organism level (Gadjev et al., 2006; Mittler et al., 2011). For the most recent reviews on RNS signaling we refer to (Astier et al., 2012; Yu et al., 2012; Lounifi et al., 2013). The accumulation of ROS was demonstrated for multiple stress conditions like wounding (Orozco-Cardenas and Ryan, 1999), chilling in the light (Wise and Naylor, 1987), excess light (Fryer et al., 2003), pathogen infection (Apostol et al., 1989; Levine et al., 1994), low CO_2 availability (Noctor et al., 2002) but also during developmental processes like root growth (Foreman et al., 2003), gravitropism (Joo et al., 2001), extracellular ATP signaling (Song et al., 2006), pollen tube growth (Potocký et al., 2007; Kaya et al., 2014) and rupture (Duan et al., 2014). Finally, the production of ROS is an intrinsic feature of multiple cellular processes like mitochondrial respiration, photosynthesis, photorespiration and β-fatty acid oxidation (Petrov and Van Breusegem, 2012). In agreement with their role as signaling molecules the levels of ROS are tightly controlled by multiple enzymatic and non-enzymatic systems (Fig. 1A). The non-enzymatic antioxidants include glutathione (GSH) and ascorbate (Asc) that are the major cellular redox buffers, as well as other compounds such as tocopherol, flavonoids, alkaloids, and carotenoids (Apel and Hirt, 2004). Although GSH and Asc are often listed as antioxidants, they are preferentially used as cofactors of glutathione peroxidases (GPX) and ascorbate peroxidases (APX) respectively, that together with catalases (CAT), superoxide dismutases (SOD) and peroxiredoxins (Prx) constitute the major enzymatic pathways of ROS scavenging (Mittler et al., 2004). Due to its high pKa (9.2, Jung et al., 1972) glutathione is fully protonated at physiological pH range which limits its reactivity towards disulfides, however, the maintenance of reduced glutathione pool is of major importance for cellular redox balance as it is used to regenerate oxidized ascorbate in a process termed glutathione-ascorbate cycle (Fig. 1A, Foyer and Halliwell, 1976; Foyer and Halliwell, 1977).

In plants, ROS have an established role in direct post-translational modifications of enzymes of which the best studied examples are those involved in Calvin cycle (Schürmann and Buchanan, 2008), sulfur metabolism and glutathione synthesis (Kopriva et al., 2012) and starch metabolism (Glaring et al., 2012). Next to the well described regulation of redox-sensitive enzymes, ROS emerge as potent regulators of multiple signal transduction proteins such as transcription factors, kinases, phosphatases, RNA-binding proteins etc. These examples (discussed in detail later) provide support for an emerging field of plant "thiol-based redox signaling" well established in animal, yeast and prokaryotic systems
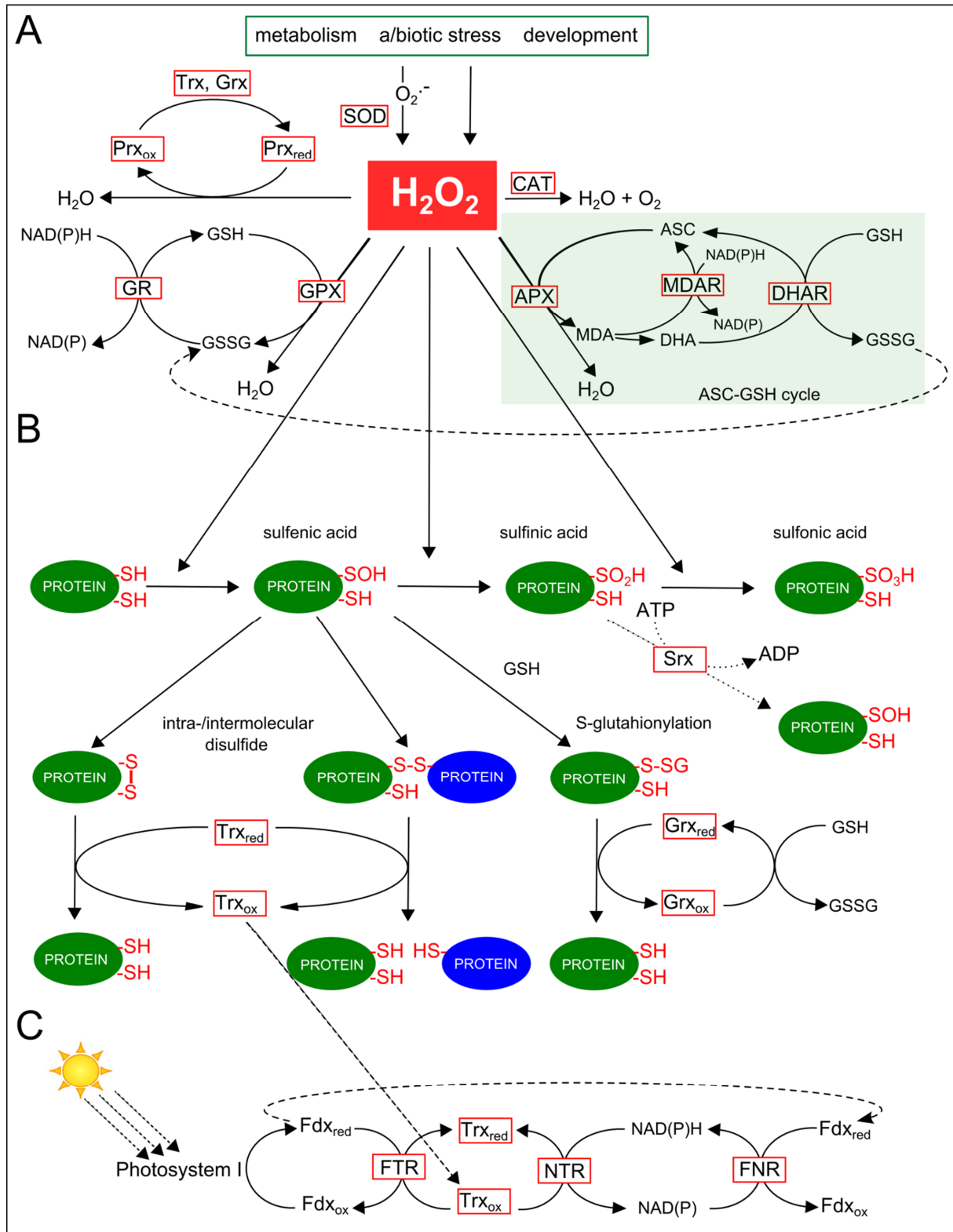
Fig. 1. The impact of H_2O_2 on plant cells. **A)** Production and enzymatic scavenging of H_2O_2. SOD, superoxide dismutase; Prx, peroxiredoxin; CAT, catalase; GR, glutathione reductase; GPX, glutathione peroxidise; APX, ascorbate peroxidase; MDAR, monodehydroascorbate reductase; DHAR, dehydroascorbate reductase, Srx, sulfiredoxin. Adapted from (Mittler et al., 2004; Dietz, 2011) **B)** Oxidative post-translational modifications of cysteine residues, adapted from (Roos and Messens, 2011). **C)** Light dependent reduction of Trx, adapted from (Schürmann and Buchanan, 2008). Fdx, ferrodoxin; FTR, ferrodoxin-thioredoxin reductase; NTR, NADPH-dependent thioredoxin reductase, FNR, ferrodoxin-NADP reductase.

(Roos and Messens, 2011; Wouters et al., 2011). The majority of oxidative post-translational modifications of proteins occurs via oxidation of cysteine residues. This is due to the presence of sulfur centers (R-SH) that make Cys residues the major sites of oxidative modifications within proteins (Davies, 2005). Between individual cysteines, the reactivity towards ROS can be largely different. This is strongly correlated with their pK_a – i.e. the ability to form the anionic form of sulfur called thiolate (R-S⁻) at physiological pH values. While free cysteine has a pK_a of 8.3-8.5 (Tajc et al., 2004; Luo et al., 2005) the most reactive Cys residues described thus far have a $pK_a \leq 3.5$ (Gan et al., 1990; Nelson and Creighton, 1994). The pK_a of Cys residues is largely determined by the local electrostatic environment i.e. presence of proximal charged residues or dipoles and the hydrogen bonding between thiols/thiolates and neighboring residues (Harris and Turner, 2002). Another important factor that controls the reactivity of Cys residues is their steric accessibility on the protein 3D structure (Marino and Gladyshev, 2010).

The first step in ROS dependent signaling involves reversible oxidation of reactive Cys residues to sulfenic acid (R-SOH; Fig 1 B). Unless stabilized within protein environment this modification is highly unstable and leads to further modifications (Claiborne et al., 1993). An excess concentration of oxidant can lead to further oxidation to sulfinic- ($R-SO_2H$), and irreversible sulphonic acid ($R-SO_3H$; Roos and Messens, 2011). The reversibility of the sulfinic acid modification has been debated, but was demonstrated by the presence of an ATP-dependent sulfiredoxin enzyme (Srx), capable of reducing sulfinic acids in plant cells (Rey et al., 2007). Thus far the only known substrates of *At*Srx are chloroplast 2-Cys Peroxiredoxins (2-Cys Prx; Rey et al., 2007; Iglesias-Baena et al., 2010) and mitochondrial PrxIIF (Iglesias-Baena et al., 2011), therefore the reduction of sulfinic acids can not be regarded as a general rule. Another fate of sulfenic acid might be the reaction with free protein thiols to form intra- or intermolecular disulfide bonds (Fig. 1 B). Alternatively sulfenic acids can be modified by low molecular weight thiols (e.g. glutathione [GSH]) leading to cysteine S-glutathionylation (Fig 1 B). The formation of intermolecular bonds and S-glutathionylation were long believed to serve as a mechanism protecting the active site Cys residues from overoxidation and permanent protein damage. Only recently the S-glutathionylation gains recognition for its role in redox signaling (Zaffagnini et al., 2012b; Zaffagnini et al., 2012c). Both, S-glutathionylation and formation of intra-/intermolecular disulfides are readily reversible and the status of these modifications is under control of glutaredoxins (Grx) and thioredoxins (Trx) respectively. Compared to prokaryotes and animals, plants are equipped with a much more complex network of Trx/Grx systems. *Arabidopsis* genome encodes for 44 Trx and 50 Grx proteins (Meyer et al., 2012). Depending on the subcellular localization thioredoxins utilize multiple sources of reducing equivalents to perform the reduction of disulfide bonds (Fig 1C). In chloroplasts light reactions reduce ferredoxin (Fdx) that in turn reduces ferredoxin-thioredoxin reductase (FTR) which ultimately regenerates the Trx sulfhydryl groups (Schürmann and Buchanan, 2008). Another source of reducing equivalents common for Trx and Grx

systems is NADPH reduced by Fdx:NADP reductase (FNR) within chloroplast stroma as well as produced during oxidative pentose phosphate pathway (Meyer et al., 2012). While Trxs are directly reduced by NADPH-dependent thioreodoxin reductases (NTR), Grxs utilize a two step reaction involving GSH and NADPH-dependent glutathione reductases (GR; Fig. 1B, C).

With the current knowledge on redox regulated metabolic enzymes covered in multiple excellent reviews (Schürmann and Buchanan, 2008; Glaring et al., 2012; Kopriva et al., 2012; Balsera et al., 2014), in this chapter we will explore the H_2O_2-mediated oxidative post-translational modifications of proteins that are involved in signal transductions events rather than metabolic pathways. We especially focused on proteins that mediate the crosstalk between ROS and signaling pathways initiated by plant stress hormones such as abscisic acid, salicylic acid, ethylene and jasmonates. Further, we explore the link between hydrogen peroxide and signaling via mitogen-activated protein kinases and list known examples of transcription factors and RNA-binding proteins directly regulated by ROS. We provide an insight into their redox regulation and its implication into the hormone and developmental signaling pathways.

ROS HORMONAL CROSS-TALK IN PLANT SIGNAL TRANSDUCTION

Abscisic acid signaling

The plant hormone abscisic acid (ABA) plays a key role in plant defense responses, growth and development (Finkelstein, 2013; Nakashima and Yamaguchi-Shinozaki, 2013). Numerous studies describe the tight association of reactive oxygen species and the ABA signaling pathways. Thus far, the best described case of such crosstalk is the control of guard cell movement (Pei et al., 2000; Kwak et al., 2003). In response to drought stress plants produce ABA that triggers a signaling cascade which ultimately results in stomata closure and reduction of water loss (Fig. 2). Upon perception of ABA by PYRABACTIN RESISTANCE/PYR1 LIKE/REGULATORY COMPONENT OF ABA RECEPTOR (PYR/PYL/RCAR) proteins (Ma et al., 2009; Park et al., 2009) a signaling cascade involving members of PROTEIN PHOSPHATASE 2C (PP2C) family (Leung et al., 1997; Merlot et al., 2001) and OPEN STOMATA 1 (OST1) kinase (Mustilli et al., 2002), activates the production of ROS by plasma membrane bound NADPH oxidases RbohD/F (Kwak et al., 2003). This oxidative burst is necessary for activation of Ca^{2+} permeable channels (discussed later in this paragraph) that mediate influx of Ca^{2+} into the cytoplasm of guard cells (Pei et al., 2000). In parallel, OST1 phosphorylates and activate anion channel SLOW ANION CHANNEL-ASSOCIATED 1 (SLAC1; Lee et al., 2009b; Vahisalu et al., 2010). The rise in cytoplasmic Ca^{2+} concentration activates CALCIUM-DEPENDENT PROTEIN KINASE 21 (CPK21) that next to regulation of SLAC1 (Geiger et al., 2010) activates the SLAC1 homolog 3 (SLAH3; Geiger et al., 2011; Demir et al., 2013). Together, these signaling steps lead to coordinated action of membrane channels that control the levels of osmotically active

ions within guard cells, described in detail by Song et al., (2014). A number of proteins involved in this complex signaling network are regulated via direct redox modifications (Fig. 2).
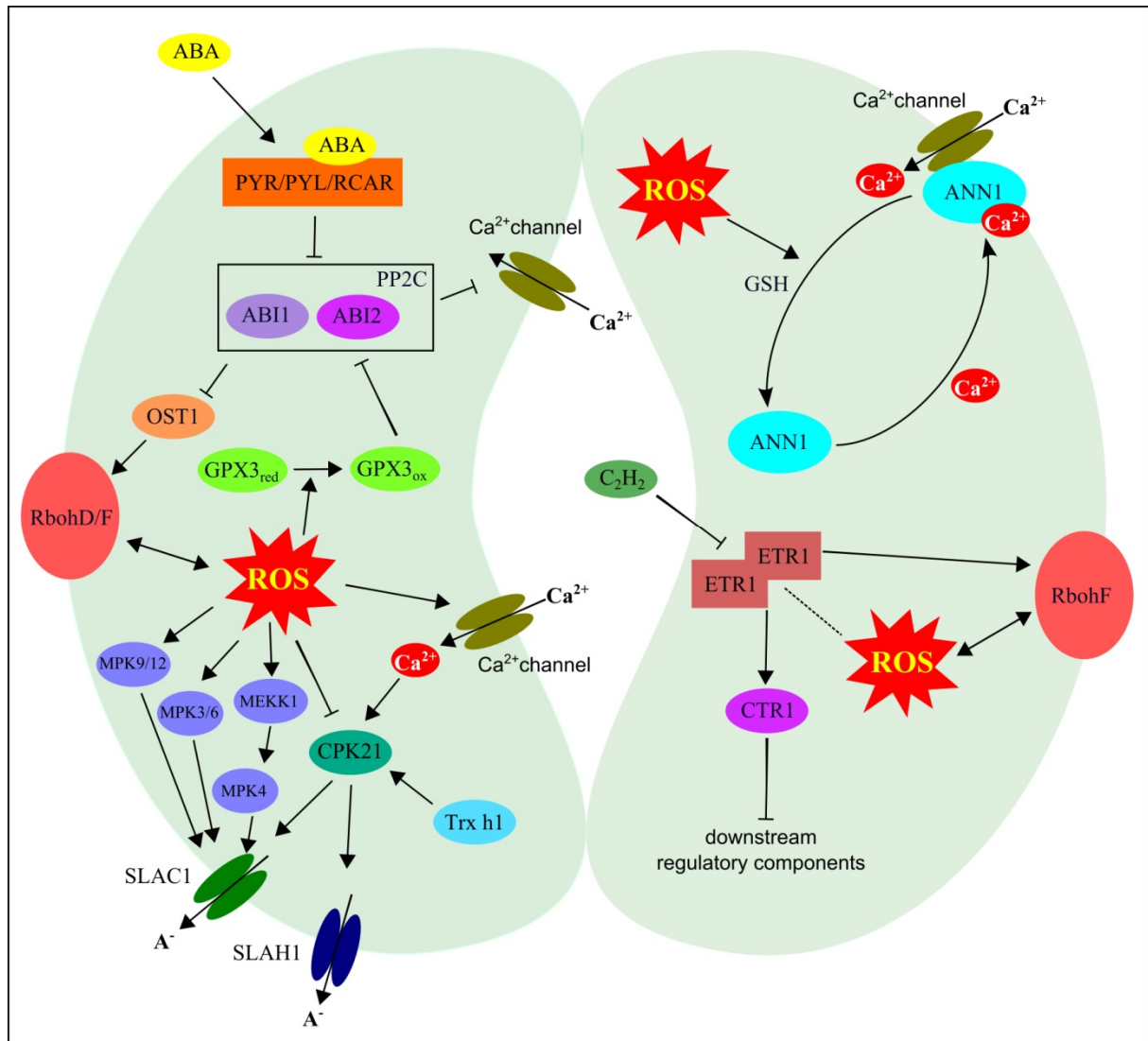

Fig. 2. Schematic and simplified representation of ROS function in guard cell signaling. For abbreviations and description of respective regulatory events see the main text.

Two members of the PP2C family ABA INSENSITIVE1 (ABI1) and ABI2 that act as negative regulators of ABA signaling (Merlot et al., 2001) were shown to undergo H_2O_2 dependent inhibition (Fig 2). In both cases oxidizing conditions lead to inactivation of their phosphatase activity *in vitro*, presumably via formation of intra-molecular disulfide bond (Meinhard and Grill, 2001; Meinhard et al., 2002). The inactivation of both phosphatases serves as a mechanism that amplifies the ABA signaling in guard cells. *In planta*, the oxidation of these enzymes is mediated by GLUTATHIONE PEROXIDASE 3 (GPX3). GPX3 acts as a sensor protein that upon perception of ROS signal relays the oxidizing equivalents to ABI2 via thiol-disulfide exchange (Miao et al., 2006). The interaction of GPX3 with ABI2 (and with a much lower affinity with ABI1) inhibits its PP2C activity (Miao et al., 2006). A similar scenario was described in yeast (*Saccharomyces cerevisiae*) cells exposed

to oxidative stress. Under these conditions the oxidation of H_2O_2 sensor Oxidant receptor protein 1 (ORP1/Gpx3) triggers a thiol-disulfide relay mechanism that ultimately leads to nuclear import of Yeast AP-1 (YAP1) transcription factor (Delaunay et al., 2000; Delaunay et al., 2002). Upon import to the nucleus YAP1 controls transcription of H_2O_2 responsive genes (Lee et al., 1999; Gasch et al., 2000). Analogous thiol-disulfide relays initiated by oxidation of thiol peroxidases were recently demonstrated also in mammalian cells (Gutscher et al., 2009) suggesting that thiol peroxidases might act as universal redox sensors. This notion is further strengthened by their cross kingdom sequence similarity indicating that these mechanisms are evolutionary conserved (Fomenko and Gladyshev, 2012).

Next to the GPX3-mediated inhibition of ABI1/2, redox conditions govern the activity of CPK21 (Fig. 2), initially identified in a screen for plasma membrane-associated Trx h1 targets (Ueoka-Nakanishi et al., 2013). CPK21 undergoes hydrogen peroxide-dependent inhibition of its kinase activity both *in vitro* and *in vivo*. This inactivation is linked with formation of intra-molecular disulfide bond (Cys97-Cys108) and is effectively restored by Trx h1 (Ueoka-Nakanishi et al., 2013).

Recent evidence suggests that the ROS-dependent Ca^{2+} fluxes in *Arabidopsis* roots and presumably also in guard cells are mediated by ANNEXIN1 (AtANN1; Konopka-Postupolska et al., 2009; Laohavisit et al., 2010; Laohavisit et al., 2012). Annexins (AtANN1-8) are a multigene family with eight members in *Arabidopsis* (Cantero et al., 2006). These multifunctional proteins are characterized by Ca^{2+} dependent binding to lipid membranes (Laohavisit and Davies, 2011). Thus far, the best characterized member of the family, ANNEXIN1, stimulates the Ca^{2+} influx in a hydroxyl radical (HO·) and peroxide-dependent manner (Laohavisit et al., 2012; Richards et al., 2013). Mutants lacking AtANN1 are impaired in ROS mediated increase in cytoplasmic Ca^{2+} concentration (Laohavisit et al., 2012). This process is of particular importance for root growth as it largely relies on cell expansion that is dependent on activation of Ca^{2+} channels that function downstream of NADPH oxidase RbohC serving as a source of ROS (Foreman et al., 2003). As a consequence, *ann1* mutants exhibit impaired root development. Furthermore, *ann1* plants are hypersensitive to drought (Konopka-Postupolska et al., 2009) suggesting they might be impaired in Ca^{2+}-dependent guard cell signaling and ultimately stomata closure. ANNEXIN1 was demonstrated to undergo S-glutathionylation on both of its cysteine residues (Cys111 and Cys239) resulting in 50% decrease in Ca^{2+} affinity (Konopka-Postupolska et al., 2009). Most probably, this mechanism serves to restrict the AtANN1 membrane association and inhibit ROS-mediated Ca^{2+} fluxes in a negative feedback loop (Fig. 2). Furthermore, AtANN1 was also found to undergo S-nitrosylation (Lindermayr et al., 2005) although the consequences of this modification remain unexplored. It might be speculated that this modification disturbs the AtANN1 function as it was demonstrated for mammalian ANNEXIN II (Liu et al., 2002).

Ethylene signaling

Guard cells exhibit a broad competence towards signaling molecules. Next to ABA-dependent signals also ethylene (ET) is able to exert the closure of stomata (Desikan et al., 2006). Ethylene is a gaseous plant hormone that despite of its chemical simplicity, regulates multiple aspects of plant growth, development and stress responses (Schaller, 2012; Wang et al., 2013). The ethylene signaling pathway starts with binding of ET to a family of ER membrane-localized receptor proteins. In *Arabidopsis*, this family of receptors consists of five members among which the best described is ETHYLENE RESPONSE 1 (ETR1). Upon ethylene binding, ETR1 inactivates CONSTITUTIVE TRIPLE RESPONSE 1 (CTR1) serine/threonine kinase that acts as a repressor of downstream signaling components. For a detailed view on ET signal transduction we refer to Shakeel et al., (2013). ETR1 acts as a disulfide-linked homodimer. As indicated by site directed mutagenesis, at least one of the N-terminal cysteines (Cys4, Cys6) is necessary for the dimerization (Schaller et al., 1995). However, it is yet not clear whether these residues are subject to redox regulation *in vivo*. In the context of guard cell signaling, perception of ethylene by ETR1 triggers accumulation of hydrogen peroxide that is pivotal for ethylene-induced stomatal closure (Fig. 2; Desikan et al., 2006). In contrast to ABA signaling that activates both guard cell NADPH oxidases RbohD and RbohF, the ET mediated pathway requires only the latter isoform (Desikan et al., 2006). The two hormones appear to act independently as *etr1* mutants exhibit normal ABA sensitivity in terms of stomatal closure and H_2O_2 synthesis (Desikan et al., 2006). Next to the ethylene mediated oxidative burst ETR1 is also necessary for stomatal closure in response to H_2O_2 (Desikan et al., 2005). Interestingly Cys65 of ETR1 is crucial for both pathways i.e. ABA and ET-signaling, but the reasons for this requirement are unrelated (Desikan et al., 2005; Desikan et al., 2006). The ethylene perception requires a copper co-factor that is stabilized by Cys65 and His69. Consequently, mutation of Cys65 results in abolished Cu and ethylene binding (Rodríguez, 1999). Conversely, the ETR1-mediated hydrogen peroxide induced stomatal closure does not require the Cu co-factor as plants treated with copper chelator diethyldithiocarbamate (DDC) that disrupts the ETR1 ethylene binding exhibit a wild type response towards H_2O_2 (Desikan et al., 2006). Similarly, the *ran1-1* (RESPONSIVE TO ANTAGONIST1) mutant deficient in incorporation of copper into ETR1 (Hirayama et al., 1999; Binder et al., 2010) exhibits wild-type like stomatal closure in response to hydrogen peroxide but fails to accumulate H_2O_2 in response to ethylene (Desikan et al., 2006). These data demonstrate a crucial role for the Cys65 of ETR1 in hydrogen peroxide mediated stomatal closure that is independent of ethylene perception. It is tempting to speculate that Cys65 serves as a site for oxidative PTM, however, further research is needed to corroborate this theory.

Salicylic acid – plant immunity

Salicylic acid (SA) is a phenolic compound that acts as a potent signaling molecule to control plant-pathogen interactions (Vlot et al., 2009) and various developmental processes (Rivas-San Vicente and Plasencia, 2011). This hormone is best known for its role in regulation of both local and systemic acquired resistance (SAR) that serve to limit the progress of pathogen infection. The transcriptional responses triggered by SA are largely governed by coordinated action of NONEXPRESSER OF PR GENES 1 (NPR1) transcriptional co-activator and its interacting transcription factors from TGA family, both regulated by changes in cellular redox status that occur upon pathogen infection (Fig.3) (Mou et al., 2003; Tada et al., 2008). Under control conditions, NPR1 localizes to the cytoplasm in a form of oligomers. This oligomerization is achieved via intra-molecular disulfide bonds involving cysteine residues Cys82 and Cys216 (Mou et al., 2003). SA triggers fluctuations in cellular redox status that lead to Trxh3/h5-dependent reduction of disulfides, monomerization of NPR1 and subsequent nuclear import (Mou et al., 2003; Tada et al., 2008). This process is in direct competition with oligomerization promoted by S-nitrosylation of Cys156 and the interplay between these two modifications provides a tight control for NPR1-dependent signaling (Tada et al., 2008). Upon import to nucleus NPR1 interacts with TGA basic leucine-zipper transcription factors to promote transcription of pathogenesis related (PR) genes. Clade 2 TGA transcription factors (TGA2/5/6) act as constitutive repressors of PR transcription.
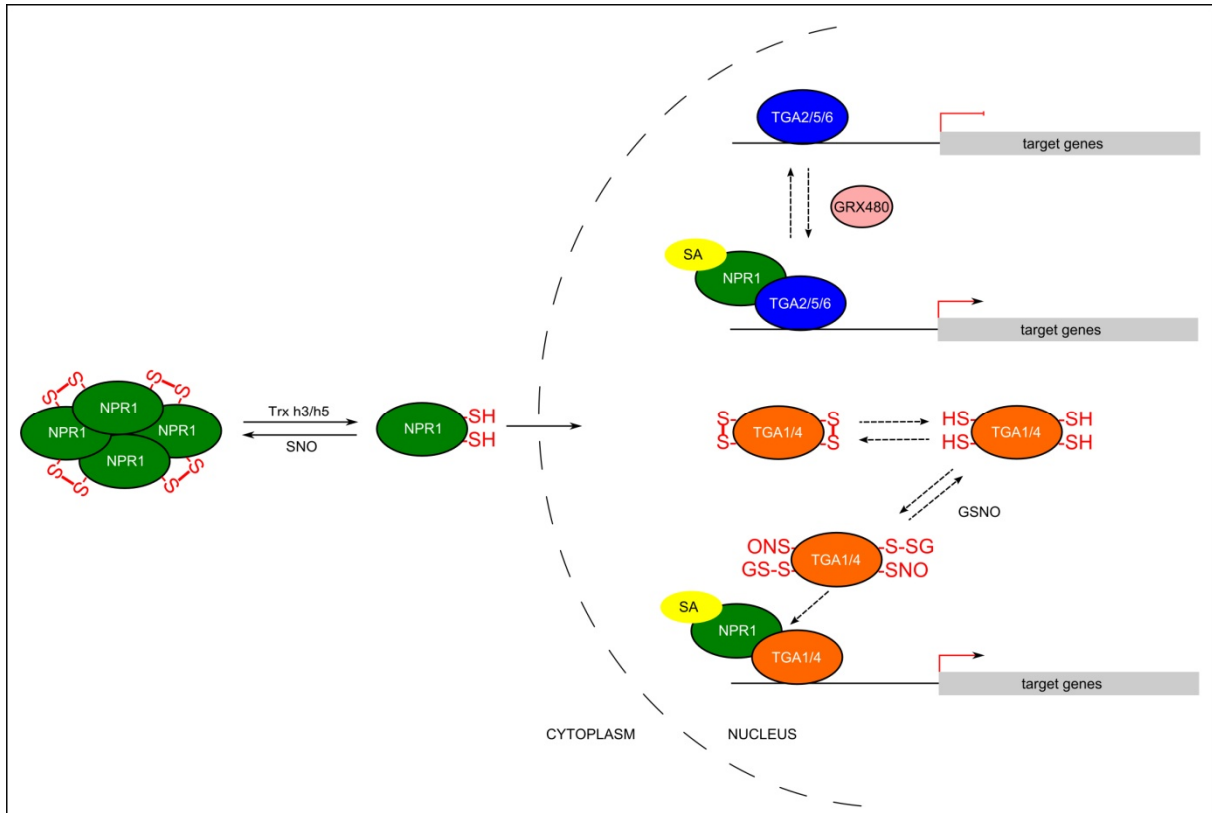

Fig. 3. Schematic representation of NPR1-based plant immune signaling. For abbreviations and description of respective regulatory events see the main text.

Binding of NPR1 to TGA2 results in co-activation of transcription and depends on NPR1 Cys521 and Cys529 required for activation of NPR1 trans-activation domain (Rochon et al., 2006). Recently it was demonstrated that NPR1 is a SA receptor and these two residues are involved in stabilization of copper atoms necessary for binding of SA (Wu et al., 2012). Furthermore, TGA2/6 interact with glutaredoxin GRX480 (ROXY 19) suggesting that GRX480 might control their redox status. This complex might also involve NPR1 which implies the role of GRX480 in regulation of interaction between TGA and NPR1 (Ndamukong et al., 2007).

The interaction of NPR1 with clade 1 TGA transcription factors (TGA1/4) relies on their redox status. When oxidized, TGA1 and/or TGA4 form an intra-molecular disulfide bridge (Cys260-Cys266) that hinders interaction with NPR1. Reduction of this disulfide stimulates formation of complex with NPR1, and subsequent binding to the as-1 element for activation of PR genes (Després et al., 2003). Recent data indicate that the two remaining TGA1 cysteine residues Cys172 and Cys287 are also involved in regulatory disulfide (Lindermayr et al., 2010). Furthermore, all four residues were found to undergo S-nitrosylation/S-glutathionylation upon treatment with S-Nitrosoglutathione (GSNO). These modifications serve to protect the Cys residues from oxidation and consequently lead to an increase in the DNA binding activity of TGA1 (Lindermayr et al., 2010).

Jasmonate signaling

Next to SA signaling plant defense responses are controlled by jasmonic acid (JA) and its derivatives collectively known as jasmonates (JAs), although the SA- and JA-signaling pathways are believed to act antagonistically (Van der Does et al., 2013). Thus far jasmonates were implemented in control of plant development and accumulation of flavonoids and a plethora of other secondary metabolites (Kazan and Manners, 2008) in response to abiotic and biotic (wounding, herbivore attack) stresses. The biologically active form of JA, JA-Ile conjugate, triggers 26 proteasome-mediated proteolysis of JASMONATE ZIM-domain (JAZ) transcriptional repressors by mediating their interaction with F-box protein CORONATINE INSENSITIVE1 (COI1), part of the Skp1/Cullin/F-box[COII] ubiquitin E3 ligase complex. Proteolysis of JAZ proteins de-represses multiple transcription factors (i.e. MYC2) and leads to global changes in gene expression. For a detailed view on JA signaling we refer to Pauwels and Goossens (2011). Apart from JA derivatives also JA precursors, such as 12-oxo-phytodienoic acid (OPDA) are able to exert transcriptional responses (Taki et al., 2005). A recent study by Park et al., (2013) extended our knowledge about OPDA signaling by identification of its chloroplastic receptor CYCLOPHYLIN 20-3 (CYP20-3). Cyclophilins are characterized by a highly conserved peptidyl-prolyl isomerase (PPIase) domain that, if functional, assists proper folding of their target proteins (Trivedi et al., 2012). CYP20-3 is targeted by Trx m (Motohashi et al., 2001) and was demonstrated to undergo oxidative inhibition mediated by formation of two intra-molecular disulfide bonds (Cys53-Cys170; Cys128-Cys175) (Motohashi et al., 2003). Thus far, in *Arabidopsis*,

the only identified target of CYP20-3 is chloroplast SERINE ACETYL-TRANSFERASE1 (SAT1) which catalyzes the rate limiting step in cysteine synthesis. The physical interaction of CYP20-3 with SAT1 is crucial for optimal synthesis of cysteine. Consequently, *cyp20-3* mutant plants exhibit low thiol content and are impaired in light dependent stress responses (Dominguez-Solis et al., 2008). Direct binding of OPDA to CYP20-3 was shown to stimulate this interaction and ultimately promote the production of cellular antioxidants (Park et al., 2013). Therefore, CYP20-3 is a redox sensitive crosstalk point linking OPDA signaling with maintenance of cellular redox balance. To our best knowledge, there are no reports on cysteine PTMs for proteins involved in JA-signaling.

Redox control of protein tyrosine phosphatases and mitogen-activated protein kinases

Mitogen-activated protein kinases (MAPKs) constitute a large family of signaling proteins involved in regulation of almost every aspect of plant growth, development and stress responses. Numerous studies describe the involvement of MAPK signaling cascades in control of pathogen signaling (Petersen et al., 2000; Dóczi et al., 2007; Suarez-Rodriguez et al., 2007), ROS signaling (Pitzschke et al., 2009), nitric oxide biosynthesis (Wang et al., 2010), jasmonate signaling (Takahashi et al., 2007), priming of stress responses (Beckers et al., 2009), as well as multiple developmental processes such as cytokinesis (Kosetsu et al., 2010), homeostasis of shoot apical meristem (Betsuyaku et al., 2011) and development of stomata (Wang et al., 2007; Khan et al., 2013). The three component MAPK signaling cascades are initiated by stimulus-triggered activation of MAPK kinase kinases (MAPKKKs) that in turn phosphorylate MAPK kinases (MAPKKs) which phosphorylate specific MAPKs. *Arabidopsis* genome encodes for more than 60 MAPKKKs, 10 MAPKKs and 20 MAPKs (Ichimura et al., 2002) that depending on the environmental and developmental stimuli regulate respective cellular processes. Several examples of MAPK signaling cascades could fall within other paragraphs of this chapter, however, the potential complexity of signaling combinations that could arise from numerous members of MAPKKK/MAPKK/MAPK families suggests that these proteins might function as convergence points linking multiple rather than single hormonal pathway. While MAPK-dependent cascades and their interactions with multiple hormonal signaling pathways were covered in multiple reviews (Colcombet and Hirt, 2008; Hahn and Harter, 2009; Pitzschke and Hirt, 2009; Rasmussen et al., 2012; Danquah et al., 2014) we focus here on mechanistic interactions linking ROS to regulation of MAPK activity.

MAPKs are well established examples of signaling proteins that undergo oxidative PTMs (Corcoran and Cotter, 2013; Truong and Carroll, 2013) although this kind of regulation was explored mainly in yeast (Day and Veal, 2010) and mammals (Cross and Templeton, 2004; Templeton et al., 2010). Thus far there are no reports describing direct oxidative post-translational modifications of plant MAPKs. However, a number of studies indicates that MAPKs are activated in response to oxidative stress. The ABA-dependent stomata closure is positively regulated by MAPK9 and MAPK12 that

function downstream of ROS in the signaling cascade (Jammes et al., 2009; Fig 2). The kinase activity of MPK12 is stimulated by both ABA and H_2O_2 (Jammes et al., 2009), however the exact mechanism of this regulation needs further investigation. Similarly, hydrogen peroxide was demonstrated to induce MAPKKK1 (ANP-1) which in turn activates MAPK3 and MAPK6 (Kovtun et al., 2000) however the redox sensing capabilities of MAPKKK1 are yet to be demonstrated. The redox regulation mechanisms of MAPK signaling cascades are likely to be evolutionary conserved as tomato (*Solanum lycopersicum*) MAPK2, which is an orthologue of *Arabidopsis* MAPK6, also undergoes oxidative activation (Zhou et al., 2014). Direct oxidative PTMs of plant MAPKs need further investigation, however, a growing evidence suggests that such modifications can take place (Chapter 2).

Thus far, in plants, the only well-established link between the redox status and MAPK activity is the oxidative stress-related negative regulation of MAPKs repressors. The activity of MAPKs depends on phosphorylation status of threonine and tyrosine of the conserved TXY motif present within the activation loop. The phosphorylation of both residues is required for optimal kinase activity (Kiegerl et al., 2000). ROS mediate inactivation of protein tyrosine phosphatases (PTPs; Xu et al., 1998) and double specificity PTPs (DsPTPs) that act on both phosphotyrosine and phosphothreonine residues and repress MAPKs (Gupta et al., 1998). As such, the PTPs were implemented in control of various processes that involve MAPK signaling component such as guard cell signaling (MacRobbie, 2002), oxidative stress tolerance (Lee and Ellis, 2007), SA homeostasis (Bartels et al., 2009), disease responses (Lumbreras et al., 2010) as well as auxin signaling (Strader et al., 2008; Lee et al., 2009a) and cortical microtubule functions (Walia et al., 2009). The activity of PTPs and DsPTPs, that apart from their active site motif do not share any sequence similarity, requires a highly conserved Cys residue, Cys265 in *At*PTP1 (Xu et al., 1998) and Cys135 in *At*DsPTP1 (Gupta et al., 1998). Alike their mammalian counterparts (Ostman et al., 2011; Meng and Zhang, 2013) *Arabidopsis* PTPs are inhibited by oxidative stress conditions. The activity of *At*PTP1 is negatively influenced by hydrogen peroxide treatment both *in vitro* and *in vivo*. Furthermore, this inactivation is positively correlated to MAPK6 activation by H_2O_2, indicating that *At*PTP1 acts as redox sensor linking oxidative stress with MAPKs activity (Gupta and Luan, 2003).

In contrast to *Arabidopsis* and mammalian PTPs, soybean (*Glycine max*) *Gm*PTP is characterized by a low sensitivity to inhibition with hydrogen peroxide and hypersensitivity towards GSSG-induced S-glutathionylation (Dixon et al., 2005a). The activity of *Gm*PTP is governed by two redox active cysteine residues (Cys78 and Cys176) that control the catalytic Cys266 which itself is not a primary target for oxidation. The sequential S-glutathionylation of Cys176 and Cys78 leads to rapid inhibition of *Gm*PTP activity and formation of Cys78-Cys266 that is believed to protect the Cys266 from oxidation (Dixon et al., 2005a).

The general paradigm of oxidative inactivation of PTPs was recently challenged by the discovery of reductant inhibited PTP from maize (*Zea mays*) *Zm*RIP (Li et al., 2012). The activity of this enzyme is insensitive to a common inhibitor H_2O_2 and irreversibly decreases upon reduction with DTT. This regulation of activity depends on Cys181 that when mutated changed the effect of reductant on PTP activity from inactivation to activation (Li et al., 2012). Authors suggest that Cys181 might be involved in disulfide bonds however the exact mechanism of this redox regulation needs further research. Interestingly, upon H_2O_2 treatment *Zm*RIP1 undergoes chloroplast-to-nucleus translocation indicative of a role in signal transduction (De Clercq et al., 2013; Ng et al., 2013). The target proteins of *Zm*RIP1 are currently not known.

REDOX CONTROL OF TRANSCRIPTION FACTORS

Redox control of flavonoid biosynthesis in maize

The first described example of redox regulated plant transcription factor is maize R2R3 MYB P1 that regulates flavonoid biosynthesis (Williams and Grotewold, 1997; Heine et al., 2004). P1 transcription factor binds to the promoter and activates expression of the A1 gene required for 3-deoxy flavonoid and phlobaphene biosynthesis (Grotewold et al., 1994). Under oxidizing conditions the disulfide bond between Cys49 and Cys53 located within the MYB DNA-binding domain inhibits binding of the P1 to the APB1 cis-regulatory element of the A1 promoter (Heine et al., 2004).

Redox control of HD-ZIP transcription factors

The plant specific homeodomain-leucine zipper (HD-ZIP) transcription factors control a wide range of developmental processes (Ariel et al., 2007). This super class consists of 48 proteins composed of DNA-binding homeodomain and a leucine zipper that mediates dimerization necessary for DNA binding. Based on evolutionary sequence analysis they can be classified into four classes (HD-ZIP I-IV), according to their intron – exon structure, presence of common motifs and physiological functions (Mukherjee et al., 2009). Thus far, a redox regulation was demonstrated for members of HD-ZIP class II, III and IV (Tron et al., 2002; Comelli and Gonzalez, 2007). Among the distinct features of class II HD-ZIPs, implemented in control of apical embryo development and meristem function (Turchi et al., 2013), is the presence of highly conserved CPSCE motif. The two cysteine residues present in this motif were demonstrated to exert the redox regulatory function in the sunflower Hahb-10 transcription factor. Oxidation and subsequent formation of intermolecular disulfide bonds, presumably occurring between the Cys residues between adjacent monomers, were shown to inhibit the DNA binding activity (Tron et al., 2002). A similar regulation was demonstrated for HD-ZIP class IV sunflower HAHR1 transcription factor, a homologue of *Arabidopsis* GLABRA2 protein controlling epidermal cell fate (Rerie et al., 1994; Masucci et al., 1996). A high conservation of CXXCG motif within this class of TFs suggests that this kind of redox regulation might be

evolutionary conserved (Tron et al., 2002). Within HD-ZIP III family that is involved in embryo development, organ polarity and meristem function (Prigge et al., 2005) a redox regulation was demonstrated for *Arabidopsis* PHAVOLUTA (PHV, AtHB9) transcription factor. Also there, oxidation of conserved cysteine residues resulting in formation of intermolecular disulfides that inhibits the DNA binding activity (Comelli and Gonzalez, 2007). The activity of all three HD-ZIP transcription factors discussed here, Hahb-10, HAHR1 and AtHB9 is positively influenced by Trx/NTR reduction system providing a mechanism for redox-dependent activation (Tron et al., 2002; Comelli and Gonzalez, 2007).

Expression of *2-CYS PEROXIREDOXIN A* is governed be the redox regulation of Rap2.4 DNA binding activity

The APETALA2-related transcription factor Rap2.4a controls expression of *2-CYS PEROXIREDOXIN A* (*2CPA*), by redox-dependent binding to the CE3-like cis-regulatory element present within its promoter (Shaikhali et al., 2008). Under reducing conditions (1 mM DTT/ASC), this transcription factor is found in its inactive monomeric form. Mildly oxidizing conditions (1 mM H_2O_2) promote formation of dimers that bind to the *2CPA* promoter and activate the expression. Under conditions of severe oxidative stress (H_2O_2 conc. > 3 mM) transcriptionally inactive oligomers are formed (Shaikhali et al., 2008). It is not clear which of the three cysteine residues present in the Rap2.4a control the formation of dimers/oligomers.

TGA transcription factors – more than control of plant immunity

Apart from their role in plant immune responses TGA transcription factors are involved in the control of plant developmental processes. The PERIANTHIA (PAN/TGA8) member of TGA family has an established role in control of floral development (Running and Meyerowitz, 1996; Chuang et al., 1999). Lack of this transcription factor results in formation of atypical pentamerous flowers (Running and Meyerowitz, 1996). PAN, together with three other TGA transcriptions factors (TGA2/3/7) directly interact with ROXY1 (Li et al., 2009) a floral monothiol glutaredoxin required for petal development (Xing et al., 2005). Mutagenesis of PAN Cys residues indicates that only Cys-340 (equivalent to Cys-266 in TGA1) is crucial for its function which supports the monothiol mechanism of its regulation. Genetic analysis indicate that PAN is epistatic to ROXY1, suggesting that ROXY1 might directly act on PAN protein to negatively regulate its activity (Li et al., 2009). TGA9 and 10 are another members of TGA family that next to PAN are involved in floral organogenesis. These two proteins are redundantly required for anther development (Murmu et al., 2010). Alike other members of the TGA family, these TFs are most likely under redox control since both TGA9 and TGA10 interact with ROXY1 and its closest homologue ROXY2 (Murmu et al., 2010). The exact mechanism and significance of this interaction is not yet understood.

Redox control of group G bZIP transcription factors

Using a high light responsive promoter fragment of LIGHT-HARVESTING CHLOROPHYLL B-BINDING 2 (LHCB2.4) in a DNA affinity trapping approach, Shaikhali et al., (2012) identified a redox-dependent DNA-binding properties of the G-group basic leucine-zipper (bZIP) transcription factor bZIP16. The DNA-binding activity of this transcriptional regulator is stimulated by reducing conditions. Oxidation leads to formation of high molecular weight oligomers that were shown to depend on intermolecular disulfides involving Cys330. Furthermore, two closely related transcription factors belonging to the same family, bZIP68 and G-BOX BINDING FACTOR 1 (GBF1) also exhibit a similar mode of redox regulation relying on redox status of Cys320 and Cys247 respectively. Interestingly, analysis of gain- and loss-of-function transgenics indicated that the three transcription factors have opposite function in *LHCB2.4* gene expression. bZIP16 acts as a repressor, while bZIP68 and GBF1 positively influence the transcript level (Shaikhali et al., 2012). Apart from positive regulation of *LHCB2.4*, GBF1 binds to *CATALASE2* (discussed in chapter 3) promoter and represses its expression. This mechanism serves to transiently elevate the H_2O_2 concentration which is necessary for developmental transition to flowering (Smykowski et al., 2010). It is tempting to speculate that after reaching necessary threshold concentration, hydrogen peroxide could de-repress the *CAT2* expression by inhibiting GBF1 function in a negative feedback loop. Alike GBF1 the bZIP16 also plays a role in regulation of developmental processes. A recent work by Hsieh et al., (2012) highlights its role in negative regulation of light-mediated inhibition of cell elongation and positive regulation of light-regulated seed germination thereby establishing bZIP16 as a key player in early seedling development.

Redox control of TCP family transcription factors

A recent work by Viola et al. (2013) has established a redox modulation for yet another family of plant transcription factors, named TCP after its best characterized members TEOSINTE BRANCHED1, CYCLOIDEA, and PROLIFERATING CELL FACTOR1. Thus far, these transcriptional regulators were implemented in control of various developmental processes (Martín-Trillo and Cubas, 2010). Members of class I of the TCP family are characterized by the presence of highly (94%) conserved cysteine residue within their DNA-binding/dimerization domain (Viola et al., 2013). This residue, located at position 20 of the TCP domain, mediates the oxidative inhibition of DNA-binding via formation of intra-molecular disulfide bonds. Using TCP15 as a model family member, Viola et al., (2013) demonstrated inhibition of DNA-binding activity upon treatment with hydrogen peroxide both *in vitro* and *in vivo*. Moreover, treatment with oxidized glutathione (GSSG) or nitric oxide (NO) donors also led to inhibition of activity indicating that the Cys20 might be subjected to S-glutathionylation and/or S-nitrosylation (Viola et al., 2013).

REDOX CONTROL OF PROTEIN TRANSLATION

Next to regulation of transcription, the control of mRNA translation by trans-acting factors is crucial for fine tuned protein expression. Thus far, the best studied case of redox-regulated control of mRNA translation occurs during expression of *Chlamydomonas reinhardtii* photosystem II reaction center protein D1 that is encoded by the chloroplast *psbA* gene (Kim and Mayfield, 1997; Yohn et al., 1998; Alergand et al., 2006). This two-component system involves the polyadenylation-binding protein RB47 and the protein disulfide isomerase RB60. RB60 regulates binding of the RB47 to the 5'-untranslated region of the *psbA* mRNA in a light-dependent manner. Binding of RB47 to the 5' UTR of the *psbA* mRNA is required for translation (Yohn et al., 1998). During the photosynthetic light reactions a reducing environment is generated by PSII. The reducing equivalents are passed through Fdx/FTR/Trx system to the chloroplast RB60 (Kim and Mayfield, 1997). RB60 contains two Trx-like –CGHC- sites that serve to interact with Cys143 or Cys259 of RB47. This interaction results in reduction of RB47 regulatory disulfides (Cys259 – Cys143 or Cys259 – Cys55) and activates the binding of RB47 to the *psbA* mRNA (Alergand et al., 2006). Upon translation the D1 protein is incorporated into PSII complexes. Importantly, under oxidizing conditions, RB60 facilitates the conversion of reduced RB47 to its inactive oxidized form (Kim and Mayfield, 1997). Evidence exists, that an analogous system could control the *psbA* mRNA translation in *Arabidopsis* as two yet unidentified RNA-binding proteins were found to interact with *psbA* mRNA in a redox dependent manner (Shen et al., 2001). Next to the control of mRNA translation also the mRNA stability might be subjected to redox control. The best characterized evidence of such regulation is the H_2O_2 induced mRNA stability of *SALT OVERLY SENSITIVE 1* (*SOS1*) which encodes for plasma membrane Na^+/H^+ antiporter crucial for the maintenance of ion homeostasis in saline stress conditions (Chung et al., 2008). Under normal conditions SOS1 mRNA is highly unstable, via yet unknown mechanisms stress induced production of H_2O_2 positively influences its stability and promotes salt stress tolerance (Chung et al., 2008).

RNA-binding proteins (RBPs) gain recognition in the field of plant stress adaptation and development (Lorković, 2009) however in higher plants the knowledge about their redox regulation limited. Examples of RBPs potentially undergoing oxidative PTMs are described in Chapter 2.

CONCLUSIONS AND PERSPECTIVES

Since the advent of proteomics numerous studies aimed at identification of proteins undergoing oxidative post-translational modifications. Among the most explored approaches towards identification of such proteins are numerous attempts to identify thioredoxin (Montrichard et al., 2009) and glutaredoxin (Rouhier et al., 2005) targets as well as proteins subjected to S-glutathionylation (Dixon et al., 2005b; Zaffagnini et al., 2012a) and S-nitrosylation (Lindermayr et al., 2005). Portfolio of techniques able of identifying common precursors of these PTMs, cysteine sulfenic acids, is now

expanding (Qian et al., 2012; Paulsen and Carroll, 2013). Among the new approaches the non-invasive *in vivo* Cys-SOH trapping genetically encoded probe based on YAP1 transcription factor gains recognition as an excellent tool for sulfenome mining purposes (see Chapter 2).

It is now clear that next to cysteine residues also methionine and tyrosine side chains are susceptible to oxidative modifications. Formation of methionine sulfoxide and tyrosine nitration are emerging redox PTMs that affect protein structure and function (Jacques et al., 2013). We expect, that in the near future the exploration of this relatively new field will result in identification of new proteins undergoing oxidative PTMs of methionine and tyrosine residues.

Thanks to the efforts of numerous research groups the amount of proteins potentially undergoing oxidative PTMs is continuously growing. However, a close look at the results of these investigations reveals an apparent gap between the number of identified proteins and the number of proteins for which the occurrence of oxidative PTMs has been confirmed. The validation of proteomic results requires a dedicated effort that in most cases focuses on a single protein at a time. This is caused by the difficulty to express recombinant proteins, lack of suitable activity assays, the absence of mutant phenotypes hampering the complementation studies, and finally, the scarce information about the role and function of identified proteins. We anticipate that future efforts towards deciphering the ROS signal transduction events will focus on functional characterization of already identified proteins, therefore exploring the sets of non validated proteomic findings.

Finally, we expect that the growing knowledge about ROS signal transduction events will stimulate efforts towards manipulation of plant stress tolerance and future translation of this knowledge into crop species.

REFERENCES

Alergand T, Peled-Zehavi H, Katz Y, Danon A (2006) The chloroplast protein disulfide isomerase RB60 reacts with a regulatory disulfide of the RNA-binding protein RB47. Plant Cell Physiol **47**: 540–8

Apel K, Hirt H (2004) Reactive oxygen species: metabolism, oxidative stress, and signal transduction. Annu Rev Plant Biol **55**: 373–99

Apostol I, Heinstein PF, Low PS (1989) Rapid stimulation of an oxidative burst during elicitation of cultured plant cells : role in defense and signal transduction. Plant Physiol **90**: 109–16

Ariel FD, Manavella PA, Dezar CA, Chan RL (2007) The true story of the HD-Zip family. Trends Plant Sci **12**: 419–26

Astier J, Kulik A, Koen E, Besson-Bard A, Bourque S, Jeandroz S, Lamotte O, Wendehenne D (2012) Protein S-nitrosylation: what's going on in plants? Free Radic Biol Med **53**: 1101–10

Balsera M, Uberegui E, Schurmann P, Buchanan BB (2014) Evolutionary development of redox regulation in chloroplasts. Antioxid Redox Signal [Epub ahead of print]

Bartels S, Anderson JC, González Besteiro MA, Carreri A, Hirt H, Buchala A, Métraux J-P, Peck SC, Ulm R (2009) MAP kinase phosphatase 1 and Protein tyrosine phosphatase 1 are repressors of salicylic acid synthesis and SNC1-mediated responses in *Arabidopsis*. Plant Cell **21**: 2884–97

Beckers GJM, Jaskiewicz M, Liu Y, Underwood WR, He SY, Zhang S, Conrath U (2009) Mitogen-activated protein kinases 3 and 6 are required for full priming of stress responses in *Arabidopsis thaliana*. Plant Cell **21**: 944–53

Betsuyaku S, Takahashi F, Kinoshita A, Miwa H, Shinozaki K, Fukuda H, Sawa S (2011) Mitogen-activated protein kinase regulated by the CLAVATA receptors contributes to shoot apical meristem homeostasis. Plant Cell Physiol **52**: 14–29

Binder BM, Rodríguez FI, Bleecker AB (2010) The copper transporter RAN1 is essential for biogenesis of ethylene receptors in *Arabidopsis*. J Biol Chem **285**: 37263–70

Cantero A, Barthakur S, Bushart TJ, Chou S, Morgan RO, Fernandez MP, Clark GB, Roux SJ (2006) Expression profiling of the *Arabidopsis* annexin gene family during germination, de-etiolation and abiotic stress. Plant Physiol Biochem **44**: 13–24

Chuang C-F, Running MP, Williams RW, Meyerowitz EM (1999) The PERIANTHIA gene encodes a bZIP protein involved in the determination of floral organ number in *Arabidopsis thaliana*. Genes Dev 334–344

Chung J-S, Zhu J-K, Bressan RA, Hasegawa PM, Shi H (2008) Reactive oxygen species mediate Na+-induced SOS1 mRNA stability in *Arabidopsis*. Plant J **53**: 554–65

Claiborne A, Miller H, Parsonage D, Ross R (1993) Protein-sulfenic acid stabilization and function in enzyme catalysis and gene regulation. FASEB J **7**: 1483–1490

De Clercq I, Vermeirssen V, Van Aken O, Vandepoele K, Murcha MW, Law SR, Inzé A, Ng S, Ivanova A, Rombaut D, et al (2013) The membrane-bound NAC transcription factor ANAC013 functions in mitochondrial retrograde regulation of the oxidative stress response in *Arabidopsis*. Plant Cell **25**: 3472–90

Colcombet J, Hirt H (2008) *Arabidopsis* MAPKs: a complex signalling network involved in multiple biological processes. Biochem J **413**: 217–26

Comelli RN, Gonzalez DH (2007) Conserved homeodomain cysteines confer redox sensitivity and influence the DNA binding properties of plant class III HD-Zip proteins. Arch Biochem Biophys **467**: 41–7

Corcoran A, Cotter TG (2013) Redox regulation of protein kinases. FEBS J **280**: 1944–65

Cross J V, Templeton DJ (2004) Oxidative stress inhibits MEKK1 by site-specific glutathionylation in the ATP-binding domain. Biochem J **381**: 675–83

Danquah A, de Zelicourt A, Colcombet J, Hirt H (2014) The role of ABA and MAPK signaling pathways in plant abiotic stress responses. Biotechnol Adv **32**: 40–52

Davies MJ (2005) The oxidative environment and protein damage. Biochim Biophys Acta **1703**: 93–109

Day AM, Veal EA (2010) Hydrogen peroxide-sensitive cysteines in the Sty1 MAPK regulate the transcriptional response to oxidative stress. J Biol Chem **285**: 7505–16

Delaunay A, Isnard A-D, Toledano MB (2000) H_2O_2 sensing through oxidation of the Yap1 transcription factor. EMBO J **19**: 5157–66

Delaunay A, Pflieger D, Barrault MB, Vinh J, Toledano MB (2002) A thiol peroxidase is an H_2O_2 receptor and redox-transducer in gene activation. Cell **111**: 471–81

Demir F, Horntrich C, Blachutzik J, Scherzer S, Reinders Y, Kierszniowska S, Schulze W, Harms G, Hedrich R, Geiger D, et al (2013) *Arabidopsis* nanodomain-delimited ABA signaling pathway regulates the anion channel SLAH3. Proc Natl Acad Sci U S A **110**: 8296–8301

Desikan R, Hancock JT, Bright J, Harrison J, Weir I, Hooley R, Neill SJ (2005) A Role for ETR1 in hydrogen peroxide signaling in stomatal guard cells. Plant Physiol **137**: 831–834

Desikan R, Last K, Harrett-Williams R, Tagliavia C, Harter K, Hooley R, Hancock JT, Neill SJ (2006) Ethylene-induced stomatal closure in *Arabidopsis* occurs via AtrbohF-mediated hydrogen peroxide synthesis. Plant J **47**: 907–16

Després C, Chubak C, Rochon A, Clark R, Bethune T, Desveaux D, Fobert PR (2003) The *Arabidopsis* NPR1 disease resistance protein is a novel cofactor that confers redox regulation of DNA binding activity to the basic domain / leucine zipper transcription factor TGA1. Plant Cell **15**: 2181–2191

Dietz K-J (2011) Peroxiredoxins in plants and cyanobacteria. Antioxid Redox Signal **15**: 1129–59

Dixon DP, Fordham-Skelton AP, Edwards R (2005a) Redox regulation of a soybean tyrosine-specific protein phosphatase. Biochemistry **44**: 7696–703

Dixon DP, Skipsey M, Grundy NM, Edwards R, Sciences B, Kingdom U (2005b) Stress-induced protein S-glutathionylation in *Arabidopsis*. Plant Physiol **138**: 2233–2244

Dóczi R, Brader G, Pettkó-Szandtner A, Rajh I, Djamei A, Pitzschke A, Teige M, Hirt H (2007) The *Arabidopsis* mitogen-activated protein kinase kinase MKK3 is upstream of group C mitogen-activated protein kinases and participates in pathogen signaling. Plant Cell **19**: 3266–79

Van der Does D, Leon-Reyes A, Koornneef A, Van Verk MC, Rodenburg N, Pauwels L, Goossens A, Körbes AP, Memelink J, Ritsema T, et al (2013) Salicylic acid suppresses jasmonic acid signaling downstream of SCFCOI1-JAZ by targeting GCC promoter motifs via transcription factor ORA59. Plant Cell **25**: 744–61

Dominguez-Solis JR, He Z, Lima A, Ting J, Buchanan BB, Luan S (2008) A cyclophilin links redox and light signals to cysteine biosynthesis and stress responses in chloroplasts. Proc Natl Acad Sci U S A **105**: 16386–16391

Duan Q, Kita D, Johnson EA, Aggarwal M, Gates L, Wu H-M, Cheung AY (2014) Reactive oxygen species mediate pollen tube rupture to release sperm for fertilization in *Arabidopsis*. Nat Commun **5**: 3129

Finkelstein R (2013) Abscisic Acid synthesis and response. *Arabidopsis* Book **11**: e0166

Fomenko DE, Gladyshev VN (2012) Comparative genomics of thiol oxidoreductases reveals widespread and essential functions of thiol-based redox control of cellular processes. Antioxid Redox Signal **16**: 193–201

Foreman J, Demidchik V, Bothwell JHF, Mylona P, Miedema H, Torres MA, Linstead P, Costa S, Brownlee C, Jones JDG, et al (2003) Reactive oxygen species produced by NADPH oxidase regulate plant cell growth. Nature **422**: 442-6

Foyer CH, Halliwell B (1976) The presence of glutathione and glutathione reductase in chloroplasts: A proposed role in ascorbic acid metabolism. Planta **133**: 21–5

Foyer CH, Halliwell B (1977) Purification and properties of dehydroascorbate reductase from spinach leaves. Phytochemistry **16**: 1347–1350

Fryer MJ, Ball L, Oxborough K, Karpinski S, Mullineaux PM, Baker NR (2003) Control of Ascorbate Peroxidase 2 expression by hydrogen peroxide and leaf water status during excess light stress reveals a functional organisation of *Arabidopsis* leaves. Plant J **33**: 691–705

Gadjev I, Vanderauwera S, Gechev T (2006) Transcriptomic footprints disclose specificity of reactive oxygen species signaling in *Arabidopsis*. Plant Physiol **141**: 436–445

Gan Z-R, Sardana MK, Jacobs JW, Polokoff MA (1990) Yeast thioltransferase—The active site cysteines display differential reactivity. Arch Biochem Biophys **282**: 110–115

Gasch AP, Spellman PT, Kao CM, Carmel-Harel O, Eisen MB, Storz G, Botstein D, Brown PO (2000) Genomic expression programs in the response of yeast cells to environmental changes. Mol Biol Cell **11**: 4241–57

Geiger D, Maierhofer T, Al-Rasheid KAS, Scherzer S, Mumm P, Liese A, Ache P, Wellmann C, Marten I, Grill E, et al (2011) Stomatal closure by fast abscisic acid signaling is mediated by the guard cell anion channel SLAH3 and the receptor RCAR1. Sci Signal **4**: 1–12

Geiger D, Scherzer S, Mumm P, Marten I, Ache P, Matschi S, Liese A, Wellmann C, Al-Rasheid KAS, Grill E, et al (2010) Guard cell anion channel SLAC1 is regulated by CDPK protein kinases with distinct Ca^{2+} affinities. Proc Natl Acad Sci U S A **107**: 8023–8

Glaring MA, Skryhan K, Kötting O, Zeeman SC, Blennow A (2012) Comprehensive survey of redox sensitive starch metabolising enzymes in *Arabidopsis thaliana*. Plant Physiol Biochem **58**: 89–97

Grotewold E, Drummond B, Bowen B, Peterson T (1994) The myb-homologous P gene controls phlobaphene pigmentation in maize floral organs by directly activating a flavonoid biosynthetic gene subset. Cell **76**: 543–53

Gupta R, Huang Y, Kieber J, Luan S (1998) Identification of a dual-specificity protein phosphatase that inactivates a MAP kinase from *Arabidopsis*. Plant J **16**: 581–9

Gupta R, Luan S (2003) Redox control of protein tyrosine phosphatases and mitogen-activated protein kinases in plants. Plant Physiol **132**: 1149–1152

Gutscher M, Sobotta MC, Wabnitz GH, Ballikaya S, Meyer AJ, Samstag Y, Dick TP (2009) Proximity-based protein thiol oxidation by H_2O_2-scavenging peroxidases. J Biol Chem **284**: 31532–40

Hahn A, Harter K (2009) Mitogen-activated protein kinase cascades and ethylene: signaling, biosynthesis, or both? Plant Physiol **149**: 1207–10

Harris TK, Turner GJ (2002) Structural basis of perturbed pK_a values of catalytic groups in enzyme active sites. IUBMB Life **53**: 85–98

Heine GF, Hernandez JM, Grotewold E (2004) Two cysteines in plant R2R3 MYB domains participate in REDOX-dependent DNA binding. J Biol Chem **279**: 37878–85

Hirayama T, Kieber JJ, Hirayama N, Kogan M, Guzman P, Nourizadeh S, Alonso JM, Dailey WP, Dancis A, Ecker JR (1999) RESPONSIVE-TO-ANTAGONIST1, a Menkes/Wilson disease-related copper transporter, is required for ethylene signaling in *Arabidopsis*. Cell **97**: 383–93

Hsieh W-P, Hsieh H-L, Wu S-H (2012) *Arabidopsis* bZIP16 transcription factor integrates light and hormone signaling pathways to regulate early seedling development. Plant Cell **24**: 3997–4011

Ichimura K, Shinozaki K, Tena G, Sheen J, Henry Y, Champion A, Kreis M, Zhang S, Hirt H, Wilson C, et al (2002) Mitogen-activated protein kinase cascades in plants: a new nomenclature. Trends Plant Sci **7**: 301–308

Iglesias-Baena I, Barranco-Medina S, Lazaro-Payo A, Lopez-Jaramillo JF, Sevilla F, Jose LJ (2010) Characterization of plant sulfiredoxin and role of sulphinic form of 2-Cys peroxiredoxin. J Exp Bot. doi: 10.1093/jxb/erq016

Iglesias-Baena I, Barranco-Medina S, Sevilla F, Lázaro J-J (2011) The dual-targeted plant sulfiredoxin retroreduces the sulfinic form of atypical mitochondrial peroxiredoxin. Plant Physiol **155**: 944–55

Jacques S, Ghesquière B, Van Breusegem F, Gevaert K (2013) Plant proteins under oxidative attack. Proteomics **13**: 932-40

Jammes F, Song C, Shin D, Munemasa S, Takeda K, Gu D, Cho D, Lee S, Giordo R, Sritubtim S, et al (2009) MAP kinases MPK9 and MPK12 are preferentially expressed in guard cells and positively regulate ROS-mediated ABA signaling. Proc Natl Acad Sci U S A **106**: 20520–5

Joo JH, Bae YS, Lee JS (2001) Role of auxin-induced reactive oxygen species in root gravitropism. Plant Physiol **126**: 1055–60

Jung G, Breitmaier E, Voelter W. (1972) Dissociation equilibrium of glutathione. A Fourier transform-13C-NMR spectroscopic study of pH-dependence and of charge densities. Eur J Biochem. 24(3):438-45

Kaya H, Nakajima R, Iwano M, Kanaoka MM, Kimura S, Takeda S, Kawarazaki T, Senzaki E, Hamamura Y, Higashiyama T, et al (2014) Ca^{2+}-activated reactive oxygen species production by *Arabidopsis* RbohH and RbohJ is essential for proper pollen tube tip growth. Plant Cell **26**: 1069–80

Kazan K, Manners JM (2008) Jasmonate signaling: toward an integrated view. Plant Physiol **146**: 1459–68

Khan M, Rozhon W, Bigeard J, Pflieger D, Husar S, Pitzschke A, Teige M, Jonak C, Hirt H, Poppenberger B (2013) Brassinosteroid-regulated GSK3/Shaggy-like kinases phosphorylate mitogen-activated protein (MAP) kinase kinases, which control stomata development in *Arabidopsis thaliana*. J Biol Chem **288**: 7519–27

Kiegerl S, Cardinale F, Siligan C, Gross A, Baudouin E, Liwosz A, Eklöf S, Till S, Bögre L, Hirt H, et al (2000) SIMKK, a mitogen-activated protein kinase (MAPK) kinase, is a specific activator of the salt stress-induced MAPK, SIMK. Plant Cell **12**: 2247–58

Kim J, Mayfield SP (1997) Protein disulfide isomerase as a regulator of chloroplast translational activation. Science **278 (5345)**: 1954–1957

Konopka-Postupolska D, Clark G, Goch G, Debski J, Floras K, Cantero A, Fijolek B, Roux S, Hennig J (2009) The role of annexin 1 in drought stress in *Arabidopsis*. Plant Physiol **150**: 1394–410

Kopriva S, Mugford SG, Baraniecka P, Lee B-R, Matthewman CA, Koprivova A (2012) Control of sulfur partitioning between primary and secondary metabolism in *Arabidopsis*. Front Plant Sci **3**: 163

Kosetsu K, Matsunaga S, Nakagami H, Colcombet J, Sasabe M, Soyano T, Takahashi Y, Hirt H, Machida Y (2010) The MAP kinase MPK4 is required for cytokinesis in *Arabidopsis thaliana*. Plant Cell **22**: 3778–90

Kovtun Y, Chiu WL, Tena G, Sheen J (2000) Functional analysis of oxidative stress-activated mitogen-activated protein kinase cascade in plants. Proc Natl Acad Sci U S A **97**: 2940–5

Kwak JM, Mori IC, Pei Z-M, Leonhardt N, Torres MA, Dangl JL, Bloom RE, Bodde S, Jones JDG, Schroeder JI (2003) NADPH oxidase AtrbohD and AtrbohF genes function in ROS-dependent ABA signaling in *Arabidopsis*. EMBO J **22**: 2623–33

Laohavisit A, Brown AT, Cicuta P, Davies JM (2010) Annexins: components of the calcium and reactive oxygen signaling network. Plant Physiol **152**: 1824–9

Laohavisit A, Davies JM (2011) Annexins. New Phytol **189**: 40–53

Laohavisit A, Shang Z, Rubio L, Cuin TA, Véry A-A, Wang A, Mortimer JC, Macpherson N, Coxon KM, Battey NH, et al (2012) *Arabidopsis* annexin1 mediates the radical-activated plasma membrane Ca^{2+}- and K^+-permeable conductance in root cells. Plant Cell **24**: 1522–33

Lee J, Godon C, Spector D, Garin J, Toledano MB (1999) Yap1 and Skn7 control two specialized oxidative stress response regulons in Yeast. J Biol Chem **274**: 16040 – 16046

Lee JS, Ellis BE (2007) *Arabidopsis* MAPK phosphatase 2 (MKP2) positively regulates oxidative stress tolerance and inactivates the MPK3 and MPK6 MAPKs. J Biol Chem **282**: 25020–9

Lee JS, Wang S, Sritubtim S, Chen J-G, Ellis BE (2009a) *Arabidopsis* mitogen-activated protein kinase MPK12 interacts with the MAPK phosphatase IBR5 and regulates auxin signaling. Plant J **57**: 975–85

Lee SC, Lan W, Buchanan BB, Luan S (2009b) A protein kinase-phosphatase pair interacts with an ion channel to regulate ABA signaling in plant guard cells. Proc Natl Acad Sci U S A **106**: 21419–24

Leung J, Merlot S, Giraudat J (1997) The *Arabidopsis* ABSCISIC ACID-INSENSITIVE2 (ABI2) and ABI1 genes encode homologous protein phosphatases 2C involved in abscisic acid signal transduction. Plant Cell **9**: 759–771

Levine A, Tenhaken R, Dixon R, Lamb C (1994) H_2O_2 from the oxidative burst orchestrates the plant hypersensitive disease resistance response. Cell **79**: 583–93

Li B, Zhao Y, Liang L, Ren H, Xing Y, Chen L, Sun M, Wang Y, Han Y, Jia H, et al (2012) Purification and characterization of *Zm*RIP1, a novel reductant-inhibited protein tyrosine phosphatase from maize. Plant Physiol **159**: 671–81

Li S, Lauri A, Ziemann M, Busch A, Bhave M, Zachgo S (2009) Nuclear activity of ROXY1, a glutaredoxin interacting with TGA factors, is required for petal development in *Arabidopsis thaliana*. Plant Cell **21**: 429–41

Lindermayr C, Saalbach G, Durner J (2005) Proteomic identification of S-nitrosylated proteins. Plant Physiol **137**: 921-930

Lindermayr C, Sell S, Müller B, Leister D, Durner J (2010) Redox regulation of the NPR1-TGA1 system of *Arabidopsis thaliana* by nitric oxide. Plant Cell **22**: 2894–907

Liu L, Enright E, Sun P, Tsai SY, Mehta P, Beckman DL, Terrian DM (2002) Inactivation of annexin II tetramer by S-nitrosoglutathione. Eur J Biochem **269**: 4277–4286

Lorković ZJ (2009) Role of plant RNA-binding proteins in development, stress response and genome organization. Trends Plant Sci **14**: 229–36

Lounifi I, Arc E, Molassiotis A, Job D, Rajjou L, Tanou G (2013) Interplay between protein carbonylation and nitrosylation in plants. Proteomics **13**: 568–78

Lumbreras V, Vilela B, Irar S, Solé M, Capellades M, Valls M, Coca M, Pagès M (2010) MAPK phosphatase MKP2 mediates disease responses in *Arabidopsis* and functionally interacts with MPK3 and MPK6. Plant J **63**: 1017–30

Luo D, Smith SW, Anderson BD (2005) Kinetics and mechanism of the reaction of cysteine and hydrogen peroxide in aqueous solution. J Pharm Sci **94**: 304–16

Ma Y, Szostkiewicz I, Korte A, Moes D, Yang Y, Christmann A, Grill E (2009) Regulators of PP2C phosphatase activity function as abscisic acid sensors. Science **324**: 1064–8

MacRobbie EA (2002) Evidence for a role for protein tyrosine phosphatase in the control of ion release from the guard cell vacuole in stomatal closure. Proc Natl Acad Sci U S A **99**: 11963–8

Marino S, Gladyshev V (2010) Cysteine function governs its conservation and degeneration and restricts its utilization on protein surfaces. J Mol Biol **404**: 902–916

Martín-Trillo M, Cubas P (2010) TCP genes: a family snapshot ten years later. Trends Plant Sci **15**: 31–9

Masucci JD, Rerie WG, Foreman DR, Zhang M, Galway ME, Marks MD, Schiefelbein JW (1996) The homeobox gene GLABRA 2 is required for position-dependent cell differentiation in the root epidermis of *Arabidopsis thaliana*. Development **122**: 1253–1260

Meinhard M, Grill E (2001) Hydrogen peroxide is a regulator of ABI1, a protein phosphatase 2C from *Arabidopsis*. FEBS Lett **508**: 443–6

Meinhard M, Rodriguez PL, Grill E (2002) The sensitivity of ABI2 to hydrogen peroxide links the abscisic acid-response regulator to redox signalling. Planta **214**: 775–82

Meng F-G, Zhang Z-Y (2013) Redox regulation of Protein Tyrosine Phosphatase activity by hydroxyl radical. Biochim Biophys Acta **1834**: 464–469

Merlot S, Gosti F, Guerrier D, Vavasseur a, Giraudat J (2001) The ABI1 and ABI2 protein phosphatases 2C act in a negative feedback regulatory loop of the abscisic acid signalling pathway. Plant J **25**: 295–303

Meyer Y, Belin C, Delorme-Hinoux V, Reichheld J-P, Riondet C (2012) Thioredoxin and glutaredoxin systems in plants: molecular mechanisms, crosstalks, and functional significance. Antioxid Redox Signal **17**: 1124–60

Miao Y, Lv D, Wang P, Wang X-C, Chen J, Miao C, Song C-P (2006) An *Arabidopsis* glutathione peroxidase functions as both a redox transducer and a scavenger in abscisic acid and drought stress responses. Plant Cell **18**: 2749–66

Mittler R, Vanderauwera S, Gollery M, Van Breusegem F (2004) Reactive oxygen gene network of plants. Trends Plant Sci **9**: 490–8

Mittler R, Vanderauwera S, Suzuki N, Miller G, Tognetti VB, Vandepoele K, Gollery M, Shulaev V, Van Breusegem F (2011) ROS signaling: the new wave? Trends Plant Sci **16**: 300–9

Montrichard F, Alkhalfioui F, Yano H, Vensel WH, Hurkman WJ, Buchanan BB (2009) Thioredoxin targets in plants: the first 30 years. J Proteomics **72**: 452–74

Motohashi K, Kondoh A, Stumpp MT, Hisabori T (2001) Comprehensive survey of proteins targeted by chloroplast thioredoxin. Proc Natl Acad Sci U S A **98**: 11224–9

Motohashi K, Koyama F, Nakanishi Y, Ueoka-Nakanishi H, Hisabori T (2003) Chloroplast cyclophilin is a target protein of thioredoxin. Thiol modulation of the peptidyl-prolyl cis-trans isomerase activity. J Biol Chem **278**: 31848–52

Mou Z, Fan W, Dong X (2003) Inducers of plant systemic acquired resistance regulate NPR1 function through redox changes. Cell **113**: 935–44

Mukherjee K, Brocchieri L, Bürglin TR (2009) A comprehensive classification and evolutionary analysis of plant homeobox genes. Mol Biol Evol **26**: 2775–94

Murmu J, Bush MJ, DeLong C, Li S, Xu M, Khan M, Malcolmson C, Fobert PR, Zachgo S, Hepworth SR (2010) *Arabidopsis* basic leucine-zipper transcription factors TGA9 and TGA10 interact with floral glutaredoxins ROXY1 and ROXY2 and are redundantly required for anther development. Plant Physiol **154**: 1492–504

Mustilli A, Merlot S, Vavasseur A, Fenzi F, Giraudat J (2002) *Arabidopsis* OST1 protein kinase mediates the regulation of stomatal aperture by abscisic acid and acts upstream of reactive oxygen species production. Proc Natl Acad Sci USA **14**: 3089–3099

Nakashima K, Yamaguchi-Shinozaki K (2013) ABA signaling in stress-response and seed development. Plant Cell Rep **32**: 959–70

Ndamukong I, Abdallat AA, Thurow C, Fode B, Zander M, Weigel R, Gatz C (2007) SA-inducible *Arabidopsis* glutaredoxin interacts with TGA factors and suppresses JA-responsive PDF1.2 transcription. Plant J **50**: 128–39

Nelson J, Creighton T (1994) Reactivity and ionization of the active site cysteine residues of DsbA, a protein required for disulfide bond formation in vivo. Biochemistry **33**: 5974–83

Ng S, Ivanova A, Duncan O, Law SR, Van Aken O, De Clercq I, Wang Y, Carrie C, Xu L, Kmiec B, et al (2013) A membrane-bound NAC transcription factor, ANAC017, mediates mitochondrial retrograde signaling in *Arabidopsis*. Plant Cell **25**: 3450–71

Noctor G, Veljovic-Jovanovic S, Driscoll S, Novitskaya L, CH F (2002) Drought and oxidative load in the leaves of C3 plants: a predominant role for photorespiration? Ann Bot **89**: 841–850

Orozco-Cardenas M, Ryan CA (1999) Hydrogen peroxide is generated systemically in plant leaves by wounding and systemin via the octadecanoid pathway. Proc Natl Acad Sci U S A **96**: 6553–7

Ostman A, Frijhoff J, Sandin A, Böhmer F-D (2011) Regulation of protein tyrosine phosphatases by reversible oxidation. J Biochem **150**: 345–56

Park S, Fung P, Nishimura N, Jensen DR, Zhao Y, Lumba S, Santiago J, Rodrigues A, Alfred SE, Bonetta D, et al (2009) Abscisic acid inhibits PP2Cs via the PYR/PYL family of ABA- binding START proteins. Science **324**: 1068-1071

Park S-W, Li W, Viehhauser A, He B, Kim S, Nilsson AK, Andersson MX, Kittle JD, Ambavaram MMR, Luan S, et al (2013) Cyclophilin 20-3 relays a 12-oxo-phytodienoic acid signal during stress responsive regulation of cellular redox homeostasis. Proc Natl Acad Sci U S A **110**: 9559–64

Paulsen CE, Carroll KS (2013) Cysteine-Mediated Redox Signaling: Chemistry, Biology, and Tools for Discovery. Chem Rev. doi: 10.1021/cr300163e

Pauwels L, Goossens A (2011) The JAZ proteins: a crucial interface in the jasmonate signaling cascade. Plant Cell **23**: 3089–100

Pei ZM, Murata Y, Benning G, Thomine S, Klüsener B, Allen GJ, Grill E, Schroeder JI (2000) Calcium channels activated by hydrogen peroxide mediate abscisic acid signalling in guard cells. Nature **406**: 731–4

Petersen M, Brodersen P, Naested H, Andreasson E, Lindhart U, Johansen B, Nielsen HB, Lacy M, Austin MJ, Parker JE, et al (2000) *Arabidopsis* map kinase 4 negatively regulates systemic acquired resistance. Cell **103**: 1111-20

Petrov VD, Van Breusegem F (2012) Hydrogen peroxide-a central hub for information flow in plant cells. AoB Plants **2012**: pls014

Pitzschke A, Djamei A, Bitton F, Hirt H (2009) A major role of the MEKK1-MKK1/2-MPK4 pathway in ROS signalling. Mol Plant **2**: 120–37

Pitzschke A, Hirt H (2009) Disentangling the complexity of mitogen-activated protein kinases and reactive oxygen species signaling. Plant Physiol **149**: 606–15

Potocký M, Jones MA, Bezvoda R, Smirnoff N, Zárský V (2007) Reactive oxygen species produced by NADPH oxidase are involved in pollen tube growth. New Phytol **174**: 742–51

Prigge M, Otsuga D, Alonso J, Ecker J, Drews G, Clark S (2005) Class III Homeodomain-Leucine Zipper gene family members have overlapping, antagonistic, and distinct roles in *Arabidopsis* development. Plant Cell **17**: 61–76

Qian J, Wani R, Klomsiri C, Poole LB, Tsang AW, Furdui CM (2012) A simple and effective strategy for labeling cysteine sulfenic acid in proteins by utilization of β-ketoesters as cleavable probes. Chem Commun (Camb) **48**: 4091-3

Rasmussen MW, Roux M, Petersen M, Mundy J (2012) MAP kinase cascades in *Arabidopsis* innate immunity. Front Plant Sci **3**: 169

Rerie WG, Feldmann KA, Marks MD (1994) The GLABRA2 gene encodes a homeo domain protein required for normal trichome development in *Arabidopsis*. Genes Dev **8**: 1388–1399

Rey P, Bécuwe N, Barrault M-B, Rumeau D, Havaux M, Biteau B, Toledano MB (2007) The *Arabidopsis thaliana* sulfiredoxin is a plastidic cysteine-sulfinic acid reductase involved in the photooxidative stress response. Plant J **49**: 505–14

Richards SL, Laohavisit A, Mortimer JC, Shabala L, Swarbreck SM, Shabala S, Davies JM (2013) Annexin 1 regulates the H2O2 -induced calcium signature in *Arabidopsis thaliana* roots. Plant J 136–145

Rivas-San Vicente M, Plasencia J (2011) Salicylic acid beyond defence: its role in plant growth and development. J Exp Bot **62**: 3321–38

Rochon A, Boyle P, Wignes T, Fobert PR, Després C (2006) The coactivator function of *Arabidopsis* NPR1 requires the core of its BTB/POZ domain and the oxidation of C-terminal cysteines. Plant Cell **18**: 3670–85

Rodríguez FI (1999) A copper cofactor for the ethylene receptor ETR1 from *Arabidopsis*. Science (80-) **283**: 996–998

Roos G, Messens J (2011) Protein sulfenic acid formation: from cellular damage to redox regulation. Free Radic Biol Med **51**: 314–26

Rouhier N, Villarejo A, Srivastava M, Gelhaye E, Keech O, Droux M, Finkemeier I, Samuelsson G, Dietz KJ, Jacquot J, et al (2005) Identification of plant glutaredoxin targets. Antioxid Redox Signal **7**: 919–929

Running MP, Meyerowitz EM (1996) Mutations in the PERIANTHIA gene of *Arabidopsis* specifically alter floral organ number and initiation pattern. Development **122**: 1261–9

Schaller G, Ladd A, Lanahan M, Spanbauer J, Bleecker A (1995) The ethylene response mediator ETR1 from *Arabidopsis* forms a disulfide-linked dimer. J Biol Chem **270**: 12526–12530

Schaller GE (2012) Ethylene and the regulation of plant development. BMC Biol. doi: 10.1186/1741-7007-10-9

Schürmann P, Buchanan BB (2008) The ferredoxin/thioredoxin system of oxygenic photosynthesis. Antioxid Redox Signal **10**: 1235–74

Shaikhali J, Heiber I, Seidel T, Ströher E, Hiltscher H, Birkmann S, Dietz K-J, Baier M (2008) The redox-sensitive transcription factor Rap2.4a controls nuclear expression of 2-Cys peroxiredoxin A and other chloroplast antioxidant enzymes. BMC Plant Biol **8**: 48

Shaikhali J, Norén L, de Dios Barajas-López J, Srivastava V, König J, Sauer UH, Wingsle G, Dietz K-J, Strand Å (2012) Redox-mediated mechanisms regulate DNA binding activity of the G-group of basic region leucine zipper (bZIP) transcription factors in *Arabidopsis*. J Biol Chem **287**: 27510–25

Shakeel SN, Wang X, Binder BM, Schaller GE (2013) Mechanisms of signal transduction by ethylene: overlapping and non-overlapping signalling roles in a receptor family. AoB Plants **5**: doi:10.1093/aobpla/plt010

Shen Y, Danon A, Christopher DA (2001) RNA binding-proteins interact specifically with the *Arabidopsis* chloroplast *psbA* mRNA 5' untranslated region in a redox-dependent manner. Plant Cell Physiol **42**: 1071–8

Smykowski A, Zimmermann P, Zentgraf U (2010) G-Box binding factor1 reduces CATALASE2 expression and regulates the onset of leaf senescence in *Arabidopsis*. Plant Physiol **153**: 1321–31

Song CJ, Steinebrunner I, Wang X, Stout SC, Roux SJ (2006) Extracellular ATP Induces the accumulation of superoxide via NADPH Oxidases in *Arabidopsis*. Plant Physiol **140**: 1222–32

Song Y, Miao Y, Song C-P (2014) Behind the scenes: the roles of reactive oxygen species in guard cells. New Phytol **201**: 1121–1140

Strader LC, Monroe-Augustus M, Bartel B (2008) The IBR5 phosphatase promotes *Arabidopsis* auxin responses through a novel mechanism distinct from TIR1-mediated repressor degradation. BMC Plant Biol **8**: 41

Suarez-Rodriguez MC, Adams-Phillips L, Liu Y, Wang H, Su S-H, Jester PJ, Zhang S, Bent AF, Krysan PJ (2007) MEKK1 is required for flg22-induced MPK4 activation in *Arabidopsis* plants. Plant Physiol **143**: 661–9

Tada Y, Spoel SH, Pajerowska-Mukhtar K, Mou Z, Song J, Wang C, Zuo J, Dong X (2008) Plant immunity requires conformational changes of NPR1 via S-nitrosylation and thioredoxins. Science **321**: 952–6

Tajc S, Tolbert B, Basavappa R, Miller B (2004) Direct determination of thiol pK_a by isothermal titration microcalorimetry. J Am Chem Soc **126**: 10508–9

Takahashi F, Yoshida R, Ichimura K, Mizoguchi T, Seo S, Yonezawa M, Maruyama K, Yamaguchi-Shinozaki K, Shinozaki K (2007) The mitogen-activated protein kinase cascade MKK3-MPK6 is an important part of the jasmonate signal transduction pathway in *Arabidopsis*. Plant Cell **19**: 805–18

Taki N, Sasaki-Sekimoto Y, Obayashi T, Kikuta A, Kobayashi K, Ainai T, Yagi K, Sakurai N, Suzuki H, Masuda T, et al (2005) 12-oxo-phytodienoic acid triggers expression of a distinct set of genes and plays a role in wound-induced gene expression in *Arabidopsis*. Plant Physiol **139**: 1268–1283

Templeton DJ, Aye M-S, Rady J, Xu F, Cross J V (2010) Purification of reversibly oxidized proteins (PROP) reveals a redox switch controlling p38 MAP kinase activity. PLoS One **5**: e15012

Trivedi DK, Yadav S, Vaid N, Tuteja N (2012) Genome wide analysis of Cyclophilin gene family from rice and *Arabidopsis* and its comparison with yeast. Plant Signal Behav **7**: 1653–66

Tron AE, Bertoncini CW, Chan RL, Gonzalez DH (2002) Redox regulation of plant homeodomain transcription factors. J Biol Chem **277**: 34800–7

Truong TH, Carroll KS (2013) Redox regulation of protein kinases. Crit Rev Biochem Mol Biol **48**: 332–56

Turchi L, Carabelli M, Ruzza V, Possenti M, Sassi M, Peñalosa A, Sessa G, Salvi S, Forte V, Morelli G, et al (2013) *Arabidopsis* HD-Zip II transcription factors control apical embryo development and meristem function. Development **140**: 2118–29

Ueoka-Nakanishi H, Sazuka T, Nakanishi Y, Maeshima M, Mori H, Hisabori T (2013) Thioredoxin h regulates calcium dependent protein kinases in plasma membranes. FEBS J **280**: 3220–31

Vahisalu T, Puzõrjova I, Brosché M, Valk E, Lepiku M, Moldau H, Pechter P, Wang Y-S, Lindgren O, Salojärvi J, et al (2010) Ozone-triggered rapid stomatal response involves the production of reactive oxygen species, and is controlled by SLAC1 and OST1. Plant J **62**: 442–53

Viola IL, Güttlein LN, Gonzalez DH (2013) Redox modulation of plant developmental regulators from the class I TCP transcription factor family. Plant Physiol **162**: 1434–47

Vlot AC, Dempsey DA, Klessig DF (2009) Salicylic Acid, a multifaceted hormone to combat disease. Annu Rev Phytopathol **47**: 177–206

Walia A, Lee JS, Wasteneys G, Ellis B (2009) *Arabidopsis* mitogen-activated protein kinase MPK18 mediates cortical microtubule functions in plant cells. Plant J **59**: 565–75

Wang F, Cui X, Sun Y, Dong C-H (2013) Ethylene signaling and regulation in plant growth and stress responses. Plant Cell Rep **32**: 1099–109

Wang H, Ngwenyama N, Liu Y, Walker JC, Zhang S (2007) Stomatal development and patterning are regulated by environmentally responsive mitogen-activated protein kinases in *Arabidopsis*. Plant Cell **19**: 63–73

Wang P, Du Y, Li Y, Ren D, Song C-P (2010) Hydrogen peroxide-mediated activation of MAP kinase 6 modulates nitric oxide biosynthesis and signal transduction in *Arabidopsis*. Plant Cell **22**: 2981–98

Williams CE, Grotewold E (1997) Differences between plant and animal Myb domains are fundamental for DNA binding activity, and chimeric Myb domains have novel DNA binding specificities. J Biol Chem **272**: 563–571

Wise RR, Naylor AW (1987) Chilling-enhanced photooxidation : evidence for the role of singlet oxygen and superoxide in the breakdown of pigments and endogenous antioxidants. Plant Physiol **83**: 278–82

Wouters MA, Iismaa S, Fan SW, Haworth NL (2011) Thiol-based redox signalling: rust never sleeps. Int J Biochem Cell Biol **43**: 1079–85

Wu Y, Zhang D, Chu JY, Boyle P, Wang Y, Brindle ID, De Luca V, Després C (2012) The *Arabidopsis* NPR1 protein is a receptor for the plant defense hormone salicylic acid. Cell Rep **1**: 639–47

Xing S, Rosso MG, Zachgo S (2005) ROXY1, a member of the plant glutaredoxin family, is required for petal development in *Arabidopsis thaliana*. Development **132**: 1555–65

Xu Q, Fu HH, Gupta R, Luan S (1998) Molecular characterization of a tyrosine-specific protein phosphatase encoded by a stress-responsive gene in *Arabidopsis*. Plant Cell **10**: 849–57

Yohn CB, Cohen A, Rosch C, Kuchka MR, Mayfield SP (1998) Translation of the chloroplast psbA mRNA requires the nuclear-encoded Poly(A)-binding protein, RB47. J Cell Biol **142**: 435–442

Yu M, Yun B-W, Spoel SH, Loake GJ (2012) A sleigh ride through the SNO: regulation of plant immune function by protein S-nitrosylation. Curr Opin Plant Biol **15**: 424–30

Zaffagnini M, Bedhomme M, Groni H, Marchand CH, Puppo C, Gontero B, Cassier-Chauvat C, Decottignies P, Lemaire SD (2012a) Glutathionylation in the photosynthetic model organism *Chlamydomonas reinhardtii*: a proteomic survey. Mol Cell Proteomics **11**: M111.014142

Zaffagnini M, Bedhomme M, Lemaire SD, Trost P (2012b) The emerging roles of protein glutathionylation in chloroplasts. Plant Sci **185-186**: 86–96

Zaffagnini M, Bedhomme M, Marchand CH, Morisse S, Trost P, Lemaire SD (2012c) Redox regulation in photosynthetic organisms: focus on glutathionylation. Antioxid Redox Signal **16**: 567–86

Zhou J, Xia X-J, Zhou Y-H, Shi K, Chen Z, Yu J-Q (2014) RBOH1-dependent H_2O_2 production and subsequent activation of MPK1/2 play an important role in acclimation-induced cross-tolerance in tomato. J Exp Bot **65**: 595–607

2

Sulfenome mining in *Arabidopsis thaliana*

Cezary Waszczak, Mosammat Salma Akter, Dominique Eeckhout, Geert Persiau, Khadija Wahni, Nandita Bodra, Inge Van Molle, Barbara De Smet, Didier Vertommen, Kris Gevaert, Geert De Jaeger, Marc Van Montagu, Joris Messens and Frank Van Breusegem

AUTHOR CONTRIBUTIONS

ABSTRACT

Reactive oxygen species (ROS) have been shown to be potent signaling molecules. Nowadays, oxidation of cysteine residues is a well-recognized posttranslational protein modification (PTM), but the signaling processes steered by such oxidations are poorly understood. To get insight into the cysteine thiol-dependent ROS signaling in *Arabidopsis thaliana*, we identified the hydrogen peroxide (H_2O_2)-dependent sulfenome, i.e., proteins with at least one cysteine thiol oxidized to a sulfenic acid. By means of a genetic construct consisting of a fusion between the C-terminal domain of the yeast (*Saccharomyces cerevisiae*) AP1 (YAP1) transcription factor and a tandem affinity purification tag, we detected ~100 sulfenylated proteins in *Arabidopsis* cell suspensions exposed to H_2O_2 stress. The *in vivo* YAP1-based trapping of sulfenylated proteins was validated by a targeted in vitro analysis of DEHYDROASCORBATE REDUCTASE 2 (DHAR2). In DHAR2, the active site nucleophilic cysteine is regulated through a sulfenic acid-dependent switch, leading to S-glutathionylation, a PTM that protects the protein against oxidative damage.

INTRODUCTION

Numerous posttranslational modifications (PTMs) have been discovered within proteomes, creating a complex landscape of protein diversity and function (Garavelli, 2004). One of the recognized reversible redox-based PTMs is the oxidation of a cysteine thiol group to a sulfenic acid (Cys-SOH) (Roos and Messens, 2011) that acts as regulatory switch in several oxidative stress signal transduction pathways (Ma et al., 2007). Unless stabilized into the protein environment, sulfenic acids can react rapidly with other protein thiols or with low-molecular weight thiols to form intramolecular and/or intermolecular disulfides. These mechanisms protect the sulfenic acids against overoxidation to sulfinic (SO_2H) or sulfonic (SO_3H) acid and allow sulfur oxygen signaling (Roos and Messens, 2011). In plants, the best-known redox regulation mechanisms are the light-dependent thiol-disulfide exchange switches in chloroplast proteins (Balsera et al., 2014). Examples of other redox-regulated proteins are the vacuolar H^+-ATPase (Tavakoli et al., 2001), the transcriptional co-activator NONEXPRESSER OF PR GENES 1 (Mou et al., 2003), and several transcription factors (TF) including the REDOX-SENSITIVE APETALA2-TYPE Rap2.4a (Shaikhali et al., 2008), the G-group of BASIC LEUCINE ZIPPER TFs (Shaikhali et al., 2012), and the class I of TFs from TEOSINTE-BRANCHED1/CYLOIDEA/PROLIFERATING CELL FACTOR family (Viola et al., 2013). The redox relay mechanisms that bridge the signal perception to the final oxidative stress response are largely unknown. Some thiol peroxidases have an H_2O_2-dependent signaling function and can act as receptor and transducer (Fomenko et al., 2011). In yeast, the H_2O_2 sensor Oxidant receptor protein1 (ORP1/Glutathione peroxidase 3) controls, together with the transcription factor YAP1, a redox regulon via a sulfenic acid thiol-disulfide relay mechanism (Delaunay et al., 2002). Upon reaction with H_2O_2, the peroxidatic cysteine of ORP1 is oxidized to a sulfenic acid that reacts with the YAP1 C-terminal cysteine-rich domain (cCRD) and forms a disulfide. This specific mixed disulfide formation has prompted us to develop a YAP1-based probe for trapping plant sulfenylated proteins *in vivo* (Takanishi et al., 2007). To categorize the sulfenome, which is the set of proteins with at least one sulfenic acid, and its dynamics at the proteome level in *Arabidopsis thaliana* cells upon oxidative stress, we implemented the YAP1-based sulfenic acid trapping method coupled to a tandem affinity purification (TAP) tag (Van Leene et al., 2008). We identified approximately 100 sulfenylated proteins during the early and late oxidative stress responses, of which 68 had previously not been recognized to undergo oxidative PTMs. Validation of sulfenylation on DEHYDROASCORBATE REDUCTASE 2 (DHAR2) demonstrates the importance of a glutathione (GSH)-dependent redox switch on its sulfenylated nucleophilic cysteine that reversibly regulates the DHAR activity.

RESULTS AND DISCUSSION

H_2O_2 triggers the formation of YAP1C heterocomplexes in a time- and dose-dependent manner

To apply the YAP1-TAP approach, we synthesized a YAP1-cCRD construct with adapted codons for expression in plants and mutated Cys620 and Cys629 to alanine and threonine (Table S1; Fig. 1A), retaining only the redox-active cysteine Cys598. Then, we fused this construct at its N-terminus to a GS tag that combines two immunoglobulin G (IgG)-binding domains of protein G with a streptavidin-binding peptide (SBP), separated by a tobacco etch virus (TEV) protease cleavage site (Van Leene et al., 2008). The Cys598 of YAP1C-GS is essential for the formation of mixed disulfides with sulfenylated proteins (Takanishi et al., 2007). In addition, we constructed a similar control version, YAP1A-GS, in which all cysteines are mutated (Table S1; Fig. 1A). The cauliflower mosaic virus (CaMV) 35S promoter-driven constructs were transformed in *Arabidopsis* cell suspensions. Western blot analysis with a specific antibody conjugate to detect the G moiety of the tag (peroxidases-anti-peroxidase [PAP] antibody conjugate) revealed that the yield of the two fusion proteins YAP1C-GS and YAP1A-GS is comparable and that they migrate as a single band at 35 kDa (Fig. 1B). Previously, a 20-mM H_2O_2 treatment of *Arabidopsis* cells had been found to provoke oxidative stress signaling (Desikan et al., 2001) and oxidative stress induced cell death, while the H_2O_2 concentrations ≤ 5 mM had little effect on cell survival (Desikan et al., 1998).
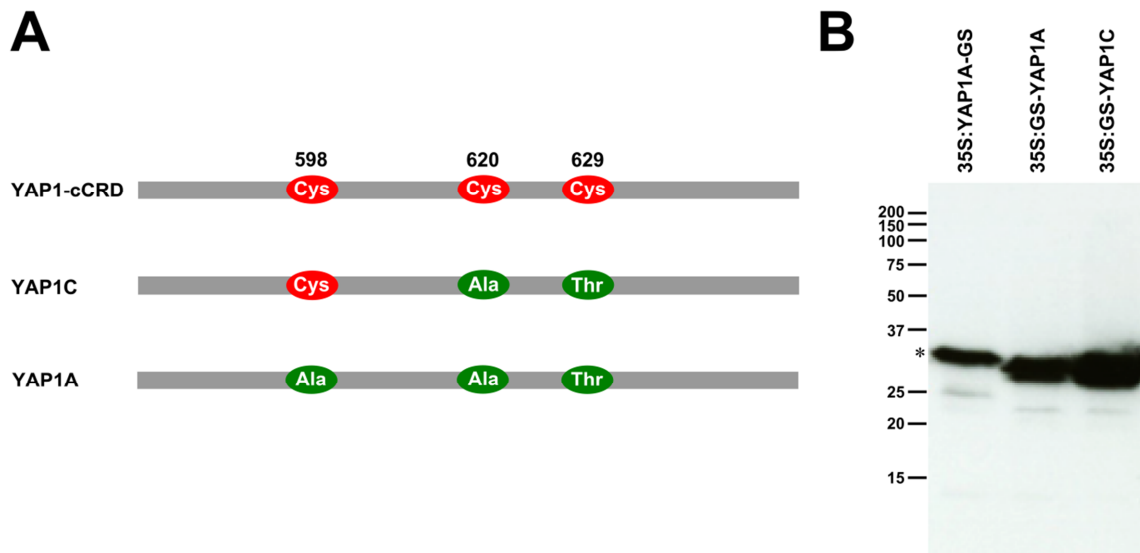

Fig. 1. Recombinant YAP1 probes used in this study. *(A)* Schematic representation of YAP1-cCRD and YAP1A/C mutants. The yeast sequence corresponding to YAP1-cCRD was codon optimized for expression in *Arabidopsis*. For YAP1C, Cys598 was retained that is necessary for heterodimer formation, whereas in the YAP1A-negative control probe, all cysteines were mutated. *(B)* CaMV 35S promoter-driven production of recombinant YAP1-GS fusion proteins in transformed *Arabidopsis* cell cultures. Proteins were extracted and probes were visualized on immunoblot with the PAP antibody complex. Under reducing conditions, probes migrate as a single band at ~35 kDa. Asterisk indicates that, due to a presence of additional c-Myc tag, the C-terminal fusion is 0.7 kDa heavier.

We treated the transformed *Arabidopsis* cell suspension cultures with 0, 0.1, 1, 5, 10 and 20 mM H_2O_2 at the mid-log phase for 1 h. To block all free thiols, we extracted the soluble protein in the presence of iodoacetamide (IAM)and *N*-Ethylmaleimide (NEM) (Fig. 2) and analyzed the disulfide bond formation on a nonreducing Western blot with the PAP antibody conjugate. In untreated cells and in cells treated with 0.1 mM H_2O_2, YAP1C-GS migrates at 35 kDa. H_2O_2 treatments ranging between 1 and 20 mM resulted in a proportional increase in the number of high-molecular weight YAP1C-GS complexes (Fig. 3A). The disulfide nature of the interactions has been proven by the disappearance of most of the high molecular weight bands on a reducing Western blot (Fig. 3A). In cells producing YAP1A-GS, only the 35-kDa monomer is detected, even after a 20-mM H_2O_2 treatment, strengthening that Cys598 is essential for the YAP1-disulfide formation in plant cells under stress. It is noteworthy that exogenous H_2O_2 is rapidly metabolized by *Arabidopsis* cell cultures with 20 mM being dissipated to the limits of detection within 5 min (Desikan et al., 1998). Therefore, it is likely that the high amount of interactions present after 1 h of treatment results from active generation of ROS by *Arabidopsis* cells after the initial H_2O_2 trigger. Previous data, indicate that the H_2O_2 from oxidative burst is required for initiation of cell death program as addition of catalase to the growth media as late as 1 h after initial treatment inhibits cell death (Desikan et al., 1998). Next, we checked the transient dynamic character of the intermolecular disulfide bond formation by YAP1C in a time course experiment. Cell cultures were pulse-treated with 1 mM H_2O_2 and harvested 5, 10, 30, 60, and 120 min after treatment. The YAP1C complexes were most abundant after 10 min. (Fig. 3B), but were almost undetectable after 2 h, possibly due to the decreased number of mixed disulfide bonds by either the activation of the reducing systems in the cell or a rapid proteolytic degradation. Taken together, these results indicate that a YAP1-based sulfenic acid trapping methodology is a solid tool to study time- and dose-dependent H_2O_2 stress responses in plant cells.
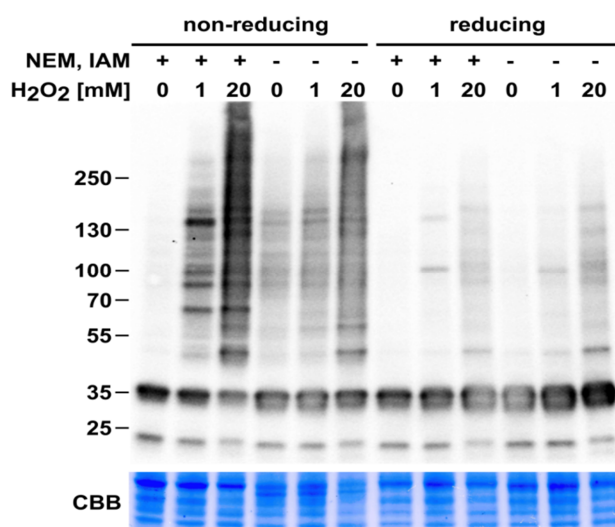
Fig. 2. Influence of IAM and NEM on post-extraction protein oxidation. Cell cultures overproducing the GS-YAP1C probe were treated with 0, 1, and 20 mM H_2O_2 for 1 h. Proteins were extracted in extraction buffer with or without IAM and NEM and visualized on immunoblot with the PAP antibody conjugate. The enhanced signal intensity under control conditions without IAM and NEM indicates the formation of YAP1C heterocomplexes upon protein extraction.

Unique sulfenylated proteins are selectively trapped with YAP1C-GS

To evaluate the early signaling events in the presence of 1 mM H_2O_2, we decided to focus on cysteine oxidation 10 min after stress. Protein extracts of cells containing YAP1C-GS and YAP1A-GS were purified by TAP (Fig. 4). Briefly, first, YAP1-GS complexes were captured on IgG-sepharose. Second, with a TEV protease cleavage step, the YAP1 fused to the SBP tag together with several mixed disulfide complexes and all possible interacting proteins was eluted. In a following SBP purification step, the mixed disulfide YAP1 complexes were enriched. The sulfenylated proteins were released by selective elution of the disulfide-bonded proteins with 5 mM dithiothreitol (DTT) followed by a 20 mM desthiobiotin elution. The majority of interactors (41/46) elute with DTT (Table S2).
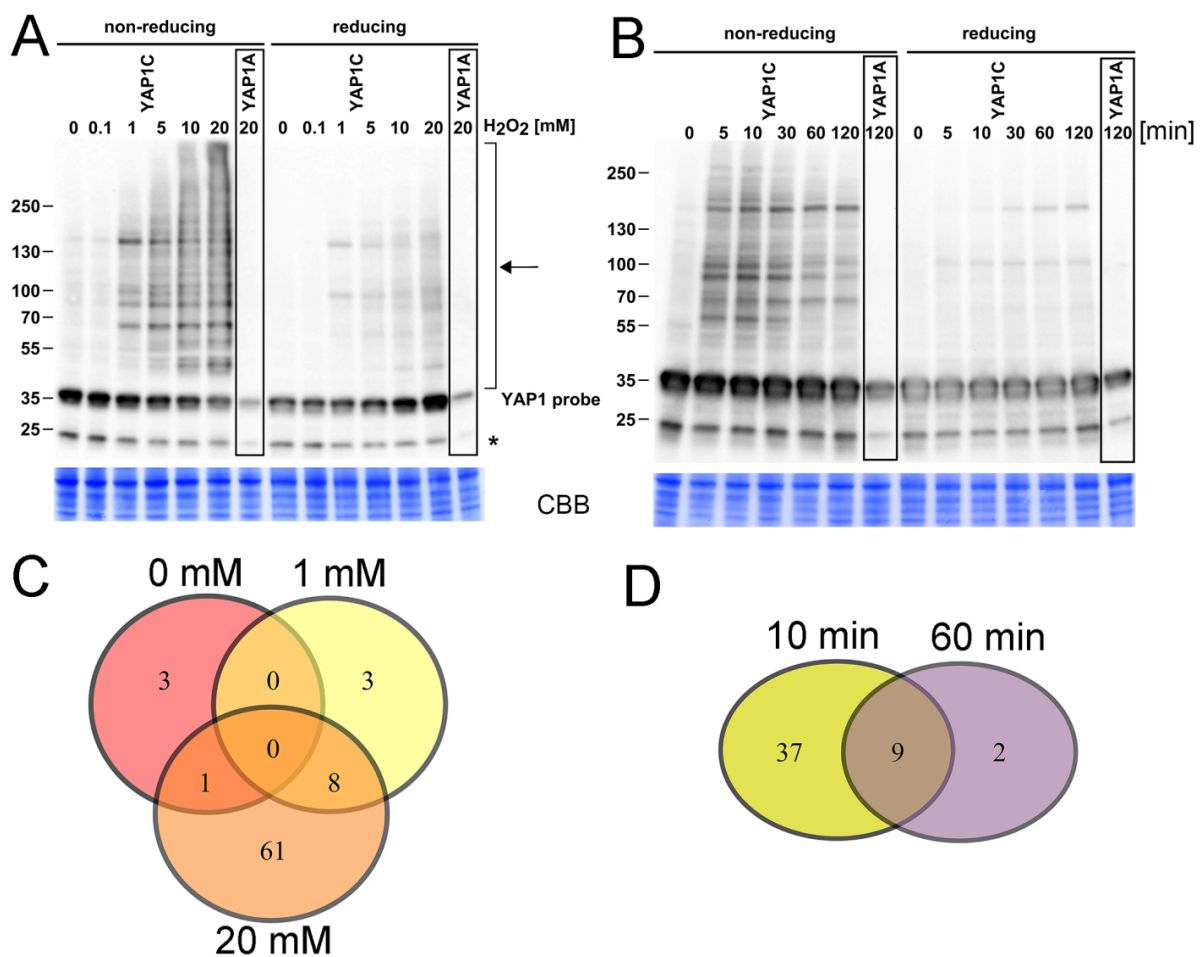

Fig. 3. Dose- and time-dependent formation of YAP1C-involving complexes. (*A*) Cell cultures overproducing the GS-YAP1C/A probe treated with 0, 0.1, 1, 5, 10, and 20 mM H_2O_2 for 1 h. Complexes (marked with an arrow) are visualized with the PAP antibody complex. The H_2O_2 concentration and the amount of signal clearly correlate. Treatment of protein samples with 50 mM Tris(2-carboxyethyl)phosphine (TCEP) led to reduction of the complexes. (*B*) Cell cultures treated with 1 mM H_2O_2. The time course was taken after 0, 5, 10, 30, 60, and 120 min. The initial signal intensity peak returns to a near basal level after 120 min of treatment. The asterisk denotes an unknown protein recognized by the antiserum. (*C* and *D*) Schematic comparison of datasets identified after treatment of cultures with 0, 1, and 20 mM H_2O_2 for 1 h (*C*) and 1 mM H_2O_2 for 10 min (early response) and 1 h (late response) (*D*).

To guarantee a complete interactor recovery, we decided to use desthiobiotin for all the TAP purifications. In a following experiment, we focused on the late-response sulfenome observed 1 h after an oxidative stress pulse with 0, 1 (sublethal dose), and 20 mM (lethal dose) H_2O_2. In agreement with the increased mixed-disulfide complex formation that positively correlates with the H_2O_2 dose (Fig. 3A), we identified 4, 11, and 70 YAP1C-specific interactors (Fig. 3C; Table S2 & S3). The majority (8/11) of the interactors detected after treatment with 1 mM H_2O_2 were also present in the set of 70 proteins identified with 20 mM H_2O_2 (Fig. 3C). Nine out of the 11 interactors derived from cells treated with 1 mM H_2O_2 for 1 h were also present in the early time point of 10 min (Fig. 3D), emphasizing their sensitivity toward oxidation and suggesting an important function in oxidative stress sensing.
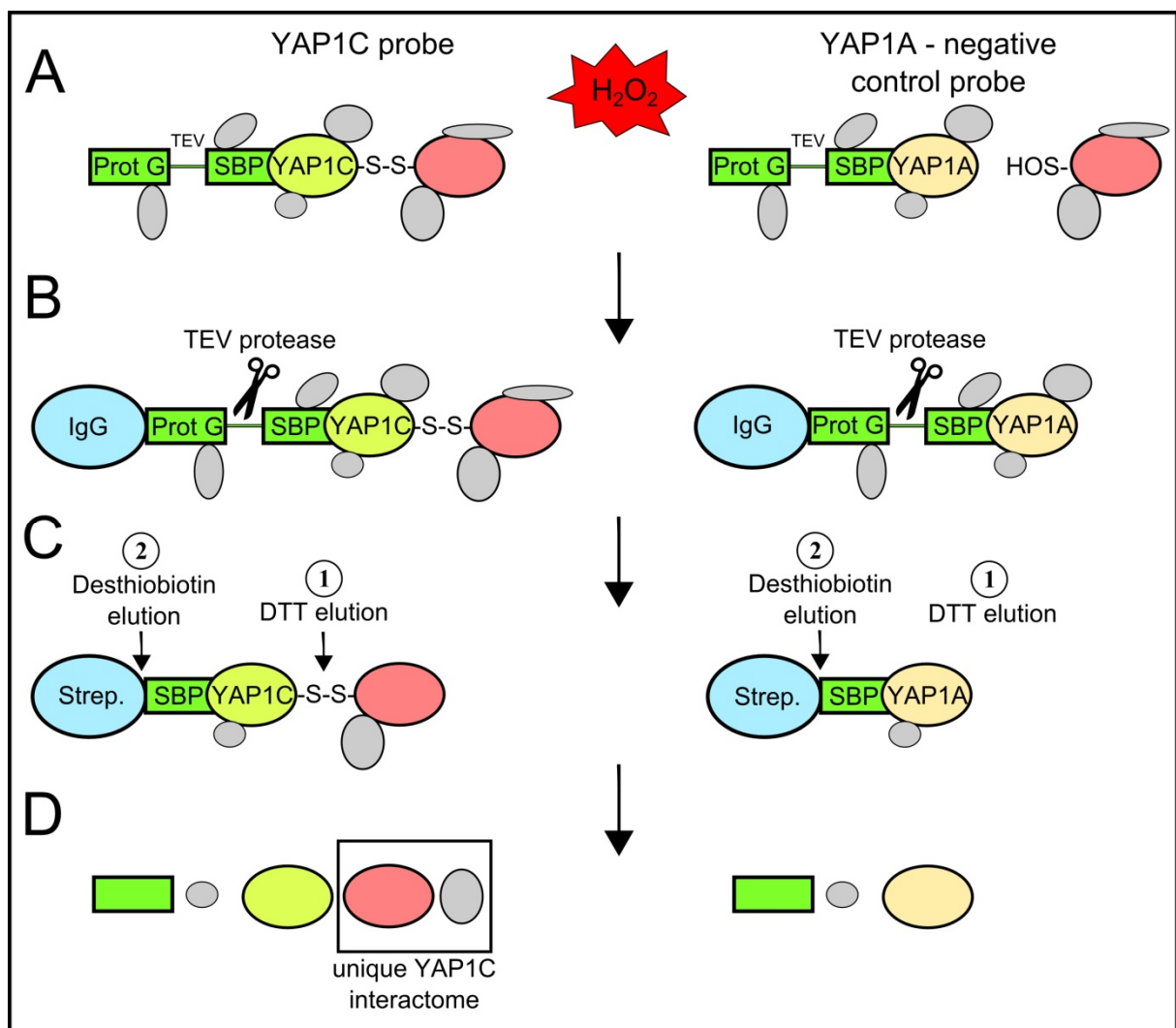
Fig. 4. Experimental setup for *in vivo* identification of the *Arabidopsis* sulfenome. (*A*) Cell cultures overproducing the YAP1C/A probes treated with H_2O_2 as described (see text). (*B* and *C*) Proteins isolated and subjected to a two-step purification procedure based on IgG-protein G and streptavidin–streptavidin binding peptide (SBP) affinity. Numbers indicate the sequence of elution steps. (*D*) LC-MS/MS analysis of proteins after elution. Comparison of interactors between the negative control probes of YAP1C and YAP1A potentially undergoing cysteine sulfenic acid (-SOH) formation under oxidative stress.

Functional categorization of the *Arabidopsis* H$_2$O$_2$-dependent sulfenome

In the *Arabidopsis* sulfenome, we detected 67 proteins that, until now, had not been classified as H$_2$O$_2$-sensitive. In addition, we found 30 proteins that had previously been reported to have oxidative modifications, such as disulfides, S-glutathiolynation, S-nitrosylation, and sulfenic acids, and some to be Trx/Grx substrates (see Table S3 for references). Within the identified set of proteins, great majority (68/97) localizes to cytoplasm (http://suba3.plantenergy.uwa.edu.au/). This is in agreement with the presumed cytoplasmic localization of YAP1C-GS probe that was not equipped with any signal peptide. For the schematic representation of subcellular localization see Fig. S2. In the identified sulfenome, proteins could be functionally categorized: 13 into signal perception and transduction, 19 into protein degradation, 7 into redox related enzymes, 7 into RNA-binding and translation, 6 into primary metabolism, 4 into hormone homeostasis, 5 into protein transport, 5 into amino acid metabolism and 31 into miscellaneous and unknown functions. For the complete list of YAP1C interactors, see Table S3. When concentrating on the 46 proteins sulfenylated within the first 10 min after the oxidative stress trigger (Table S3), we found several signal perception and transduction proteins. In addition, almost one fourth of them is involved in proteasomal activities and several redox-related enzymes were identified, of which some present at an early (10 min) as well as a late (1 h) oxidative stress response, whereas additional members of these functional classes are present within the late response (Table S3).

Signal perception and transduction. Three different mitogen-activated protein kinases (MAPKs) have been found to be sulfenylated: MAPK2, MAPK4, and MAPK7. The MAPK signaling cascades are integrate parts of plant biotic and abiotic stress signaling pathways and are activated by H$_2$O$_2$ (Kovtun et al., 2000; Zhou et al., 2014). In yeast and human model systems, MAPKs are redox regulated through upstream regulators and through direct cysteine oxidation events (Truong and Carroll, 2013). A cysteine oxidation event in the human p38 MAPK had been shown to act as a functional regulatory switch (Templeton et al., 2010), whereas, in plant MAPK modules, such thiol modification has not been reported yet. The fast sulfenylation after an oxidative stress stimulus suggests that MAPK2, MAPK4, and MAPK7 could function as redox sensors downstream of a ROS-producing event. The MAPK activity is also controlled through dephosphorylation by redox-sensitive phosphatases (Truong and Carroll, 2013). Sulfenylation of the catalytic nucleophilic cysteine leads to the inhibition of protein tyrosine phosphatases (PTPs) (Tanner et al., 2011). The identified *Arabidopsis* AtPTP1 undergoes cysteine-dependent inhibition by H$_2$O$_2$ and negatively regulates the MAPKs (Gupta and Luan, 2003), suggesting that the oxidation-dependent AtPTP1 inhibition might be a primary step in the oxidative stress response leading to MAPK signaling de-repression (Bartels et al., 2009). Furthermore, at least two members of the plant-specific SNF1-RELATED PROTEIN KINASE 2 (SnRK2) protein kinase family are rapidly sulfenylated. The plant stress response SnRK2 pathways are regulated by direct phosphorylation of various

downstream targets, including the RESPIRATORY BURST OXIDASE HOMOLOG F (AtRbohF) and transcription factors, and are required for the expression of numerous stress response genes (Kulik et al., 2011). Only recently, a redox-regulated rapeseed (*Brassica napus*) SnRK2 had been shown to be involved in guard cell signaling (Zhu et al., 2014).

PROTEIN PHOSPHATASE 2A (PP2A) is a holoenzyme consisting of a catalytic subunit C, a structural subunit A, and a highly variable regulatory subunit B that determines its target specificity. We identified two B subunits PP2A-b55α and PP2A-b'γ as potential redox sensitive proteins. Both subunits were found to have opposite effect on regulation of flowering time (Heidari et al., 2013). Moreover, PP2A-b'γ was suggested to control premature senescence and basal repression of defense responses in *Arabidopsis* (Trotta et al., 2011). PP2A-b'γ knockout plants were reported to exhibit disintegration of chloroplasts, constitutive expression of disease resistance genes and accumulation of ROS. In agreement with previous results a recent study by Li et al., (2014) consolidated the function of PP2A-b'γ in SA-dependent defense responses. It would be of interest to investigate the influence of the cellular redox balance on substrate specificity of these B subunits.

Protein degradation. Approximately 20% of the YAP1C-GS interactors are involved in proteolysis, with a clear enrichment for proteins participating in proteasome-mediated degradation, among which five control ubiquitination, such as the UBIQUITIN-CONJUGATING ENZYME27 (UBC27), two subunits of the SKP/CULLIN/F-BOX (SCF) E3-ubiquitin ligase complex (ASK1 and ASK2), and the 3 and 5A subunits of the CONSTITUTE PHOTOMORPHOGENIC9 (COP9) signalosome (Table S3). In the 26S proteasome, we identified the REGULATORY PARTICLE NON-ATPASE 12A (RPN12A) as a potentially H_2O_2-modified protein. Interestingly, RPN12A has been established as a cytoplasmic thioredoxin h (Trxh) target protein (Yamazaki et al., 2004), acting as a potential crosstalk point between ROS and cytokinin signaling (Ryu et al., 2009). The removal of oxidatively damaged proteins is an important event in the stress responses (Jung and Grune, 2013), but oxidative modifications of the proteasome and the ubiquitin-proteasome system itself trigger changes in activities in such a manner that it manages both the removal of oxidized proteins and the adaptation of the cellular metabolism to the stress situation (Höhn and Grune, 2014). In maize (*Zea mays*), sugar starvation-triggered oxidative stress leads to oxidative modifications of the 20S proteasome, modulating its proteolytic activity (Basset et al., 2002). In addition, our dataset includes a number of de-ubiquitinating enzymes (DUBs), such as UBIQUITIN C-TERMINAL HYDROLASE 3 (UCH3) and the ubiquitin-specific proteases, UBP12, UBP13, and UBP24. Redox regulation of multiple ovarian tumor DUBs had been reported to occur via reversible sulfenylation of a catalytic cysteine residue (Kulathu et al., 2013), but until now, this inhibition mode has not been described for plant DUBs.

RNA binding proteins, translational machinery, post-transcriptional regulation events. Synthesis of certain proteins is activated in redox dependent manner in response to light exposure without an increase in the corresponding mRNA levels and therefore relays on post-transcriptional regulation. Such mechanisms of redox-dependent translational activation were studied mostly in the context of *psbA* mRNA translation in algae (Kim and Mayfield, 1997; Alergand et al., 2006) and higher plants (Shen et al., 2001). In *Chlamydomonas*, this two-component system involves the POLY(A) BINDING PROTEIN RB47 and PROTEIN DISULFIDE ISOMERASE RB60. RB60 regulates the binding of RB47 to the 5'-UTR of *psbA* mRNA through redox equivalents thereby providing a mechanism for its redox-dependent translation (Kim and Mayfield, 1997; Alergand et al., 2006). In this study, we identified seven proteins involved in control of protein translation mechanisms including RNA BINDING PROTEIN 45C, POLY(A) BINDING PROTEIN 8 (PAB8) and PROTEIN ARGININE METHYLTRANSFERASE 5 (PRMT5) that was shown to link the circadian clock to the control of alternative splicing in plants (Sanchez et al., 2010). Ample evidence supports the role of RNA binding proteins in control of plant development and stress responses (Lorković, 2009) however further studies are necessary to investigate the potential redox dependent RNA-binding properties of proteins identified here.

Primary metabolism and energy homeostasis. Next to well established redox regulated proteins including CYTOSOLIC-NAD-DEPENDENT MALATE DEHYDROGENASE 1 (Hara et al., 2006), VACUOLAR ATP SYNTHASE SUBUNIT A (Seidel et al., 2012) and cytosolic FRUCTOSE-BISPHOSPHATE ALDOLASE 4 (van der Linde et al., 2011); we identified a number of new potential redox regulated enzymes involved in primary metabolism and energy homeostasis. The properties of maize chloroplastic NADP-MALIC ENZYME (ZmC$_4$-NADP-ME) involved in C$_4$ photosynthesis have been explored recently (Alvarez et al., 2012). In this enzyme, the oxidation of cysteine residues induces conformational change that limits the catalytic process. Yet, the information about similar regulation of cytosolic enzymes such as NADP-ME2 identified in this study is lacking. In agreement with our results NADP-ME2 was reported earlier to undergo stress induced S-glutathionylation (Dixon et al., 2005) and identified as a Trx y2 target protein (Marchand et al., 2010). However, a recent study (Li et al., 2013) indicates that this enzyme is not essential for oxidative stress response. ATP-CITRATE LYASE (ACL) is a cytosolic enzyme catalyzing ATP-dependent conversion of citrate and CoA to acetyl-CoA and oxaloacetate. This heteromeric enzyme composed of two distinct subunits, ACLA and B is of crucial importance for plant metabolism as acetyl-CoA serves as an initial metabolite for a plethora of natural products (Fatland et al., 2002; Fatland et al., 2005). ACL is of particular interest in modern medicine as recent studies highlight its role in metabolism of cancer cells (Zaidi et al., 2012; Hanai et al., 2013). So far, the redox-dependent modulation of ACL activity was demonstrated for rat liver enzyme (Wells and

Saxty, 1992), however a similar observation for plant isoforms is still missing. Our results demonstrate a possibility for direct regulation of *Arabidopsis* ACL activity via redox modification of B subunit(s).

Hormone homeostasis. ROS-hormonal interplay was shown to affect abscisic acid (Suzuki et al., 2013; Song et al., 2014) and auxin (Tognetti et al., 2010; Tognetti et al., 2012) signaling pathways. Here, we identified four proteins tightly associated with hormonal homeostasis including ABA DEFICIENT 2 (ABA2) and NITRILASE 1 & 2 (NIT1, NIT2) involved in synthesis of abscisic acid (ABA; Léon-Kloosterziel et al., 1996) and 3-indoleacetic acid (IAA; Bartel and Fink, 1994) respectively. Hydrogen peroxide was shown before to be involved in the ABA signaling pathway via direct post-translational modifications of ABA INSENSITIVE 1 (ABI1) and ABI2. Oxidizing conditions promote inactivation of both phosphatases that act as negative regulators of ABA signaling (Meinhard and Grill, 2001; Meinhard et al., 2002) thereby providing a positive feedback loop. NIT1 and NIT2 identified in this study were reported earlier as potential targets for Cys PTM (Dixon et al., 2005; Wang et al., 2012). Together, our results provide a new perspective towards further investigation of ROS hormonal crosstalk with a main scope on ABA- and auxin-regulated pathways.

Redox proteins. At least four redox-related proteins have been detected: MONOTHIOL GLUTAREDOXIN17 (GRXS17), THIOREDOXIN-DEPENDENT PEROXIDASE1 (TPX1), GLUTAREDOXIN C2 (GRXC2), and a DEHYDROASCORBATE REDUCTASE 2 (DHAR2). TPX1 had been identified as a target of cytosolic Trxh3 (Marchand et al., 2006) and also in a subset of early-responsive redox-sensitive proteins (Wang et al., 2012). GRXC2 and GRXS17 function in early plant development during embryonic (Riondet et al., 2012) and temperature-dependent postembryonic (Cheng et al., 2011) growth, respectively, but their specific substrate proteins are unknown. DHAR2 was sulfenylated in both the early and late oxidative stress responses (Table S3). Dehydroascorbate reductase plays an important role in counterbalancing oxidative stress by catalyzing the regeneration of ascorbate, a major antioxidant in plants. In *Arabidopsis*, three isoforms are present: the mitochondrial DHAR1, the cytosolic DHAR2, and a chloroplastic DHAR3. In planta it had been shown that perturbation of DHAR limits ascorbate recycling, as a consequence, influences the rate of plant growth and leaf aging due to ROS-mediated damage (Chen and Gallie, 2006).

DHAR2 kinetics are affected by H_2O_2 treatment

Next, we aimed to confirm our findings by in vitro validation of sulfenic acid formation on proteins present within the identified set of YAP1C-GS interactors. Among candidates selected for the validation experiments we obtained the highest yield of soluble protein for DHAR2. DHAR2 catalyzes the reduction of oxidized ascorbate with a concomitant oxidation of GSH to GSSG; therefore, it is one of the core enzymes of the GSH/ascorbate cycle that maintains ascorbate pools reduced (Foyer and Halliwell, 1977). We recombinantly produced and purified His-tagged DHAR2. Recombinant DHAR2 eluted as a monomer from the Ni^{2+}-immobilized metal-affinity column and

migrated as a single band at 30 kDa on a sodium dodecyl sulfate-polyacrylamide gel electrophoresis (SDS-PAGE) gel. Its molecular weight was confirmed by mass spectrometry (MS) with a total mass of 26,748 Da after loss of the N-terminal methionine (Fig. S1). We analyzed the activity of recombinant DHAR2 by following the ascorbate formation in progress curves in function of time at 265 nm. The initial velocities were measured at varying dehydroascorbate (DHA) concentrations in a 5-mM excess of GSH. Plots of the initial velocities versus the DHA concentrations revealed a sigmoidal curve with a Hill factor of 2.65, indicative for positive cooperativity and hinting at the positive influence of the GSH binding at increasing DHA concentrations. We determined for DHAR2 a $k_{cat}/K_{0.5}$ value of $9.3{\times}10^5$ $M^{-1}s^{-1}$ with $K_{0.5}$ of 23.8 ± 1.2 µM, whereas for DHAR1 and DHAR3, K_M values of 260 µM and 500 µM had been reported (Dixon et al., 2002). To understand the possible role of the cysteine thiols of DHAR2 in its catalytic cycle, we modified the free thiols with 1 mM IAM and oxidized DHAR2 with increasing concentrations of H_2O_2 (Fig. 5A). In both cases, the activity is affected, indicating that reduced cysteines are essential for catalytic DHAR2 activity, as observed previously for DHAR1 (Dixon et al., 2002).

DHAR2 is sulfenylated and S-glutathionylated on its nucleophilic cysteine

DHAR2 contains two cysteines (Cys6 and Cys20). To prove the sulfenylation of DHAR2 by H_2O_2, we used 5,5-dimethyl-1,3-cyclohexadione (dimedone), a chemical compound that forms a thioether bond with the electrophilic sulfur atom of sulfenylated proteins (Benitez and Allison, 1974). Previously, dimedone and its derivatives have successfully been applied to study sulfenylation in many important physiological pathways in various organisms and in recombinant proteins (Paulsen and Carroll, 2009; Paulsen et al., 2011).We analyzed the H_2O_2-induced DHAR2 sulfenylation in the presence and absence of GSH on Western blots with antibodies that specifically recognize dimedone-tagged sulfenic acids (Fig. 5B). After a 30-min treatment with 100 µM H_2O_2 in the presence of dimedone, DHAR2 was sulfenylated. Remarkably, sulfenylation was lower in H_2O_2-treated samples than in nontreated samples, possibly due to overoxidation to sulfinic or sulfonic acids, or to the formation of a disulfide bond (Roos and Messens, 2011). Dimedone signal present in untreated protein sample indicates that DHAR2 undergoes oxidation with atmospheric oxygen. In the presence of 1 mM GSH, the sulfenylation signal did not depend on the H_2O_2 treatment, suggesting that the majority of the formed sulfenic acid is unavailable for dimedone because a mixed disulfide is formed with GSH. To confirm this observation, we analyzed H_2O_2-treated DHAR2 in the presence of dimedone or GSH by liquid chromatography-tandem MS (Table 1). After treatment with 100 µM H_2O_2 in the presence of dimedone, we blocked all free thiols. A tryptic digest revealed a dimedone adduct on the Cys20 peptide, resulting in a 138-Da mass increase of this peptide when compared to the parent peptide (Fig. 5C), confirming that Cys20 is sulfenylated. Cys20 is also partially overoxidized to sulfonic acid (48 Da larger than the parent peptides).
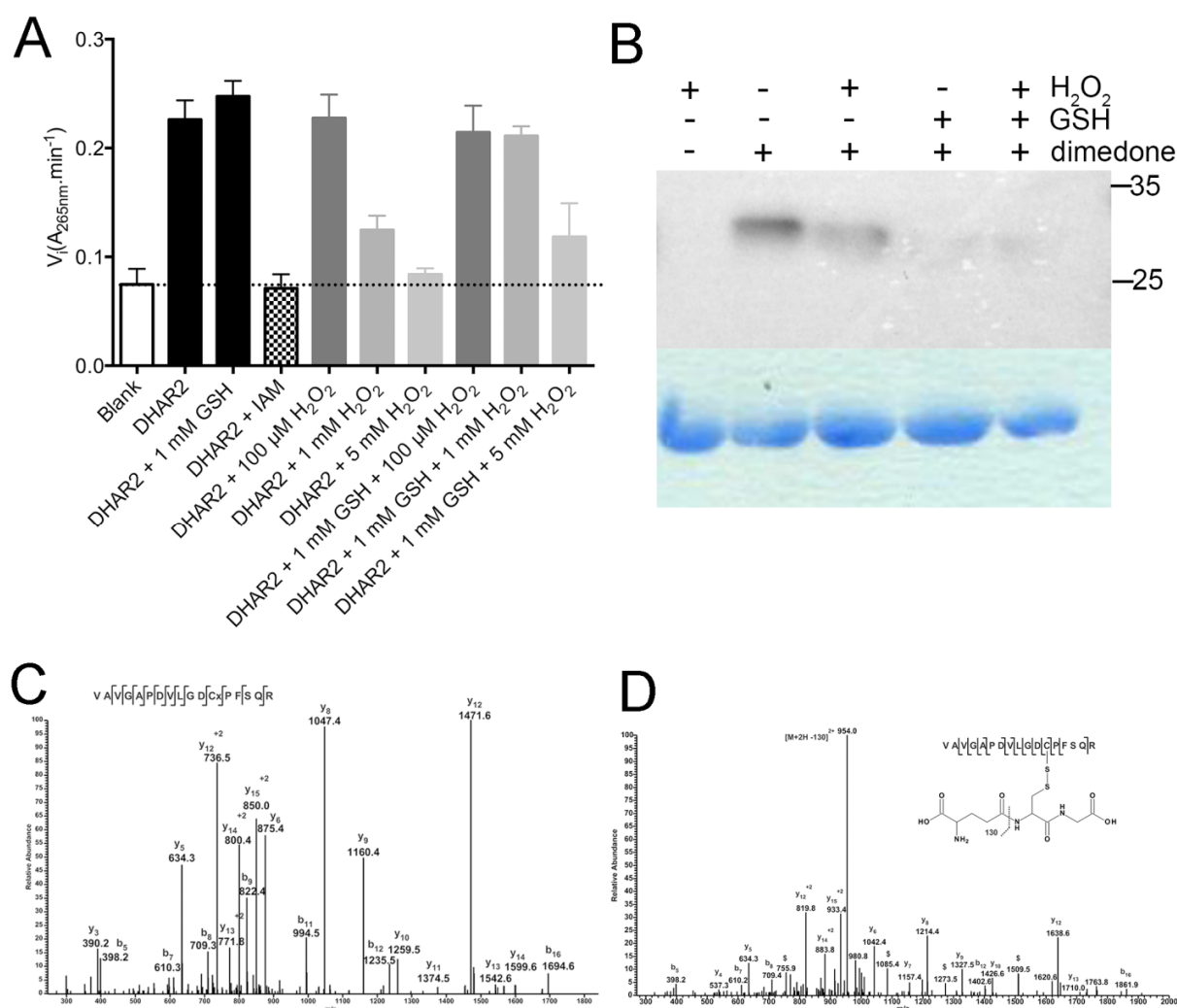
Fig. 5. Requirement of DHAR2 cysteines and GSH protection against overoxidation. (*A*) The average initial velocities (n=3) of DHAR2 under different conditions were determined on progress curves. DTT-reduced DHAR2 was treated with 100 µM, 1 mM and 5 mM H_2O_2 in the presence or absence of 1 mM GSH incubated for 30 min at room temperature. IAM-blocked DHAR2 was prepared by 10 mM IAM treated 30 min in the dark at room temperature. Excess of H_2O_2, IAM, and GSH was removed on a Micro Bio-Spin[TM] P-6 gel column (Bio-Rad) equilibrated with 50 mM potassium phosphate (pH 7.0) assay buffer. The reaction was started under Vmax conditions by adding 100 µM DHA to a final concentration of 30 nM DHAR2 in the presence of 5 mM GSH. (*B*) Dimedone labeling of DHAR2-SOH *in vitro*. DHAR2 (20 µM) nontreated or treated with 1 mM GSH was either not or incubated with 100 µM H_2O_2 in the presence or absence of dimedone (1 mM). DHAR2-SOH formation was analyzed by immunoblot with an anti-cysteine sulfenic acid antibody. (*C*) Identification of the dimedone modification Cys20 of DHAR2. The LC-MS/MS spectrum shows data obtained from a +2 parent ion with *m/z* 935.5. The cysteine residue corresponds to a dimedone-modified sulfenic acid, which produces a +138-Da mass increment. The *y*- and *b*-series of ions allow the modified cysteine to be localized exactly. (*D*) Identification of S-glutathionylation on Cys20 of DHAR2. The LC-MS/MS spectrum shows data obtained from a +2 parent ion with *m/z* 1019.0. The spectrum displays a major fragment ion at *m/z* 954.0, corresponding to the neutral loss of glutamic acid (130 Da) after fragmentation at a peptide bond within GSH. The mixed disulfide between GSH and the cysteine residue is located precisely by means of the *y*- and *b*-series of ions. Ions that were generated from loss of glutamic acid are marked ($).

Samples	Reduced (CIAM)	Sulfenic Dimedone	Sulfinic	Sulfonic	GSH	S-S
DHAR2 + H_2O_2	C6 (7*) C20 (18)	nd	nd	nd	nd	$^{\$}C_6\text{-}C_{20}$
DHAR2 + dimedone + H_2O_2	C6 (24) C20 (22)	C20 (1)	nd	C20 (2)	nd	$C_6\text{-}C_6$ $C_6\text{-}C_{20}$
DHAR2 + GSH + H_2O_2	C6 (6) C20 (18)	nd	nd	nd	C20 (13)	nd

Table 1. Detection of redox PTMs of DHAR2 by mass spectrometry. Recombinant DHAR2 was treated with H_2O_2 in presence of dimedone or GSH. Free thiols were blocked with excess of CIAM. The peptides were analyzed by LC-MS/MS. Two tryptic peptides were detectable: AGFEVLFQGPMALDIC₆VK and VAVGAPDVLGDC₂₀PFSQR. (*) numbers in brackets indicate the number of peptide spectral matches; ($) indicates the disulfide with the highest score in Dbond; nd, not detectable.

In contrast, in the absence of dimedone, but in the presence of GSH, MS data clearly show S-glutathionylation at Cys20 (Fig. 5D). To test the 1-mM GSH protection on the DHAR2 activity, we added increasing concentrations of H_2O_2 to DHAR2 in the presence of 1 mM GSH and determined the initial velocities (*Vi*) of the progress curves (Fig. 5A). The *Vi* of GSH-pretreated DHAR2 sample is even higher than that of the nontreated sample, which is, at least, partially sulfenylated after purification (Fig. 5B). Furthermore, is it clear that GSH (1 mM) rescues the 1-mM H_2O_2 sulfenylation of DHAR2. At 5 mM H_2O_2, however, the DHAR2 activity was only partially rescued by GSH (Fig. 5A), possibly because the overoxidation rate to sulfinic or sulfonic acids seems too fast for 1 mM GSH to react with the sulfenic acid and to recover all activity (Fig. 5A). Thus, in the absence of substrate, S-glutathionylation occurs after sulfenylation of Cys20 as a reversible protection mechanism, recovering DHAR2 activity, which results in increased initial velocities. All together, the nucleophilic Cys20 in DHAR2 is vulnerable to oxidation and becomes sulfenylated under H_2O_2 stress. The formation of a Cys20-Cys6 disulfide bond or the Cys20 S-glutathionylation might protect DHAR2 against irreversible overoxidation.

Generation of transgenic *A. thaliana* plants overexpressing YAP1-GS probes

Plants exhibit unique capabilities of adaptation to adverse environmental conditions. Generally, the cellular response to oxidative stress differs among tissues or organs and might be influenced by factors such as plant growth stage, nutritional status or internal developmental programs all coordinated at the whole organism level. Moreover, it is now well established that phenotypes observed in tightly controlled laboratory conditions cannot be related to those observed in the field (Wituszyńska et al., 2013a; Wituszyńska et al., 2013b). In order to get a more holistic view into oxidative stress signal perception at the whole organism level we set out to apply the YAP1TAP technology to field conditions.

As an initial step towards proof-of-concept experiments we generated transgenic *A. thaliana* lines overexpressing YAP1-GS probes used throughout this study. Formation of YAP1C-GS-involving complexes is in direct competition with reaction catalyzed by antioxidant system, therefore next to Col-0 wild type also CATALASE 2 deficient line *cat2-2* (Queval et al., 2007; see Chapter 3) was transformed with vectors used before to obtain transgenic cell cultures (see Materials & methods). For each construct and within each parent line at least three independent transformation events were selected on basis of recombinant protein yield. In a view of future optimization experiments the selection included lines with high, medium and low yield of recombinant protein. An exemplary immunoblot summarizing portfolio of *cat2-2* background lines expressing YAP1-GS probes is shown on Fig. 6. Among the most important advantages supporting the use of plants instead of cell cultures is the possibility for application of physiological stress treatments and exploration of tissue specificity with the use of tissue specific promoters driving the expression of YAP1C-GS probe. Transgenic lines generated in this study pave the way towards exploration of organ- and stimuli-specific sulfenomes in field conditions.
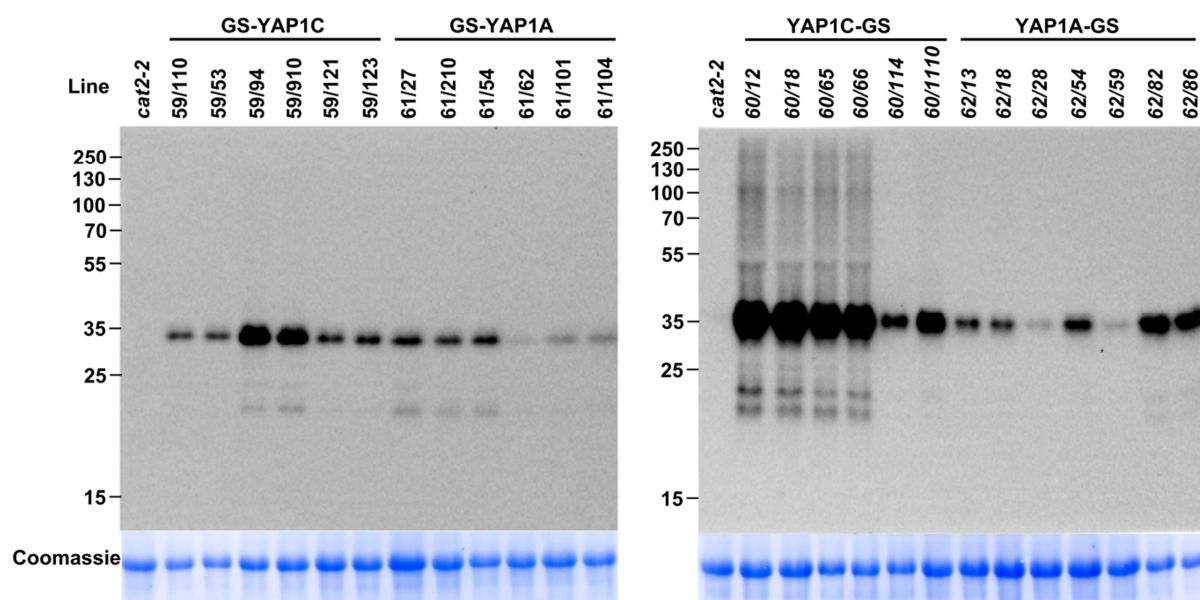

Fig. 6. Compendium of transgenic *cat2-2* mutant lines overexpressing YAP1-GS probes. Proteins were isolated and visualized as described in 'Materials and methods'. Prior to SDS-PAGE samples were reduced with 50 mM TCEP.

CONCLUSIONS AND PERSPECTIVES

This work describes the first successful application of YAP1-based sulfenome mining strategy in plants. By a unique combination of Cys-SOH trapping with tandem affinity purification we identified a set of 97 proteins potentially involved in redox-regulated cellular processes. Next to the well established players in oxidative stress response a number of regulatory proteins with previously unreported mode of oxidative regulation were identified. Exploration of these findings will

lead to a better understanding of signaling events that govern adaptation of plants to environmental stimuli. As a first step towards transfer of YAP1TAP technology to field conditions, we generated a set of transgenic *A. thaliana* lines overexpressing YAP1 probes. Further research implementing various target peptides and tissue specific promoters will focus on identification of subcellular, tissue- and organ-specific sulfenomes. Furthermore, studies at the whole plant level open a possibility for application of broad range of stress treatments related to needs dictated by modern agriculture.

MATERIALS AND METHODS

Arabidopsis suspension cultures

The *Saccharomyces cerevisiae* YAP1-coding region fragment corresponding to Asn^{565} to Asn^{650} was codon optimized for expression in *Arabidopsis thaliana*, synthesized, and cloned by Integrated DNA Technologies into the pIDTSmart vector with introduction of mutations to create YAP1C and YAP1A probes: YAP1C – C^{620}A, C^{629}T; YAP1A – C^{598}A, C^{620}A, C^{629}T according to strategy described (Takanishi et al., 2007). The sequences of these synthetic fragments can be found in Table S1. Both synthetic DNA sequences were amplified with specific primers (Table S4) to introduce the attB sites and START or STOP codon for expression of C- and N-terminal GS tag fusions, respectively. The PCR reactions were carried out in two steps; in a second step, the initial amplicons were amplified with attB1 and attB2 primers (Table S4) to complete the attB sites. Both PCR reactions were run with Pfu proofreading polymerase (Promega). Subsequently, sequences were inserted into pDONR221 vector by means of the Gateway TM technology (Life Technologies) according to the manufacturer's instructions. Vectors were sequenced with M13 primers (Table S4) to verify the accuracy of the gene synthesis and PCR amplifications. Expression clones were generated as previously described (Van Leene et al., 2007). The *Arabidopsis* cell suspension cultures (NASC stock no. CCL84840) were transformed and maintained as described (Van Leene et al., 2007).

Stress treatments

Mid-log phase cell cultures (dark grown, 3 day old, approximately 10 mg fresh weight ml^{-1}) expressing the YAP1C/YAP1A N-terminal GS-tag fusions were treated with 0.1, 1, 5, 10, and 20 mM H$_2$O$_2$. Cells were harvested after 1 h. For the time-dependent experiments, 1 mM H$_2$O$_2$ was added to mid-log phase cell cultures and cells were sampled after 5, 10, 30, 60, and 120 min.

Protein extractions and Western blot analysis.

Plant material was ground on ice in the presence of sand and TAP extraction buffer (Van Leene et al., 2007) without DTT and supplemented with 10 mM NEM and 10 mM IAM (unless otherwise specified) to prevent de novo oxidation of cysteine residues. For the Western blot analysis, soluble proteins were separated on SDS-PAGE gradient gel (Bio-Rad), blotted, and hybridized with a 1:5000

dilution of PAP-soluble complex (Sigma-Aldrich) to detect the GS tag. Sulfenic acid residues were visualized with a 1:10000 dilution of polyclonal rabbit anti-cysteine sulfenic acid antibody (Millipore).

Tandem affinity purification

Tandem affinity purification of protein complexes was performed using the GS tag strategy (Van Leene et al., 2008) according to GS protocol described previously (Van Leene et al., 2011) adapted herein for use with redox active bait proteins. In short, 10g of cells were ground at 4 °C in a presence of extraction buffer supplemented with 10mM NEM and 10mM IAM to prevent de novo oxidation of cysteine residues. Protein extracts were cleared by two subsequent centrifugation steps at 36,900 x g for 20 min. In the first purification step, a protein input of 25 mg was incubated with 25 µl of IgG-Sepharose 6 Fast Flow beads (GE Healthcare), the complexes were released from the column by cleavage with AcTEV^{TM} Protease (Invitrogen). In a second affinity step 25 µl of Streptavidin Sepharose High Performance (Amersham) was used. For specified experiments the final elution step was preceded by incubation of beads with elution buffer containing 5 mM DTT for 30 min at room temperature. Finally, proteins were eluted by incubation of beads for 5 minutes with 40 µl 1 x NuPAGE sample buffer containing 20 mM Desthiobiotin. Beads were separated from eluate in a 1-ml Mobicol column (MoBiTec, Göttingen, Germany).

LC-MS/MS analysis

Eluted proteins were separated in a short run of 7 min on a 4-12% gradient NuPAGE gel (Invitrogen) and visualized with colloidal Coomassie Brilliant Blue staining. The protein gel was washed for 2 h in water, polypeptide disulfide bridges were reduced for 40 min with 6,66 mM DTT in 50 mM NH_4HCO_3 and sequentially the thiol groups were alkylated for 30 min with 55 mM IAM in 50 mM NH_4HCO_3. After washing with water, broad zones containing the proteins were excised from the protein gel and sliced. Gel plugs were washed with water, this was followed by two steps of dehydration with 95% acetonitrile (v/v) separated by rehydration with water. Dehydrated gel particles were rehydrated in 60 µL digest buffer containing 750 ng trypsin (MS Gold; Promega, Madison, WI), 50 mM NH_4HCO_3 and 10% acetonitrile (v/v) for 30 min at 4° C. Proteins were digested at 37° C for 3.5 hours. Peptide mixtures were introduced into LC-MS/MS system consisting of the UltiMate 3000 RSLCnano (Dionex, Amsterdam, The Netherlands) coupled to LTQ Orbitrap Velos (Thermo Fisher Scientific, Bremen, Germany). The sample mixture was loaded on an in-house made trapping column (100 µm x 20 mm) filled with 5 µm C18 Reprosil-HD beads (Dr. Maisch GmbH, Ammerbuch-Entringen, Germany). After back-flushing from the trapping column, the sample was loaded on an in-house made reverse-phase column (75 µm. x 150 mm, 5 µm C18 Reprosil-HD beads). Peptides were loaded with solvent A (0.1% trifluoroacetic acid, 2% acetonitrile), and separated with a linear gradient from 2% solvent A' (0.1% formic acid) to 50% solvent B' (0.1% formic acid and 80% acetonitrile) at a flow rate of 300 nl/min, followed by a wash step reaching 100% solvent B'.

The mass spectrometer was operated in data-dependent mode, automatically switching between MS and MS/MS acquisition for the ten most abundant peaks in a given MS spectrum. In the LTQ Orbitrap Velos, full scan MS spectra were acquired in the Orbitrap at a target value of 1E6 with a resolution of 60,000. The ten most intense ions were then isolated for fragmentation in the linear ion trap, with a dynamic exclusion of 20 seconds. Peptides were fragmented after filling the ion trap at a target value of 1E4 ion counts. From the MS/MS data in each LC run, Mascot Generic Files were created using the Mascot Distiller software v2.4.1.0 (Matrix Science). Grouping of spectra was allowed with a maximum intermediate retention time of 30 seconds and a maximum intermediate scan count of 5 was used where possible. Grouping was done with 0.005 Da precursor tolerance. A peak list was only generated when the MS/MS spectrum contained more than 10 peaks. There was no de-isotoping and the relative signal-to-noise limit was set to 2. Peak lists were then searched with the Mascot search engine v2.3 (MatrixScience) using the Mascot Daemon interface (Matrix Science). Spectra were searched against the TAIR10 database containing 35386 sequence entries extended with cRAP sequences (http://www.thegpm.org/crap/). Variable modifications were set to methionine oxidation and methylation of aspartic acid and glutamic acid. Fixed modifications were set to carbamidomethylation of cysteines. Mass tolerance on MS was set to 10 ppm (with Mascot's C13 option set to 1) and the MS/MS tolerance at 0.5 Da. The peptide charge was set to 1+, 2+ and 3+ and the instrument setting was set to ESI-TRAP. Trypsin was set as the protease used, allowing for 1 missed cleavage, and cleavage when arginine or lysine was followed by proline. Only high confident peptides, ranked one and with scores above the threshold score, set at 99% confidence, were withheld. Proteins identified by at least one (for YAP1A identifications) or two (for YAP1C identifications) high-confident peptides were retained (Table S5).

Cloning and purification of recombinant DHAR2

The DHAR2-coding sequence was amplified by PCR (Table S4) from the *Arabidopsis* Biological Resource Center clone (stock No U25352, Yamada et al., 2003). The sequence was inserted into the pDONR221 vector and subcloned in the pDEST17 expression vector by means of the Gateway technology (Life Technologies). *Escherichia coli* C41 (DE3) strain was transformed and grown aerobically overnight at 37ºC in Luria-Bertani Broth (LB) supplemented with 100 µg/ml ampicillin. Subsequently, 1-liter LB cultures were inoculated with this overnight culture. After the culture had reached the exponential growth phase, it was cooled down to 16ºC, supplemented with 0.2 mM isopropyl β-D-1-thiogalactopyranoside, and further grown overnight. Cells were pelleted and resuspended in lysis buffer (20 mM 4-(2-hydroxyethyl)-1-piperazineethanesulfonic acid (Hepes), pH 7.5, 1 M NaCl, 1 mM DTT, 5 mM imidazole, 1 µg/ml leupeptine, 0.1 mg/ml 4-(2-aminoethyl) benzenesulfonyl fluoride hydrochloride, 50 µg/ml DNaseI, and 20 mM $MgCl_2$). The cells were homogenized by cell cracker at 20 kilopound per square inches and then centrifuged at 40,000×g for 30 min, 4°C to remove cell debris. The supernatant was passed through a 0.45-µm filter, and

loaded onto a Ni^{2+}-Sepharose column equilibrated with 20 mM Hepes, pH 7.5, 1 M NaCl, 1 mM DTT, 5 mM imidazole. Protein peaks under the imidazole elution were pooled, concentrated by 10 kDa molecular weight cutoff (Millipore), and injected on a size exclusion Superdex75 column equilibrated with 20 mM Tris, pH 7.5, 150 mM NaCl, 1 mM ethylenediaminetetraacetic acid (EDTA) and 1 mM DTT. Protein samples analyzed by SDS-PAGE were flash-frozen for storage at -80ºC.

DHAR2 activity/inhibition assay and in vitro sulfenic acid labeling.

DHAR2 activity was monitored by GSH-dependent reduction of DHA to ascorbate (ε = 14,000 M^{-1} cm^{-1}) by following the associated absorption increase at 265 nm (Hossain and Asada, 1984). The assay was done for 2 min at 30ºC in a buffer containing 50 mM potassium phosphate (pH 7.0), 150 mM NaCl, and 1 mM EDTA. The buffer was incubated for 1 min at 30ºC and the reaction was started by adding DHAR2 followed by the premix of DHA and GSH. In this assay, freshly prepared DHA, reduced GSH, and DTT-reduced DHAR2 were used (1 h incubation at room temperature). Excess DTT was removed by a size exclusion chromatography in a Superdex75 column equilibrated with the assay buffer. The initial velocity of the ascorbate production was measured at increasing concentrations of DHA (1, 3, 5, 10, 15, 20, 30, 40, 50, 100, 150, 200, and 500 µM), whereas GSH was fixed at 5 mM. Non-enzymatic DHA conversion by GSH was subtracted from the corresponding enzymatic assay. To understand the role of the cysteine residue on the DHAR2 activity, the reduced enzyme was incubated 30 min in the dark with 10 mM IAM or oxidized in the presence or absence of 1 mM reduced GSH with 100 µM, 1 mM, and 5 mM H_2O_2 at room temperature. We removed excess IAM, GSH, and H_2O_2 with Micro Bio-SpinTM P-6 gel column (Bio-Rad) equilibrated with the assay buffer. The reaction was started under Vmax conditions by adding 100 µM DHA at a final concentration of 30 nM DHAR2 in the presence of 5 mM GSH. Initial rates of the progress curves were determined with the Cary 100 Bio UV-Visible Spectrophotometer (Agilent). For dimedone-based in vitro sulfenic acid labeling, DHAR2 (1 mg/ml) was reduced by 1 mM DTT and excess DTT was removed by the Micro Bio-SpinTM P-6 gel column (Bio-Rad) equilibrated with phosphate buffered saline (pH 7.4). Reduced DHAR2 (20 µM) was incubated for 30 min at room temperature with 1 mM dimedone, in the presence or absence of 100 µM H_2O_2 (dimedone stocks in dimethoxy sulfoxide: 100 mM Bis-Tris-HCl, pH 7.4 [1:1]). When GSH was added to the samples, DHAR2 was mixed with 1 mM GSH before oxidation and dimedone treatment.

MS on DHAR2

The intact mass was measured by direct infusion in a microelectrospray ionization ion trap mass spectrometer (LTQ XL; ThermoFisher Scientific). The mass spectra were deconvoluted with the ProMass Deconvolution software (ThermoFisher Scientific). To identify redox-active cysteine residues, DHAR2 was oxidized with H_2O_2 in the presence of dimedone or GSH as for the dimedone labeling experiment. All the free thiols were blocked with excess of iodoacetamide for 10 min before

tryptic digestion. The peptides were analyzed by LC-MS/MS as described (Pyr Dit Ruys et al., 2012). The resulting peak lists were searched with SEQUEST against an *Arabidopsis* protein database containing the recombinant DHAR2 sequence (Uniprot Q9FRL8) and the introduced polyhistidine tag. Peptide matches were filtered by means of the PERCOLATOR program within the Proteome Discoverer software (ThermoFischer Scientific) and manually validated. The considered dynamic modifications on the cysteine residues were +138.0 Da for sulfenic dimedone, +32.0 Da for sulfinic acid, +48.0 Da for sulfonic acid, +305.1 Da for GSH, and +57.0 Da for CIAM modifications. The mixed disulfide peptide between C6 and C20 of DHAR2 was identified by means of the DBond software (Choi et al., 2010) and manually validated.

Generation of transgenic *A. thaliana* lines

To generate *A. thaliana* lines overexpressing YAP1C/A N- and C-terminal TAP tag fusion proteins Col-0 wild type and *cat2-2* mutant plants (Queval et al., 2007) were transformed by means of floral dip transformation (Clough and Bent, 1998) with *Agrobacterium tumefaciens* strain C58C1 carrying expression vectors used before to transform the cell suspensions. Primary transformants were selected through resistance to kanamycin. For every construct and genotype 12 T1 plants were transferred to soil to set T2 generation seeds. Each T1 plant was screened for expression of fusion protein by means of western blot analysis. In order to determine the number of T-DNA insertion loci 70 T2 seeds harvested from respective T1 plants were grown on selective 1 x MS medium (35 mg/L kanamycin). Only T2 populations exhibiting segregation ratio close to theoretical 3:1 characteristic for single T-DNA insertion locus were used to generate homozygous T3 plants.

SUPPLEMENTARY INFORMATION

Table S1. YAP1 probes used for *Arabidopsis thaliana*

Probe	YAP1-cCRD DNA sequences: codon optimized for *Arabidopsis thaliana*

YAP1C	N	G	S	S	L	Q	N	A	D	K	I	N	N	G	N	D	N	D	N	D	N
	AAC	GGT	TCT	TCG	CTT	CAA	AAC	GCC	GAT	AAG	ATA	AAT	AAT	GGT	AAC	GAT	AAT	GAT	AAC	GAT	AAT
	D	V	V	P	S	K	E	G	S	L	L	R	**C**	S	E	I	W	D	R	I	T
	GAC	GTT	GTT	CCG	AGC	AAA	GAG	GGC	TCC	CTT	TTG	AGG	**TGT**	AGC	GAG	ATA	TGG	GAT	CGT	ATA	ACC
	T	H	P	K	Y	S	D	I	D	V	D	G	L	A	S	E	L	M	A	K	A
	ACC	CAC	CCC	AAG	TAC	TCT	GAT	ATA	GAT	GTC	GAT	GGG	CTC	GCC	TCA	GAA	TTA	ATG	GCT	AAA	GCT
	K	T	S	E	R	G	V	V	I	N	A	E	D	V	Q	L	A	L	N	K	H
	AAG	ACG	TCT	GAA	AGG	GGT	GTA	GTG	ATC	AAT	GCT	GAA	GAT	GTG	CAG	CTT	GCA	CTT	AAT	AAA	CAT
	M	N																			
	ATG	AAT																			

YAP1A	N	G	S	S	L	Q	N	A	D	K	I	N	N	G	N	D	N	D	N	D	N
	AAT	GGG	TCG	AGT	CTC	CAG	AAT	GCA	GAC	AAA	ATT	AAT	AAT	GGT	AAT	GAC	AAC	GAC	AAT	GAT	AAT
	D	V	V	P	S	K	E	G	S	L	L	R	**A**	S	E	I	W	D	R	I	T
	GAC	GTC	GTC	CCT	TCA	AAA	GAA	GGC	TCA	CTA	TTG	CGA	**GCG**	TCA	GAG	ATC	TGG	GAT	CGT	ATA	ACG
	T	H	P	K	Y	S	D	I	D	V	D	G	L	A	S	E	L	M	A	K	A
	ACT	CAT	CCT	AAG	TAC	TCA	GAT	ATA	GAT	GTC	GAT	GGA	TTG	GCA	TCA	GAA	CTT	ATG	GCG	AAG	GCC
	K	T	S	E	R	G	V	V	I	N	A	E	D	V	Q	L	A	L	N	K	H
	AAG	ACC	AGT	GAA	AGA	GGA	GTT	GTT	ATC	AAC	GCT	GAA	GAT	GTT	CAA	CTC	GCG	CTA	AAT	AAG	CAT
	M	N																			
	ATG	AAT																			

Table S2. [Enclosed on a CD attached to this thesis] Database of all YAP1C/A interacting proteins identified in this study.

Table S3. Unique YAP1C interactors identified in *Arabidopsis* cell cultures

AGI code	Description	Early response (10 min) 1mM	Late response (1h) 0 mM	Late response (1h) 1 mM	Late response (1h) 20 mM	Cys residues	Cys PTM	Reference
SIGNAL PERCEPTION & TRANSDUCTION								
AT1G59580	MITOGEN ACTIVATED PROTEIN KINASE 2 (MPK2)	x		1	1	8		
AT4G01370	MITOGEN ACTIVATED PROTEIN KINASE 4 (MPK4)	x			1	8		
AT2G18170	MITOGEN ACTIVATED PROTEIN KINASE 7 (MPK7)	x		1	1	8		
AT3G50500	SNF1-RELATED PROTEIN KINASE 2-2 (SNRK2-2)	x				7		
AT5G66880	SNF1-RELATED PROTEIN KINASE 2-3 (SNRK2-3)					8		
AT4G33950	SNF1-RELATED PROTEIN KINASE 2-6 (SNRK2-6)					6		
AT1G60940	SNF1-RELATED PROTEIN KINASE 2-10 (SNRK2-10)	x			1	6		
AT1G35670	CALCIUM-DEPENDENT PROTEIN KINASE 2 (CPK2)				1	9		
AT4G09570	CALCIUM-DEPENDENT PROTEIN KINASE 4 (CPK4)					10		
AT2G18790	PHYTOCHROME B (PHYB)	x				25		(Liu et al., 2014)
AT4G16250	PHYTOCHROME D (PHYD)					25		
AT2G43980	INOSITOL 1,3,4-TRISPHOSPHATE 5/6-KINASE 4 (ITPK4)	x			1	9		
AT2G42810	PHYTOCHROME-ASSOCIATED PROTEIN PHOSPHATASE 5 (PAPP5)				2	8		
AT1G71860	PROTEIN TYROSINE PHOSPHATASE 1 (PTP1)	x				7		(Gupta and Luan, 2003; Wang et al., 2012; Liu et al., 2014)
AT1G51690	PROTEIN PHOSPHATASE 2A 55kDa REGULATORY SUBUNIT (PP2A-b55α)	x		2	2	15		
AT4G15410	PROTEIN PHOSPHATASE 2A 55 kDa REGULATORY SUBUNIT (PP2A-b'γ)				1	1		
AT2G46900	bHLH protein	x			2	6		
PROTEIN DEGRADATION								
AT1G22920	COP9 SIGNALOSOME 5A (CSN5A)				1	2		
AT5G14250	COP9 SIGNALOSOME SUBUNIT 3 (CSN3)	x			1	8		
AT1G64520	REGULATORY PARTICLE NON-ATPASE 12A (RPN12A)	x				4	Trxs target	(Lemaire et al., 2004*; Yamazaki et al., 2004)

AT ID	Protein					Modification	Reference
AT1G75950	S-PHASE KINASE-ASSOCIATED PROTEIN 1 (SKP1)	x	2	2	3		
AT2G45240	METHIONINE AMINOPEPTIDASE 1A (MAP1A)			2	17		
AT2G47790	GIGANTUS 1 (GTS1)	x			12		
AT5G06600	UBIQUITIN-SPECIFIC PROTEASE 12 (UBP12)	x			11		
AT3G11910	UBIQUITIN-SPECIFIC PROTEASE 13 (UBP13)	x			10		
AT4G30890	UBIQUITIN-SPECIFIC PROTEASE 24 (UBP24)	x			3		
AT4G17510	UBIQUITIN C-TERMINAL HYDROLASE 3 (UCH3)	x	1		4	SOH	(Kulathu et al., 2013*)
AT5G50870	UBIQUITIN-CONJUGATING ENZYME 27 (UBC27)	x		1	4		
AT3G18060	transducin family protein / WD-40 repeat family protein			1	14		
AT3G51800	ERBB-3 BINDING PROTEIN 1 (EBP1)			2	7	SNO	(Fares et al., 2011)
AT4G11260	ENHANCED DOWNY MILDEW 1 (EDM1)			1	4		
AT5G13520	peptidase M1 family protein			1	7		
AT4G17830	Peptidase M20/M25/M40 family protein	x		1	8	S-SG	(Dixon et al., 2005)
AT5G15400	MUTANT SNC1-ENHANCING 3 (MUSE3)			1	12		
AT5G36210	α/β-Hydrolases superfamily protein			1	13		
AT5G42190	SKP-LIKE PROTEIN 1B (SKP1B)	x	1	2	3		
REDOX RELATED							
AT1G65980	THIOREDOXIN-DEPENDENT PEROXIDASE 1 (TPX1)	x	1		2	SNO, Trxs target. Grxs target	(Lindermayr et al., 2005; Rouhier et al., 2005*; Marchand et al., 2006; Wang et al., 2012)
AT1G75270	DEHYDROASCORBATE REDUCTASE 2 (DHAR2)	x		1	2	S-SG; Trxs target; S-S	(Dixon et al., 2005; Marchand et al., 2010; Wang et al., 2012)
AT4G04950	MONOTHIOL GLUTAREDOXIN 17 (GRXS17)	x	2	2	6		
AT1G01800	NAD(P)-binding Rossmann-fold superfamily protein	x			4	S-S	(Wang et al., 2012)
AT3G44190	FAD/NAD(P)-binding oxidoreductase family protein	x		2	3		
AT5G40370	GLUTAREDOXIN C2 (GRXC2)			1	5		
AT1G37130	NITRATE REDUCTASE 2 (NR2)		1	1	16		

Locus	Protein				Modification	Reference
RNA BINDING- TRANSLATION						
AT1G15930	Ribosomal protein L7Ae/L30e/S12e/Gadd45 family protein	x	**1**	6	Trxs target	(Hagglund et al., 2008*)
AT2G32060	Ribosomal protein L7Ae/L30e/S12e/Gadd45 family protein		**1**	6	Trxs target	(Hagglund et al., 2008*)
AT1G49760	POLY(A) BINDING PROTEIN 8 (PABP8)		**2**	4		
AT3G57290	EUKARYOTIC TRANSLATION INITIATION FACTOR 3E (EIF3E)		**1**	5		
AT4G27000	RNA-BINDING FAMILY PROTEIN (ATRBP45C)	x		3		
AT1G70980	Class II aminoacyl-tRNA and biotin synthetases superfamily protein (SYNC3)		**1**	9		
AT4G31120	PROTEIN ARGININE METHYLTRANSFERASE 5 (PRMT5)	x		12		
PRIMARY METABOLISM						
AT1G04410	CYTOSOLIC-NAD-DEPENDENT MALATE DEHYDROGENASE 1 (C-NAD-MDH1)		**2**	6	SNO, Trxs target	(Yamazaki et al., 2004; Lindermayr et al., 2005; Hara et al., 2006)
AT3G06650	ATP-CITRATE LYASE SUBUNIT B-1 (ACLB-1)		**1**	10		
AT5G49460	ATP CITRATE LYASE SUBUNIT B 2 (ACLB-2)			10		
AT4G35260	ISOCITRATE DEHYDROGENASE 1 (IDH1)		**1**	7	Trxs target	(Balmer et al., 2006; Yoshida et al., 2013)
AT5G03690	FRUCTOSE-BISPHOSPHATE ALDOLASE 4 (FBA4)		**1**	5	S-SG, SNO & S-S bond	(van der Linde et al., 2011)*
AT5G11670	NADP-MALIC ENZYME 2 (NADP-ME2)	x	**2**	7	S-SG	(Dixon et al., 2005)
AT1G78900	VACUOLAR ATP SYNTHASE SUBUNIT A (VHA-A)	x	**2**	6	S-S	(Seidel et al., 2012)
HORMONE HOMEOSTASIS						
AT1G48630	RECEPTOR FOR ACTIVATED C KINASE 1B (RACK1B)		**1**	8		(Liu et al., 2014)
AT3G18130	RECEPTOR FOR ACTIVATED C KINASE 1C (RACK1C)			7		
AT1G52340	ABA DEFICIENT 2 (ABA2)		**1**	7		
AT3G44310	NITRILASE 1 (NIT1)		**2**	7	S-SG	(Dixon et al., 2005)
AT3G44300	NITRILASE 2 (NIT2)	x	**2**	7	S-S	(Wang et al., 2012)
PROTEIN TRANSPORT						
AT5G58590	RAN BINDING PROTEIN 1 (RANBP1)		**2**	4	Trxs target	(Alkhalfioui et al., 2007)*

AT ID	Protein					Modification	Reference
AT1G07140	PUTATIVE RAN-BINDING PROTEIN (SIRANBP)			**1**	4	Trxs target	(Alkhalfioui et al., 2007)*
AT3G56190	ALPHA-SOLUBLE NSF ATTACHMENT PROTEIN 2 (ASNAP)	x			8		
AT3G59020	ARM repeat superfamily protein			**1**	16		
AT4G30550	GAMMA-GLUTAMYL PEPTIDASE 3 (GGP3)	x			8		
AMINO ACID METABOLISM							
AT5G10870	CHORISMATE MUTASE 2 (CM2)			**1**	3		
AT4G24830	Arginosuccinate synthase family protein			**1**	6	Trxs target; S-S	(Hagglund et al., 2008)*, (Wang et al., 2012)
AT5G17330	GLUTAMATE DECARBOXYLASE 1 (GAD1)	x	1	**2**	7		
AT1G49820	5-METHYLTHIORIBOSE KINASE 1 (MTK1)			**1**	5		
AT5G01410	PYRIDOXINE BIOSYNTHESIS 1.3 (PDX1.3)	x		**2**	5	S-S	(Wang et al., 2012)
MISCELLANEOUS AND UNKNOWN FUNCTIONS							
AT3G16050	PYRIDOXINE BIOSYNTHESIS 1.2 (PDX1.2)			**2**	4		
AT1G04690	POTASSIUM CHANNEL BETA SUBUNIT 1 (KAB1)		1	**1**	4		
AT1G07660	Histone superfamily protein		1		0		
AT1G09080	BINDING PROTEIN 3 (BIP3)		1		4		
AT1G10270	GLUTAMINE-RICH PROTEIN 23 (GRP23)		1		9		
AT1G62740	HOP2			**1**	5		
AT1G69800	Cystathionine beta-synthase (CBS) protein			**2**	6		
AT1G70310	SPERMIDINE SYNTHASE 2 (SPDS2)			**2**	9		
AT2G27860	UDP-D-APIOSE/UDP-D-XYLOSE SYNTHASE 1 (AXS1)			**2**	8	S-SG	(Dixon et al., 2005)
AT2G42910	Phosphoribosyltransferase family protein	x	1	**2**	7		
AT3G03250	UDP-GLUCOSE PYROPHOSPHORYLASE (UGP1)			**1**	3	S-SG; Trxs target	(Wong et al., 2004)*, (Dixon et al., 2005), (Alkhalfioui et al., 2007)*
AT3G07720	Galactose oxidase/kelch repeat superfamily protein	x			6	S-S	(Wang et al., 2012)

AGI	Protein			Count	PTM	Reference
AT3G12110	ACTIN-11 (ACT11)	1		4	Trxs target; SOH	(Wong et al., 2004)*, (Alkhalfioui et al., 2007)*, (Oger et al., 2012)*
AT3G46010	ACTIN DEPOLYMERIZING FACTOR 1 (ADF1)		1	5		
AT3G16520	UDP-GLUCOSYL TRANSFERASE 88A1 (UGT88A1)	x	1	9		
AT3G53180	NODULIN/GLUTAMINE SYNTHASE-LIKE PROTEIN (NODGS)	x		9	S-SG	(Dixon et al., 2005)
AT3G63000	NPL4-LIKE PROTEIN 1 (NPL41)			5		
AT4G02340	alpha/beta-Hydrolases superfamily protein		1	3		
AT4G02860	Phenazine biosynthesis PhzC/PhzF protein		1	10		
AT4G13730	Ypt/Rab-GAP domain of gyp1p superfamily protein		2	4		
AT4G14710	ACIREDUCTONE DIOXYGENASE 2 (ATARD2)	x		5		
AT4G29350	PROFILIN 2 (PFN2)	x		2	Trxs target	(Wong et al., 2004)*
AT4G29510	ARGININE METHYLTRANSFERASE 11 (PRMT11)		1	6		
AT5G13050	5-FORMYLTETRAHYDROFOLATE CYCLOLIGASE (5-FCL)	x		5		
AT5G17270	Protein prenylyltransferase superfamily protein	x	2	20		
AT5G17620	AUGMIN SUBUNIT 7 (AUG7)		2	2		
AT5G49650	XYLULOSE KINASE 2 (XK2)		1	8		
AT3G29280	unknown protein	x		6		
AT3G52610	unknown protein		2	8		
AT4G27450	unknown protein	x	2	7	Trxs target	(Hagglund et al., 2008)*
AT5G11810	unknown protein		2	5		

Annotation according to TAIR10. Abbreviations of PTMs are as follows: SOH, sulfenic acid; S-S, disulphide bridge; S-SG, S-glutathionylation; SNO, S-nitrosylation; Trxs/Grxs target, thioredoxins/gluteredoxins target proteins. X indicates presence within early response identifications. Numbers indicate the occurrence of proteins in two independent experiments. References describing identification of homolog/ortholog are marked with *

Table S4. Primers used for cloning

Primer	Sequence (5'- 3')
Cloning – 1st PCR (YAP1(C/A)-cCRD)	
YAP1C_N_LP	AAAAAGCAGGCTTCAACGGTTCTTCGCTTCAAAACG
YAP1C_N_RP	AGAAAGCTGGGTCTTAATTCATATGTTTATTAAGT
YAP1A_N_LP	AAAAAGCAGGCTTCAATGGGTCGAGTCTCCAGAATGC
YAP1A_N_RP	AGAAAGCTGGGTCTTAATTCATATGCTTATTTAGCG
YAP1A_C_LP	AAAAAGCAGGCTCCACCATGAATGGGTCGAGTCTCCAGAATG
YAP1A_C_RP	AGAAAGCTGGGTCATTCATATGCTTATTTAGCGCGAG
Cloning – 1st PCR (DHAR2)	
DHAR2_LP	AAAAAGCAGGCTTCGAAGTGCTGTTTCAGGGCCCGATGGCTCTAGATATCTGCGTGAAG
DHAR2_RP	AGAAAGCTGGGTCTCACGCATTCACCTTCGAT
Cloning – 2nd PCR	
attB1	GGGGACAAGTTTGTACAAAAAAGCAGGCT
attB2	GGGGACCACTTTGTACAAGAAAGCTGGGT
Sequencing	
GWM13-LP	GTAAAACGACGGCCAGTCTTA
GWM13-RP	CCAGGAAACAGCTATGACCAT

Table S5. [Enclosed on a CD attached to this thesis]. Protein identification details.
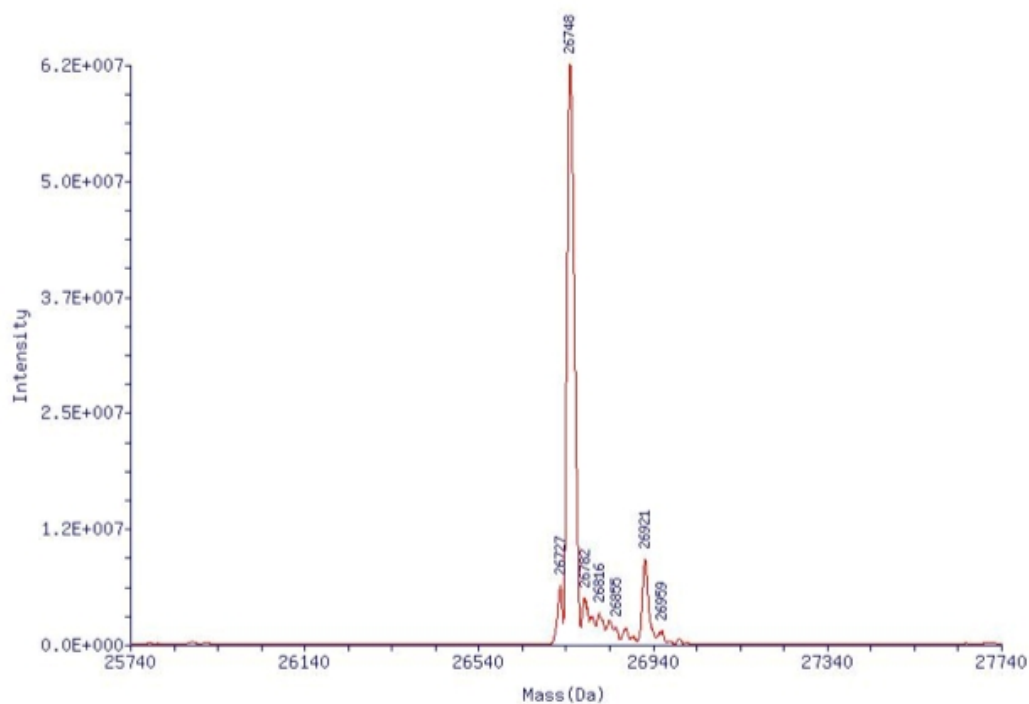
Fig. S1. Recombinant DHAR2 identity confirmed by MS. Total mass equals 26,748 Da after loss of the N-terminal methionine.
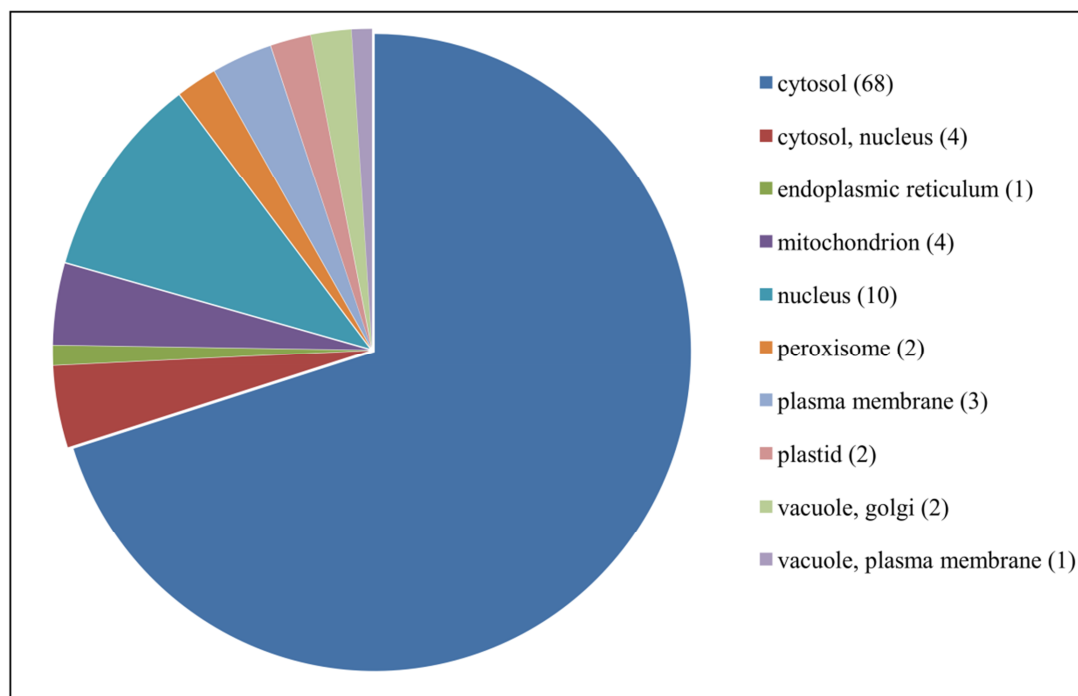
Fig. S2. Schematic representation of subcellular localizations for 97 YAP1C-GS interacting proteins. Numbers in brackets indicate amount of proteins predicted to localize within respective subcellular compartment. Localization data obtained from the subcellular localization database for *Arabidopsis* proteins (http://suba3.plantenergy.uwa.edu.au/).

REFERENCES

Alergand T, Peled-Zehavi H, Katz Y, Danon A (2006) The chloroplast protein disulfide isomerase RB60 reacts with a regulatory disulfide of the RNA-binding protein RB47. Plant Cell Physiol **47**: 540–8

Alkhalfioui F, Renard M, Vensel WH, Wong J, Tanaka CK, Hurkman WJ, Buchanan BB, Montrichard F (2007) Thioredoxin-linked proteins are reduced during germination of *Medicago truncatula* seeds. Plant Physiol **144**: 1559-79

Alvarez CE, Detarsio E, Moreno S, Andreo CS, Drincovich MF (2012) Functional characterization of residues involved in redox modulation of maize photosynthetic NADP-malic enzyme activity. Plant Cell Physiol **53**: 1144–53

Balmer Y, Vensel WH, Hurkman WJ, Buchanan BB (2006) Thioredoxin target proteins in chloroplast thylakoid membranes. Antioxid Redox Signal **8**: 1829–34

Balsera M, Uberegui E, Schurmann P, Buchanan BB (2014) Evolutionary development of redox regulation in chloroplasts. Antioxid Redox Signal [Epub ahead of print]

Bartel B, Fink GR (1994) Differential regulation of an auxin-producing nitrilase gene family in *Arabidopsis thaliana*. Proc Natl Acad Sci U S A **91**: 6649–6653

Bartels S, Anderson JC, González Besteiro MA, Carreri A, Hirt H, Buchala A, Métraux J-P, Peck SC, Ulm R (2009) MAP kinase phosphatase 1 and Protein tyrosine phosphatase 1 are repressors of salicylic acid synthesis and SNC1-mediated responses in *Arabidopsis*. Plant Cell **21**: 2884–97

Basset G, Raymond P, Malek L, Brouquisse R (2002) Changes in the expression and the enzymic properties of the 20S proteasome in sugar-starved maize roots. Evidence for an in vivo oxidation of the proteasome. Plant Physiol **128**: 1149–1162

Benitez L V, Allison WS (1974) The inactivation of the acyl phosphatase activity catalyzed by the sulfenic acid form of glyceraldehyde 3-phosphate dehydrogenase by dimedone and olefins. J Biol Chem **249**: 6234–6243

Chen Z, Gallie DR (2006) Dehydroascorbate reductase affects leaf growth, development, and function. Plant Physiol **142**: 775–787

Cheng N-H, Liu J-Z, Liu X, Wu Q, Thompson SM, Lin J, Chang J, Whitham SA, Park S, Cohen JD, et al (2011) *Arabidopsis* monothiol glutaredoxin, AtGRXS17, is critical for temperature-dependent postembryonic growth and development via modulating auxin response. J Biol Chem **286**: 20398–406

Choi S, Jeong J, Na S, Lee HS, Kim H-Y, Lee K-J, Paek E (2010) New algorithm for the identification of intact disulfide linkages based on fragmentation characteristics in tandem mass spectra. J Proteome Res **9**: 626–635

Clough SJ, Bent AF (1998) Floral dip: a simplified method for *Agrobacterium*-mediated transformation of *Arabidopsis thaliana*. Plant J **16**: 735–43

Delaunay A, Pflieger D, Barrault MB, Vinh J, Toledano MB (2002) A thiol peroxidase is an H_2O_2 receptor and redox-transducer in gene activation. Cell **111**: 471–81

Desikan R, Reynolds A, Hancock JT, Neill SJ (1998) Harpin and hydrogen peroxide both initiate programmed cell death but have differential effects on defence gene expression in *Arabidopsis* suspension cultures. Biochem J. 1998 Feb 15;330 (Pt 1):115-20.

Desikan R, A.-H.-Mackerness S, Hancock JT, Neill SJ (2001) Regulation of the *Arabidopsis* transcriptome by oxidative stress. Plant Physiol **127**: 159–72

Dixon DP, Davis BG, Edwards R (2002) Functional divergence in the glutathione transferase superfamily in plants. Identification of two classes with putative functions in redox homeostasis in *Arabidopsis thaliana*. J Biol Chem **277**: 30859–69

Dixon DP, Skipsey M, Grundy NM, Edwards R, Sciences B, Kingdom U (2005) Stress-induced protein S-glutathionylation in *Arabidopsis*. Plant Physiol **138**: 2233–2244

Fares A, Rossignol M, Peltier J-B (2011) Proteomics investigation of endogenous S-nitrosylation in *Arabidopsis*. Biochem Biophys Res Commun **416**: 331–6

Fatland BL, Ke J, Anderson MD, Mentzen WI, Cui LW, Allred CC, Johnston JL, Nikolau BJ, Wurtele ES (2002) Molecular characterization of a heteromeric ATP-Citrate Lyase that generates cytosolic acetyl-coenzyme A in *Arabidopsis*. Plant Physiol **130**: 740–756

Fatland BL, Nikolau BJ, Wurtele ES (2005) Reverse genetic characterization of cytosolic acetyl-CoA generation by ATP-citrate lyase in *Arabidopsis*. Plant Cell **17**: 182–203

Fomenko DE, Koc A, Agisheva N, Jacobsen M, Kaya A, Malinouski M, Rutherford JC, Siu K-L, Jin D-Y, Winge DR, et al (2011) Thiol peroxidases mediate specific genome-wide regulation of gene expression in response to hydrogen peroxide. Proc Natl Acad Sci U S A **108**: 2729–34

Foyer CH, Halliwell B (1977) Purification and properties of dehydroascorbate reductase from spinach leaves. Phytochemistry **16**: 1347–1350

Garavelli JS (2004) The RESID Database of Protein Modifications as a resource and annotation tool. Proteomics 1527–1533

Gupta R, Luan S (2003) Redox control of protein tyrosine phosphatases and mitogen-activated protein kinases in plants. Plant Physiol **132**: 1149–1152

Hagglund P, Bunkenborg J, Maeda K, Svensson B (2008) Identification of thioredoxin disulfide targets using a quantitative proteomics approach based on isotope-coded affinity tags. J Proteome Res **7**: 5270–5276

Hanai J, Doro N, Seth P, Sukhatme VP (2013) ATP citrate lyase knockdown impacts cancer stem cells in vitro. Cell Death Dis **4**: e696

Hara S, Motohashi K, Arisaka F, Romano PGN, Hosoya-Matsuda N, Kikuchi N, Fusada N, Hisabori T (2006) Thioredoxin-h1 reduces and reactivates the oxidized cytosolic malate dehydrogenase dimer in higher plants. J Biol Chem **281**: 32065–71

Heidari B, Nemie-Feyissa D, Kangasjärvi S, Lillo C (2013) Antagonistic regulation of flowering time through distinct regulatory subunits of Protein phosphatase 2A. PLoS One **8**: e67987

Höhn TJA, Grune T (2014) The proteasome and the degradation of oxidized proteins: Part III-Redox regulation of the proteasomal system. Redox Biol **2**: 388–394

Hossain MA, Asada K (1984) Purification of dehydroascorbate reductase from spinach and its characterization as a thiol enzyme. Plant Cell Physiol **25**: 85–92

Jung T, Grune T (2013) The proteasome and the degradation of oxidized proteins: Part I-structure of proteasomes. Redox Biol **1**: 178–182

Kim J, Mayfield SP (1997) Protein disulfide isomerase as a regulator of chloroplast translational activation. Science **278**: 1954–1957

Kovtun Y, Chiu WL, Tena G, Sheen J (2000) Functional analysis of oxidative stress-activated mitogen-activated protein kinase cascade in plants. Proc Natl Acad Sci U S A **97**: 2940–5

Kulathu Y, Garcia FJ, Mevissen TET, Busch M, Arnaudo N, Carroll KS, Barford D, Komander D (2013) Regulation of A20 and other OTU deubiquitinases by reversible oxidation. Nat Commun **4**: 1569

Kulik A, Wawer I, Krzywińska E, Bucholc M, Dobrowolska G (2011) SnRK2 protein kinases--key regulators of plant response to abiotic stresses. OMICS **15**: 859–72

Van Leene J, Stals H, Eeckhout D, Persiau G, Van De Slijke E, Van Isterdael G, De Clercq A, Bonnet E, Laukens K, Remmerie N, et al (2007) A tandem affinity purification-based technology platform to study the cell cycle interactome in *Arabidopsis thaliana*. Mol Cell Proteomics **6**: 1226–38

Van Leene J, Witters E, Inzé D, De Jaeger G (2008) Boosting tandem affinity purification of plant proteins complexes. Trends Plant Sci **13**: 517–520

Van Leene J, Eeckhout D, Persiau G, Van De Slijke E, Geerinck J, Van Isterdael G, Witters E, De Jaeger G. (2011) Isolation of transcription factor complexes from *Arabidopsis* cell suspension cultures by tandem affinity purification. Methods Mol Biol. 754:195-218

Lemaire SD, Guillon B, Le Maréchal P, Keryer E, Miginiac-Maslow M, Decottignies P (2004) New thioredoxin targets in the unicellular photosynthetic eukaryote *Chlamydomonas reinhardtii*. Proc Natl Acad Sci U S A **101**: 7475–80

Léon-Kloosterziel KM, Alvarez Gil M, Ruijs GJ, Jacobsen SE, Olszewski NE, Schwartz SH, Zeevart JA, Korneef M (1996) Isolation and characterization of abscisic acid-deficient *Arabidopsis* mutants at two new loci. Plant J **10**: 655-661

Li S, Mhamdi A, Clement C, Jolivet Y, Noctor G (2013) Analysis of knockout mutants suggests that *Arabidopsis* NADP-MALIC ENZYME2 does not play an essential role in responses to oxidative stress of intracellular or extracellular origin. J Exp Bot **64**: 3605–14

Li S, Mhamdi A, Trotta A, Kangasjarvi S, Noctor G (2014) The protein phosphatase subunit PP2A-B'γ is required to suppress day length-dependent pathogenesis responses triggered by intracellular oxidative stress. New Phytol **202**: 2–145–60

Van der Linde K, Gutsche N, Leffers H-M, Lindermayr C, Müller B, Holtgrefe S, Scheibe R (2011) Regulation of plant cytosolic aldolase functions by redox-modifications. Plant Physiol Biochem **49**: 946–57

Lindermayr C, Saalbach G, Durner J (2005) Proteomic identification of S-nitrosylated proteins. Plant Physiol **137**: 921-930

Liu P, Zhang H, Wang H, Xia Y (2014) Identification of redox-sensitive cysteines in the *Arabidopsis* proteome using OxiTRAQ, a quantitative redox proteomics method. Proteomics **14**: 750–62

Lorković ZJ (2009) Role of plant RNA-binding proteins in development, stress response and genome organization. Trends Plant Sci **14**: 229–36

Ma L-H, Takanishi CL, Wood MJ (2007) Molecular mechanism of oxidative stress perception by the Orp1 protein. J Biol Chem **282**: 31429–36

Marchand C, Le Maréchal P, Meyer Y, Decottignies P (2006) Comparative proteomic approaches for the isolation of proteins interacting with thioredoxin. Proteomics **6**: 6528–6537

Marchand C, Vanacker H, Collin V, Issakidis-Bourguet E, Maréchal P, Decottignies P (2010) Thioredoxin targets in *Arabidopsis* roots. Proteomics **10**: 2418–28

Meinhard M, Grill E (2001) Hydrogen peroxide is a regulator of ABI1, a protein phosphatase 2C from *Arabidopsis*. FEBS Lett **508**: 443–6

Meinhard M, Rodriguez PL, Grill E (2002) The sensitivity of ABI2 to hydrogen peroxide links the abscisic acid-response regulator to redox signalling. Planta **214**: 775–82

Mou Z, Fan W, Dong X (2003) Inducers of plant systemic acquired resistance regulate NPR1 function through redox changes. Cell **113**: 935–44

Oger E, Marino D, Guigonis J-M, Pauly N, Puppo A (2012) Sulfenylated proteins in the *Medicago truncatula-Sinorhizobium meliloti* symbiosis. J Proteomics **75**: 4102–4113

Paulsen CE, Carroll KS (2009) Chemical dissection of an essential redox switch in yeast. Chem Biol **16**: 217–225

Paulsen CE, Truong TH, Garcia FJ, Homann A, Gupta V, Leonard SE, Carroll KS (2011) Peroxide-dependent sulfenylation of the EGFR catalytic site enhances kinase activity. Nat Chem Biol **8**: 57–64

Pyr Dit Ruys S, Wang X, Smith EM, Herinckx G, Hussain N, Rider MH, Vertommen D, Proud CG (2012) Identification of autophosphorylation sites in eukaryotic elongation factor-2 kinase. Biochem J **442**: 681–692

Queval G, Issakidis-Bourguet E, Hoeberichts FA, Vandorpe M, Gakière B, Vanacker H, Miginiac-Maslow M, Van Breusegem F, Noctor G (2007) Conditional oxidative stress responses in the *Arabidopsis* photorespiratory mutant *cat2* demonstrate that redox state is a key modulator of daylength-dependent gene expression, and define photoperiod as a crucial factor in the regulation of H_2O_2-induced cell death. Plant J **52**: 640–57

Riondet C, Desouris JP, Montoya JG, Chartier Y, Meyer Y, Reichheld J-P (2012) A dicotyledon-specific glutaredoxin GRXC1 family with dimer-dependent redox regulation is functionally redundant with GRXC2. Plant Cell Environ **35**: 360–73

Roos G, Messens J (2011) Protein sulfenic acid formation: from cellular damage to redox regulation. Free Radic Biol Med **51**: 314–26

Rouhier N, Villarejo A, Srivastava M, Gelhaye E, Keech O, Droux M, Finkemeier I, Samuelsson G, Dietz KJ, Jacquot J, et al (2005) Identification of plant glutaredoxin targets. Antioxid Redox Signal **7**: 919–929

Ryu MY, Cho SK, Kim WT (2009) RNAi suppression of RPN12a decreases the expression of type-A ARRs, negative regulators of cytokinin signaling pathway, in *Arabidopsis*. Mol Cells **28**: 375–82

Sanchez SE, Petrillo E, Beckwith EJ, Zhang X, Rugnone ML, Hernando CE, Cuevas JC, Godoy Herz MA, Depetris-Chauvin A, Simpson CG, et al (2010) A methyl transferase links the circadian clock to the regulation of alternative splicing. Nature **468**: 112–6

Seidel T, Scholl S, Krebs M, Rienmüller F, Marten I, Hedrich R, Hanitzsch M, Janetzki P, Dietz K-J, Schumacher K (2012) Regulation of the V-type ATPase by redox modulation. Biochem J **448**: 243–51

Shaikhali J, Heiber I, Seidel T, Ströher E, Hiltscher H, Birkmann S, Dietz K-J, Baier M (2008) The redox-sensitive transcription factor Rap2.4a controls nuclear expression of 2-Cys peroxiredoxin A and other chloroplast antioxidant enzymes. BMC Plant Biol **8**: 48

Shaikhali J, Norén L, de Dios Barajas-López J, Srivastava V, König J, Sauer UH, Wingsle G, Dietz K-J, Strand Å (2012) Redox-mediated mechanisms regulate DNA binding activity of the G-group of basic region leucine zipper (bZIP) transcription factors in *Arabidopsis*. J Biol Chem **287**: 27510–25

Shen Y, Danon A, Christopher DA (2001) RNA binding-proteins interact specifically with the *Arabidopsis* chloroplast psbA mRNA 5' untranslated region in a redox-dependent manner. Plant Cell Physiol **42**: 1071–8

Song Y, Miao Y, Song C-P (2014) Behind the scenes: the roles of reactive oxygen species in guard cells. New Phytol **201**: 1121–1140

Suzuki N, Miller G, Salazar C, Mondal HA, Shulaev E, Cortes DF, Shuman JL, Luo X, Shah J, Schlauch K, et al (2013) Temporal-spatial interaction between reactive oxygen species and abscisic acid regulates rapid systemic acclimation in plants. Plant Cell. doi: 10.1105/tpc.113.114595

Takanishi CL, Ma L-H, Wood MJ (2007) A genetically encoded probe for cysteine sulfenic acid protein modification *in vivo*. Biochemistry **46**: 14725–32

Tanner JJ, Parsons ZD, Cummings AH, Zhou H, Gates KS (2011) Redox regulation of protein tyrosine phosphatases: structural and chemical aspects. Antioxid Redox Signal **15**: 77–97

Tavakoli N, Kluge C, Golldack D, Mimura T, Dietz KJ (2001) Reversible redox control of plant vacuolar H+-ATPase activity is related to disulfide bridge formation in subunit E as well as subunit A. Plant J **28**: 51–9

Templeton DJ, Aye M-S, Rady J, Xu F, Cross J V (2010) Purification of reversibly oxidized proteins (PROP) reveals a redox switch controlling p38 MAP kinase activity. PLoS One **5**: e15012

Tognetti VB, Van Aken O, Morreel K, Vandenbroucke K, van de Cotte B, De Clercq I, Chiwocha S, Fenske R, Prinsen E, Boerjan W, et al (2010) Perturbation of indole-3-butyric acid homeostasis by the UDP-glucosyltransferase UGT74E2 modulates *Arabidopsis* architecture and water stress tolerance. Plant Cell **22**: 2660–79

Tognetti VB, Mühlenbock P, Van Breusegem F (2012) Stress homeostasis - the redox and auxin perspective. Plant Cell Environ **35**: 321–33

Trotta A, Wrzaczek M, Scharte J, Tikkanen M, Konert G, Rahikainen M, Holmström M, Hiltunen H-M, Rips S, Sipari N, et al (2011) Regulatory subunit B'gamma of protein phosphatase 2A prevents unnecessary defense reactions under low light in *Arabidopsis*. Plant Physiol **156**: 1464–80

Truong TH, Carroll KS (2013) Redox regulation of protein kinases. Crit Rev Biochem Mol Biol **48**: 332–56

Vercruyssen L, Verkest A, Gonzalez N, Heyndrickx KS, Eeckhout D, Han SK, Jégu T, Archacki R, Van Leene J, Andriankaja M, et al (2014) ANGUSTIFOLIA3 binds to SWI/SNF chromatin remodeling complexes to regulate transcription during *Arabidopsis* leaf development. Plant Cell **26**: 210–29

Viola IL, Güttlein LN, Gonzalez DH (2013) Redox modulation of plant developmental regulators from the class I TCP transcription factor family. Plant Physiol **162**: 1434–47

Wang H, Wang S, Lu Y, Alvarez S, Hicks LM, Ge X, Xia Y (2012) Proteomic analysis of early-responsive redox-sensitive proteins in *Arabidopsis*. J Proteome Res **11**: 412–24

Wells TNC, Saxty BA (1992) Redox control of catalysis in ATP-citrate lyase from rat liver. Eur J Biochem **204**: 249–255

Wituszyńska W, Gałązka K, Rusaczonek A, Vanderauwera S, Van Breusegem F, Karpiński S (2013a) Multivariable environmental conditions promote photosynthetic adaptation potential in *Arabidopsis thaliana*. J Plant Physiol **170**: 548–59

Wituszyńska W, Slesak I, Vanderauwera S, Szechynska-Hebda M, Kornas A, Van Der Kelen K, Mühlenbock P, Karpinska B, Mackowski S, Van Breusegem F, et al (2013b) Lesion simulating disease1, enhanced disease susceptibility1, and phytoalexin deficient4 conditionally regulate cellular signaling homeostasis, photosynthesis, water use efficiency, and seed yield in *Arabidopsis*. Plant Physiol **161**: 1795–805

Wong JH, Cai N, Balmer Y, Tanaka CK, Vensel WH, Hurkman WJ, Buchanan BB (2004) Thioredoxin targets of developing wheat seeds identified by complementary proteomic approaches. Phytochemistry **65**: 1629–1640

Yamada K, Lim J, Dale JM, Chen H, Shinn P, Palm CJ, Southwick AM, Wu HC, Kim C, Nguyen M, et al (2003) Empirical analysis of transcriptional activity in the *Arabidopsis* genome. Science (80-) **302**: 842–6

Yamazaki D, Motohashi K, Kasama T, Hara Y, Hisabori T (2004) Target proteins of the cytosolic thioredoxins in *Arabidopsis thaliana*. Plant Cell Physiol **45**: 18–27

Yoshida K, Noguchi K, Motohashi K, Hisabori T (2013) Systematic exploration of thioredoxin target proteins in plant mitochondria. Plant Cell Physiol **54**: 875–92

Zaidi N, Swinnen J V, Smans K (2012) ATP-citrate lyase: a key player in cancer metabolism. Cancer Res **72**: 3709–14

Zhou J, Xia X-J, Zhou Y-H, Shi K, Chen Z, Yu J-Q (2014) RBOH1-dependent H_2O_2 production and subsequent activation of MPK1/2 play an important role in acclimation-induced cross-tolerance in tomato. J Exp Bot **65**: 595–607

Zhu M, Zhu N, Song W, Harmon AC, Assmann SM, Chen S (2014) Thiol-based redox proteins in *Brassica napus* guard cell abscisic acid and methyl jasmonate signalling. Plant J in press (doi: 10.1111/tpj.12490)

3

Forward genetic screen to identify modulators of photorespiratory H$_2$O$_2$-induced cell death

Cezary Waszczak, Pavel Kerchev, Jordi Denecker, Per Mühlenbock, Frank A. Hoeberichts,
Katrien Van Der Kelen, Brigitte van de Cotte, Michaël Vandorpe,
Joris Messens, Frank Van Breusegem

AUTHOR CONTRIBUTIONS

PM developed RGCL assay; PM, FAH, KVDK, MV performed mutant screen; CW, JD – identified causative mutations; BVDC provided technical assistance; PK, CW performed metabolome profiling and gas exchange measurements; CW mentored by PK performed all remaining experiments; CW wrote the chapter with the help of PK, JM and FVB; all authors contributed to the experimental design at respective stages of this work.

ABSTRACT

Initially recognized solely as a wasteful process leading to losses in photosynthetic carbon fixation, photorespiration is now recognized to play a role in multiple plant metabolic pathways. However, the knowledge about the signaling events linking photorespiratory metabolism with transcriptional responses is fragmentary. Our previous results indicated that photorespiratory hydrogen peroxide serves as a signaling molecule that controls nuclear gene expression. To explore the possibilities for tuning of photorespiratory metabolism, we conducted a forward genetics screen and identified 13 second-site mutations that alleviate the negative effects of photorespiration in *Arabidopsis thaliana* mutants lacking peroxisomal CATALASE 2 (*cat2*). Among the polymorphisms that could rescue the photorespiratory phenotype of *cat2* were mutations in *SHORT-ROOT* (*SHR*), encoding for a transcription factor that is involved in controlling the developmental processes, and *GLYCOLATE OXIDASE1* (*GOX1*), encoding a core photorespiratory enzyme that catalyzes the oxidation of glycolate to glyoxylate. Both rescue phenotypes were confirmed in genetic crosses of *cat2* plants with independent loss-of-function lines of SHR and GOX1. The analysis of mutants lacking different glycolate oxidase isoforms established a central role for GOX1 in the photorespiratory metabolism. A detailed functional characterization of *shr* mutants by transcriptome and metabolome profiling indicated an effect of early developmental processes on oxidative stress tolerance.

INTRODUCTION

In C3 plants the biochemical process of carbon fixation starts with the carboxylation of ribulose-1,5-biphosphate (RuBP) by ribulose-1,5-biphosphate carboxylase/oxygenase (RuBisCO). This reaction yields two molecules of 3-phosphoglycerate (3-PGA), the entry metabolite of the Calvin-Benson cycle. However, in ambient air, approximately 25% of the catalytic RuBisCO activity corresponds to oxygenation rather than carboxylation of RuBP and results in the formation of equimolar amounts of 3-PGA and 2-phosphoglycolate (2-PG; Peterhansel and Maurino, 2011). The balance between these two reactions depends on the CO_2/O_2 ratio in the chloroplast and the CO_2/O_2 specificity factor (the relative rates of the two reactions at any given CO_2 and O_2 concentrations) of RubisCO (Maurino and Peterhansel, 2010). Due to the high toxicity of 2-PG (Anderson, 1971), the level of this metabolite has to be tightly regulated by the process of photorespiration which central function is to recycle the 2-PG into 3-PGA that can be utilized in the Calvin-Benson cycle (Figure 1). In higher plants, this complex pathway of reactions involves at least eight core enzymes distributed among the chloroplast, the peroxisome and the mitochondrion (Bauwe et al., 2012) and is complemented by a cytosolic bypass (Timm et al., 2008). Over the last 30 years, a broad collection of photorespiratory mutants has been isolated. The majority of them corresponds to core photorespiratory enzymes, metabolite transporters or regulators of associated processes and are characterized by lethal/sub-lethal phenotypes exhibited under ambient air that can be readily reverted by growth in high CO_2 atmosphere (Timm and Bauwe, 2012). Detailed investigation of photorespiratory mutants revealed a tight interplay between photorespiration and plant metabolism. Glycolate, the direct metabolite of 2-PG was shown to negatively influence RubisCO activity (Gonzalez-Moro et al., 1997). Photorespiratory flux serves as the main source of glycine that is used in glutathione (GSH) (Noctor et al., 1999) and serine (Somerville and Ogren, 1981) synthesis. Hydrogen peroxide (H_2O_2) produced during oxidation of glycolate to glyoxylate catalyzed by glycolate oxidase (GOX) had been shown to participate in hypersensitive response in plant pathogen interactions (Rojas et al., 2012). Importantly, hydrogen peroxide serves as a potent signaling molecule (Levine et al., 1994) that interacts with multiple hormonal pathways (Petrov and Van Breusegem, 2012). Over the last decade, mutant plants defective in peroxisomal CATALASE 2, a major scavenger of photorespiratory H_2O_2, were instrumental in deciphering the transcriptional responses towards hydrogen peroxide accumulation (Vandenabeele et al., 2004; Vanderauwera et al., 2005; Queval et al., 2007; Queval et al., 2012). Increased H_2O_2 levels observed in *cat2* mutants have a direct impact on the cellular redox balance as demonstrated by enhanced glutathione synthesis and low GSH/GSSG ratio (Queval et al., 2007). Under ambient air, CATALASE2-deficient plants exhibit stunted growth accompanied with the formation of cell death lesions (Queval et al., 2007). Next to the CO_2 concentration, the occurrence of these phenotypes is governed by light intensity and photoperiod (Queval et al., 2007; Queval et al., 2012), and depends on SA accumulation (Chaouch et al., 2010).
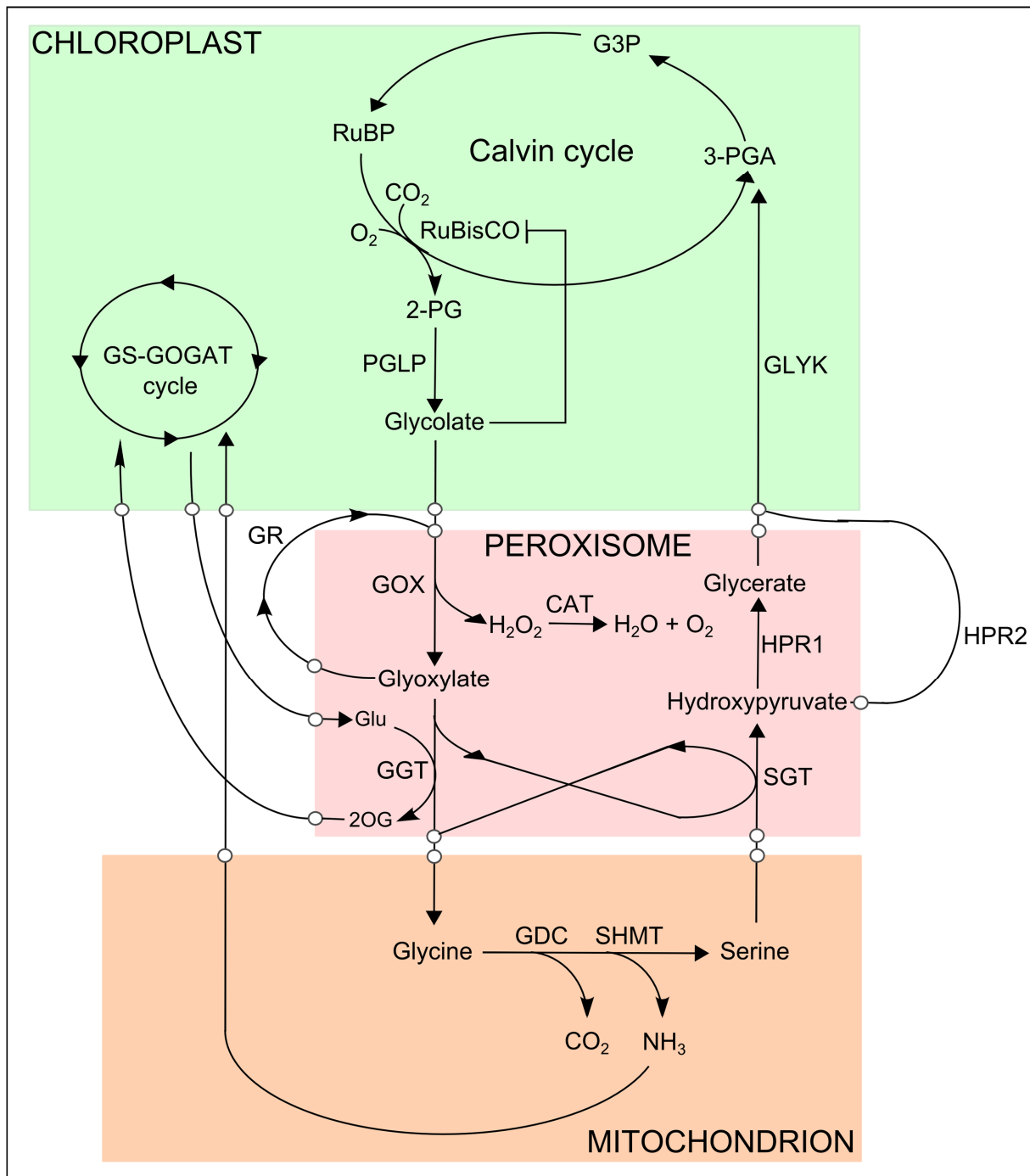
Figure 1. Schematic and simplified representation of photorespiratory metabolism, adapted from Bauwe et al., (2012). RuBisCo, ribulose-1,5-biphosphate carboxylase/oxygenase; PGLP, 2-phosphoglycolate phosphatase; GOX, glycolate oxidase; GR, glyoxylate reductase; CAT, catalase; GGT, glutamate-glyoxylate aminotransferase; GDC, glycine decarboxylase; SHMT, serine hydroxymethyltransferase; SGT serine-glyoxylate aminotransferase; HPR, hydroxypyruvate reductase; GLYK, glycerate kinase; GS, glutamine synthase; GOGAT, glutamine:2-oxoglutarate amidotransferase; RuBP, ribulose 1,5-biphosphate; 2-PG, 2-phosphoglycolate; 2OG, 2-oxoglutarate; 3-PGA, 3-phosphoglycerate; G3P, glyceraldehyde 3-phosphate.

Due to the losses in carbon fixation associated with photorespiratory metabolism this pathway has attracted multiple efforts aiming at reducing its rate. Next to yet unsuccessful efforts towards modification of RuBisCO oxygenase activity (Parry et al., 2013), three independent strategies

targeting downstream photorespiratory reactions were described (Kebeish et al., 2007; Carvalho et al., 2011; Maier et al., 2012). The first approach (Kebeish et al., 2007) is based on heterologous overexpression of *E. coli* enzymes constituting the glycolate catabolic pathway. In this strategy, glycolate is converted to glycerate directly in the chloroplast, which significantly reduces the photorespiratory flux through peroxisomes and mitochondria. Plants that utilize this photorespiratory bypass exhibited improved biomass production and increased sugar content (Kebeish et al., 2007). The next attempt (Carvalho et al., 2011) aimed at reducing the release of ammonia that is produced during conversion of glycine into serine at the mitochondrial stage of the photorespiration. In this peroxisomal bypass glycolate is decarboxylated to tartronic semialdehyde that is directed back into photorespiration by the hydroxypyruvate isomerase. However, despite reducing the necessity of ammonia recycling the application of this approach did not lead to increased biomass accumulation (Carvalho et al., 2011). Similarly to the first approach, the third strategy (Maier et al., 2012) introduced a complete glycolate catabolic cycle in chloroplasts. The pathway comprised of glycolate oxidase, malate synthase and catalase, and was designed to metabolise glycolate into malate that is catalyzed by endogenous enzymes into pyruvate with the release of CO_2 (Maier et al., 2012). This approach remains controversial since no 3-PGA is recycled and therefore the reaction depletes the Calvin cycle from intermediates (Peterhansel et al., 2013). Nevertheless, a growth improvement was reported for transgenics generated in this study (Maier et al., 2012).

Next to the efforts towards avoiding negative consequences of photorespiratory metabolism, numerous studies performed in the past aimed at identifying mutants with elevated tolerance to oxidative stress triggered by other forms of ROS that are often associated with formation of hydrogen peroxide. Methyl viologen (MV), a herbicide that triggers formation of superoxide anions $O_2^{\bullet-}$ at the photosystem I (PSI), was often used as a selection factor for these mutant screening purposes (Chen et al., 2009; Fujita et al., 2012; Xi et al., 2012; Li et al., 2013). However, the majority of mutants identified so far corresponds to proteins that are responsible for the uptake of MV such as PLEIOTROPIC DRUG RESISTANCE 11 (Xi et al., 2012) and RESISTANT TO METHYL VIOLOGEN 1 (Fujita et al., 2012) or transport of this compound from cytoplasm to chloroplast (Li et al., 2013) and therefore present avoidance mechanisms rather than genuine oxidative stress tolerance. This is in contrast to the mutation in the highly conserved S-nitrosoglutathione reductase GSNOR1 that acts downstream of superoxide to regulate cell death (Chen et al., 2009). Additionally, it has been demonstrated that the resistance to MV is positively correlated to a late flowering phenotype such as the one observed in *gi-3* (*gigantea*) mutants (Kurepa et al., 1998) Another treatment used to identify mutants that have altered oxidative stress tolerance was exposure to elevated ozone (O_3) concentrations (Overmyer et al., 2000; Saji et al., 2008; Vahisalu et al., 2008). These efforts lead to the characterization of two genes that upon mutation decrease resistance to oxidative stress namely *RADICAL INDUCED CELL DEATH1* (*RCD1*; Overmyer et al., 2000) and *SLOW ANION CHANNEL-*

ASSOCIATED1 (*SLAC1*); the latter being impaired in O_3 induced stomatal closure which explains its decreased performance under ozone enriched atmosphere (Saji et al., 2008; Vahisalu et al., 2008). On the other hand, the *RCD1* was shown to be involved in control of programmed cell death events (Overmyer et al., 2005). Apart from the effort of Gechev et al., (2013), who described forward genetic screen for mutants with elevated tolerance towards 3-aminotriazole, a potent catalase inhibitor, so far and to the best of our knowledge, there are no reports describing genetic screens to identify mutants with enhanced resistance towards photorespiratory hydrogen peroxide.

When challenged with photorespiratory conditions, CATALASE2-deficient plants exhibit a decline in photosynthetic efficiency and cell death (Queval et al., 2007; Fig. 2). To identify modulators of photorespiratory H_2O_2-induced cell death, we used an EMS-mutagenesis approach to identify mutations that revert this phenotype. We designed a novel high-throughput photorespiratory stress assay and screened approximately 113,000 M2 *cat2-2* seeds for mutations that alleviate the negative effects of enhanced photorespiratory fluxes. We identified 13 mutant lines that demonstrated increased viability under conditions promoting photorespiration. Two of these mutations are mapped in this study and found to reside in genes encoding SHORT-ROOT (SHR) transcription factor and GLYCOLATE OXIDASE 1 (GOX1). We demonstrate that SHR-deficiency induces metabolite rearrangements that via the induction of heterotrophic growth promote survival during photorespiratory stress. Additionally, we highlight GOX1 as the major GOX isoform in the shoot and discuss its potential for engineering oxidative stress tolerance.

RESULTS

ISOLATION OF MUTANTS THAT SUPPRESS PHOTORESPIRATORY H_2O_2-INDUCED CELL DEATH CONDITIONED BY CAT2 DEFICIENCY

A high throughput *in vitro* photorespiratory stress assay

A prerequisite for a successful forward genetics screen is a robust assay to screen large populations of mutant plants for a particular phenotype. Here we developed a high throughput *in vitro* photorespiratory stress bioassay that promotes the production of photorespiratory hydrogen peroxide (Vanderauwera et al., 2012; Kerchev et al., 2014). Wild-type and *cat2-2* mutant plants (Queval et al., 2007) were grown in vitro under long day conditions (16h light/ 8 h dark) at 100 $\mu mol·m^{-2}·s^{-1}$ light intensity, 21°C, on 1 x MS medium supplemented with 1% sucrose. After 3 weeks, the gas exchange in the Petri dishes was blocked by replacement of the surgical tape that sealed the dishes with multiple layers of parafilm (Parafilm M®, Bemis) and subsequently plants were transferred to continuous light and hence the name of the assay, <u>R</u>estricted <u>G</u>as <u>C</u>ontinuous <u>L</u>ight (RGCL). This treatment resulted in a rapid decrease of CO_2 levels inside the plates demonstrated by direct measurement with Dräger CO_2 diffusion tubes (Kerchev et al., 2014). Low CO_2 availability promotes oxygenase activity of RuBisCO,

and consequently enhances production of photorespiratory H_2O_2 which cannot be scavenged efficiently in *cat2-2* mutant plants. Increased H_2O_2 levels were evidenced by DAB staining (Fig 2E) and the induction of H_2O_2 responsive genes (described later in the text).
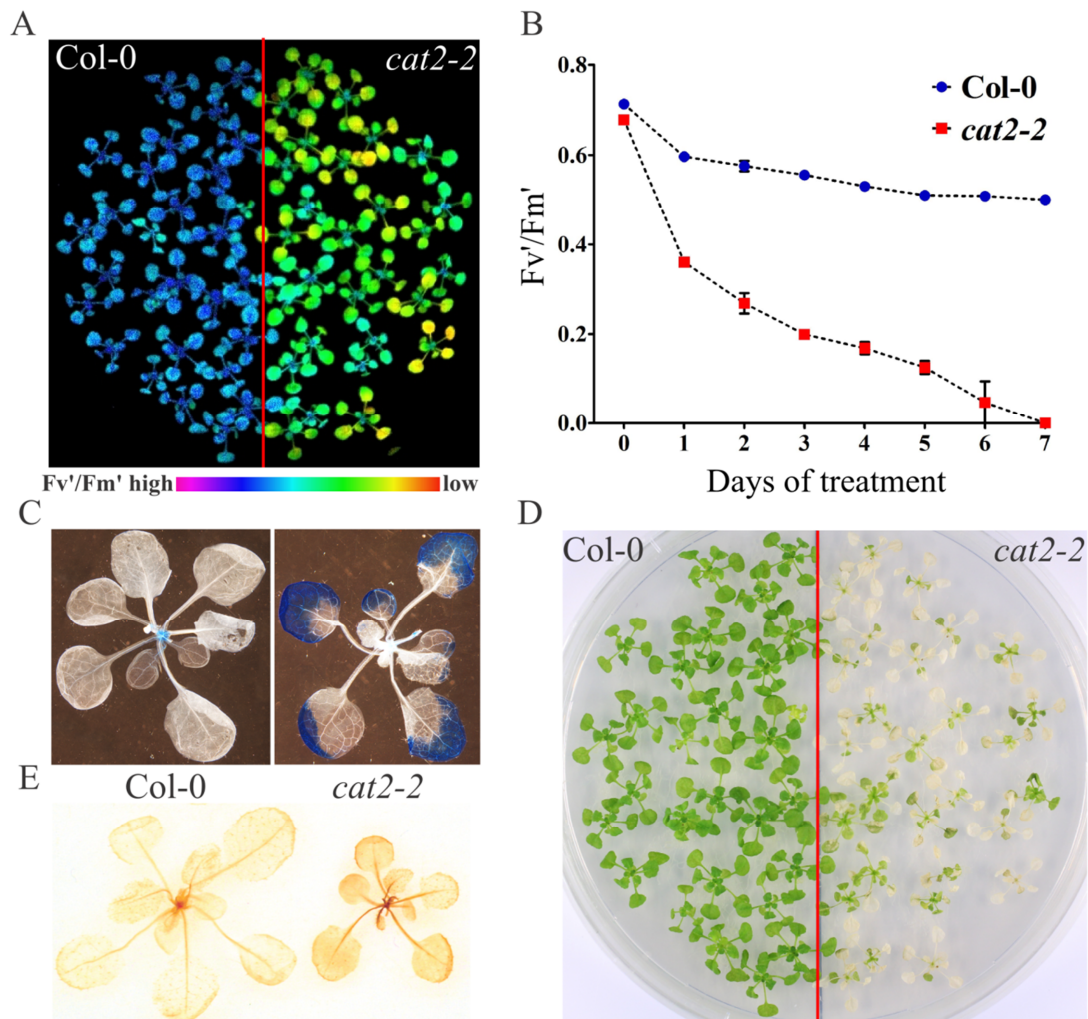

Figure 2. Induction of photorespiratory stress in RGCL assay. Three-week old Col-0 and *cat2-2* plants grown in vitro under control conditions were subjected to photorespiratory stress by mechanical restriction of gas exchange and transfer to continuous light. **A)** PSII maximum efficiency (Fv'/Fm') after 24 hours of treatment. **B)** Changes of Fv'/Fm' during RGCL assay, bars represent means of three biological replicates ± SE. **C)** Cell death progression visualized by trypan blue staining 3 days after the onset of photorespiratory stress. Staining visible in the apex of Col-0 plant corresponds to vasculature **D)** Phenotype of Col-0 and *cat2-2* plants after 7 days of RGCL treatment. **E)** Accumulation of H_2O_2 visualised by 3,3′-Diaminobenzidine staining after 3 days of treatment.

Maximum efficiency of the photosystem II (PSII) photochemistry (Fv'/Fm') was used as an indicator for plant stress (Baker, 2008). After 24 hours of stress treatment the Fv'/Fm' parameter decreased by approximately 50 % in case of *cat2-2* mutant and 15 % in Col-0 wild type plants (Fig. 2 A, B). The progressive decrease in efficiency of PSII photochemistry was followed by the appearance of cell death lesions in CATALASE2-deficient plants after 3 days of treatment as evidenced by trypan blue staining that detects dead plant cells (Fig. 2C). After 7 days, all catalase-deficient plants were dead in contrast to Col-0 wild-type plants, which did not exhibit any visible lesions (Fig. 2D).

Identification of second-site mutations that revert the cell death phenotype of CAT2-deficient plants under oxidative stress conditions

To identify second site mutations capable of reverting the *cat2-2* cell death phenotype within the RGCL bioassay, approximately 12,000 *cat2-2* seeds were subjected to EMS-induced mutagenesis and a total number of 113,000 M2 seedlings were screened with the RGCL assay for improved survival. The selection of mutants was based on their attenuated cell death phenotype and decreased drop of Fv'/Fm'. In a first round, 216 (~0.2%) revertants were rescued from the screen. M3 seeds of 142 plants were retested in the RGCL assay and confirmed the cell death reversion phenotype for 47 mutants (33%). All lines tested showed similar catalase activity levels (approx. 5-7 % of wild-type plants; data not shown) to the original *cat2-2* knockout plants. A total of 13 mutants with most prominent phenotypes were retained for further characterization. Here, two mutants (238.3 and 378.3) were characterized in more detail. Figure 3 shows the oxidative stress related phenotypes of these mutants. Upon RGCL treatment line 238.3 retained higher maximum efficiency of PSII photochemistry and exhibited a one-day delay in formation of lesions when compared to *cat2-2* knockout line. After 7 days of RGCL treatment, a 50% survival rate (47 survivors / 93 plants) was observed for line 238.3 and 84% (86 survivors / 102 plants) for line 378.3 while *cat2-2* control plants
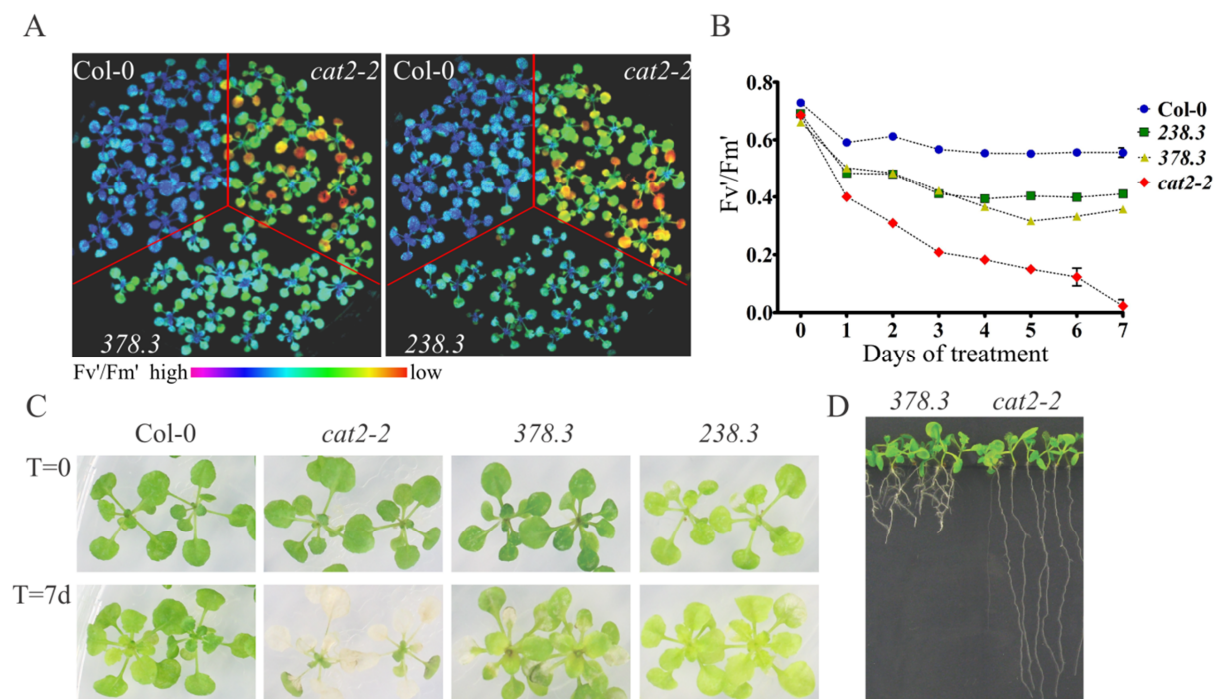
Figure 3. Oxidative stress related phenotypes of 378.3 and 238.3 mutant lines. Three-week old plants grown in vitro under control conditions were subjected to photorespiratory stress by mechanical restriction of gas exchange and transfer to continuous light. **A)** PSII maximum efficiency (Fv'/Fm') after 24 hours of treatment. **B)** Changes of Fv'/Fm' during RGCL assay, bars represent means of three biological replicates ± SE. **C)** Representative images of Col-0, *cat2-2*, 378.3 and 238.3 line before (upper row) and after 7 days (bottom row) of RGCL treatment. **D)** Short root phenotype of line 378.3, plants were grown vertically for two weeks on 1 x MS medium supplemented with 1% sucrose under long day conditions at 100 μmol·m^{-2}·s^{-1}.

exhibited 100% mortality. In 378.3, lesion formation was delayed by three days and the decrease in Fv'/Fm' was significantly lower compared to CAT2-deficient plants (Fig 3A, B, C). In order to understand the genetic basis of the observed phenotypes we sought to reveal the causative mutations in both mutant lines.

Isolation and characterization of *CATALASE 2* mutant in Ler-0 ecotype

Map-based identification of causative mutations requires an introduction of high-density genetic markers that can be achieved by outcrossing the mutant line with a highly divergent ecotype. The most commonly used combination for such positional mapping purposes is Landsberg erecta x Columbia-0 (Lukowitz et al., 2000). It was proven useful for simultaneous mapping and mutation identification with a SHOREmap strategy based on analysis of deep sequencing data from a large pool of F2 recombinants (Schneeberger et al., 2009). To avoid the necessity for pre-screening large numbers of F2 individuals for CAT2 deficiency (as only 25% of obtained F2 individuals would be homozygous for the mutated *CAT2* allele when outcrossing to wild-type Ler-0), we first isolated a *CAT2* knockout line in Ler-0 ecotype to be used as maternal line in the development of mapping populations.
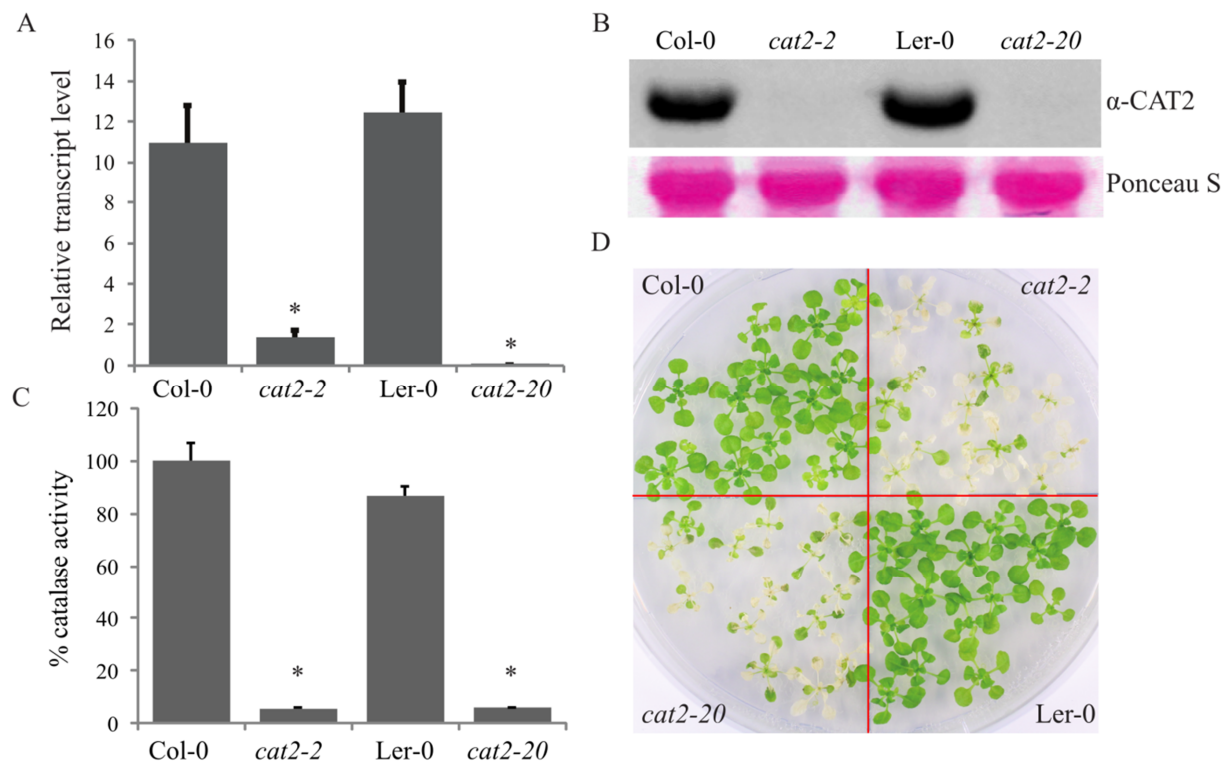
Figure 4. Characterisation of CAT2-deficient Ler-0 mutant (*cat2-20*). Plants were grown in vitro for two weeks on 1 x MS medium supplemented with 1% sucrose under long day conditions at 100 $\mu mol \cdot m^{-2} \cdot s^{-1}$. **A)** Relative *CAT2* transcript levels were analyzed by qRT-PCR. Bars represent means from 3 biological replicates ± SE. Asterisks indicate significant differences to respective control lines (One-way ANOVA followed by Tukey's multiple comparison test, p-value < 0.05). **B)** Immunoblot detection of CATALASE 2 with α-CAT2 antibody. **C)** Measurement of extractable catalase activity. Bars represent percentage of activity related to wild type (Col-0) averaged from 3 biological replicates ± SE. Asterisks indicate significant differences to respective control lines (One-way ANOVA followed by Tukey's multiple comparison test). **D)** Phenotype of *cat2-2* and *cat2-20*, and respective control lines after 7 days of RGCL treatment. Three-week old plants grown in vitro under control conditions were subjected to photorespiratory stress by mechanical restriction of gas exchange and transfer to continuous light.

The enhancer trap line ET8347 carrying a transposable DsE T-DNA insertion in the genomic region corresponding to *CATALASE2* was identified in the TRAPPER collection (http://genetrap.cshl.edu; Sundaresan et al., 1995). The presence and exact location of the DsE element were verified by PCR with genomic DNA and sequencing of PCR products. The genomic sequence was disrupted 4 bp upstream of the *CATALASE 2* start codon (data not shown). The absence of *CAT2* transcript and protein was confirmed by Q-PCR and Western blot analysis (Fig. 4A, B) with α-CAT2 antiserum developed herein (for details, see Materials and Methods). In a spectrophotometric catalase activity assay line ET8347 was shown to exhibit 7% residual activity when compared to Ler-0 WT plants (Fig. 4 C). Finally, the phenotypic response towards RGCL conditions closely resembled that of *cat2-2* plants (Fig 4 D). We concluded that CATALASE 2 is equally important for maintenance of cellular redox balance in Col-0 and Ler-0 accessions and therefore a novel *CAT2* knockout line (hereafter named *cat2-20*) could be used in our mapping strategy.

SECTION I - CHARACTERISATION OF MUTANT 378.3

RESULTS

Identification of the causative mutation 378.3

For the identification of the causative mutation in mutant 378.3, we combined deep sequencing-based discovery of EMS-induced polymorphisms with a positional mapping approach. First, we prepared a nuclear DNA sample from a pool of approximately 200 M3 individuals to construct an Illumina library, which was sequenced to an average 83-fold genome coverage. In total 548 EMS specific polymorphisms (G → A, C → T) were identified of which 210 were located within coding sequences. Within these 210 mutations 159 resulted in nonsynonymous changes causing an amino acid change (149) or leading to the introduction of a premature stop codon (10).

In a complementary approach, we analyzed an F2 mapping population derived from a cross between line *cat2-20* and 378.3 mutant. A total of 1235 F2 individuals were subjected to the RGCL assay and about 25% of plants (289) exhibited reversion of cell death phenotype which fitted the Mendelian 1:3 ratio ($\chi^2 = 2.698$, $p > 0.05$) indicating that the trait was determined by a single recessive mutation. Interestingly, the improved survival perfectly co-segregated with a short-root phenotype, decreased rosette area and increased anthocyanin content (Fig. 3C, D). We then examined the inventory of 378.3 EMS-induced mutations in order to identify candidate mutations for the observed phenotypes. As a result, a mutation introducing a premature STOP codon in a coding sequence of SHORT-ROOT transcription factor (W417X; Fig. S1) was identified as a potential causative factor. SHORT-ROOT (SHR) belongs to a GRAS family of transcription factors and is involved in control of root radial patterning, root growth and leaf development. Null *shr* mutants exhibit terminate root growth resulting from disorganisation of quiescent centre (QC) and consequent loss of stem cell activity (Benfey et al., 1993; Helariutta et al., 2000). Besides strong reduction in primary root growth, *shr* mutants display a severely dwarfed shoot phenotype with a 6.1 fold reduction of rosette size independent from root development (Dhondt et al., 2010). We therefore considered a mutation in *SHR* gene being either the 378.3 causative mutation or tightly linked with the causative factor. To verify our hypothesis, we genotyped 177 F2 individuals that exhibited the revertant phenotype with a CAPS marker detecting the mutation in the SHR gene. In addition, we assessed the prevalence of the nonsynonymous mutation (A311V) in *UDP-GLUCOSYL TRANSFERASE 73B1* (*UGT73B1*), an early salicylic acid-responsive gene (Uquillas et al., 2004), that is localized in the proximity (1.34 Mbp) of *SHR*. All plants tested were positive for *SHR* mutation while the SNP in *UGT73B1* co-segregated with the observed phenotypes incompletely (94% of F2 plants). Next we sought to examine whether the introduction of the *shr-6* null allele (Dhondt et al., 2010) into *cat2-2* background would mimic the oxidative stress related phenotype of 378.3 mutant. In agreement with our genetic analysis
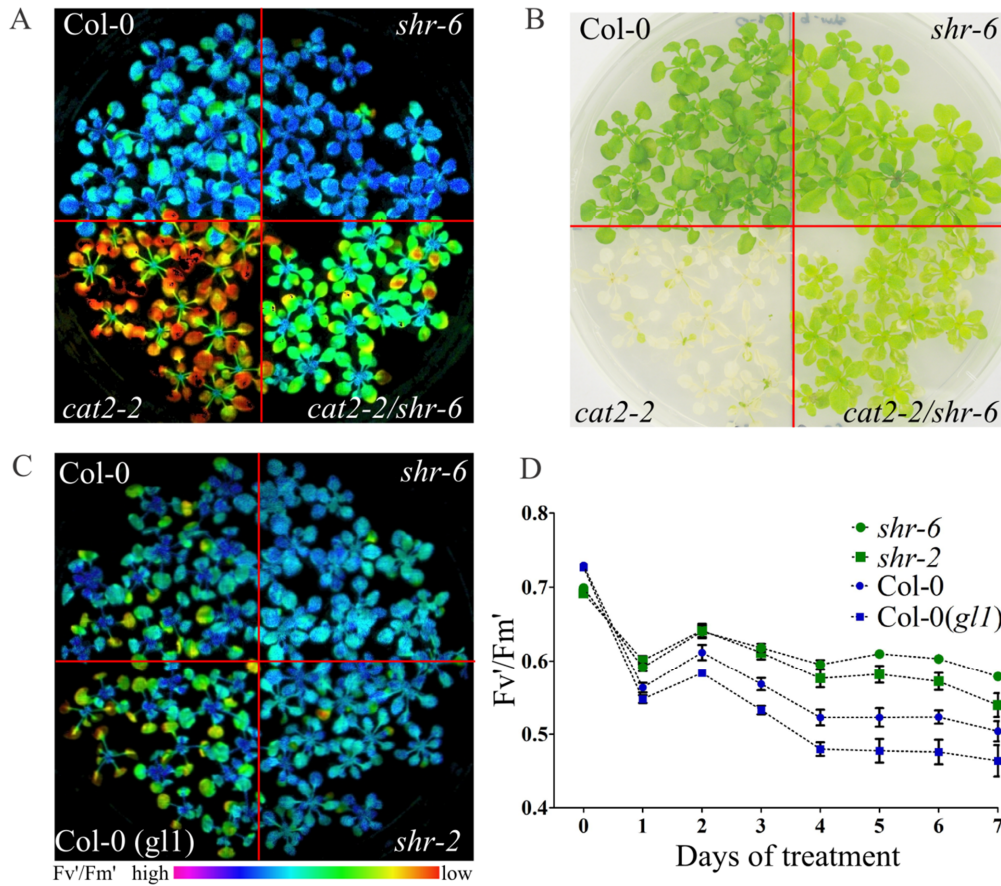
Figure 5. SHORT-ROOT deficiency influences oxidative stress tolerance. Three-week old plants grown under long day conditions at 100 μmol·m^{-2}·s^{-1} on 1 x MS medium supplemented with 1% sucrose were subjected to photorespiratory stress by mechanical restriction of gas exchange and transfer to continuous light. **A)** Introduction of *shr-6* mutation into *cat2-2* background reverts oxidative stress related phenotypes in RGCL conditions, PSII maximum efficiency after 2 days of treatment. **B)** Representative image of Col-0, *cat2-2*, *shr-6* and *shr-6/cat2-2* line after 7 days of RGCL treatment. **C)** *shr* mutants outperform wild type plants in RGCL conditions, PSII maximum efficiency after 7 days of treatment. **D)** Changes of Fv'/Fm' during RGCL assay, bars represent means of three biological replicates ± SE.

cat2-2/shr-6 double knockout line exhibited reversion of cell death when subjected to RGCL assay (Fig. 5 A, B). Strikingly, independent shr mutant lines *shr-6* and *shr-2* perform significantly better in photorespiratory promoting conditions when compared to respective wild type plants (Fig. 5 C, D). However, after the onset of the treatment both *shr* mutants and *shr-6/cat2-2* plants exhibited progressive yellowing of the leaves, most probably due to the loss of chlorophyll (Fig. 5B).We concluded that a missense mutation in SHR coding sequence is responsible for the reversion of cell death phenotype in mutant 378.3. Interestingly, when tested in a WT background independent *shr* mutant lines *shr-6* and *shr-2* exhibited increased resistance to photorespiratory stress when compared to respective control plants (Fig. 5 C, D). Interestingly, after the onset of the treatment both *shr* mutants as well as *shr-6/cat2-2* plants displayed progressive yellowing of the leaves, most probably due to the loss of chlorophyll (Fig. 5 B). All together, our genetic and physiological studies provide evidence for the modulation of oxidative stress response by the SHORT-ROOT transcription factor.

SHORT-ROOT modulates oxidative stress tolerance independently of root size

SHORT-ROOT is a key player in the determination of radial patterning and indeterminacy of primary root growth (Benfey et al., 1993; Helariutta et al., 2000). We therefore set out to elucidate whether the oxidative stress related phenotype of *shr* plants could be explained by compromised root growth. We compared the oxidative stress tolerance of *cat2-2* and Col-0 WT plants in which the root length was reduced to the same extent as in *shr-6* mutant line. For this, roots of vertically grown plants were cut to the length of ~ 2 cm every 3 DAS, during the 12-days growth period. Subsequently, plants were subjected to the RGCL assay. Truncating of roots did not enhance the oxidative stress tolerance of *cat2-2* and Col-0 plants as evidenced by a decrease in Fv'/Fm' comparable to that of intact plants (Fig. S2). Therefore, it is unlikely that the observed phenotypes might be related to a reduced root size. It had been demonstrated that decreased levels of SHR protein observed in hybrid poplar *P. tremula* x *P. tremuloides* (RNAi knockdown, 20 - 80 % res. transcript level) and *A. thaliana* (heterozygous for *shr-2* allele), positively influence growth and fresh weight (Wang et al., 2011; Koizumi et al., 2012). Therefore, we investigated whether there is a link between oxidative stress tolerance and growth promoting effects of moderate SHR levels. For this, we have examined the oxidative stress performance of F1 seedlings from crosses Col-0 x *shr-6* and *cat2-2* x *cat2-2/shr-6*. Both F1 populations developed at an accelerated rate as demonstrated by a 23 % and 27 % increase in projected rosette area for plants heterozygous for *shr-6* mutation in Col-0 and *cat2-2* background respectively (Fig. S3A). However, the oxidative stress performance of F1 plants closely resembles that of parental lines (Fig. S3B). In the light of these observations we concluded that dose-dependent growth-promoting effects of SHR do not enhance oxidative stress tolerance. Together, our physiological and genetic experiments provide evidence that the oxidative stress tolerance of *shr* plants is due to the complete, rather than partial, loss of the SHR function in the shoot.

SHORT-ROOT deficiency leads to sugar-dependent oxidative stress tolerance

To evaluate the impact of SHORT-ROOT deficiency on oxidative stress performance in more physiologically relevant conditions we tested whether the reversion of cell death phenotype conferred by lack of SHR function also occurs in soil grown plants. For this, 378.3 BC4 and *cat2-2/shr-6* plants were grown together with respective control plants for 21 days under a long day (16 h light/8 h dark) photoperiod at elevated CO_2 concentration (3000 ppm). These conditions were shown to limit photorespiration and consequently hamper the induction of cell death lesions and H_2O_2 responsive transcripts in *cat2-2* mutant (Queval et al., 2007). Next, plants were transferred to ambient air (300-400 ppm CO_2) and exposed to continuous excess light irradiation (1100-1200 $\mu mol \cdot m^{-2} \cdot s^{-1}$) for 24 hours. This resulted in a dramatic reduction of maximum efficiency of PSII and the formation of cell death lesions in the *cat2-2* line, with both symptoms generally limited to mature tissues. The progression of cell death was most pronounced at the tips of mature rosette leaves, while

the young emerging leaves were protected. Similarly, the highest decrease in Fv'/Fm' parameter was observed for old leaves (Fig. 6). Strikingly, the lack of SHR function did not revert these phenotypes as both *cat2-2/shr-6* and 378.3 BC4 mutant lines displayed cell death symptoms similar to those of *cat2-2* (Fig 6). These results are in contrast to those observed in RGCL assay, and hence indicate that SHR deficiency does not lead to enhanced oxidative stress tolerance in soil conditions.

The application of exogenous sugars had been shown to induce tolerance towards atrazine-induced oxidative stress injury, and similarly, the pre-stress carbohydrate status is linked to oxidative stress tolerance (Ramel et al., 2009a; Ramel et al., 2009b). Therefore, we set out to investigate whether lack of SHR enhances oxidative stress tolerance in RGCL conditions when grown on a sugar-free medium. Interestingly, the *shr-6* mutant line exhibited abnormal development when grown on medium with no sucrose. Plants were chlorotic with necrotic lesions and the growth rate was significantly reduced when compared to the growth on sucrose supplemented medium. Additionally, a fraction of seedlings exhibited growth arrest at the early post-embryonic growth stage (Fig. S4). In order to avoid the influence of pre-stress conditions, plants were first grown on nylon mesh membranes placed over medium supplemented with 1% sucrose and transferred to a sugar-free medium three days before the RGCL treatment. In these conditions the *cat2-2/shr-6* double mutant exhibited decreased oxidative stress tolerance compared to *cat2-2* line. Furthermore the *shr-6* mutant line displayed a significant drop in Fv'/Fm' parameter followed by appearance of cell death lesions similar to that of *cat2-2* mutant after five days of RGCL assay (Fig. 7 A - D). Our results indicate that exogenous sugar supplementation is a pivotal factor that determines the tolerance of *shr-6/cat2-2* double mutants towards photorespiratory stress. The lack of SHORT-ROOT negatively influences oxidative stress tolerance under autotrophic growth conditions, which clearly indicates a novel function for this transcription factor.

Lack of SCARECROW does not lead to sugar-dependent oxidative stress tolerance

To better understand the mechanism of SHR-sucrose interaction we sought to investigate the oxidative stress tolerance mediated by downstream targets of SHR. The SCARECROW (SCR) transcription factor acts directly downstream of SHR as SHR binds to the *SCR* promoter positively regulating its expression (Levesque et al., 2006; Cui et al., 2007). Furthermore, the scr mutants exhibit a similar phenotype to that of shr plants as demonstrated by reduced root length and rosette size (Di Laurenzio et al., 1996; Dhondt et al., 2010). *SCR* expression is reduced in *shr* background both in root and shoot tissues (Helariutta et al., 2000; Dhondt et al., 2010) and a great majority of transcripts differentially expressed in *shr* are also affected in *scr* (Dhondt et al., 2010). We therefore tested the oxidative stress performance of *scr-3/cat2-2* double mutants. Surprisingly, the introduction of *scr-3* mutation into *cat2-2* background not only did not revert the cell death phenotype, but further decreased the oxidative stress tolerance of *cat2-2* line in RGCL conditions (Fig 8A, C). The reversion was also not observed in soil after high light treatment (Fig. S5).
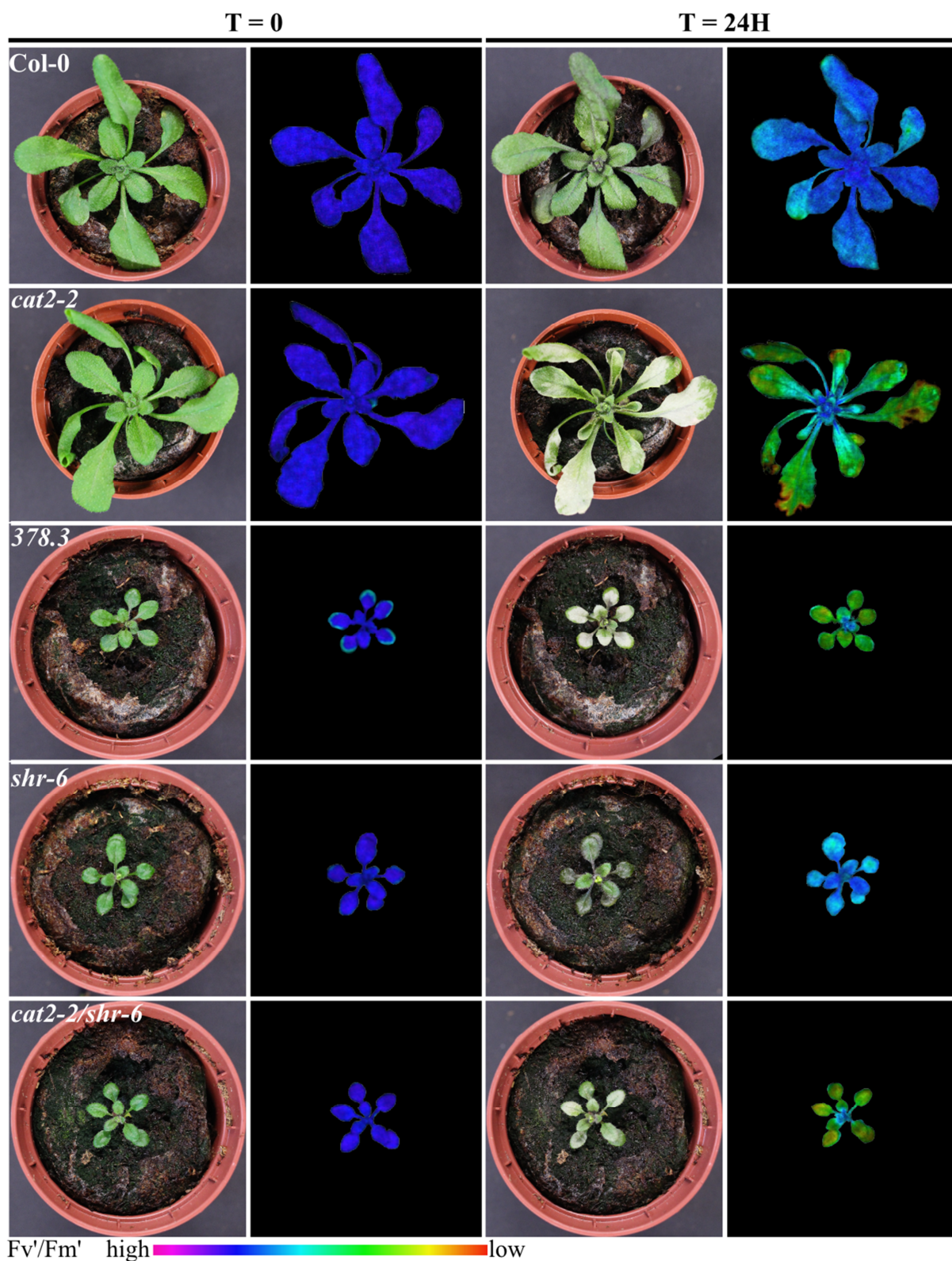
Figure 6. SHORT-ROOT deficiency does not lead to enhanced oxidative stress tolerance in soil conditions. Plants were grown for three weeks under long day photoperiod (120-130 $\mu mol \cdot m^{-2} \cdot s^{-1}$) at elevated CO_2 concentration (3000 ppm) and subsequently exposed to 24 hours of continuous excess light irradiation (1100-1200 $\mu mol \cdot m^{-2} \cdot s^{-1}$) in ambient air. Representative images demonstrate formation of cell death lesions and reduction of PSII maximum efficiency.
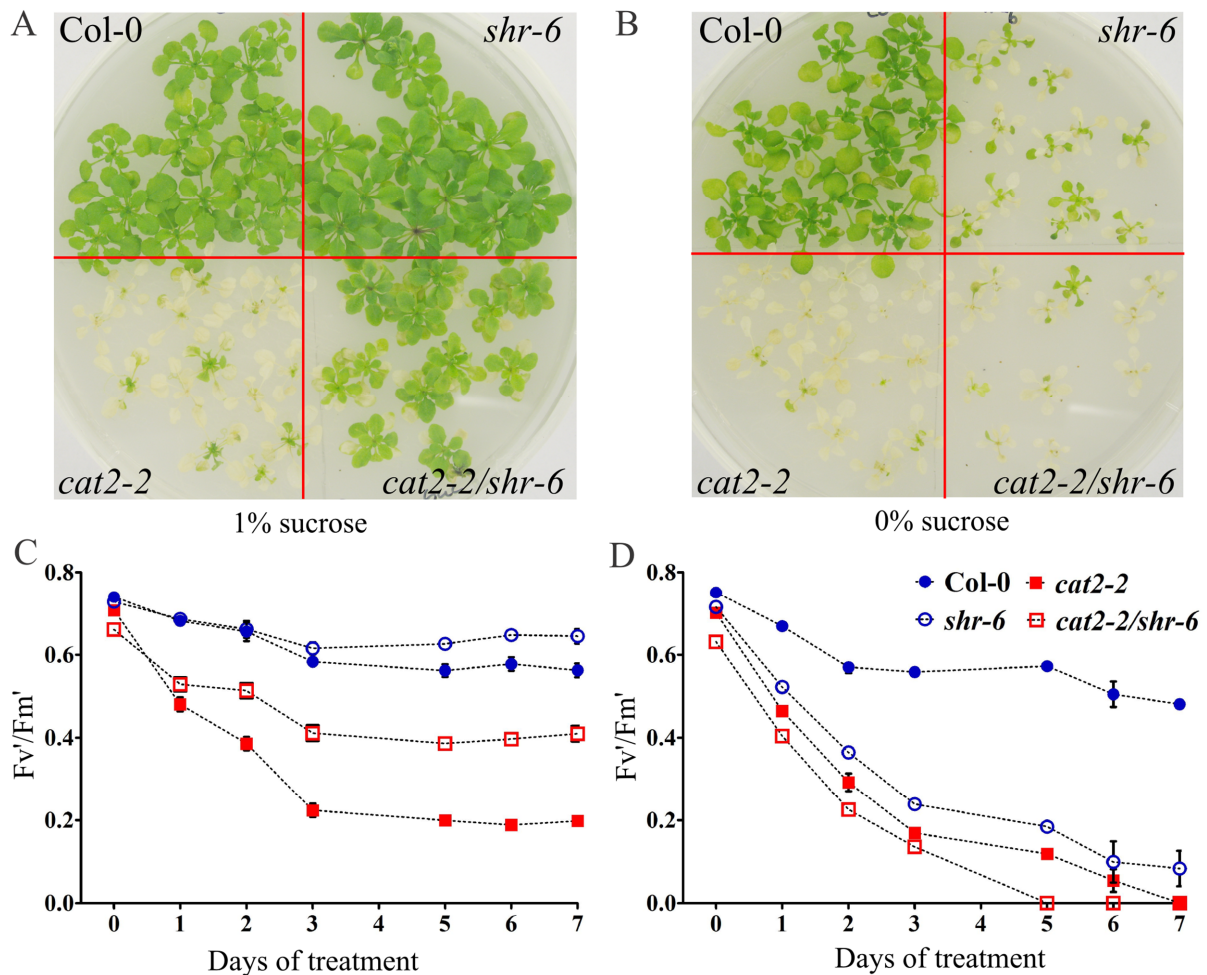
Figure 7. Exogenous sucrose supplementation determines tolerance of *shr* mutants towards oxidative stress. Plants were grown under long day conditions at 100 μmol·m^{-2}·s^{-}1 on nylon mesh membranes placed over medium supplemented with 1% sucrose and transferred to 1% sucrose (**A, C**) or 0% sucrose (**B, D**) medium three days before the RGCL treatment. **A, B)** Images illustrating cell death lesions after 7 days of RGCL treatment. **C, D)** Changes of Fv'/Fm' during RGCL assay, bars represent means of three biological replicates ± SE.

Additionally, mutant lines *scr-3* and *scr-1* exhibited significantly reduced oxidative stress tolerance in RGCL assay when compared to respective control lines Col-0 and Ws-0 respectively (Fig. 8B, D). These data indicate that SHR acts independently from SCR in modulating sugar-related oxidative stress tolerance.

Transcript profiling reveals distinct responses of SHR-deficient plants to oxidative stress

Next, we set out to investigate the molecular basis of the observed phenotypes. Affymetrix ATH1 microarrays were used to perform a genome-wide transcriptome analysis on shoot tissue of *cat2-2* and *shr-6/cat2-2* plants that were grown *in vitro* for three weeks and subsequently subjected to the RGCL assay for 24 hours. Principal component analysis demonstrated high consistency between biological replicates (Fig. 9A). Using a false discovery rate of 0.05 and a 2-fold expression level cut-off we identified 438 and 1328 genotype- and treatment-responsive genes (Table S1). 63 genes responded to RGCL treatment in a genotype specific manner (Table S2).
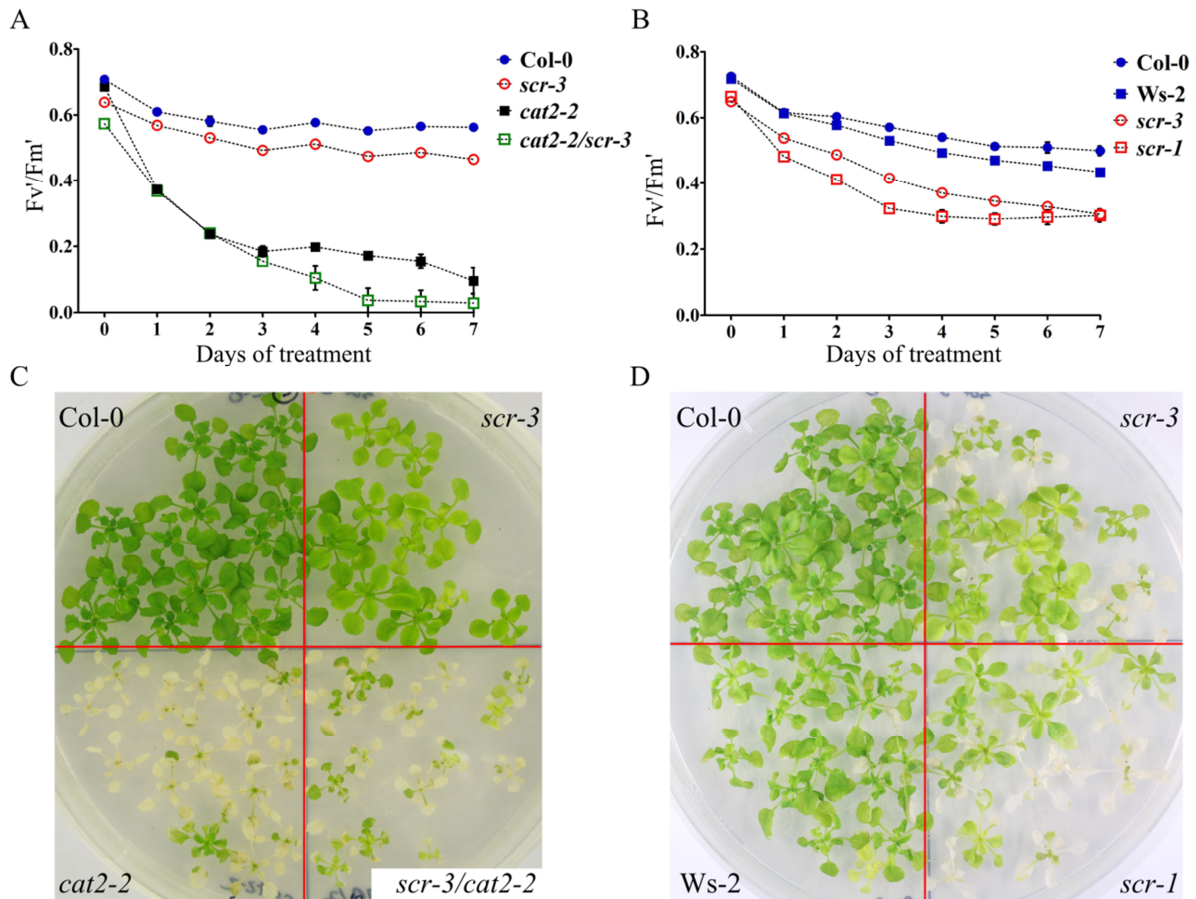
Figure 8. Lack of SCARECROW negatively influences oxidative stress tolerance. Three-week old plants grown under long day conditions at 100 μmol·m^{-2}·s^{-1} on 1 x MS medium supplemented with 1% sucrose were subjected to photorespiratory stress by mechanical restriction of gas exchange and transfer to continuous light. **A, B)** Comparison of changes in PSII maximum efficiency during RGCL assay for **(A)** *Col-0*, *scr-3*, *cat2-2*, *scr-3/cat2-2* **(B)** *scr-3, scr-1* and respective control lines. Bars represent means of three biological replicates ± SE. **C, D)** Images illustrating cell death lesions after **(C)** 7 days and **(D)** 13 days of RGCL treatment.

Comparison of genes affected by SHR deficiency in a genotype specific manner with gene expression pattern identified in similar study performed on *shr-6* shoot tissue in wild-type genetic background (Dhondt et al., 2010) exhibited an overlap between the two signatures (33% of up-regulated and 27% of down-regulated genes; Fig. 9B). To identify mutations or treatments that most closely resemble the transcriptomic response to SHR deficiency, a comparative data analysis was performed between highly significant transcripts (p-value < 0.001; log2 ratio ≥1.5, 106 transcripts up- and 34 down-regulated) and all publicly available Affymetrix microarray data sets using the Signature tool in Genevestigator (Hruz et al., 2008). Top 10 most similar microarray experiments are listed in Table S3. The highest similarity was revealed between SHR-deficiency and microarray experiment investigating transcriptome of *Arabidopsis* cytokinin receptor *HISTIDINE KINASE 2, 3, 4* triple mutant *ahk2/ahk3/ahk4* (ArrayExpress accession no. E-MEXP-1262) as well as *SET DOMAIN GROUP 2* (*sdg2-1*) mutant (Gene Expression Omnibus accession no. GSE23208; Guo et al., 2010).
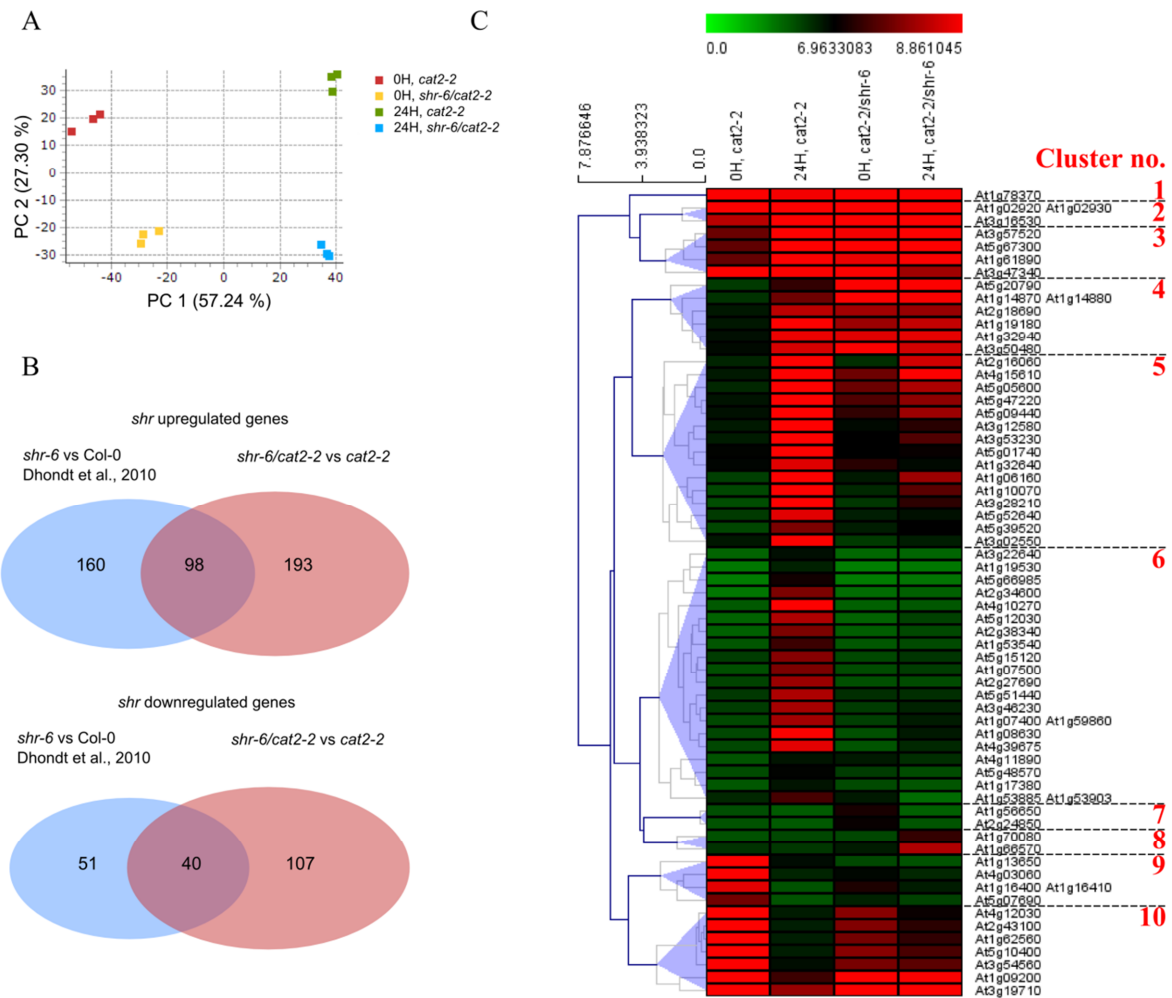
Figure 9. Lack of SHORT-ROOT affects transcriptomic response to oxidative stress conditions. **A)** Principal component analysis of transcriptomic profiles of *cat2-2* and *shr-6/cat2-2* lines before and after oxidative stress treatment. **B)** Comparison of *shr* responsive genes identified herein with previous data (Dhondt et al., 2010). **C)** Hierarchical clustering of 63 genes that responded to RGCL treatment in a genotype-specific manner with a distance threshold set to 3.7. See Table S2 for gene annotation.

Strikingly, five mutants transcriptionally resembling SHR-deficiency were shown to exhibit developmental abnormalities leading to a dwarf phenotype and altered root morphologies: *ahk2/ahk3/ahk4* (Nishimura et al., 2004), *sdg2* (Guo et al., 2010), *OBERON1/2* double mutant *obe1/obe2* (Saiga et al., 2008; Thomas et al., 2009), *Arabidopsis RESPONSE REGULATOR 20 (ARR20)* overexpression line (Kiba et al., 2004) and double mutant of plastidial *GLYCERALDEHYDE 3-PHOSPHATE DEHYDROGENASE* (*gapcp1/gapcp2)* (Muñoz-Bertomeu et al., 2009). Next to these perturbations a significant similarity was found for studies dealing with Pi starvation (Misson et al., 2005), cold treatment of *INDUCER OF CBF EXPRESSION 1* (*ice1*) mutant (Lee et al., 2005) as well as transcriptomic profiling of *IMMUTANS* (*im*) green sectors (Aluru et al., 2009). Together, our comparative study suggests that transcriptomic patterns evoked by the introduction of *shr-6* mutation into *cat2-2* background are similar to mutations leading to abnormal development and bears signatures of impaired cytokinin signaling. Next, we sought

to identify physiological or genetic conditions that most closely resemble the transcriptomic signature provoked by the RGCL assay. Due to the limitations of Gevestigator Signature tool (max. input = 400 genes) a stringent gene selection was applied (p-value < 0.001; log2 ratio ≥ 2; 144 transcripts up- and 63 down-regulated) and resulting subset was subjected to comparative data analysis as described before. The highest similarity was revealed between RGCL and nine microarray experiments dealing with late (53 → 93 hours) responses to nicotinamide supplementation in the context of disturbed circadian clock regulation (GEO acc. no. GSE19271; Dalchau et al., 2010). The genetic perturbation that most closely resembled the RGCL signature was a mutation in *SPEECHLESS* (*spch*) a bHLH transcription factor necessary for stomata differentiation. The RGCL transcriptomic pattern was also significantly similar to responses evoked by treatment with clothianidin and imidacloprid two neonicotinoid insecticides that induce salicylate-associated plant defense responses (GEO acc. no. GSE20188; Ford et al., 2010). Surprisingly, among the significantly similar gene expression patterns we did not identify "classical" experiments dealing with oxidative stress (Gadjev et al., 2006) which might suggest that a large fraction of differentially regulated genes responds to a change in the photoperiod conditions (long day → continuous light).

In a next step, we focused on transcripts that respond to RGCL treatment in a genotype specific manner. Hierarchical clustering of 63 differentially responsive genes (Table S2) revealed distinct responses that are clustered into 10 groups based on their expression profiles (Fig. 9C). The largest cluster (no. 6) containing almost one-third of identified genes (20) comprises of genes up-regulated in response to RGCL treatment in *cat2-2* line, but not induced in *shr-6/cat2-2* double knockout. The biggest gene ontology (GO) group within this cluster was "response to heat" ($p = 7.3e^{-6}$) represented by 5 heat shock proteins. Interestingly, another significant GO group was "transcription" ($p = 3.6e^{-1}$) represented by *JASMONATE-ZIM-DOMAIN* (*JAZ*) *5 & 7* and *DEHYDRATION RESPONSE ELEMENT-BINDING PROTEIN 19* (*DREB19*). The opposite direction of transcriptional regulation was observed for cluster 8 comprising of *SUCROSE-PROTON SYMPORTER 7* and *AT1G70080* encoding for terpenoid cyclase class superfamily protein. Similarly to cluster no. 6, genes grouped in cluster 5 (15 genes) were highly up-regulated in *cat2-2* line by RGCL treatment with a moderate response in *shr-6/cat2-2* line. Interestingly, this cluster is also significantly enriched in genes related to jasmonate signaling with "response to jasmonic acid stimulus" group ($p = 7.1e^{-3}$) represented by *ETHYLENE RESPONSE FACTOR 2 & 59* and *JASMONATE INSENSITIVE 1* (*JIN1, MYC2*). Together, our transcriptomic study indicates that a large fraction of transcriptomic response present in *cat2-2* line (of which a significant part is involved in JA signaling) is abolished or diminished by introduction of *shr-6* mutation (discussed later in the text).

Lack of SHR results in hyperaccumulation of glycolate and phosphate deficiency

We performed a metabolite analysis on Col-0 and *cat2-2*, *shr-6*, *cat2-2/shr-6* mutant lines under control and oxidative stress conditions. Plants were grown in conditions identical to those applied in the transcriptomic study. For each genotype, shoot tissue was harvested before, and after 24 h of oxidative stress treatment. Analysis of polar metabolites was performed with gas chromatography-mass spectrometry (GC-MS). Interestingly, we found that the levels of photorespiratory metabolites such as glycolate, glycine and serine were significantly affected by SHR depletion (Fig. 10 A-C). Under control conditions, *cat2-2/shr-6* double mutant accumulated glycolate at a level 9-fold higher than that of Col-0. Single knockouts *cat2-2* and *shr-6* also exhibited elevated levels (albeit not statistically significant). Application of RGCL treatment did not affect the glycolate level in Col-0 plants in sharp contrast to *cat2-2*, *shr-6* and *cat2-2/shr-6* lines in which glycolate levels were 3.3-, 5.5- and 70-fold higher when compared to Col-0 line respectively. An opposite trend was observed for glycine. Under control conditions both *shr-6* and *shr-6/cat2-2* mutants exhibited levels of Gly that were ~3 times lower than that of Col-0 and *cat2-2* lines. RGCL treatment led to ~7 fold increase of Gly levels in the Col-0 line in contrast to the *cat2-2* mutant that exhibited no increase. SHR deficiency in both Col-0 and *cat2-2* background had a negative impact on Gly accumulation reaching 33% and 42% of the levels in respective control lines. In contrary to glycolate and glycine, serine levels were largely unaffected by oxidative stress treatment. However under both control and stress conditions CAT2-deficient lines exhibited significantly higher levels of this intermediate although markedly lower in *shr-6/cat2-2* double mutant. It is noteworthy that serine biosynthesis occurs also via non-photorespiratory routes i.e. glycerate pathway and phophorylated pathway (Ros et al., 2012) that might possibly compensate for the loss of serine generated in photorespiratory pathway. RGCL treatment influenced levels of branched-chain amino acids (BCAA) and phenylalanine (Fig. 10 D-G). Under control conditions all four amino acids (Val, Leu, Ile, Phe) were slightly increased in *cat2-2*, *shr-6* and *shr-6/cat2-2* line when compared to Col-0 line. Oxidative stress led to a significant increase in levels of these AA in Col-0 and to a much higher extent in *cat2-2* line. SHR deficiency impaired this induction completely. The opposite situation could be observed in case of metabolites commonly associated with responses to environmental stress such as proline (Szabados and Savouré, 2010) and putrescine (Cuevas et al., 2008; Alet et al., 2011). Both SHR-deficient lines accumulated these metabolites to a much higher extent than respective control lines (Fig. 10 H, I) although their content was generally not responsive to oxidative stress treatment. Another metabolite affected by SHR-deficiency was myo-inositol (Fig. 10 J). Low levels of this compound in *cat2-2* line were previously correlated with cell death (Chaouch and Noctor, 2010) and mutants defective in myo-inositol biosynthesis display spontaneous lesion formation (Donahue et al., 2010). Interestingly, the introduction of *shr-6* mutation into *cat2-2* background completely reverted the myo-inositol deficiency raising its level to ~ 125% of the wild type value. In agreement with our microarray analysis that
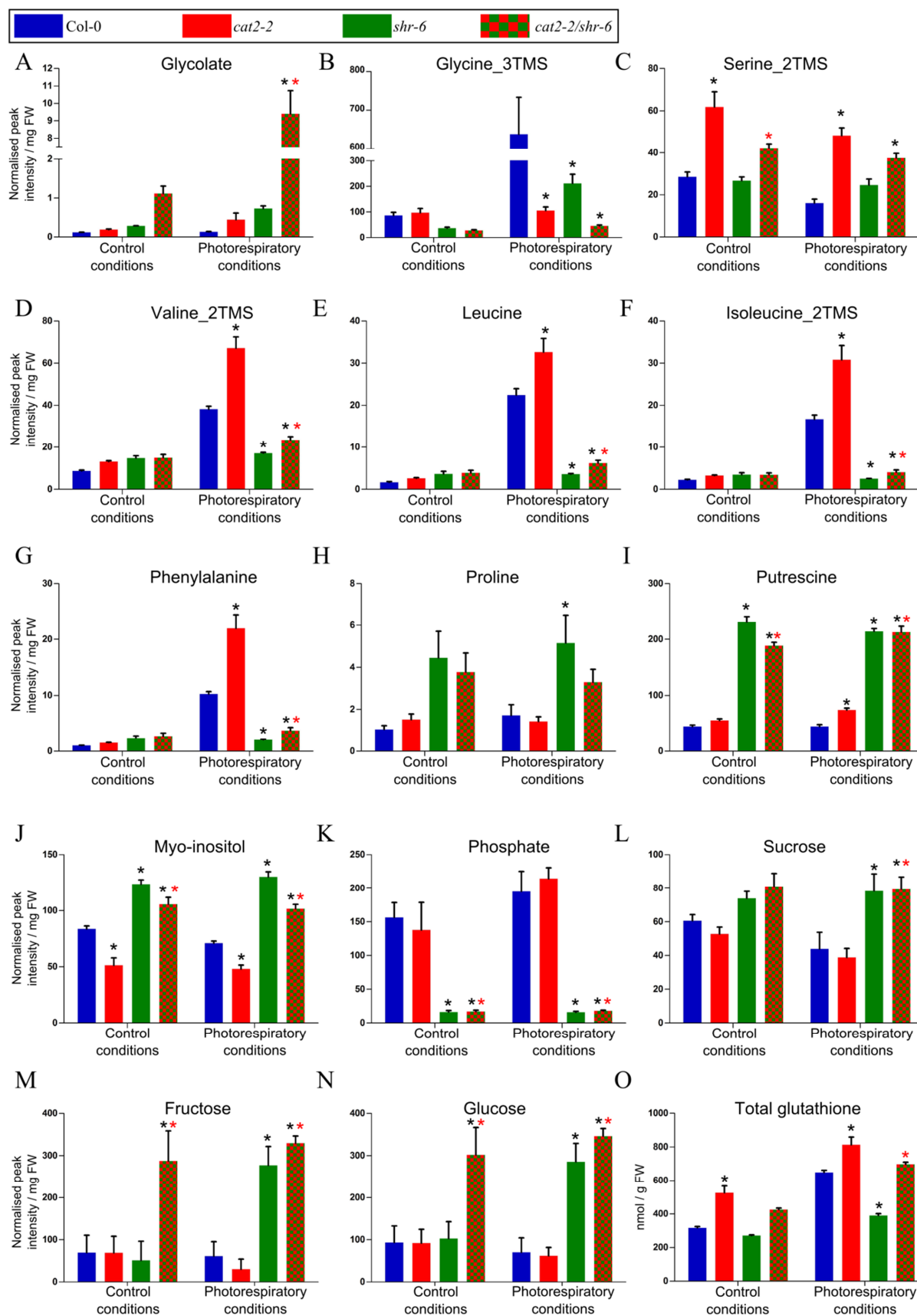
Figure 10. SHORT-ROOT deficiency affects metabolite rearrangements in *cat2-2* mutant plants during photorespiratory stress (continued on next page).

identified transcriptomic response to phosphate starvation in *shr-6/cat2-2* double mutant line the metabolic analysis demonstrated that SHR deficiency results in a severely reduced shoot phosphate content (Fig. 10 K).Under both control and stress conditions phosphate levels in *shr-6* and *shr-6/cat2-2* line were reduced by approximately 10 fold when compared to Col-0 and *cat2-2* control lines. Moreover, as indicated earlier (Cui et al., 2012), we found that lack of SHORT-ROOT influences carbohydrate metabolism (Fig. 10 L-N). Under control conditions sucrose content was slightly elevated in SHR-deficient lines and remained at nearly the same level after RGCL treatment while dropping significantly in both Col-0 and *cat2-2* line. On the contrary, RGCL treatment had positive influence on fructose and glucose levels in SHR-deficient lines (Fig. 10 M-N). Under control conditions, *shr-6/cat2-2* double mutant line accumulated these sugars to a significantly higher level than the remaining lines. Oxidative stress induced accumulation of Glu and Fru in *shr-6* line and a slight decrease in Col-0 and *cat2-2* line. At present we are not able to explain these remarkably high levels of Glu and Fru observed in *shr-6/cat2-2* line under control and stress conditions. Considering the fact that this mutant is not capable of *in vitro* autotrophic growth it is plausible that these sugars originate from the growth medium. Additionally, we observed significant alterations in the levels of TCA cycle intermediates as demonstrated by highly increased content of citrate and malate in SHR-deficient lines (Fig. S6).

Accumulation of glutathione serves as a well-established hallmark of oxidative stress and has been documented before for *cat2-2* mutants (Queval et al., 2007). In order to estimate the influence of SHR deficiency on cellular antioxidant potential, we complemented our metabolomic survey with measurements of glutathione content (Queval and Noctor, 2007). As expected, the total level of this antioxidant was markedly higher in *cat2-2* line already in control conditions and exhibited positive correlation with RGCL treatment. Surprisingly, the *shr-6* line was impaired in stress-related glutathione accumulation (Fig. 10 O). Furthermore, the introduction of *shr-6* mutation into *cat2-2* background significantly diminished glutathione content. Taken together, our metabolome analysis indicates that lack of SHORT-ROOT leads to pleiotropic effects demonstrated by changes in multiple metabolic pathways.

Figure 10. (continued) Three-week-old Col-0, *cat2-2*, *shr-6* and *shr-6/cat2-2* mutant plants grown on 1 x MS medium supplemented with 1% sucrose were sealed with parafilm and moved to continuous light. Rosettes were harvested before and after 24 hours of treatment. Values represent means of 5 biological replicates ± SE. Data were analyzed with two-way ANOVA using photorespiratory stress (photorespiratory conditions vs control conditions) and genotype as main factors, and followed by Bonferroni multiple comparisons post-hoc test ($p < 0.05$). Black asterisks (*) show significant differences to Col-0, red asterisks (*) mark significant differences between *cat2-2* and *shr-6/cat2-2* line within respective conditions. **A-N)** GC-MS profiling of polar metabolites. **O)** Quantification of total glutathione level (GSH + GSSG) performed according to (Queval and Noctor, 2007).

SHORT-ROOT deficiency influences the photorespiratory pathway and CO$_2$ assimilation

We have shown that under both control and stress conditions, plants lacking SHR hyperaccumulate glycolate. High levels of this metabolite were previously shown to inhibit the RuBisCO activity and to decrease CO$_2$ fixation (Gonzalez-Moro et al., 1997).Therefore we sought to investigate CO$_2$ photoassimilation in *shr-6* and *cat2-2/shr-6* double mutant line. As reversion of *cat2-2* phenotype by SHORT-ROOT deficiency is sugar dependent we decided to perform gas exchange measurements on plants grown on sucrose-supplemented medium. For this, three-week-old in vitro grown seedlings were subjected to analysis of CO$_2$ fixation (see Materials & Methods). The photosynthetic performance of *shr-6* and *cat2-2/shr-6* lines was significantly lower compared to Col-0 plants, reaching only 63% and 45% of wild type level respectively while a *cat2-2* line exhibited only slight decrease in CO$_2$ assimilation (Fig. 11 A). Given that SHR deficiency leads to reduced photosynthetic performance and decreased levels of intermediate photorespiratory metabolites such as serine and glycine we set out to investigate levels of glycolate oxidase (GOX) and catalase, two enzymes participating in the peroxisomal phase of the photorespiratory pathway. Strikingly, activities of both enzymes were significantly reduced in *shr-6* line with a 60% and 40% decrease for GOX and CAT activity respectively (Fig. 11 B, C; the low activity of GOX in *cat2-2* line is discussed in the 238.3 result section). In support of our metabolome profiling data, both physiological and biochemical experiments conducted herein indicate that SHR deficiency leads to the deregulation of the photorespiratory pathway, which might affect the rate of photosynthesis. Accumulation of glycolate and low abundance of downstream photorespiratory metabolites together with partial requirement for exogenous sucrose supplementation to support post-embryonic growth
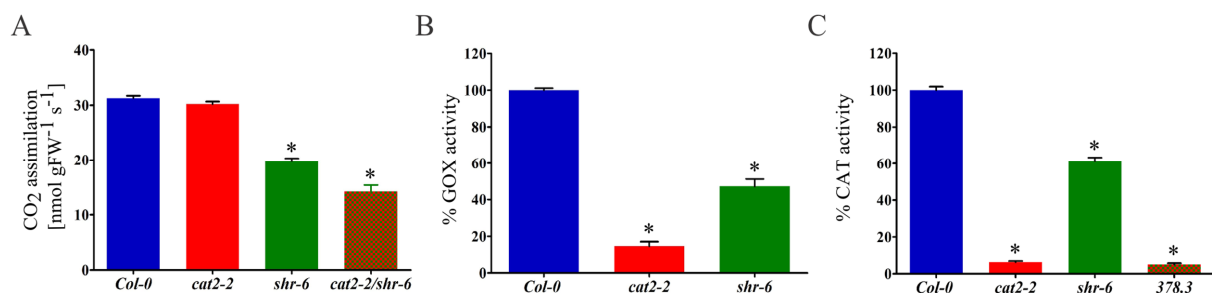

Figure 11. SHR deficiency affects photosynthesis and activity of photorespiratory enzymes. **A)** Lack of SHR reduces CO$_2$ assymilation. Plants were grown in vitro on 1 x MS medium 1% sucrose for three weeks. Whole plates were used for gas exchange measurements and resulting values were divided by rosettes' fresh weight. Values represent means of 8 biological replicates ± SE. Data were analyzed with one-way ANOVA followed by Dunnett's multiple comparisons post-hoc test (p < 0.05). Asterisks show significant differences to Col-0. **B-C)** SHR deficiency decreases shoot **(B)** glycolate oxidase and **(C)** catalase activity. Plants were grown in vitro on 1 x MS medium 1% sucrose for two weeks. Enzymatic assays were performed as described before (Rojas et al., 2012) and (Clare et al., 1984) respectively. Values represent percentage means of 3 biological replicates ± SE related to Col-0 (100%). Data were analyzed with one-way ANOVA followed by Dunnett's multiple comparisons test (p < 0.05). Asterisks show significant differences to Col-0.

are characteristic of peroxisome biogenesis mutants (*pex*; Nito et al., 2007). This indicates that *shr* mutants might be deficient in general peroxisome function. The majority of *pex* mutants exhibit indole-3-butyric acid (IBA) and 2,4-dichlorophenoxybutyric acid (2,4-DB) insensitive germination as conversion of these compounds to the active indole-3-acetic acid (IAA) and 2,4-dichlorophenoxyacetic acid (2,4-D) respectively requires glyoxysomal/peroxisomal β-oxidation (Hayashi et al., 1998; Zolman and Bartel, 2004; Strader et al., 2010). To test this hypothesis, we have investigated the germination of *shr-6* line on media supplemented with these auxin precursors. Interestingly, IBA and 2,4-DB inhibited germination of *shr-6* mutant to the same extent as in the Col-0 line (data not shown) indicating that the peroxisomal β-oxidation pathway functions properly. Next, we crossed the *shr-6* mutant with a peroxisomal marker line (35S:PTS1:GFP; Zolman and Bartel, 2004) in order to investigate the peroxisome number and dynamics. However, the F2 GFP-positive *shr-6* plants did not exhibit any apparent phenotypes related to peroxisome development (data not shown). All together, our results indicate that phenotypes associated to SHR deficiency described in this chapter are independent from peroxisome biogenesis.

DISCUSSION

THE ROLE OF SHORT-ROOT IN OXIDATIVE STRESS TOLERANCE

In higher plants exposure to environmental stresses lead to disruption of the balance between production and scavenging of reactive oxygen species (Mittler et al., 2011). Among multiple forms of ROS, hydrogen peroxide has the highest potential for acting as a signaling molecule due to its relative stability, participation in numerous post-translational modifications of proteins (discussed in Chapter 1) and ability to cross membranes (Bienert et al., 2006). CATALASE 2 serves as a major hydrogen peroxide scavenger in peroxisomes, hence mutants lacking this enzyme were used in the past as a model to study oxidative stress responses (Mhamdi et al., 2010). In this study we have used an EMS-mutagenesis approach to identify modulators of photorespiratory H_2O_2-induced cell death. We describe the identification and functional characterization of two novel mutations that suppress the oxidative stress related phenotypes of *cat2* plants. Thus far, only two such mutations have been described (Chaouch et al., 2010; Vanderauwera et al., 2011). Lesion formation triggered by peroxisomal H_2O_2 was abolished in *cat2*/*sid2* double mutants lacking ISOCHORISMATE SYNTHASE 1 (ICS1), a key enzyme within the salicylic acid synthesis pathway, demonstrating that the formation of cell death lesions results from an active process dependent on SA signaling rather than random oxidative damage of cell components (Chaouch et al., 2010). Another mechanism of suppression was observed in case of *apx1/cat2* double mutant lacking cytosolic ASCORBATE PEROXIDASE 1 (Vanderauwera et al., 2011). In this line, a DNA damage response was constitutively activated, suppressing growth via a WEE1 kinase-dependent cell-cycle checkpoint. This adaptation correlated positively with oxidative stress tolerance (Vanderauwera et al., 2011). A novel mutation

that reverts the *cat2* phenotype under oxidative stress identified herein resides in the SHORT-ROOT transcription factor involved in regulation of root radial patterning.

Control of early development by SHORT-ROOT is necessary for oxidative stress tolerance

The development of higher plants relies on the coordinated control of cell divisions leading to proper patterning and organ formation. In this study we identified a role for SHR transcription factor in determination of oxidative stress tolerance. SHR has an established role in the control of root and leaf development. In roots, the SHR protein is expressed in the vascular tissue and migrates outwards to the adjacent cell layers, where it is sequestered to the nucleus via formation of a complex with SCARECROW (Nakajima et al., 2001; Cui et al., 2007). This interaction is necessary for proper root radial patterning. Plants lacking SHR develop, instead of an endodermis and a cortex, a single cell layer lacking endodermal differentiation markers (Casparian strip; arabinogalactan proteins) (Benfey et al., 1993). Apart from their function in root development, recently both genes were also shown to control leaf growth (Dhondt et al., 2010) and SCR was implemented in the development of Kranz-type morphology in maize leaves (Slewinski et al., 2012) and bundle sheath cells in *Arabidopsis* (Cui et al., 2014).

Although initially isolated as a mutation that reverts the hydrogen peroxide dependent cell death in *cat2-2* mutant, the lack of SHR cannot be directly considered as a feature that increases oxidative stress tolerance. This is because oxidative stress related phenotypes observed in *shr* plants are fully dependent on exogenous sucrose supplementation. The transfer experiments (Fig. 7) clearly indicate that the addition of sucrose is a major factor contributing to the suppression of the cell death phenotype observed in this assay. Furthermore, when deprived of external sucrose sources *shr* mutants exhibit formation of cell death lesions that could be compared to those observed in *cat2-2* line. The combination of these mutations in *shr-6/cat2-2* double mutant further reduces plant survival as compared to single *shr-6* and *cat2-2* lines. In line with these observations, lack of SHR does not lead to increased oxidative stress tolerance in soil conditions. The expression of SHR in the leaves correlates with the developmental stages. While abundant in proliferating leaves, it becomes confined to the vascular tissue at the end of cell proliferation (Dhondt et al., 2010). At the onset of RGCL treatment (21DAS) the expression of SHR is limited to the vascular bundle (xylem) and does not occur in the mesophyll cells (Cui et al., 2014) that are especially affected by photorespiratory hydrogen peroxide. In transcriptomic studies with the use of CATALASE2-deficient plants we did not observe the oxidative stress related up-regulation of SHR transcript levels (Vanderauwera et al., 2005; this study). Therefore, it is likely that the oxidative stress related phenotypes observed in this study result from the early developmental defects observed in *shr* mutants or are an indirect result of SHR deficiency in leaf vascular tissue (lack of bundle sheath layer).

Lack of SHORT-ROOT affects photorespiratory metabolism

Our metabolome profiling indicates that SHR-deficiency impairs the conversion of glycolate to glycine through the photorespiratory flux. Upon shift to photorespiratory conditions *shr* plants accumulate glycolate while Gly synthesis is impaired. These results are in line with the reduced glutathione content in *shr* background as photorespiratory glycine was shown to be required for maximal GSH synthesis (Noctor et al., 1999). A plausible explanation for the accumulation of glycolate could be the low activity of downstream photorespiratory enzymes. Indeed, the activity of glycolate oxidase catalyzing the oxidation of glycolate to glyoxylate, and catalase were markedly decreased in *shr-6* mutant. The low activity of these enzymes cannot be explained by a transcriptional repression as genes encoding for CATALASE1, 2 & 3 are not differentially transcribed in *shr-6* background while among five genes encoding glycolate oxidase isoforms only GOX3 was differentially regulated (Log2 FC = 1.25; Dhondt et al., 2010). The deficiency in activity of catalase and glycolate oxidase suggested that the SHR mutants could be deficient in general peroxisome function. The development of peroxisomes, relies on coordinated import of nuclear-encoded peroxisomal proteins through the peroxisome membrane into the matrix (Hu et al., 2012). We therefore speculated that low GOX and CAT activities might be related to impaired import of these enzymes (and others using the same import machinery) into peroxisomes. However we were not able to find evidence to support this notion as *shr-6* line exhibited normal peroxisome morphology and β-fatty acid oxidation (data not shown). A much more detailed discussion on phenotypic effects of GOX deficiency is enclosed in section II of this chapter. Another explanation for the hyperaccumulation of glycolate could be its impaired export from the chloroplasts. However, the recently identified chloroplastic glycolate/glycerate transporter PLGG1 (Pick et al., 2013) is not affected by SHR deficiency at the transcriptomic level (Dhondt et al., 2010). An alternative explanation for impaired glycolate metabolism arose from the discovery of extremely low phosphate (Pi) levels in *shr* plants. The phosphate deficiency phenotype observed on metabolome and transcriptome level might lead to altered composition of plant membrane structures, that in turn may hamper diffusion/transport of metabolites. It has been demonstrated that under Pi limiting conditions (Essigmann et al., 1998) plants replace phosphatidylglycerol, the major component of photosynthetic membranes, with the sulfolipid sulfoquinovosyl diacylglycerol. This exchange results in altered organization of thylakoid membrane as observed in *pho1* mutant (Härtel et al., 1998). Therefore, it can be hypothesized that altered composition of membranes could hamper the transport of glycolate. Additionally, the increased consumption of sulfur that is necessary to produce sulfolipids might be another factor contributing to the impaired glutathione synthesis in *shr* mutants. The impaired GSH production might explain reduced abundance of transcripts linked to jasmonate (JA) signaling observed in *shr-6/cat2-2* double mutant as low levels of GSH are known to repress

the induction of JA signaling (Han et al., 2013). In a view of our results, it would be of interest to assess the ratio of reduced to oxidized glutathione (GSH/GSSG).

It is noteworthy that SCR and most likely SHR are crucial for a proper development of the Kranz-type anatomy in C4 plants by participating in the development of bundle sheath chloroplasts. Therefore their role in the development of chloroplasts in C3 plants might be speculated. One line of evidence supporting this theory is a significant similarity between transcript signatures of *shr-6/cat2-2* and *immutans* mutant exhibiting a variegated phenotype linked to chloroplast development (Carol et al., 1999). Furthermore, our metabolome profiling data show the SHR deficiency impairs synthesis of BCAA (Val, Leu, Ile) and Phe that are synthesized in the chloroplast (Rippert et al., 2009; Binder, 2010) suggesting a general decrease in chloroplast function. Further research efforts with the use of electron microscopy are necessary to investigate the ultrastructure of *shr* chloroplasts.

Phosphate deficiency might explain other phenotypes related to *shr* deficiency such as the impaired starch degradation observed in *shr* (Cui et al., 2014), as the phosphorylation of transitory starch is crucial for its mobilization (Yu et al., 2001; Ritte et al., 2004). Another *shr* phenotype that might be attributed to Pi starvation is anthocyanin accumulation, which occurs under low Pi levels (Rubio et al., 2001; Yin et al., 2012). Multiple studies had demonstrated the link between phosphate starvation and sucrose accumulation (Hammond and White, 2008). A more recent study (Lei et al., 2011) indicates that elevated sucrose levels are able to exert a transcriptomic response that largely resembles transcriptomic footprints of Pi starvation establishing sucrose as global regulator of plant response to Pi deficiency. In agreement with these findings, we observed largely increased levels of sucrose, fructose and glucose in *shr* shoots. It seems most likely that the elevated concentration of these sugars results from enhanced uptake from the growth medium. This notion is supported by significant overexpression of *SUCROSE-PROTON SYMPORTER 7* that might create a sink force in *shr* shoot. It is also noteworthy that development of *shr* mutants is impaired on medium with no sucrose (Cui et al., 2012; this work) which suggests that their photosynthetic capacity is not sufficient to sustain proper growth. It would be of interest to investigate at which stage Pi transport is inhibited in SHR-deficient plants. Measurement of phosphate level in the SHR root could indicate whether the uptake or long distance Pi transport is impaired in *shr* mutants.

The impact of the carbohydrate nutritional status on oxidative stress tolerance

Our results clearly indicate that exogenous sucrose supplementation is a crucial factor controlling oxidative stress related phenotype of *shr* mutants. Gas exchange measurements performed in this study demonstrate a significant decrease in net CO_2 assimilation related to SHR deficiency. This, together with the exogenous sucrose-dependent growth of *shr* mutants implicates that SHR-deficient plants are at least partially heterotrophic. It was demonstrated earlier that exogenous sucrose supplementation increases oxidative stress tolerance (Ramel et al., 2009a; Ramel et al., 2009b). Similarly,

in Chapter IV of this thesis we demonstrated that *cat2* plants grown on media with elevated sucrose levels exhibit significant increase in survival in RGCL assay. The heterotrophic lifestyle of *shr* mutants appears to be linked with altered mitochondrial metabolism as levels of TCA cycle metabolites (especially citrate and malate) were greatly increased in *shr* background.

In line with the previous observations (Chaouch and Noctor, 2010) we observed significantly lower content of myo-inositol (MI) in *cat2-2* line. It has been shown that exogenous application of MI blocked lesion formation and SA accumulation in *cat2* plants, and closely resembled the effects of genetic perturbation of SA synthesis observed in *cat2/sid2* double mutant (Chaouch et al., 2010; Chaouch and Noctor, 2010). Strikingly, we found that introduction of *shr-6* mutation into *cat2-2* background raised the myo-inositol level well above that of Col-0 value. It would be of interest to investigate whether the sugar dependent reversion of lesion formation observed in *shr-6/cat2-2* line occurs on growth medium deprived of myo-inositol.

SECTION II - CHARACTERISATION OF MUTANT 238.3

RESULTS

Identification of causative mutation 238.3

In order to identify the causative mutation of line 238.3 we applied the SHOREmap pipeline (Schneeberger et al., 2009; Hartwig et al., 2012). For this, we analyzed an F2 mapping population derived from a cross between *cat2-2* and 238.3 mutant line, as the oxidative stress-related phenotype was not present in F2 progeny of *cat2-20* x 238.3 (data not shown). In total, 1794 F2 individuals were subjected to RGCL conditions and about 13% of plants (234) exhibited reversion of cell death phenotype. This segregation did not fit the Mendelian 1:3 ratio ($\chi^2 = 137.319$, p < 0.0001) presumably due to the limited penetrance of the revertant phenotype (described earlier in the text).

Surviving plants were harvested and used for preparation of nuclear DNA. This sample was used to prepare an Illumina library, which was sequenced to an average 53.6-fold genome coverage. Backcrossing of a mutant to its parent line does not introduce pre-specified markers into the mapping population. Therefore, we have applied a SHOREmap backcross strategy (Hartwig et al., 2012) that uses EMS-induced markers as novel markers in order to determine the mapping interval. Using a concordance threshold set to 0.8 we identified 10 EMS-specific SNPs (Table S4) significantly enriched in plants displaying a revertant phenotype. All polymorphisms localised to the upper arm of chromosome III within 3.3 – 7.4Mb physical interval (Fig. S7). The most frequent SNP was localized within *GLYCOLATE OXIDASE 1* (*GOX1*, AT3G14420) coding sequence at position 1 of third exon. Analysis of *GOX1* mutant sequence performed with NetGene2 software (http://www.cbs.dtu.dk/services/NetGene2/) indicated that this G → A substitution could potentially disrupt the splicing site between second intron and third exon. To validate whether the identified mutation led to a decrease in total glycolate oxidase activity we analyzed GOX activity in the 238.3 mutant line. Shoots of two-week-old seedlings grown under LD conditions on MS medium supplemented with 1% sucrose were used to determine glycolate oxidase activity. In agreement with our mapping results, we observed only 4.5% of wild-type GOX activity in the 238.3 line (Fig. 12A). Unexpectedly, this activity was reduced to 23% of wild-type level also in *cat2-2* mutant, (Fig. 12A). These results provide evidence for alterations of the photorespiratory pathway in the *cat2-2* mutant. Furthermore, disruption of GOX1 coding sequence combined with CATALASE 2 deficiency in line 238.3 led to almost complete lack of glycolate oxidase activity, which is the major source of H_2O_2 in the peroxisomes.

Photorespiratory H₂O₂ decreases GLYCOLATE OXIDASE activity by a negative feedback loop

A plausible explanation for the observation that CATALASE 2 deficiency leads to a significant reduction in glycolate oxidase activity is that *GOX* transcript levels are down-regulated in a *cat2-2* background. However, we did not observe this kind of regulation in plants subjected to 24 h of RGCL treatment (Table S1). Similarly, a down-regulation of the GOX transcript levels from all five isoforms was not observed in earlier microarray experiments (Vanderauwera et al., 2005) describing transcriptomic responses of CATALASE2-deficient plants to high light. As an alternative hypothesis, we assumed that the enzymatic activity of glycolate oxidase could be inhibited at the protein level hereby providing much faster mechanism of its regulation. As first step towards investigation of these possibilities we followed the dynamics of changes in GOX activity upon oxidative stress challenge in both Col-0 and *cat2-2* lines. Plants were grown in soil for three weeks under conditions limiting photorespiration, and transferred to a photorespiration promoting environment as described before. Tissue samples were harvested after 0, 3, 8 and 24 h of HL treatment at ambient CO_2 atmosphere.
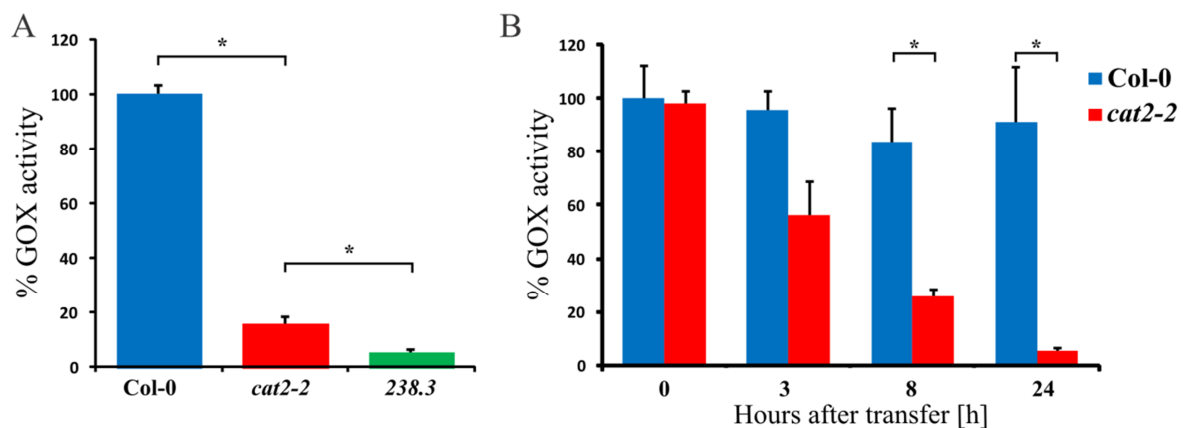

Figure 12. Oxidative stress affects glycolate oxidase activity. **A)** Line 238.3 has reduced GOX activity. Plants were grown *in vitro* on 1 x MS medium 1% sucrose for two weeks. Enzymatic assays were performed as described before (Rojas et al., 2012). Values represent percentage means of 3 biological replicates ± SE related to Col-0 (100%). Data were analyzed with one-way ANOVA followed by Bonferroni's multiple comparisons test ($p < 0.05$). Asterisks show significant differences between indicated genotypes. **B)** Oxidative stress decreases glycolate oxidase activity. Plants were grown for 21 days in soil at conditions limiting photorespiration and exposed to continuous HL 1100-1200 $\mu mol \cdot m^{-2} \cdot s^{-1}$ illumination at ambient CO_2 concentration. Rosettes were harvested in the course of experiment and used for GOX activity assay. Values represent percentage means of 3 biological replicates ± SE related to initial Col-0 GOX activity (100%). Data were analyzed with two-way ANOVA followed by Bonferroni's multiple comparisons test ($p < 0.05$). Asterisks show significant differences at indicated time points.

In contrast to previous experiments performed on ambient air grown plants, enzyme activity assays revealed a wild-type levels of GOX activity in *cat2-2* line (t = 0 h). Transfer to photorespiratory conditions resulted in gradual decrease of *cat2-2* GOX activity reaching ~10% of initial value after 24 h of stress treatment (Fig 12 B). Remarkably, in the same conditions wild type plants retained ~90% of initial GOX activity. Together, our results provide evidence for existence of negative feedback loop that leads to inhibition of GOX activity by photorespiratory hydrogen peroxide.

Decrease in GOX activity modulates the photorespiratory pathway

To further confirm that the decrease in glycolate oxidase activity leads to reversion of cell death phenotype in the *cat2-2* line under oxidative stress conditions the following double and triple mutant lines were generated and subjected to RGCL assay: *gox1-1/cat2-2, gox2-1/cat2-2, gox3-1/cat2-2, haox1-1/cat2-2* (HAOX – α-HYDROXY ACID OXIDASE (Rojas et al., 2012)), *haox2-1/cat2-2* and *gox1-1/gox3-1/cat2-2*. In agreement with our mapping results, introduction of *gox1-1* mutation into *cat2-2* background resulted in a delay of cell death to a degree observed in the 238.3 mutant line as demonstrated by chlorophyll fluorescence parameters and delayed progression of lesions in *gox1-1/cat2-2* double and *gox1-1/gox3-1/cat2-2* triple mutant (Fig 13 A-C). Interestingly, introduction of *gox2-1* mutation also resulted in a delayed progression of cell death although to a much lower extent (Fig 13 C). Mutations in *GOX3, HAOX1* or *HAOX2* did not affect the phenotype of *cat2-2* line. Interestingly, when tested in wild-type background, none of the mutant lines exhibited altered oxidative stress tolerance in RGCL assay (data not shown). Next, we tested whether the reversion of cell death phenotype occurs in soil conditions. For this, plants were grown for three weeks in high CO_2 atmosphere and subsequently exposed to continuous high light intensities at ambient CO_2 as described before. In agreement with results of RGCL assay, the lesion formation was significantly reduced in *gox1-1/cat2-2* double mutant when compared with *cat2-2* line (Fig 14 A). Mutations in the four other isoforms of glycolate oxidase in Col-0 and *cat2-2* background did not lead to any related phenotypes in soil conditions.
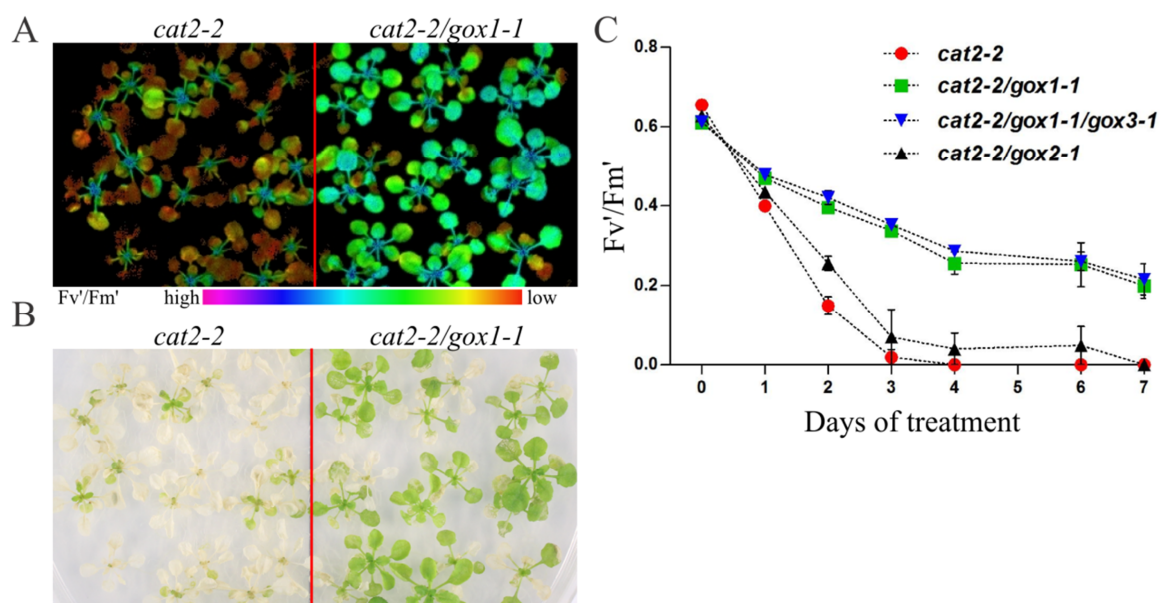

Figure 13. Lack of GLYCOLATE OXIDASE 1 delays symptoms of CATALASE 2 deficiency under oxidative stress conditions. Three-week old plants grown under long day conditions at 100 μmol·m^{-2}·s^{-1} on 1 x MS medium supplemented with 1% sucrose were subjected to photorespiratory stress by mechanical restriction of gas exchange and transfer to continuous light. **A)** PSII maximum efficiency after 2 days of treatment. **B)** Representative image of *cat2-2* and *gox1-1/cat2-2* line after 6 days of RGCL treatment. **C)** Changes of Fv'/Fm' in the course of RGCL assay, bars represent means of three biological replicates ± SE.

Lack of GOX1 enhances biomass accumulation under moderate light intensities

In a next step, we sought to investigate whether introduction of *GOX/HAOX* mutations into *cat2-2* background could revert the long-term effects of growth under low and moderate light intensities such as decreased biomass accumulation (Queval et al., 2007). In a pilot experiment, plants were grown at light intensities of 100 and 300 µmol·m^{-2}·s^{-1} under LD photoperiod for four and three weeks respectively. Measurement of rosette fresh weight demonstrated that plants grown at irradiance of 100 µmol·m^{-2}·s^{-1} were not significantly different in terms of biomass accumulation when compared to Col-0 reference (Fig. 14 B). In agreement with a previous report (Queval et al., 2007), growth under higher irradiance (300 µmol·m^{-2}·s^{-1}) lead to a 75% decrease in biomass accumulation in the *cat2-2* line. This effect was significantly attenuated in *gox1-1/cat2-2* and *gox1-1/gox3-1/cat2-2* line (~43% of WT value, Fig. 14 C), but not for other double mutants tested. Together, our results indicate that lack of GOX1 alleviates reduction in biomass accumulation observed for *cat2* plants under conditions promoting photorespiration.

GOX 1 is responsible for the majority of GOX activity in the shoot

From our previous results it can be inferred that GOX1 is the major isoform of glycolate oxidase in the shoot tissues at the rosette stage. In order to evaluate this hypothesis we measured the total GOX activity in all single and multiple mutant lines generated throughout this study (Fig 14 D). Results of enzymatic assays indicated that lack of GOX1 or GOX2 reduces shoot glycolate oxidase activity to 33 and 40 % respectively when compared with Col-0 control line. Introduction of *gox1-1* or *gox2-1* mutations into *cat2-2* background had similar effects and reduced the residual activity to ~7%. Lack of remaining glycolate oxidase isoforms had no significant influence on total GOX activity in both backgrounds. These data demonstrate that GOX1, followed by GOX2, is the major glycolate oxidase isoform in the shoot.
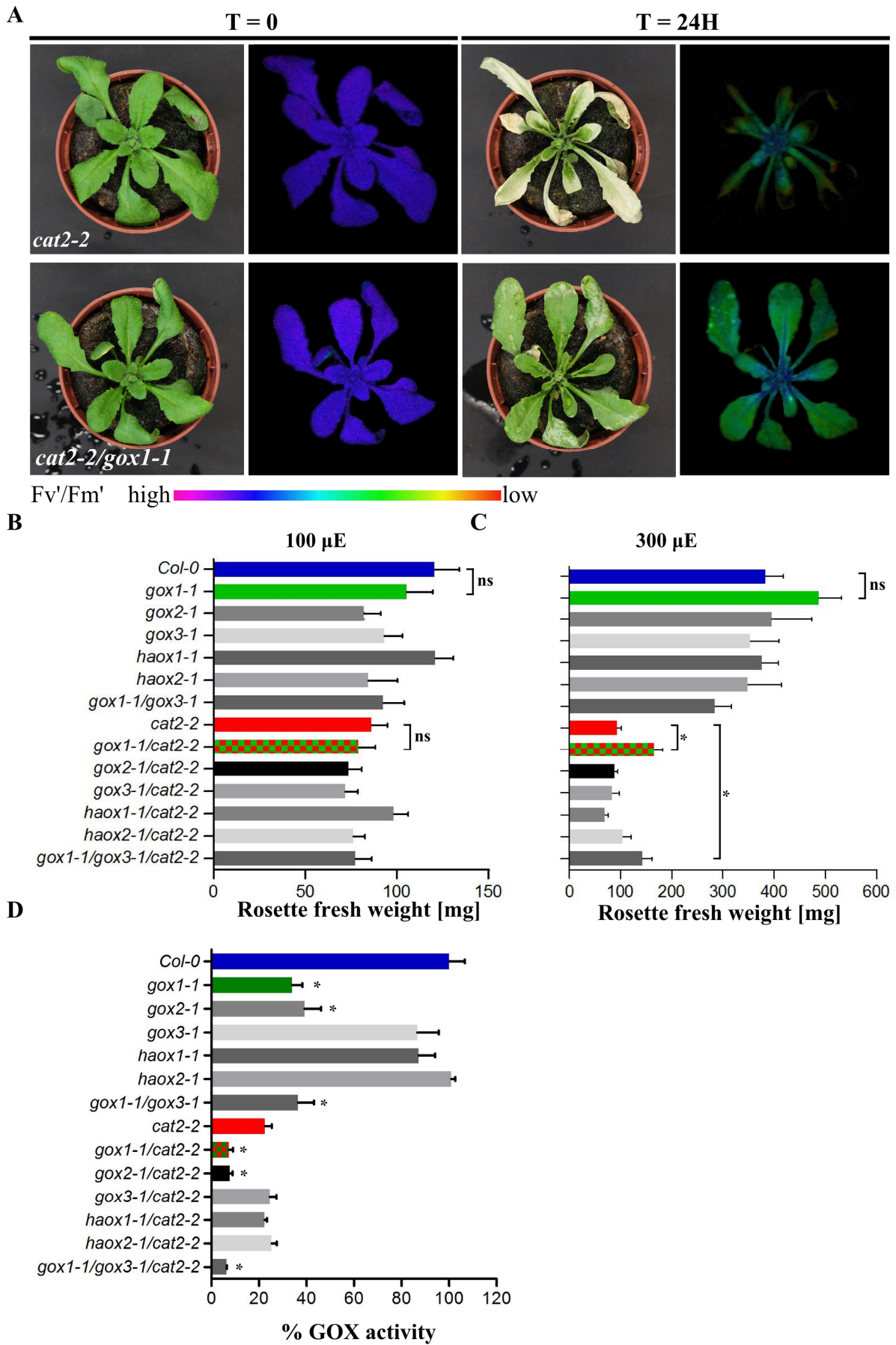
DISCUSSION

ROLE OF GLYCOLATE OXIDASE IN MODULATION OF THE PHOTORESPIRATORY PATHWAY

GOX1 is the major photorespiratory glycolate oxidase

The glycolate oxidase (GOX) is a peroxisomal flavoenzyme (FMN - dependent) that converts glycolate to glyoxylate with the formation of H_2O_2. *Arabidopsis* contains five genes encoding for GOX isoforms *GOX1* (At3g14420), *GOX2* (At3g14415), *GOX3* (At4g18360), *HAOX1* (At1g14130) and *HAOX2* (At3g14150). Comparison of expression profiles indicates that GOX1 & 2 are 60-fold more expressed in *Arabidopsis* rosette leaves than the three other GOX with GOX3 expressed mainly in roots and HAOX1 & 2 in seed tissues (Rojas et al., 2012; Hodges et al., 2013). Considering the fact that peroxisomal H_2O_2 triggers formation of cell death lesions in *cat2* plants, it is not surprising that reduction of foliar GOX activity observed in the 238.3 mutant and subsequently in *gox1-1/cat2-2* and *gox2-1/cat2-2* double mutants alleviated this phenotype. Glycolate oxidase activity measurements performed on mutant lines of all five GOX isoforms clearly indicate the major contribution of GOX1 and 2 to total foliar glycolate oxidase activity. These results are in line with their transcript levels and explain why the mutations GOX3, HAOX1and HAOX2 are not able to reduce the formation of cell death lesions in *cat2-2* background. Results of enzymatic assays performed in this study are in direct contradiction to those obtained by Rojas et al. (2012), describing similar residual GOX activities (~80%) in all five mutant lines. These differences might be explained by different age of plants used for analysis (6 weeks vs 2 weeks used herein) or different growth conditions (soil vs MS medium). Despite similar reduction of residual GOX activity observed in both mutant lines, the lack of GOX1 had a more pronounced effect demonstrated by a delay of lesion formation observed both in soil and *in vitro* conditions. The *gox2-1/cat2-2* double mutant exhibited only slight increase in survival under RGCL conditions and had no cell death inhibitory effects when

---

Fig. 14 (previous page) GOX1 influences oxidative stress performance in soil. **A)** Lack of GOX1 activity confers increased resistance towards photorespiratory conditions. Plants were grown for three weeks under conditions limiting photorespiration and subsequently exposed to 24 hours of continuous excess light irradiation (1100-1200 $\mu mol \cdot m^{-2} \cdot s^{-1}$) in ambient air. Representative images demonstrate formation of cell death lesions and reduction of PSII maximum efficiency after 24 hours of exposure. **B, C)** GOX1 deficiency promotes growth under photorespiratory conditions. Plants were grown in soil in LD at **(B)** 100 $\mu mol \cdot m^{-2} \cdot s^{-1}$ and **(C)** 300 $\mu mol \cdot m^{-2} \cdot s^{-1}$ for four and three weeks respectively. Ten rosettes/line were collected for fresh weight determination. Bars represent means of 10 biological replicates ± SE. Asterisk indicates significant difference to respective control lines according to one-way ANOVA followed by Dunnet's multiple comparison test (p < 0.05). **D)** GOX1 and GOX2 are major shoot glycolate oxidases isoforms. Plants were grown in vitro on 1 x MS medium 1% sucrose for two weeks. Enzymatic assays were performed as described before (Rojas et al., 2012). Values represent percentage means of 3 biological replicates ± SE related to Col-0 (100%). Data were analyzed with one-way ANOVA followed by Dunnett's multiple comparisons test (p < 0.05). Asterisks show significant differences to respective control lines

tested in soil. This difference might be attributed to a slightly lower residual GOX activity in *gox1-1/cat2-2* double knockout and indicates the existence of a threshold concentration of photorespiratory H_2O_2 that is necessary for induction of cell death. Taken together, our results demonstrate that GOX1 is the major shoot glycolate oxidase isoform with a role in photorespiratory metabolism.

Normal development of *gox/cat2* plants suggests alternative pathways for glycolate metabolism

The functional redundancy between GOX1 and GOX2 identified in this study might explain why thus far no glycolate oxidase mutant exhibiting a photorespiratory phenotype has been identified (Timm and Bauwe, 2012). In agreement with this hypothesis, we did not identify any oxidative stress related phenotypes for single *gox1-1* and *gox2-1* mutants both harboring 33 - 40% of residual GOX activity, respectively. Interestingly, we showed that under control conditions in *cat2-2* plants the glycolate oxidase activity is constitutively reduced to approx. 23% when compared to the WT value (discussed in next paragraph). In *gox1-1/cat2-2* and *gox2-1/cat2-2* this activity is further reduced to ~7%. This phenomenon raises a question about the metabolic fate of photorespiratory glycolate in these mutant lines. In maize, a similar decrease in residual GOX activity (5 - 10% of WT activity) observed for *go1* mutant line, conditions a lethal phenotype which supports the importance of photorespiration in maintaining low levels of glycolate in C4 plants (Zelitch et al., 2009). This phenotype was attributed to the inhibitory effect of glycolate accumulation on photosynthesis and supported the earlier study (Gonzalez-Moro et al., 1997) that demonstrated the negative influence of glycolate on RuBisCO activity. A similar phenotype was observed for rice lines with inducible antisense suppression of glycolate oxidase (Xu et al., 2009). Upon induction, the GOX activity in transgenic rice plants was decreased by > 90% and resulted in a severely stunted phenotype related to the inhibition of photosynthesis (Xu et al., 2009). Interestingly, in both cases the levels of downstream photorespiratory metabolites, glyoxylate, glycine and serine were not affected suggesting the existence of an alternative pathway for glyoxylate synthesis (Xu et al., 2009; Zelitch et al., 2009). Surprisingly, in a recent follow-up study using rice lines with constitutively suppressed glycolate oxidase activity Lu et al., (2013) demonstrated that the decrease in GOX activity leads to accumulation of glyoxylate, and that glyoxylate rather than glycolate acts as an inhibitory factor of photosynthesis. This notion was supported by earlier work (Chastain and Ogren, 1989; Campbell and Ogren, 1990) indicating the indirect inhibitory effect of glyoxylate on RUBISCO activation. Evidently, the literature data about the inhibitory effects of glycolate/glyoxylate on photosynthetic CO_2 assimilation remain equivocal and further research is needed to elucidate which of the two metabolites leads to inhibition of this process. Interestingly, none of these inhibitory effects seem to occur for *gox1/cat2* and *gox2/cat2* double mutants described in this study. In contrast, the introduction of *gox1* mutation into *cat2-2* background positively influenced the accumulation of biomass under conditions promoting photorespiration. A plausible explanation for the observed phenomenon is the existence of an alternative pathway that

is constitutively activated in these double mutants and enables efficient removal of photorespiratory glycolate/glyoxylate. Indeed, Goyal and Tolbert (1996) reported the light dependent oxidation of glycolate by isolated chloroplast thylakoids from spinach leaves. The oxidation of glyoxylate by envelope-free spinach chloroplast resulting in release of CO_2 was reported earlier by Zelitch (1972). These data were recently corroborated by Kebeish et al. (2007) who demonstrated that the chloroplast overexpression of bacterial glycolate dehydrogenase alone is sufficient to enhance photosynthesis and correlates with an increased chloroplastic CO_2 concentration. These findings were recently complemented by demonstration that the release of CO_2 originating from metabolism of glycolate and glyoxylate can be inhibited by pyruvate (Blume et al., 2013). In this study, authors provide ample evidence for the possible role of the chloroplast pyruvate dehydrogenase complex in glyoxylate decarboxylation, however the enzymatic activity catalysing the oxidation of glycolate to glyoxylate in the chloroplast awaits characterisation. We anticipate that further investigation of photorespiratory metabolism in the *gox/cat2* double mutants generated in this study will lead to a better understanding of alternative chloroplast photorespiratory pathways.

Loss of GOX activity under oxidative stress conditions

We observed a constitutive decrease of GOX activity in *cat2* plants grown under low light intensities in a long day photoperiod. This phenotype could be fully reverted by growth in atmosphere enriched with CO_2 indicating the link with photorespiratory metabolism. Upon transfer to photorespiratory conditions gradual decrease of GOX activity was observed for *cat2-2* but not in Col-0 plants indicating that the capability for H_2O_2 scavenging regulates the activity of glycolate oxidase. A similar decline in activity was reported for pea glycoate oxidase upon in vivo inhibition of catalase activity with 3-amino-1,2,4-triazole (Schäfer and Feierabend, 2000). These results are in line with our metabolome profiling data demonstrating increased steady state level of glycolate in *cat2-2* plants that is further increased upon RGCL treatment. Our observations indicate the existence of a feedback regulatory mechanism that adjusts the production of hydrogen peroxide towards the peroxisomal redox status. This adaptation might involve triggering of alternative pathways of glycolate metabolism. However, the fact that *cat2* plants develop cell death lesions upon rapid changes in CO_2 availability combined with exposure to continuous excess light clearly indicates that reduction of GOX activity observed in this conditions is not sufficient or not rapid enough to inhibit formation of photorespiratory H_2O_2. Therefore, this mechanism likely participates in a long term acclimation towards mild increases in photorespiratory flux. In agreement with results obtained in this work, earlier study conducted in our group (Vanderauwera et al., 2005) did not identify changes in transcript levels for the GOX genes therefore it can be suggested that the regulation of GOX activity occurs at the posttranslational level. Among multiple ways by which the redox status can regulate enzyme activities the most profound are oxidative modifications of Cys residues (discussed in Chapter 1 and 2). A well described example of redox-dependent core photorespiratory enzyme is maize glycerate

kinase, that becomes inhibited by formation of regulatory disulfide bond (Bartsch et al., 2010). Both GOX1 and GOX2 possess a single highly conserved Cys residue (http://bioinformatics.psb.ugent.be/plaza; Proost et al., 2009) that could potentially serve as a site for redox PTM. Indeed, an inhibitory effect of hydrogen peroxide on pea glycolate oxidase activity was demonstrated (Schäfer and Feierabend, 2000). Furthermore, glycolate oxidase was photoinactivated in leaves when the endogenous GSH was depleted by the application of buthionine sulfoximine (Schäfer and Feierabend, 2000) indicating the role for S-glutathionylation in protection of GOX from over-oxidation. This hypothesis was corroborated later by Rouhier et al. (2005) who isolated *At*GOX1 using an affinity chromatography column made with poplar GLUTAREDOXIN C4 mutated on the second active-site cysteine indicating that the protein could be subjected to S-glutathionylation. Another possibility of oxidative regulation of GOX activity arose from recent studies in the CAM plant *Kalanchoe pinnata* (Abat et al., 2008) and pea (Ortega-Galisteo et al., 2012) both describing GOX as a target for S-nitrosylation. Furthermore, in the latter study, a direct inhibitory effect of nitric oxide (NO) on glycolate oxidase activity was demonstrated. These results are in line with the recent discovery of a potent peroxisomal nitric oxide synthase (NOS) activity in that is required for NO accumulation in cytoplasm under stress conditions (Corpas et al., 2009). Another PTM potentially regulating GOX activity is phosphorylation (Hodges et al., 2013). The *Arabidopsis* Protein Phosphorylation Site Database (PhosPhAt, Heazlewood et al., 2008; Durek et al., 2010) contains information about two phospho-peptides that could be associated to both GOX1 or GOX2 however the significance of this modification needs further investigation.

Together with previous literature data, our results strongly suggest the role for glycolate oxidase in regulation of photorespiratory pathway. Further research efforts with the use of purified enzyme are necessary to elucidate the exact mechanism that leads to inhibition of its activity under oxidative stress conditions. In vivo validation of these data might implement complementation of respective mutant lines of GOX lacking potential regulatory residues.

GOX1 - a potential target in amelioration of oxidative stress tolerance in crop species

Our results indicate that a decrease in glycolate oxidase activity conferred by lack of GOX1 might contribute to increased biomass accumulation under conditions promoting photorespiration. Demonstrated by 60% increase in fresh weight, these beneficial effects were most evident in *cat2-2* background. This phenotype is likely linked with an existence of intrinsic adaptations of photorespiratory pathway in the *gox1-1/cat2-2* double knockout. These kind of adaptations are clearly species-specific as GOX-deficient maize and rice both require elevated CO_2 atmosphere for normal growth (Xu et al., 2009; Zelitch et al., 2009). Previous efforts towards chemical inhibition of glycolate oxidase activity conducted on soybean leaf cells demonstrated similar effects (Servaites and Ogren, 1977). However, during interpretation of these data it is necessary to consider

the difference between inducible and constitutive lack of enzyme activity that might force metabolic rearrangement early in the plant development. Although statistically significant, our findings need to be repeated in multiple independent experiments performed on much larger amount of individuals before launching similar efforts in crop species. Nonetheless, we propose the modulation of glycolate oxidase activity as a potential target in amelioration of oxidative stress tolerance in crop species.

MATERIALS AND METHODS

Plant material

The following mutant lines used in this study were described before: *cat2-2* (Queval et al., 2007); *shr-6* (Dhondt et al., 2010; Yu et al., 2010); *shr-2* (Fukaki et al., 1998); *scr-1* (Di Laurenzio et al., 1996); *scr-3* (Fukaki et al., 1996); *gox1-1, gox2-1, gox3-1, haox1-1, haox2-1, gox1-1/haox1-1, gox1-1/gox3-1* (Rojas et al., 2012). Line ET8347 was obtained from Cold Spring Harbour Laboratory (CSHL) TRAPPER collection http://genetrap.cshl.edu (Sundaresan et al., 1995). Plants homozygous for the DsE insertion were selected by PCR, the DsE-gene junctions were sequenced with primers used for their amplification (Table S5) in order to map the insertion site. *scr-3/cat2-2, shr-6/cat2-2, gox1-1/cat2-2, gox2-1/cat2-2, gox3-1/cat2-2, haox1-1/cat2-2, haox2-1/cat2-2* and *gox1-1/gox3-1/cat2-2* double knockout lines were generated by crossing *cat2-2* plants (pollen acceptors) with respective mutant lines (pollen donors). Double mutant plants were identified in F2 segregating populations by root length phenotype and PCR/CAPS genotyping with respective primers/restriction enzymes (Table S5). dCAPS markers were designed with dCAPS Finder 2.0 (Neff et al., 2002). *shr-6* mutants were crossed with Col-0 plants and *shr-6/cat2-2* double mutant line was crossed with *cat2-2* plants to obtain F1 individuals heterozygous in *SHR* locus in Col-0 and *cat2-2* background respectively.

Mutagenesis and screening for revertants of *cat2-2* photorespiratory phenotype

Seeds of *cat2-2* T-DNA mutant line (Queval et al., 2007) were treated with 0.3 % EMS solution for 7.5 h, washed extensively with water and sown in vinyl pots. M1 plants were grown at 21°C under short day 8h light (100 μmol·m^{-2}·s^{-1})/16h dark regime. Before harvesting of M2 seeds the number of M1 plants per each pot was determined. Recessive mutants segregate in a ratio of 7:1 in an M2 population therefore 10 M2 plants per each M1 plant were analysed. Mutagenised M2 plants were grown in Petri dishes (150 x 25 mm, Becton-Dickinson, USA) on full-strength Murashige and Skoog agar solidified medium supplemented with 1% sucrose, 100 mg/L myo-inositol, nicotinic acid 0.5 mg/L, pyridoxine 0.5 mg/L, thiamine 1 mg/L at 21°C and long day 16h light (100 μmol·m^{-2}·s^{-1})/8h dark conditions. Each plate contained approximately 60 M2 plants and 6 wild-type Col-0 seedlings. After 21 days of growth the surgical tape that sealed the plates (Micropore) was replaced by two layers of parafilm M (Bemis) to restrict gas exchange, then plants

were transferred to a continuous light regime. Changes in maximum efficiency of the PSII photochemistry (Fv'/Fm') were determined using a PAM-2000 chlorophyll fluorometer and ImagingWin software (Walz). The putative mutants that showed decreased formation of lesions and reduced drop in Fv'/Fm' ratio were transplanted to soil to obtain M3 seeds. The M3 plants were subjected to RGCL test to determine whether they exhibited the parental phenotype. Confirmed mutants were rescued in order to produce M4 seeds. In a next step the absence of wild type *CATALASE2* allele was determined by means of PCR genotyping with respective primers (Table S5).

Development of anti-CATALASE2 rabbit polyclonal antibodies.

CATALASE 2 coding sequence was amplified from *Arabidopsis thaliana* Col-0 cDNA with Phusion® High-Fidelity DNA Polymerase (Finnzymes) with primers cat2_F_attB1 and cat2_R_attB2 (Table S5) according to manufacturer's instructions. The PCR product was cloned by recombination into pDONR221 plasmid (Invitrogen). After sequence verification coding sequence was subcloned into pDEST17 Expression Vector (Invitrogen). The expression vector was transformed into *Escherichia coli* BL21(DE3)pLysS strain. A 5 mL volume of Luria-Bertani broth with 100 mg/mL ampicillin and 25mg/mL chloramphenicol was inoculated and grown overnight at 37°C and 220 rpm. This culture was diluted to 500 mL, grown for 2 h at 37°C and 220 rpm, and induced with 0.2 mM IPTG. After 24 h of induction at 20°C and 220 rpm, cells were harvested by centrifugation at 4000 x g for 10 minutes and resuspended in 100 mL of lysis buffer (20 mM AMPSO pH 8.5; 0.3 M NaCl, 1 mM PMSF, 2U/ml DNase I). Bacterial cells were disrupted by sonication and centrifuged at 16,100 x g for 20 min at 4°C. Insoluble protein fraction was denatured at 96°C in loading buffer supplemented with 5 mM β-Mercaptoethanol and examined by SDS-PAGE. Protein band corresponding to CATALASE 2 protein was excised from gel and submitted for generation of polyclonal rabbit antibodies (Eurogentec).

Enzyme activity measurements, western blot analysis

For catalase activity measurements tissue was ground with ball mill (Retsch, Germany) and mixed with extraction buffer (60 mM Tris pH = 6.9, 10 mM DTT, 20 % glycerol, 1 mM PMSF) at a 1:1 ratio (v/v). The homogenate was centrifuged at 16,100 g for 15 minutes at 4°C. The supernatant was used in spectrophotometric catalase activity assay and for SDS-PAGE protein separation. Catalase activity was assayed by monitoring the decomposition of H_2O_2 (ε = 43.6 M^{-1} cm^{-1}) to H_2O and O_2 by following the associated absorbtion decrease at 240 nm (Clare et al., 1984).

For Western blot analysis 10 µg of leaf proteins were separated on a 12.5% SDS-PAGE gel, blotted onto a PVDF membrane (Millipore) and hybridized with a 1:3500 dilution of rabbit antiserum against *A. thaliana* CATALASE2 developed herein.

The glycolate oxidase activity measurements were performed according to a protocol described before (Rojas et al., 2012) downscaled for 200 mg of ground tissue. Briefly, shoot tissue was collected,

frozen in liquid nitrogen and ground with ball mill (Retsch, Germany). Subsequently, material was mixed with 1 ml of extraction buffer by vortexing and centrifuged at 16,100 g for 30 minutes at 4°C. Protein concentration in soluble phase was determined with Bradford Assay (Bio-Rad). Next, 10 µl of supernatant was used in spectrophotometric glycolate oxidase activity assay conducted in VersaMax microplate reader (Molecular Devices) at room temperature for 1 hour. The activity of glycolate oxidase was measured by monitoring two coupled reactions. In this assay, GOX converts glycolate to glyoxylate with the concomitant release of H_2O_2 that in turn (in the presence of HRP) oxidizes O-dianisidine into a colored O-dianisidine radical cation (ε = 11.6 M^{-1} cm^{-1}) that can be quantified spectrophotometrically by following associated absorbtion increase at 440 nm. Specific activity was calculated by dividing ΔA by time and amount of soluble protein present in the sample, and expressed as percentage of control.

All enzymatic assays were performed on three biological replicates with at least three technical repeats.

Real-time PCR

For the quantification of transcript levels total RNA was prepared with RNeasy Plant Mini Kit (Qiagen). First strand cDNA synthesis was performed with iScript cDNA Synthesis Kit with 1 µg of total RNA used as input material. Five microliters of the 1:8 diluted first strand cDNA was used as a template in subsequent PCR performed on the iCycler iQ (Bio-Rad) with respective gene specific primers (Table S5). Reactions were performed in three technical repeats with the SYBR Green I Master Kit according to manufacturer's instructions. Expression analysis was performed with qBASEPlus software (Biogazelle) with *ACTIN-RELATED PROTEIN 7* (*ARP7*) and *SERINE/THREONINE PROTEIN PHOSPHATASE 2A* (*PP2A*) used for data normalisation. All experiments were performed with three biological replicates. Statistical analysis was carried out with one-way ANOVA followed by the Tukey-Kramer post-hoc test.

Next generation sequencing and SHORE mapping

For identification of EMS-induced mutations in mutants 238.3 and 378.3 M3 plants were grown for 21 days in long day conditions 16h light (100 µmol·m^{-2}·s^{-1})/8h dark on agar solidified MS medium supplemented with 1% sucrose. For identification of 238.3 causative mutation revertant plants were selected in RGCL assay according to the procedures used in the mutant screen. Bulked shoot tissue was ground in liquid nitrogen and 2g of powder were used as starting material for extraction of nuclear DNA according to a protocol described before (Schneeberger et al., 2009). The gradual enrichment of nuclear DNA was confirmed by performing a quantitative PCR analysis with primers described before (Schneeberger et al., 2009).

For sequencing of 378.3 mutant the library preparation, sequencing and annotation of SNP/InDel was performed by Fasteris SA (Geneva, Switzerland). Paired-end libraries were sequenced with Illumina Hi-Seq 2000 sequencing system with a TruSeq SBS Kit v5 (Illumina, San Diego, USA), the number of sequencing cycles was 2 x 100. The reads were mapped to *Arabidopsis thaliana* reference genome (TAIR10) using the Burrows-Wheeler Alignment Tool v 0.5.9 (Li and Durbin, 2009). The SNP/InDels were prefiltered with the coverage threshold set to 10 and only those supported by at least 3 reads in forward and 3 reads in reverse direction were retained. Further SNP/InDel calling was performed with SAMtools software (v 0.1.17, http://samtools.sourceforge.net/).

For determination of the 238.3 causative mutation the library preparation and sequencing were performed by VIB Nucleomics Core (www.nucleomics.be). Paired-end libraries were sequenced with Illumina Hi-Seq 2000 sequencing system with 2 x 100 sequencing cycles. The reads were mapped to *Arabidopsis thaliana* reference genome (v TAIR10) with SHORE 0.7.1 software (Ossowski et al., 2008). Annotation of SNPs, generation of prioritized SNP list and visualisation of results was performed with SHOREmap 2.0 (Schneeberger et al., 2009) according to SHOREmap backcross strategy described before (Hartwig et al., 2012).

Analysis of all NGS results generated in this study implemented subtraction of inherent *cat2-2* polymorphisms (Denecker et al., unpublished data).

Stress treatments

The RGCL oxidative stress assay was conducted according to the procedures used in the *cat2-2* revertant screen. For stress experiments including media change, seeds were grown on nylon mesh (ø = 20 µM, Prosep) and transferred to specified media 3 days before the treatment. For a high light (HL) treatment in soil, plants were grown in a controlled climate chamber (Vötsch Industrietechnik) at 3000ppm CO_2, 21°C, 50% relative humidity and 16h light (120-130 $\mu mol \cdot m^{-2} \cdot s^{-1}$)/8h dark regime. After 21 days of growth plants were exposed to continuous HL 1100-1200 $\mu mol \cdot m^{-2} \cdot s^{-1}$ illumination (Sanyo Fitotron plant growth chamber) at ambient CO_2 concentration, 21°C and 50% relative humidity for a specified time period. Before transfer plants were well watered to exclude to possible influence of drought.

Microarray transcript profiling

Three-week-old *cat2-2* and *shr-6/cat2-2* plants were subjected to RGCL assay as described earlier. Shoot tissue from both genotypes was sampled in three biological replicates before (T = 0) and after 24 hours (T = 24H) of RGCL treatment. Each replicate consisted of at least 15 rosettes. RNA was extracted with Spectrum Plant Total RNA Kit (Sigma). *Arabidopsis* ATH1 microarrays (Affymetrix) were hybridized at the VIB Nucleomics Core (www.nucleomics.be) according to manufacturer's instructions. Expression data were analyzed with FlexArray software (http://genomequebec.mcgill.ca/FlexArray; Blazejczyk et al., 2007). First, background correction,

normalisation and calculation of expression values were performed with Robust Multi-array Average method (Irizarry et al., 2003). Next, expression data were subjected to a two-way ANOVA analysis using the false discovery rate method (Benjamini and Hochberg, 1995). The corrected p-value threshold was set to 0.05. Searches for similarities between expression profiles were conducted with Genevestigator Signature tool implementing Euclidean distance method (http://genevestigator.com). Hierarchical clustering of the normalized expression values was performed with the MultiExperiment Viewer v4.9.0 (www.tm4.org). The analysis implemented Euclidean distance metric and average linkage cluctering method with distance threshold set to 3.7. Gene ontology analysis was performed with Database for Annotation, Visualization and Integrated Discovery (DAVID) v6.7 (http://david.abcc.ncifcrf.gov/; Huang et al., 2009).

GCMS metabolite profiling, glutathione assay

For analysis of primary metabolites plants were subjected to RGCL assay according to the procedures described before. Tissue samples were collected after 0 and 24 hours of oxidative stress treatment. At each time point 5 samples (57 – 64 mg) of shoot tissue per genotype were harvested, frozen immediately in liquid nitrogen and homogenised with ball mill (Retsch, Germany). Powdered tissue was extracted with 300 µl methanol and 30 µl of internal standard (ribitol 0.1 mg/ml) for 15 min at 70°C. Then, 200 µl of chloroform was added and samples were incubated in a rotating shaker for 5 min at 37°C, next 400 µl of water was added and samples were vortexed and centrifuged for 15 min at 16,100 x g. Aliquots of polar phase (160 µl) were dried in the speed-vac. The dried residue was redissolved and derivatized for 90 min at 30°C in 40 µl of 20 mg/ml O-Methylhydroxyamine hydrochloride in pyridine. Next 70 µl of MSTFA and 10 µl of retention time standard mixture (C12, C15, C19, C22, C28, C32, C36 n-alkane mix) were added and samples were incubated for 30 min at 37°C in rotating shaker. GC-MS analyses were carried out with a quadrupole mass-selective detector (model 5973, Hewlett-Packard), coupled to a GC system (6890 series, Hewlett-Packard) equipped with an automated sample injector and an VF-5ms capillary column (30m x 0.25mm). The sample volume was 1 µl. The injector operated in a splitless mode at 230°C with a constant helium flow of 1 ml/min. The oven temperature was held at 70°C for 5 min post injection, then raised to 325°C at a rate of 5°C/min, maintained at 325°C for 1 min and cooled down to a final temperature of 70°C at 50°C/min. The MS transfer line was set to 250°C, the MS ion source to 230°C and the detector to 150°C, throughout the analysis. A full mass spectra were recorded by scanning the m/z range of 60-600 with a solvent delay of 7.8 min. Peak alignment and integration was performed with xcms package (Smith et al., 2006) implemented in Bioconductor (www.bioconductor.org). Normalisation and statistical analysis was performed with MetaboAnalyst 2.0 (www.metaboanalyst.ca, Xia et al., 2012). Custom mass spectra library from the Golm Metabolome Database (Q_MSRI_ID) was imported in AMDIS software (Stein, 1999) in order to annotate peaks of interest.

Measurement of total glutathione level was performed according to a protocol described before (Queval and Noctor, 2007).

Gas exchange

For gas exchange measurements plants were grown in 55 mm square Petri dishes as described for RGCL assay at a density of 5 plants per plate. After three-weeks growth lids were removed and whole plates were analysed with LI-6400XT Portable Photosynthesis System equipped with tightly sealed Licor 6400-17 Whole Plant *Arabidopsis* Chamber and the Licor 6400-18 RGB Light Source. Parameters used for the measurement were as follows: light intensity, 100 $\mu mol \cdot m^{-2} \cdot s^{-1}$; CO_2 level, 400 $\mu mol \cdot M^{-1}$; ambient temperature, 23°C; flow 400 $\mu mol \cdot s^{-1}$ and stomatal ratio set to 1. After the measurement, for each plate, fresh weight of rosettes was determined with analytical balance.

ACKNOWLEDGEMENTS
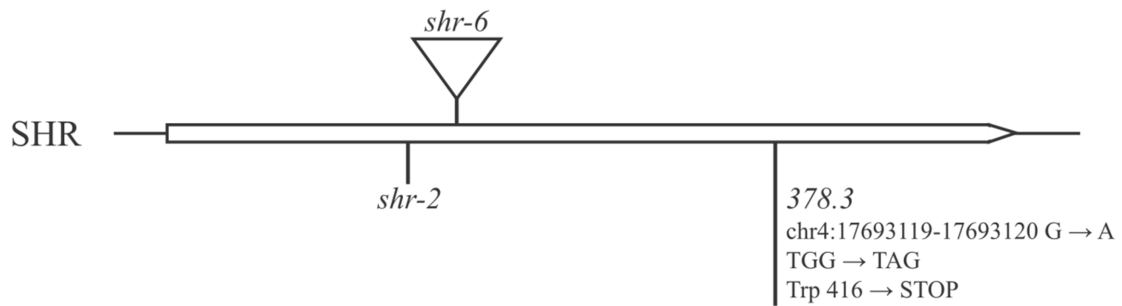
SUPPLEMENTARY INFORMATION

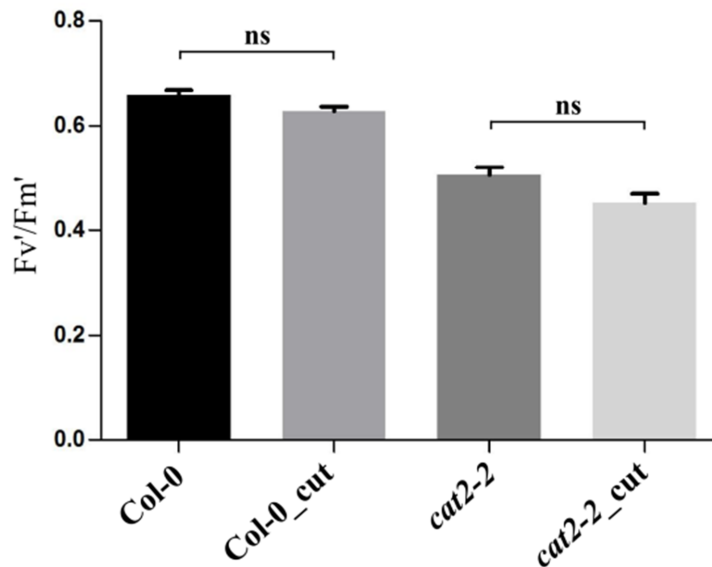**Figure S1.** SHORT-ROOT mutant alleles used in this study.

Figure S2. Mechanical restriction of root size does not affect oxidative stress performance. Plants were grown vertically on 1 x MS medium 1% sucrose in LD conditions. Roots were cut to the length of ~ 2cm every 3 DAS, during the 12-days growth period. Subsequently plants were subjected to RGCL assay. Bars demonstrate Fv'/Fm' value after 7 days of RGCL treatment averaged from 4 biological replicates. Data analyzed with one-way ANOVA followed by Bonferroni's multiple comparison test ($p < 0.05$).
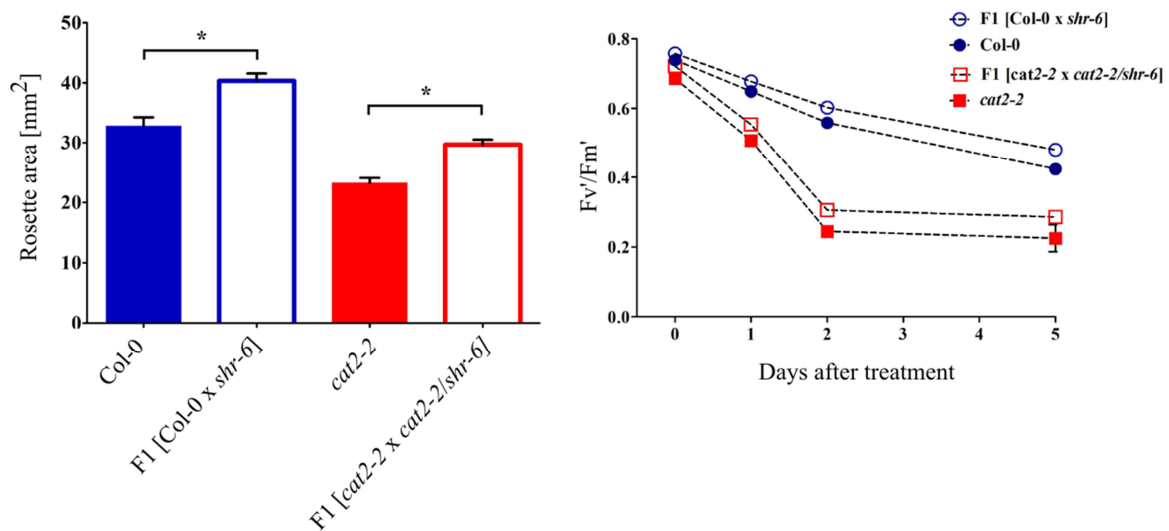
Figure S3. Heterozygous *shr* mutants exhibit enhanced growth but not oxidative stress tolerance. **A)** Projected rosette area for plants heterozygous for *shr-6* mutation in Col-0 and *cat2-2* background. Plants were grown two weeks on 1 x MS medium 1% sucrose. Projected rosette areas were determined with ImageJ software. Bars represent means for approx. 55 plants per line ± SE. Asterisks indicate significant differences to respective control lines according to one-way ANOVA followed by Bonferroni's multiple comparison test ($p < 0.05$). **B)** Changes of Fv'/Fm' during RGCL assay. Three-week old plants grown under long day conditions at 100 $\mu mol \cdot m^{-2} \cdot s^{-1}$ on 1 x MS medium supplemented with 1% sucrose were subjected to photorespiratory stress by mechanical restriction of gas exchange and transfer to continuous light. Data points represent means of three biological replicates ± SE.
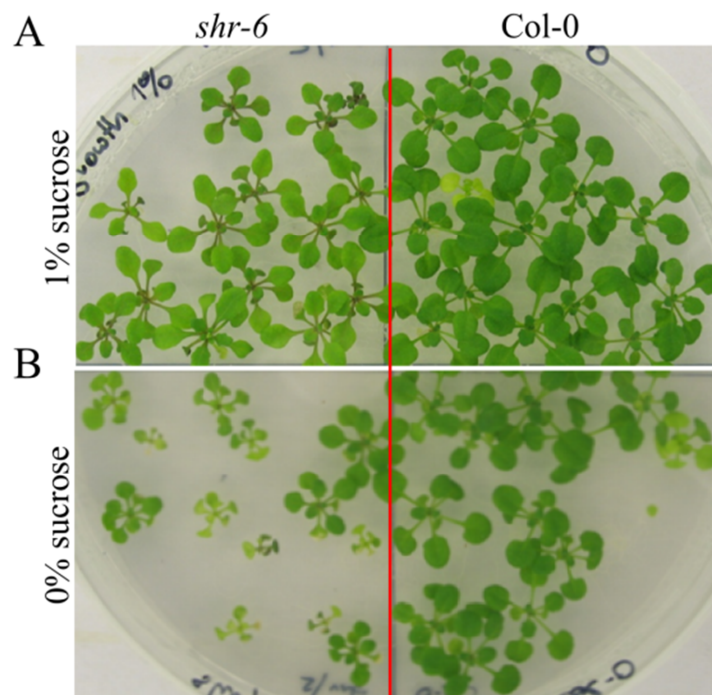

Figure S4. SHORT-ROOT-deficient plants require exogenous sucrose supplementation for normal growth *in vitro*. **A, B)** Three-week old plants grown under long day conditions (16h light / 8h dark) at 100 $\mu mol \cdot m^{-2} \cdot s^{-1}$ on 1 x MS medium supplemented with 1% sucrose **(A)** or without sucrose **(B).**

Figure S5. Lack of SCARECROW does not lead to enhanced oxidative stress tolerance in soil conditions. Plants were grown for three weeks under long day photoperiod (120-130 μmol·m^{-2}·s^{-1}) at elevated CO2 concentration (3000 ppm) and subsequently exposed to 24 hours of continuous excess light irradiation (1100-1200 μmol·m^{-2}·s^{-1}) in ambient air. Representative images demonstrate formation of cell death lesions and reduction of PSII maximum efficiency.
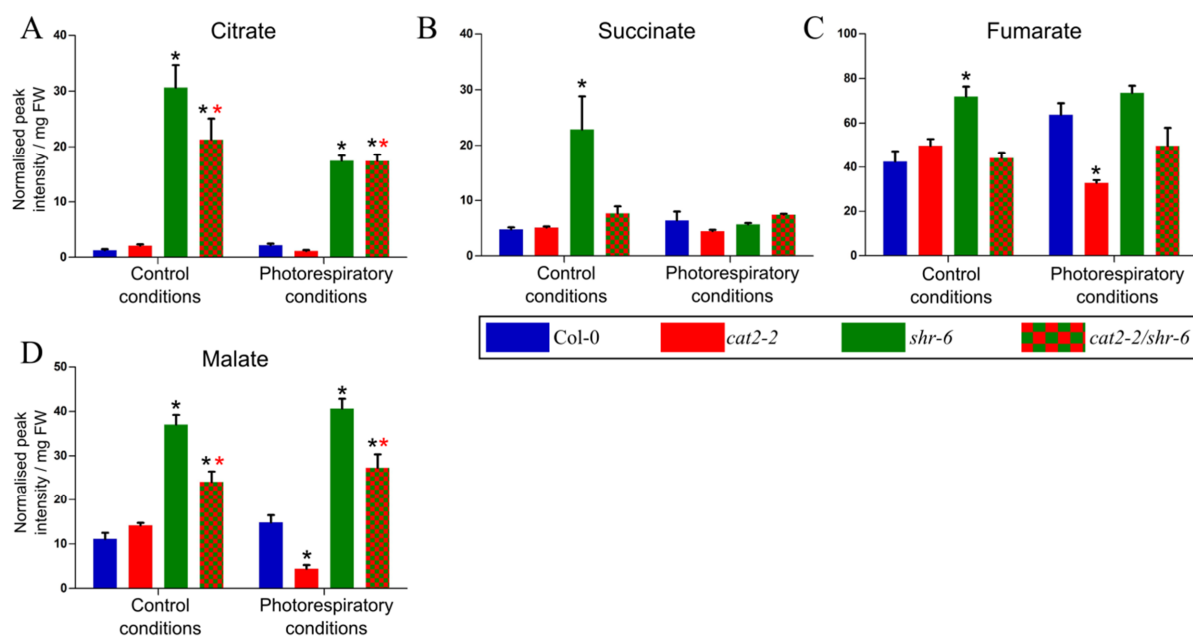
Figure S6. SHORT-ROOT deficiency affects levels of TCA cycle metabolites. **A-D)** GC-MS profiling of polar TCA cycle metabolites. Three-week-old Col-0, *cat2-2*, *shr-6* and *shr-6/cat2-2* mutant plants grown on 1 x MS medium supplemented with 1% sucrose were sealed with parafilm and moved to continuous light. Rosettes were harvested before and after 24 hours of treatment. Values represent means of 5 biological replicates ± SE. Data were analyzed with two-way ANOVA using photorespiratory stress (photorespiratory conditions vs control conditions) and genotype as main factors, and followed by Bonferroni multiple comparisons post-hoc test ($p<0.05$). Black asterisks (*) show significant differences to Col-0, red asterisks (*) mark significant differences between *cat2-2* and *shr-6/cat2-2* line within respective conditions.

Figure S7. Visual output of SHOREmap analysis performed on 238.3 mutant line. Dots represent polymorphisms, color of the dots corresponds to the SHORE score.
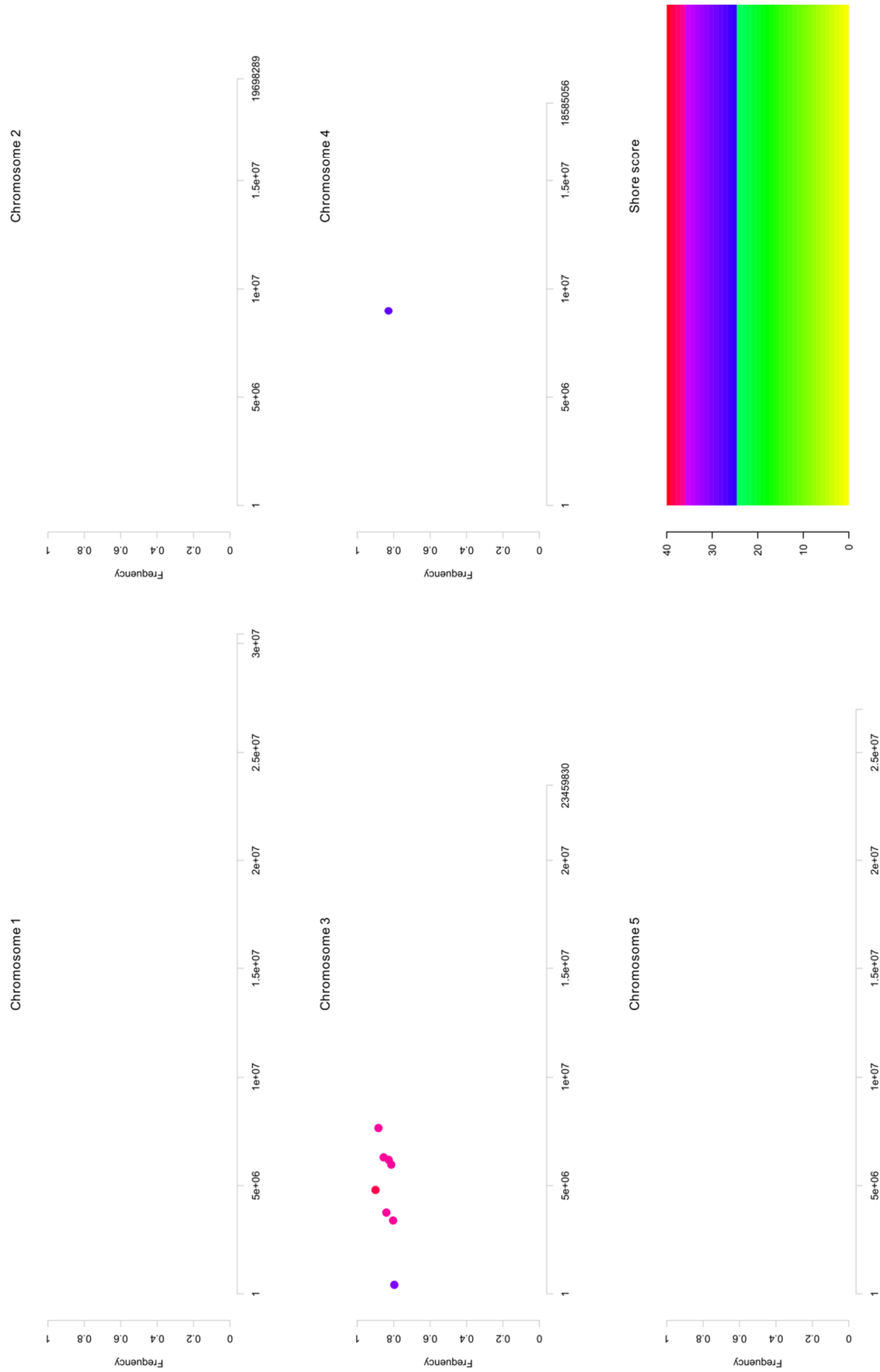
Table S1. [Enclosed on a CD attached to this thesis]. List of differentially expressed genes.

Table S2. List of genes that responded to RGCL treatment in a genotype-specific manner [FC>2, adj. p-value < 0.05]. The order of the genes corresponds to Fig. 8

AGI code	Annotation	0H, cat2-2	0H, shr-6/cat2-2	24H, cat2-2	24H cat2-2/shr-6	Treatment x Genotype log2FC	Adj. p-value	Cluster
At1g78370	ATGSTU20 GSTU20 glutathione S-transferase TAU 20	11.92	11.71	8.80	10.63	-1.02	0.0007	1
At1g02920	GSTF7 glutathione S-transferase 7	9.52	11.93	11.48	11.76	1.07	0.0003	2
At1g02930	GSTF6 glutathione S-transferase 6	8.34	11.10	11.29	11.90	1.07	0.0031	3
At3g16530	Legume lectin family protein	7.77	8.80	11.59	10.57	1.02	0.0019	
At3g57520	AtSIP2 RS2 SIP2 seed imbibition 2	7.70	9.04	11.00	10.26	1.04	0.0016	
At5g67300	ATMYB44 ATMYBR1 MYB44 MYBR1	7.72	8.72	10.38	9.37	1.01	0.0010	
At1g61890	MATE efflux family protein	9.39	9.07	10.73	8.17	1.12	0.0027	
At3g47340	DIN6 glutamine-dependent asparagine synthase 1	5.37	10.09	7.35	9.84	1.11	0.0099	4
At5g20790	unknown protein	5.58	8.93	7.79	8.84	1.15	0.0032	
At1g14870	AtPCR2 PCR2 PLANT CADMIUM RESISTANCE 2	6.33	8.19	8.36	8.10	1.06	0.0369	
At1g14880	AtPCR1 PCR1 PLANT CADMIUM RESISTANCE 1	6.36	8.13	9.13	8.43	1.24	0.0027	
At2g18690	unknown protein	6.56	8.65	8.73	8.70	1.06	0.0034	
At1g19180	JAZ1 TIFY10A jasmonate-zim-domain protein 1	6.73	8.90	8.57	8.54	1.10	0.0010	
At1g32940	ATSBT3.5 SBT3.5 Subtilase family protein							
At3g50480	HR4 homolog of RPW8 4							
At2g16060	AHB1 ARATH GLB1 ATGLB1 GLB1 HB1 NSHB1 hemoglobin 1	5.97	5.68	11.05	8.53	1.11	0.0044	5
At4g15610	Uncharacterised protein family (UPF0497)	6.26	7.79	10.13	9.19	1.23	0.0109	
At5g05600	2-oxoglutarate (2OG) and Fe(II)-dependent oxygenase superfamily protein	5.92	7.77	9.84	8.25	1.72	0.0003	
At5g47220	ERF2 ethylene responsive element binding factor 2	6.41	7.57	9.52	8.03	1.32	0.0013	
At5g09440	EXL4 EXORDIUM like 4	6.50	7.35	9.41	8.14	1.06	0.0024	
At3g12580	ATHSP70 HSP70 heat shock protein 70	6.27	6.74	9.76	7.26	1.48	0.0005	
At3g53230	ATPase, AAA-type, CDC48 protein	6.24	6.95	9.03	7.58	1.08	0.0014	
At5g01740	Nuclear transport factor 2 (NTF2) family protein	6.87	6.96	9.26	7.02	1.17	0.0008	
At1g32640	ATMYC2 JAI1 JIN1 MYC2	6.81	7.26	8.63	6.72	1.19	0.0021	
At1g06160	ORA59 octadecanoid-responsive Arabidopsis AP2/ERF 59	5.24	6.28	9.22	8.13	1.07	0.0023	
At1g10070	BCAT-2 branched-chain amino acid transaminase 2	5.04	5.86	10.05	7.65	1.61	0.0010	
At3g28210	PMZ SAP12 zinc finger (AN1-like) family protein	4.84	5.44	9.37	7.31	1.33	0.0054	
At5g52640	HSP90.1 heat shock protein 90.1	5.36	6.14	8.66	6.50	1.47	0.0019	

Gene	Annotation							Group
At5g39520	Protein of unknown function (DUF1997)	5.05	6.15	7.89	6.96	1.01	0.0027	5
At3g02550	LBD41__LOB domain-containing protein 41	6.32	5.37	10.03	6.17	1.46	0.0007	
At3g22640	PAP85__cupin family protein	4.19	4.07	6.55	4.13	1.15	0.0001	6
At1g19530	unknown protein	3.66	3.50	6.06	3.65	1.13	0.0003	
At5g66985	unknown protein	3.55	3.52	7.10	3.76	1.66	0.0003	
At2g34600	JAZ7_TIFY5B__jasmonate-zim-domain protein 7	3.69	3.97	7.90	4.32	1.93	0.0035	
At4g10270	Wound-responsive family protein	4.53	4.32	9.24	4.60	2.21	0.0003	
At4g12030	BASS5_BAT5__bile acid transporter 5	9.22	7.99	6.25	7.05	-1.02	0.0012	
At2g38340	DREB19__Integrase-type DNA-binding superfamily protein	4.33	4.43	7.90	4.97	1.51	0.0030	
At1g53540	HSP20-like chaperones superfamily protein	4.64	4.61	7.41	4.92	1.23	0.0006	
At5g15120	Protein of unknown function (DUF1637)	5.32	4.98	7.97	5.50	1.07	0.0009	
At1g07500	unknown protein	4.79	4.91	7.89	5.32	1.34	0.0015	
At2g27690	CYP94C1__cytochrome P450, family 94, subfamily C, polypeptide 1	5.14	4.78	8.12	4.90	1.43	0.0010	
At5g51440	HSP20-like chaperones superfamily protein	5.40	5.67	8.25	5.70	1.41	0.0029	
At3g46230	ATHSP17.4_HSP17.4__heat shock protein 17.4	5.31	5.34	8.20	6.01	1.11	0.0059	
At1g07400	HSP20-like chaperones superfamily protein	4.97	5.22	8.18	6.23	1.10	0.0021	
At1g59860	HSP20-like chaperones superfamily protein							
At1g08630	THA1__threonine aldolase 1	5.05	4.80	8.85	6.26	1.17	0.0008	
At4g39675	unknown protein	5.03	4.66	8.67	5.83	1.23	0.0006	
At4g11890	Protein kinase superfamily protein	4.69	6.30	6.38	5.67	1.16	0.0025	
At5g48570	ATFKBP65_FKBP-type peptidyl-prolyl cis-trans isomerase family protein	4.91	5.31	6.87	4.86	1.20	0.0008	
At1g17380	JAZ5_TIFY11A__jasmonate-zim-domain protein 5	4.61	4.94	6.37	4.63	1.04	0.0175	
At1g53885	Protein of unknown function (DUF581)	5.88	6.29	7.51	4.00	1.96	0.0020	
At1g53903	Protein of unknown function (DUF581)							
At1g56650	ATMYB75_MYB75_PAP1_SIAA1__production of anthocyanin pigment 1	4.81	7.15	4.50	4.33	1.26	0.0037	7
At2g24850	TAT_TAT3__tyrosine aminotransferase 3	4.71	7.03	4.51	4.66	1.08	0.0105	
At1g70080	Terpenoid cyclases/Protein prenyltransferases superfamily protein	4.74	5.03	5.01	7.37	-1.04	0.0004	8
At1g66570	ATSUC7_SUC7__sucrose-proton symporter 7	5.59	6.24	5.44	8.28	-1.09	0.0221	
At1g13650	Unknown protein	9.46	4.96	6.64	4.70	-1.28	0.0010	9
At4g03060	Unknown protein	8.86	6.75	5.95	5.89	-1.02	0.0022	
At1g16400	CYP79F2__cytochrome P450, family 79, subfamily F, polypeptide 2	8.67	7.18	4.70	6.21	-1.50	0.0013	
At1g16410	BUS1_CYP79F1_SPS1__cytochrome p450 79f1							
At5g07690	ATMYB29_MYB29	7.83	6.04	4.67	5.18	-1.15	0.0002	
At5g12030	AT-HSP17.6A_HSP17.6_HSP17.6A__heat shock protein 17.6A	4.22	4.25	8.28	5.18	1.57	0.0039	10
At2g43100	ATLEUD1_IPMI2__isopropylmalate isomerase 2	9.11	7.93	6.13	7.29	-1.17	0.0019	
At1g62560	FMO GS-OX3__flavin-monooxygenase glucosinolate S-oxygenase 3	9.02	7.85	6.12	7.33	-1.19	0.0012	
At5g10400	Histone superfamily protein	8.87	7.99	6.15	7.51	-1.13	0.0021	
At3g54560	HTA11__histone H2A 11	8.95	7.88	6.61	7.66	-1.06	0.0005	
At1g09200	Histone superfamily protein	10.05	9.34	7.42	8.84	-1.06	0.0005	
At3g19710	BCAT4__branched-chain aminotransferase4	11.50	9.04	8.10	9.28	-1.82	0.0002	

Table S3. List of microarray experiments significantly resembling transcriptomic patterns evoked by SHORT-ROOT deficiency.

No.	Experiment description	Relative similarity	Repository ID / Reference
1	Cytokinin receptor triple mutant *ahk2/ahk3/ahk4* vs Col-0	1.748	E-MEXP-1262 / -
2	SET DOMAIN GROUP 2-deficient mutant *sdg2-1* vs Col-0	1.491	GSE23208 / (Guo et al., 2010)
3	*Arabidopsis* line overexpressing rice full lenght cDNA of LBD37 (Os-LBD37) vs empty vector control line	1.397	GSE14646 / (Albinsky et al., 2010)
4	*Immutans (im)* green sectors vs Col-1	1.380	NASCARRAYS-343 / (Aluru et al., 2009)
5	RNAi line with silenced *OBERON1* and *OBERON2* vs Col-0	1.376	GSE19341 /-
6	Cold treatment, *ice1* mutant vs ctrl line (pCBF3::LUC)	1.333	GSE3326 / (Lee et al., 2005)
7	*Arabidopsis* line overexpressing RESPONSE REGULATOR 22 (ARR22) vs Col-0	1.332	GSE5698 / (Goda et al., 2008)
8	Double mutant of chloroplast GAPDH isoforms *gapcp1/gapcp2* vs Col-0	1.331	GSE14765 / (Muñoz-Bertomeu et al., 2009)
9	Col-0 seedlings exposed to low vs high Pi concentration	1.282	E-MEXP-791 / (Misson et al., 2005)
10	ABSCISIC ACID INSENSITIVE 4 / VITAMIN C DEFECTIVE 2 double mutant *abi4/vtc2* vs Col-0	1.275	GSE23329 / (Kerchev et al., 2011)

Table S4. Summary of EMS-specific polimorphisms significantly enriched in 238.3 mutant plants. Polymorphisms were filtered with frequency threshold set to 0.8.

Chromosome	Position	Reference base	Mutant	Coverage	Frequency	Region	AGI code	Position in gene	Position in codon	Reference aa	Mutant
3	4822263	G	A	65	0.9	CDS	AT3G14420	263	2	G	E
3	7636562	G	A	40	0.89	intergenic					
3	6290758	G	A	60	0.86	intergenic					
3	3807077	G	A	54	0.84	intergenic					
3	6145283	G	A	43	0.83	five_prime_UTR	AT3G17940				
4	8981113	G	A	5	0.83	intronic/noncoding	AT4G15780				
3	6021032	G	A	50	0.82	CDS	AT3G17600	9	3	V	V
3	436295	C	T	60	0.8	CDS	AT3G02260	11022	3	E	E
3	3397230	G	A	37	0.8	intronic/noncoding	AT3G10845				
3	6031593	G	A	51	0.8	CDS	AT3G17630	2223	3	K	K

Table S5. List of primers used in this study

Primer	Sequence (5' - 3')	RE
CAT2_LP	CCCAGAGGTACCTCTTCTTCTCCCATG	
CAT2_RP	TCAGGGAACTTCATCCCATCGC	
SALK_NewLB1	TGGACCGCTTGCTGCAACTCTC	
ET8347_LP	GTTCTCGGGAACCTAAATTCG	
ET8347_RP	TCATGGAGGAGTTGTTGTTCC	
DS3.2	CGATTACCGTATTTATCCCGTTC	
DS5.1	GAAACGGTCGGGAAACTAGCTCTAC	
cat2_F_attB1	GGGGACAAGTTTGTACAAAAAAGCAGGCTTC-ATGGATCCTTACAAGTATCGTCCAG	
cat2_R_attB2	GGGGACCACTTTGTACAAGAAAGCTGGGTC-TTAGATGCTTGGTCTCACGTTCAGACGGCTTGCC	
SHR_NcoI_F	GAGGGTTTGGAGAATGTTTACCAT	NcoI
SHR_dCAPS_R	CCGCTCCAAACCCACTATTCCT	
UGT73B1_HpaII_F	ATCATGTCCTGACATATCTAAACCG	HpaII
UGT73B1_dCAPS_R	AAAAGAGCGTGGCATATCGG	
cat2_qRT_LP	GCTGGCAAGCCGTCTGAAC	
cat2_qRT_RP	AGCACAGAAGATCCACATGATGAAG	
ARP7_qRT_LP	AACTTGTGCTCATCTGCCATTAGG	
ARP7_qRT_RP	TGATTCTGCGGAAACACCACTTTAG	
PP2A_qRT_LP	GACCGGAGCCAACTAGGAC	
PP2A_qRT_RP	AAAACTTGGTAACTTTTCCAGCA	

REFERENCES

Abat JK, Mattoo AK, Deswal R (2008) S-nitrosylated proteins of a medicinal CAM plant *Kalanchoe pinnata* ribulose-1,5-bisphosphate carboxylase/oxygenase activity targeted for inhibition. FEBS J **275**: 2862–72

Albinsky D, Kusano M, Higuchi M, Hayashi N, Kobayashi M, Fukushima A, Mori M, Ichikawa T, Matsui K, Kuroda H, et al (2010) Metabolomic screening applied to rice FOX *Arabidopsis* lines leads to the identification of a gene changing nitrogen metabolism. Mol Plant **3**: 125–42

Alet AI, Sanchez DH, Cuevas JC, del Valle S, Altabella T, Tiburcio AF, Marco F, Ferrando A, Espasandín FD, González ME, et al (2011) Putrescine accumulation in *Arabidopsis thaliana* transgenic lines enhances tolerance to dehydration and freezing stress. Plant Signal Behav **6**: 278–286

Aluru MR, Zola J, Foudree A, Rodermel SR (2009) Chloroplast photooxidation-induced transcriptome reprogramming in *Arabidopsis* immutans white leaf sectors. Plant Physiol **150**: 904–23

Anderson L (1971) Chloroplast and cytoplasmic enzymes. II. Pea leaf triose phosphate isomerases. Biochim Biophys Acta **235**: 237–44

Baker NR (2008) Chlorophyll fluorescence: a probe of photosynthesis in vivo. Annu Rev Plant Biol **59**: 89–113

Bartsch O, Mikkat S, Hagemann M, Bauwe H (2010) An autoinhibitory domain confers redox regulation to maize glycerate kinase. Plant Physiol **153**: 832–40

Bauwe H, Hagemann M, Kern R, Timm S (2012) Photorespiration has a dual origin and manifold links to central metabolism. Curr Opin Plant Biol **15**: 269–275

Benfey PN, Linstead PJ, Roberts K, Schiefelbein JW, Hauser MT, Aeschbacher RA (1993) Root development in *Arabidopsis*: four mutants with dramatically altered root morphogenesis. Development **119**: 57–70

Benjamini Y, Hochberg Y (1995) Controlling the false discovery rate: a practical and powerful approach to multiple testing. J R Stat Soc Ser B **57**: 289–300

Bienert GP, Schjoerring JK, Jahn TP (2006) Membrane transport of hydrogen peroxide. Biochim Biophys Acta **1758**: 994–1003

Binder S (2010) Branched-chain amino acid metabolism in *Arabidopsis thaliana*. *Arabidopsis* Book e0137

Blume C, Behrens C, Eubel H, Braun H-P, Peterhansel C (2013) A possible role for the chloroplast pyruvate dehydrogenase complex in plant glycolate and glyoxylate metabolism. Phytochemistry **95**: 168–76

Campbell WJ, Ogren WL (1990) Glyoxylate inhibition of ribulosebisphosphate carboxylase/oxygenase activation in intact, lysed , and reconstituted chloroplasts. Photosynth Res **23**: 257–268

Carol P, Stevenson D, Bisanz C, Breitenbach J, Sandmann G, Mache R, Coupland G, Kuntz M (1999) Mutations in the *Arabidopsis* gene *IMMUTANS* cause a variegated phenotype by inactivating a chloroplast terminal oxidase associated with phytoene desaturation. Plant Cell **11**: 57–68

Carvalho JDFC, Madgwick PJ, Powers SJ, Keys AJ, Lea PJ, Parry MAJ (2011) An engineered pathway for glyoxylate metabolism in tobacco plants aimed to avoid the release of ammonia in photorespiration. BMC Biotechnol **11**: 111

Chaouch S, Noctor G (2010) Myo -inositol abolishes salicylic acid-dependent cell death and pathogen defence responses triggered by peroxisomal hydrogen peroxide. New Phytol 711–718

Chaouch S, Queval G, Vanderauwera S, Mhamdi A, Vandorpe M, Langlois-Meurinne M, Van Breusegem F, Saindrenan P, Noctor G (2010) Peroxisomal hydrogen peroxide is coupled to biotic defense responses by ISOCHORISMATE SYNTHASE1 in a daylength-related manner. Plant Physiol **153**: 1692–705

Chastain C, Ogren W (1989) Glyoxylate inhibition of ribulosebisphosphate carboxylase/oxygenase activation state in vivo. Plant Cell Physiol **30**: 937–944

Chen R, Sun S, Wang C, Li Y, Liang Y, An F, Li C, Dong H, Yang X, Zhang J, et al (2009) The *Arabidopsis PARAQUAT RESISTANT2* gene encodes an S-nitrosoglutathione reductase that is a key regulator of cell death. Cell Res **19**: 1377–87

Clare DA, Duong MN, Darr D, Archibald F, Fridovich I (1984) Effects of molecular oxygen on detection of superoxide radical with nitroblue tetrazolium and on activity stains for catalase. Anal Biochem **140**: 532–7

Corpas FJ, Hayashi M, Mano S, Nishimura M, Barroso JB (2009) Peroxisomes are required for in vivo nitric oxide accumulation in the cytosol following salinity stress. Plant Physiol **151**: 2083–2094

Cuevas JC, López-Cobollo R, Alcázar R, Zarza X, Koncz C, Altabella T, Salinas J, Tiburcio AF, Ferrando A (2008) Putrescine is involved in *Arabidopsis* freezing tolerance and cold acclimation by regulating abscisic acid levels in response to low temperature. Plant Physiol **148**: 1094–105

Cui H, Hao Y, Kong D (2012) SCARECROW has a SHORT-ROOT-independent role in modulating the sugar response. Plant Physiol **158**: 1769–78

Cui H, Kong D, Liu X, Hao Y (2014) SCARECROW, SCR-like 23 and SHORT-ROOT control bundle sheath cell fate and function in *Arabidopsis thaliana*. Plant J doi: 10.1111/tpj.12470

Cui H, Levesque MP, Vernoux T, Jung JW, Paquette AJ, Gallagher KL, Wang JY, Blilou I, Scheres B, Benfey PN (2007) An evolutionarily conserved mechanism delimiting SHR movement defines a single layer of endodermis in plants. Science **316**: 421–5

Dalchau N, Hubbard KE, Robertson FC, Hotta CT, Briggs HM, Stan G-B, Gonçalves JM, Webb AAR (2010) Correct biological timing in *Arabidopsis* requires multiple light-signaling pathways. Proc Natl Acad Sci U S A **107**: 13171–6

Dhondt S, Coppens F, De Winter F, Swarup K, Merks RMH, Inzé D, Bennett MJ, Beemster GTS (2010) SHORT-ROOT and SCARECROW regulate leaf growth in *Arabidopsis* by stimulating S-phase progression of the cell cycle. Plant Physiol **154**: 1183–95

Donahue JL, Alford SR, Torabinejad J, Kerwin RE, Nourbakhsh A, Ray WK, Hernick M, Huang X, Lyons BM, Hein PP, et al (2010) The *Arabidopsis thaliana* Myo-inositol 1-phosphate synthase1 gene is required for myo-inositol synthesis and suppression of cell death. Plant Cell **22**: 888–903

Durek P, Schmidt R, Heazlewood JL, Jones A, Maclean D, Nagel A, Kersten B, Schulze WX (2010) PhosPhAt : the *Arabidopsis thaliana* phosphorylation site database . An update. Nucleic Acids Res **38**: 828–834

Essigmann B, Güler S, Narang RA, Linke D, Benning C (1998) Phosphate availability affects the thylakoid lipid composition and the expression of *SQD1*, a gene required for sulfolipid biosynthesis in *Arabidopsis thaliana*. Proc Natl Acad Sci U S A **95**: 1950–5

Ford KA, Casida JE, Chandran D, Gulevich AG, Okrent RA, Durkin KA, Sarpong R, Bunnelle EM, Wildermuth MC (2010) Neonicotinoid insecticides induce salicylate-associated plant defense responses. Proc Natl Acad Sci U S A **107**: 17527–32

Fujita M, Fujita Y, Iuchi S, Yamada K, Kobayashi Y, Urano K, Kobayashi M, Yamaguchi-Shinozaki K, Shinozaki K (2012) Natural variation in a polyamine transporter determines paraquat tolerance in *Arabidopsis*. Proc Natl Acad Sci U S A **109**: 6343–7

Fukaki H, Fujisawa H, Tasaka M (1996) SGR1, SGR2, and SGR3: novel genetic loci involved in shoot gravitropism in *Arabidopsis thaliana*. **110**: 945–955

Fukaki H, Wysocka-Diller J, Kato T, Fujisawa H, Benfey PN, Tasaka M (1998) Genetic evidence that the endodermis is essential for shoot gravitropism in *Arabidopsis thaliana*. Plant J **14**: 425–30

Gadjev I, Vanderauwera S, Gechev T (2006) Transcriptomic footprints disclose specificity of reactive oxygen species signaling in *Arabidopsis*. Plant Physiol **141**: 436–445

Gechev T, Mehterov N, Denev I, Hille J (2013) A simple and powerful approach for isolation of *Arabidopsis* mutants with increased tolerance to H_2O_2-induced cell death., 1st ed. Methods Enzymol **527**: 203–20

Goda H, Sasaki E, Akiyama K, Maruyama-Nakashita A, Nakabayashi K, Li W, Ogawa M, Yamauchi Y, Preston J, Aoki K, et al (2008) The AtGenExpress hormone and chemical treatment data set: experimental design, data evaluation, model data analysis and data access. Plant J **55**: 526–542

Gonzalez-Moro B, Lacuesta M, Becerril JM, Gonzalez-Murua C, Munoz-Rueda A (1997) Glycolate accumulation causes a decrease of photosynthesis by inhibiting RUBISCO activity in maize. J Plant Physiol **150**: 388–394

Goyal A, Tolbert N (1996) Association of glycolate oxidation with photosynthetic electron transport in plant and algal chloroplasts. Proc Natl Acad Sci U S A **93**: 3319–24

Guo L, Yu Y, Law JA, Zhang X (2010) SET DOMAIN GROUP2 is the major histone H3 lysine 4 trimethyltransferase in *Arabidopsis*. Proc Natl Acad Sci U S A **107**: 18557–62

Hammond JP, White PJ (2008) Sucrose transport in the phloem: integrating root responses to phosphorus starvation. J Exp Bot **59**: 93–109

Han Y, Mhamdi A, Chaouch S, Noctor G (2013) Regulation of basal and oxidative stress-triggered jasmonic acid-related gene expression by glutathione. Plant cell Environ **36**: 1135–46

Härtel H, Essigmann B, Lokstein H, Hoffmann-Benning S, Peters-Kottig M, Benning C (1998) The phospholipid deficient *pho1* mutant of *Arabidopsis thaliana* is affected in the organization, but not in the light acclimation, of the thylakoid membrane. Biochim Biophys Acta **1415**: 205–18

Hartwig B, James GV, Konrad K, Schneeberger K, Turck F (2012) Fast isogenic mapping-by-sequencing of ethyl methanesulfonate-induced mutant bulks. Plant Physiol **160**: 591–600

Hayashi M, Toriyama K, Kondo M, Nishimura M (1998) 2,4-Dichlorophenoxybutyric acid-resistant mutants of *Arabidopsis* have defects in glyoxysomal fatty acid beta-oxidation. Plant Cell **10**: 183–95

Heazlewood JL, Durek P, Hummel J, Selbig J, Weckwerth W, Walther D, Schulze WX (2008) PhosPhAt : a database of phosphorylation sites in *Arabidopsis thaliana* and a plant-specific phosphorylation site predictor. Nucleic Acids Res **36**: 1015–1021

Helariutta Y, Fukaki H, Wysocka-Diller J, Nakajima K, Jung J, Sena G, Hauser MT, Benfey PN (2000) The SHORT-ROOT gene controls radial patterning of the *Arabidopsis* root through radial signaling. Cell **101**: 555–67

Hodges M, Jossier M, Boex-Fontvieille E, Tcherkez G (2013) Protein phosphorylation and photorespiration. Plant Biol (Stuttg) **15**: 694–706

Hruz T, Laule O, Szabo G, Wessendorp F, Bleuler S, Oertle L, Widmayer P, Gruissem W, Zimmermann P (2008) Genevestigator v3: a reference expression database for the meta-analysis of transcriptomes. Adv Bioinformatics **2008**: 420747

Hu J, Baker A, Bartel B, Linka N, Mullen RT, Reumann S, Zolman BK. Plant peroxisomes: biogenesis and function. Plant Cell. 2012 Jun;24(6):2279-303

Huang DW, Sherman BT, Lempicki RA (2009) Systematic and integrative analysis of large gene lists using DAVID bioinformatics resources. Nat Protoc **4**: 44–57

Irizarry RA, Bolstad BM, Collin F, Cope LM, Hobbs B, Speed TP (2003) Summaries of Affymetrix GeneChip probe level data. Nucleic Acids Res. doi: 10.1093/nar/gng015

Kebeish R, Niessen M, Thiruveedhi K, Bari R, Hirsch H-J, Rosenkranz R, Stäbler N, Schönfeld B, Kreuzaler F, Peterhänsel C (2007) Chloroplastic photorespiratory bypass increases photosynthesis and biomass production in *Arabidopsis thaliana*. Nat Biotechnol **25**: 593–9

Kerchev P, Mühlenbock P, Denecker J, Morreel K, Hoeberichts FA, Van Der Kelen K, Vandorpe M, Nguyen L, Audenaert D, Van Breusegem F (2014) Activation of auxin signaling counteracts photorespiratory H_2O_2-dependent cell death. Plant Cell Environ DOI: 10.1111/pce.12250

Kerchev PI, Pellny TK, Vivancos PD, Kiddle G, Hedden P, Driscoll S, Vanacker H, Verrier P, Hancock RD, Foyer CH (2011) The transcription factor ABI4 Is required for the ascorbic acid-dependent regulation of growth and regulation of jasmonate-dependent defense signaling pathways in *Arabidopsis*. Plant Cell **23**: 3319–34

Kiba T, Aoki K, Sakakibara H, Mizuno T (2004) *Arabidopsis* response regulator, ARR22, ectopic expression of which results in phenotypes similar to the *wol* cytokinin-receptor mutant. Plant Cell Physiol **45**: 1063–77

Koizumi K, Hayashi T, Wu S, Gallagher KL (2012) The SHORT-ROOT protein acts as a mobile , dose- dependent signal in patterning the ground tissue. Proc Natl Acad Sci U S A **109**: 13010–13015

Kurepa J, Smalle J, Van Montagu M, Inzé D (1998) Oxidative stress tolerance and longevity in *Arabidopsis*: the late flowering mutant *gigantea* is tolerant to paraquat. Plant J **14**: 759–64

Di Laurenzio L, Wysocka-Diller J, Malamy JE, Pysh L, Helariutta Y, Freshour G, Hahn MG, Feldmann KA, Benfey PN (1996) The SCARECROW gene regulates an asymmetric cell division that is essential for generating the radial organization of the *Arabidopsis* root. Cell **86**: 423–33

Lee B, Henderson DA, Zhu J-K (2005) The *Arabidopsis* cold-responsive transcriptome and its regulation by ICE1. Plant Cell **17**: 3155–3175

Lei M, Liu Y, Zhang B, Zhao Y, Wang X, Zhou Y, Raghothama KG, Liu D (2011) Genetic and genomic evidence that sucrose is a global regulator of plant responses to phosphate starvation in *Arabidopsis*. Plant Physiol **156**: 1116–30

Levesque MP, Vernoux T, Busch W, Cui H, Wang JY, Blilou I, Hassan H, Nakajima K, Matsumoto N, Lohmann JU, et al (2006) Whole-genome analysis of the SHORT-ROOT developmental pathway in *Arabidopsis*. PLoS Biol **4**: e143

Levine A, Tenhaken R, Dixon R, Lamb C (1994) H_2O_2 from the oxidative burst orchestrates the plant hypersensitive disease resistance response. Cell **79**: 583–93

Li H, Durbin R (2009) Fast and accurate short read alignment with Burrows-Wheeler transform. Bioinformatics **25**: 1754-60

Li J, Mu J, Bai J, Fu F, Zou T, An F, Zhang J, Jing H, Wang Q, Li Z, et al (2013) PARAQUAT RESISTANT 1, a Golgi-localized putative transporter protein, is involved in intracellular transport of paraquat. Plant Physiol. doi: 10.1104/pp.113.213892

Lu Y, Li Y, Yang Q, Zhang Z, Chen Y, Zhang S, Peng X-X (2013) Suppression of glycolate oxidase causes glyoxylate accumulation that inhibits photosynthesis through deactivating Rubisco in rice. Physiol Plant doi:10.1111/ppl.12104

Lukowitz W, Gillmor CS, Scheible WR (2000) Positional cloning in *Arabidopsis*. Why it feels good to have a genome initiative working for you. Plant Physiol **123**: 795–805

Maier A, Fahnenstich H, von Caemmerer S, Engqvist MKM, Weber APM, Flügge U-I, Maurino VG (2012) Transgenic introduction of a glycolate oxidative cycle into *A. thaliana* chloroplasts leads to growth improvement. Front Plant Sci **3**: 38

Maurino VG, Peterhansel C (2010) Photorespiration: current status and approaches for metabolic engineering. Curr Opin Plant Biol **13**: 249–56

Mhamdi A, Queval G, Chaouch S, Vanderauwera S, Van Breusegem F, Noctor G (2010) Catalase function in plants: a focus on *Arabidopsis* mutants as stress-mimic models. J Exp Bot **61**: 4197–220

Misson J, Raghothama KG, Jain A, Jouhet J, Block MA, Bligny R, Ortet P, Creff A, Somerville S, Rolland N, et al (2005) A genome-wide transcriptional analysis using *Arabidopsis thaliana* Affymetrix gene chips determined plant responses to phosphate deprivation. Proc Natl Acad Sci U S A **102**: 11934–9

Mittler R, Vanderauwera S, Suzuki N, Miller G, Tognetti VB, Vandepoele K, Gollery M, Shulaev V, Van Breusegem F (2011) ROS signaling: the new wave? Trends Plant Sci **16**: 300–9

Muñoz-Bertomeu J, Cascales-Miñana B, Mulet JM, Baroja-Fernández E, Pozueta-Romero J, Kuhn JM, Segura J, Ros R (2009) Plastidial glyceraldehyde-3-phosphate dehydrogenase deficiency leads to altered root development and affects the sugar and amino acid balance in *Arabidopsis*. Plant Physiol **151**: 541–58

Nakajima K, Sena G, Nawy T, Benfey PN (2001) Intercellular movement of theputative transcription factor SHR in root patterning. Nature **413**: 307–311

Neff MM, Turk E, Kalishman M (2002) Web-based primer design for single nucleotide polymorphism analysis. Trends Genet **18**: 613–5

Nishimura C, Ohashi Y, Sato S, Kato T, Tabata S, Ueguchi C (2004) Histidine kinase homologs that act as cytokinin receptors possess overlapping functions in the regulation of shoot and root growth in *Arabidopsis*. Plant Cell **16**: 1365-1377

Nito K, Kamigaki A, Kondo M, Hayashi M, Nishimura M (2007) Functional classification of *Arabidopsis* peroxisome biogenesis factors proposed from analyses of knockdown mutants. Plant Cell Physiol **48**: 763–74

Noctor G, Arisi A-CM, Jouanin L, Foyer CH (1999) Photorespiratory glycine enhances glutathione accumulation in both the chloroplastic and cytosolic compartments. J Exp Bot **50**: 1157–1167

Ortega-Galisteo AP, Rodríguez-Serrano M, Pazmiño DM, Gupta DK, Sandalio LM, Romero-Puertas MC (2012) S-nitrosylated proteins in pea (*Pisum sativum* L.) leaf peroxisomes: changes under abiotic stress. J Exp Bot **63**: 2089-103

Ossowski S, Schneeberger K, Clark RM, Lanz C, Warthmann N, Weigel D (2008) Sequencing of natural strains of *Arabidopsis thaliana* with short reads. Genome Res **18**: 2024–2033

Overmyer K, Brosche M, Pellinen R, Kuittinen T, Tuominen H, Ahlfors R, Keinanen M, Saarma M, Scheel D, Kangasjarvi J (2005) Ozone-induced programmed cell death in the *Arabidopsis radical-induced cell death 1* mutant. Plant physiology **137**: 1092–1104

Overmyer K, Tuominen H, Kettunen R, Betz C, Langebartels C, Sandermann H, Kangasjärvi J (2000) Ozone-sensitive *Arabidopsis rcd1* mutant reveals opposite roles for ethylene and jasmonate signaling pathways in regulating superoxide-dependent cell death. Plant Cell **12**: 1849–62

Parry MAJ, Andralojc PJ, Scales JC, Salvucci ME, Carmo-Silva EA, Alonso H, Whitney SM (2013) Rubisco activity and regulation as tagrets for crop improvement. J Exp Bot **64**: 717–730

Peterhansel C, Blume C, Offermann S (2013) Photorespiratory bypasses: how can they work? J Exp Bot **64**: 709–715

Peterhansel C, Maurino VG (2011) Photorespiration redesigned. Plant Physiol **155**: 49–55

Petrov VD, Van Breusegem F (2012) Hydrogen peroxide-a central hub for information flow in plant cells. AoB Plants **2012**: pls014

Pick TR, Bräutigam A, Schulz MA, Obata T, Fernie AR, Weber APM (2013) PLGG1, a plastidic glycolate glycerate transporter, is required for photorespiration and defines a unique class of metabolite transporters. Proc Natl Acad Sci U S A **110**: 3185–90

Proost S, Van Bel M, Sterck L, Billiau K, Van Parys T, Van de Peer Y, Vandepoele K (2009) PLAZA: a comparative genomics resource to study gene and genome evolution in plants. Plant Cell **21**: 3718–31

Queval G, Issakidis-Bourguet E, Hoeberichts FA, Vandorpe M, Gakière B, Vanacker H, Miginiac-Maslow M, Van Breusegem F, Noctor G (2007) Conditional oxidative stress responses in the *Arabidopsis* photorespiratory mutant *cat2* demonstrate that redox state is a key modulator of daylength-dependent gene expression, and define photoperiod as a crucial factor in the regulation of H_2O_2-induced cell death. Plant J **52**: 640–57

Queval G, Neukermans J, Vanderauwera S, Van Breusegem F, Noctor G (2012) Day length is a key regulator of transcriptomic responses to both CO_2 and H_2O_2 in *Arabidopsis*. Plant cell Environ **35**: 374–87

Queval G, Noctor G (2007) A plate reader method for the measurement of NAD, NADP, glutathione, and ascorbate in tissue extracts: Application to redox profiling during *Arabidopsis* rosette development. Anal Biochem **363**: 58–69

Ramel F, Sulmon C, Bogard M, Couée I, Gouesbet G (2009a) Differential patterns of reactive oxygen species and antioxidative mechanisms during atrazine injury and sucrose-induced tolerance in *Arabidopsis thaliana* plantlets. BMC Plant Biol **9**: 28

Ramel F, Sulmon C, Gouesbet G, Couée I (2009b) Natural variation reveals relationships between pre-stress carbohydrate nutritional status and subsequent responses to xenobiotic and oxidative stress in *Arabidopsis thaliana*. Ann Bot **104**: 1323–37

Rippert P, Puyaubert J, Grisollet D, Derrier L, Matringe M (2009) Tyrosine and phenylalanine are synthesized within the plastids in *Arabidopsis*. Plant Physiol **149**: 1251–60

Ritte G, Scharf A, Eckermann N, Haebel S, Steup M (2004) Phosphorylation of transitory starch is increased during degradation. Plant physilogy **135**: 2068–2077

Rojas CM, Senthil-Kumar M, Wang K, Ryu C-M, Kaundal A, Mysore KS (2012) Glycolate oxidase modulates reactive oxygen species-mediated signal transduction during nonhost resistance in Nicotiana benthamiana and *Arabidopsis*. Plant Cell **24**: 336–52

Ros R, Cascales-Miñana B, Segura J, Anoman AD, Toujani W, Flores-Tornero M, Rosa-Tellez S, Muñoz-Bertomeu J (2012) Serine biosynthesis by photorespiratory and non-photorespiratory pathways: an interesting interplay with unknown regulatory networks. Plant Biol (Stuttg). 2013 Jul;15(4):707-12

Rouhier N, Villarejo A, Srivastava M, Gelhaye E, Keech O, Droux M, Finkemeier I, Samuelsson G, Dietz KJ, Jacquot J, et al (2005) Identification of plant glutaredoxin targets. Antioxid Redox Signal **7**: 919–929

Rubio V, Linhares F, Solano R, Martín AC, Iglesias J, Leyva A, Paz-Ares J (2001) A conserved MYB transcription factor involved in phosphate starvation signaling both in vascular plants and in unicellular algae. Genes Dev **15**: 2122-33

Saiga S, Furumizu C, Yokoyama R, Kurata T, Sato S, Kato T, Tabata S, Suzuki M, Komeda Y (2008) The *Arabidopsis OBERON1* and *OBERON2* genes encode plant homeodomain finger proteins and are required for apical meristem maintenance. Development **135**: 1751–9

Saji S, Bathula S, Kubo A, Tamaoki M, Kanna M, Aono M, Nakajima N, Nakaji T, Takeda T, Asayama M, et al (2008) Disruption of a gene encoding C4-dicarboxylate transporter-like protein increases ozone sensitivity through deregulation of the stomatal response in *Arabidopsis thaliana*. Plant Cell Physiol **49**: 2–10

Schäfer L, Feierabend J (2000) Photoinactivation and protection of glycolate oxidase in vitro and in leaves. Z Naturforsch **55c**: 361–372

Schneeberger K, Ossowski S, Lanz C, Juul T, Petersen AH, Nielsen KL, Jørgensen J-E, Weigel D, Andersen SU (2009) SHOREmap: simultaneous mapping and mutation identification by deep sequencing. Nat Methods **6**: 550–1

Servaites JC, Ogren WL (1977) Chemical inhibition of the glycolate pathway in soybean leaf cells. Plant Physiol **60**: 461-466

Slewinski TL, Anderson AA, Zhang C, Turgeon R (2012) SCARECROW plays a role in establishing Kranz anatomy in maize leaves. Plant Cell Physiol **53**: 2030–7

Smith CA, Want EJ, O'Maille G, Abagyan R, Siuzdak G (2006) XCMS: Processing mass spectrometry data for metabolite profiling using nonlinear peak alignment, matching, and identification. Anal Chem **78**: 779–787

Somerville CR, Ogren WL (1981) Photorespiration-deficient mutants of *Arabidopsis thaliana* lacking mitochondrial serine transhydroxymethylase activity. Plant Physiol **67**: 666–71

Stein SE (1999) An integrated method for spectrum extraction and compound identification from gas chromatography/mass spectrometry data. J Am Soc Mass Spectrom **10**: 770–781

Strader LC, Culler AH, Cohen JD, Bartel B (2010) Conversion of endogenous indole-3-butyric acid to indole-3-acetic acid drives cell expansion in *Arabidopsis* seedlings. Plant Physiol **153**: 1577–86

Sundaresan V, Springer P, Volpe T, Haward S, Jones JD, Dean C, Ma H, Martienssen R (1995) Patterns of gene action in plant development revealed by enhancer trap and gene trap transposable elements. Genes Dev **9**: 1797–1810

Szabados L, Savouré A (2010) Proline: a multifunctional amino acid. Trends Plant Sci **15**: 89–97

Thomas CL, Schmidt D, Bayer EM, Dreos R, Maule AJ (2009) *Arabidopsis* plant homeodomain finger proteins operate downstream of auxin accumulation in specifying the vasculature and primary root meristem. Plant J **59**: 426–36

Timm S, Bauwe H (2012) The variety of photorespiratory phenotypes - employing the current status for future research directions on photorespiration. Plant Biol (Stuttg) 1–11

Timm S, Nunes-Nesi A, Pärnik T, Morgenthal K, Wienkoop S, Keerberg O, Weckwerth W, Kleczkowski LA, Fernie AR, Bauwe H (2008) A cytosolic pathway for the conversion of hydroxypyruvate to glycerate during photorespiration in *Arabidopsis*. Plant Cell **20**: 2848–59

Uquillas C, Letelier I, Blanco F, Jordana X, Holuigue L (2004) NPR1-independent activation of immediate early salicylic acid-responsive genes in *Arabidopsis*. Mol Plant Microbe Interact **17**: 34–42

Vahisalu T, Kollist H, Wang Y, Nishimura N, Valerio G, Lamminmäki A, Brosché M, Moldau H, Schroeder JI, Kangasjärvi J (2008) SLAC1 is required for plant guard cell S-type anion channel function in stomatal signalling. Nature **452**: 487–491

Vandenabeele S, Vanderauwera S, Vuylsteke M, Rombauts S, Langebartels C, Seidlitz HK, Zabeau M, Van Montagu M, Inzé D, Van Breusegem F (2004) Catalase deficiency drastically affects gene expression induced by high light in *Arabidopsis thaliana*. Plant J **39**: 45–58

Vanderauwera S, Suzuki N, Miller G, van de Cotte B, Morsa S, Ravanat J-L, Hegie A, Triantaphylidès C, Shulaev V, Van Montagu MCE, et al (2011) Extranuclear protection of chromosomal DNA from oxidative stress. Proc Natl Acad Sci U S A **108**: 1711–6

Vanderauwera S, Vandenbroucke K, Inzé A, van de Cotte B, Mühlenbock P, De Rycke R, Naouar N, Van Gaever T, Van Montagu MCE, Van Breusegem F (2012) *At*WRKY15 perturbation abolishes the mitochondrial stress response that steers osmotic stress tolerance in *Arabidopsis*. Proc Natl Acad Sci U S A **109**: 20113–8

Vanderauwera S, Zimmermann P, Rombauts S, Vandenabeele S, Langebartels C, Gruissem W, Inze D, Van Breusegem F (2005) Genome-wide analysis of hydrogen peroxide-regulated gene expression in *Arabidopsis* reveals a high light-induced transcriptional cluster involved in anthocyanin biosynthesis. Plant Physiol **139**: 806–821

Wang J, Andersson-Gunnerås S, Gaboreanu I, Hertzberg M, Tucker MR, Zheng B, Leśniewska J, Mellerowicz EJ, Laux T, Sandberg G, et al (2011) Reduced expression of the *SHORT-ROOT* gene increases the rates of growth and development in hybrid poplar and *Arabidopsis*. PLoS One **6**: e28878

Xi J, Xu P, Xiang C-B (2012) Loss of AtPDR11, a plasma membrane-localized ABC transporter, confers paraquat tolerance in *Arabidopsis thaliana*. Plant J **69**: 782–91

Xia J, Mandal R, Sinelnikov I V., Broadhurst D, Wishart DS (2012) MetaboAnalyst 2.0 - a comprehensive server for metabolomic data analysis. Nucleic Acids Res **40**: W127–W133

Xu H, Zhang J, Zeng J, Jiang L, Liu E, Peng C, He Z, Peng X (2009) Inducible antisense suppression of glycolate oxidase reveals its strong regulation over photosynthesis in rice. J Exp Bot **60**: 1799–809

Yin Y, Borges G, Sakuta M, Crozier A, Ashihara H (2012) Effect of phosphate deficiency on the content and biosynthesis of anthocyanins and the expression of related genes in suspension-cultured grape (*Vitis sp* .) cells. Plant Physiol Biochem **55**: 77–84

Yu N-I, Lee SA, Lee M-H, Heo J-O, Chang KS, Lim J (2010) Characterization of SHORT-ROOT function in the *Arabidopsis* root vascular system. Mol Cells **30**: 113–9

Yu TS, Kofler H, Häusler RE, Hille D, Flügge UI, Zeeman SC, Smith AM, Kossmann J, Lloyd J, Ritte G, et al (2001) The *Arabidopsis sex1* mutant is defective in the R1 protein, a general regulator of starch degradation in plants, and not in the chloroplast hexose transporter. Plant Cell **13**: 1907–18

Zelitch I (1972) The photooxidation of glyoxylate by envelope-free spinach chloroplasts and its relation to photorespiration. Arch Biochem Biophys **150**: 698–707

Zelitch I, Schultes NP, Peterson RB, Brown P, Brutnell TP (2009) High glycolate oxidase activity is required for survival of maize in normal air. Plant Physiol **149**: 195–204

Zolman BK, Bartel B (2004) An *Arabidopsis* indole-3-butyric acid-response mutant defective in PEROXIN6, an apparent ATPase implicated in peroxisomal function. Proc Natl Acad Sci U S A **101**: 1786–91

4

Reverse genetic screen reveals an interplay between photorespiratory H_2O_2 and energy signaling

Cezary Waszczak, Pavel Kerchev, Annelies Inzé, Patrick Willems, Sandy Vanderauwera,
Per Mühlenbock, Brigitte van de Cotte, Debbie Rombaut, Joris Messens and Frank Van Breusegem

AUTHOR CONTRIBUTIONS

ABSTRACT

In order to survive in constantly changing environments plants developed efficient systems that allow adaptation towards multiple stress conditions. The interactions with environment are associated with tailored expression of nuclear genes that ultimately lead to changes in cellular metabolism and at the whole organism level. Previously, we identified photorespiratory hydrogen peroxide as a signaling molecule that provokes changes in expression of over 700 genes (H_2O_2-induced genes; HIGs). To gain insight into the oxidative stress-related functions of these HIGs we took a reverse genetic approach and screened the corresponding T-DNA insertion mutants for ~ 200 of these genes for altered oxidative stress tolerance. A loss-of-function mutation in *SUGAR TRANSPORT PROTEIN 13* (*stp13-1*) which encodes for a high affinity H^+/D-hexose symporter, had a significant impact on oxidative stress resistance. Under stress conditions, plants lacking STP13 exhibited early decrease in PSII maximum efficiency that was associated with enhanced survival. Overexpression of STP13 led to opposite phenotypes and resulted in early progress of chlorosis. The analysis of loss- and gain-of-function STP13 transgenics indicated an important role for sugar availability in the oxidative stress response. Further experiments provided a link between energy signaling and plant stress responses with a major role of SNF1-RELATED PROTEIN KINASE 1.

INTRODUCTION

Dynamic reactions towards changing environmental conditions are crucial for survival of all living organisms. Plants, due to their sessile lifestyle, are among organisms that exhibit the highest metabolic plasticity and a unique potential towards survival in harsh conditions. These adaptations are largely dependent on reprogramming of nuclear transcription. Upon perception of stress stimulus, various signaling cascades convey the signal towards the nucleus, where respective transcription regulators activate/repress expression of a stimulus-specific subset of genes. These transcriptomic responses are later fine-tuned via posttranscriptional control of translation and post-translational control of protein activity/stability and ultimately result in changes at the metabolome level. Reactive oxygen species such as singlet oxygen ($^1O_2$), hydrogen peroxide (H_2O_2), superoxide anion ($O_2^{\cdot-}$) and hydroxyl radical ($HO\cdot$), collectively termed as ROS, are potent signaling molecules that trigger plant adaptation responses (Petrov and Van Breusegem, 2012). Thus far, the ROS signal was shown to be transmitted via i) direct posttranslational modifications of redox-sensitive transcription factors (reviewed in Chapter 1) ii) activation of multi-component signaling cascades such as those involving MAPKs (reviewed in Chapter 1) iii) oxidation products of various cellular metabolites or structures that serve as site specific signaling molecules. Thus far, the best described case of such metabolite is β-cyclocitral, a carotenoid oxidation product able to exert transcriptomic reprogramming (Ramel et al., 2012). A meta-analysis of ROS transcript signatures indicates that next to the core transcriptomic response towards ROS signal specific sets of marker genes are regulated in response to H_2O_2, $^1O_2$, $HO\cdot$, O_2^- and depend on the site of the ROS production (Gadjev et al., 2006). Our previous efforts aimed at exploration of transcriptomic responses towards H_2O_2 produced during peroxisomal phase of photorespiration and made use of CATALASE2-deficient plants as a model system for conditional elevation of photorespiratory H_2O_2 concentrations (Vandenabeele et al., 2004; Vanderauwera et al., 2005; Vanderauwera et al., 2011; Hoeberichts et al., unpublished; Chapter 3 of this thesis). Thus far, this detailed information about the transcriptomic responses towards photorespiratory hydrogen peroxide led to discovery of new genes controlling anthocyanin production (Vanderauwera et al., 2005) and indicted a link between ROS and auxin signaling (Tognetti et al., 2010; Tognetti et al., 2012). The latter case serves as a good proof that transcriptomic data can aid the discovery of genes controlling traits of agricultural importance. The overexpression of UDP-glucosyltransferase UGT74E2, which is among the top most responsive genes controlled by photorespiratory hydrogen peroxide, results in significantly improved survival during drought and salt stress (Tognetti et al., 2010;. Patent no. PCT/EP2008/005213).

Next to signaling via reactive oxygen species, plant growth and development depends on availability and distribution of nutrients, of which sugars play the major role in plant energy signaling. In contrast to animals that perceive changes in AMP/ATP ratio via AMP-activated protein kinase [AMPK; Hardie, (2011) and references therein] regulating nearly all aspects of cellular metabolism, plants

sense the level of sugars via at least three major pathways to ensure the proper energy perception (Jang et al., 1997; Moore et al., 2003; Baena-González et al., 2007; Xiong et al., 2013). Glucose sensing via HEXOKINASE1 (HXK1) which is the first enzyme in hexose assimilation pathway, coordinates the glucose availability signal with expansion of roots, leaves and inflorescence, and repression of photosynthesis genes (Moore et al., 2003). The pathways involving SNF1-RELATED PROTEIN KINASE 1 are largely responsible for control of stress-related sugar starvation responses that promote utilization of alternative energy sources (Baena-González et al., 2007). Finally, the most recent discovery of sugar sensing mechanism involving TARGET OF RAPAMYCIN (TOR) provided an evidence for photosynthetic/sugar control of root meristem activity (Xiong et al., 2013). The three described sugar sensing mechanisms regulate and depend on source-sink relationships between the respective plant organs. There is a growing evidence that stress conditions and associated hormonal signaling are able to exert changes in distribution of nutrients (Lemoine et al., 2013). The development and strength of the sink-force, characterized as the availability to effectively lower the concentration of photo-assimilates (transported in the form of sucrose) in the sieve elements (Wardlaw, 1990) largely depends on localized expression of cell-wall invertases (that convert sucrose to hexoses) and hexose transporters (importing hexoses into the cells) (Lemoine et al., 2013).

The results of this study contribute to a better understanding of interactions between oxidative stress, nutrient distribution and energy signaling. Under photorespiratory conditions, CATALASE 2-deficient plants trigger mechanisms that reprogram the transcriptome with over 700 genes undergoing rapid transcriptional induction (Inzé et al., 2012). To identify novel determinants of oxidative stress tolerance, we employed a reverse genetics approach and investigated the oxidative stress tolerance of T-DNA insertion lines for ~200 of these genes. We designed a novel high-throughput oxidative stress assay and screened these mutant lines for altered oxidative stress tolerance. Our efforts led to identification of SUGAR TRANSPORT PROTEIN (STP13) as a key player controlling survival under oxidative stress induced sugar starvation conditions. Furthermore, we demonstrated that phenotypes conditioned by lack/overexpression of STP13 are largely dependent on levels of trehalose-6-phosphate and activity of SNF1-RELATED PROTEIN KINASE 1. Our results highlight the importance of sugar signaling as a novel factor that controls the oxidative stress tolerance.

RESULTS AND DISCUSSION

An inventory of photorespiratory hydrogen peroxide responsive genes

A first step towards a successful reverse genetic screen is the identification of a set of genes that are of particular interest for the biological process of choice (Alonso and Ecker, 2006). In this study we focused on genes that are responsive towards accumulation of photorespiratory hydrogen peroxide. To build a robust inventory of H_2O_2 responsive genes a meta-analysis of three independent microarray experiments that describe transcriptomic responses of CATALASE2-deficient plants towards photorespiration-promoting conditions (exposure to excess light intensities) has been performed (Inzé et al., 2012). Brief characterization of experimental design of respective microarray studies is presented in Table 1.

Platform	Transgenic line	Residual CAT activity	Light intensity [$\mu mol \cdot m^{-2} \cdot s^{-1}$]	CO_2 conc.	Timepoints [h]	Reference
ATH1 GeneChip (Affymetrix)	CAT2HP1	20%	2000	ambient	0, 3, 8	(Vanderauwera et al., 2005)
Arabidopsis V3 (Agilent)	CAT2HP2	7%	1000	ambient	0, 1	(Vanderauwera et al., 2011)
CATMA v2.3	CAT2HP1	20%	2000	3000 ppm → ambient	0, 1, 8	(Hoebrichts et al., unpub.)

Table 1. Summary of experimental design of microarray-based transcript profiling experiments used for the meta-analysis.

From the Affymetrix ATH1 data set (Vanderauwera et al., 2005), genes showing at least a threefold induction in CAT2HP1 plants (vs Col-0 control) after 3 h of HL exposure were selected, whereas from the Agilent *Arabidopsis* V3 data set (Vanderauwera et al., 2011), genes showing a significant induction [interaction significance + genotype and treatment significance ($P < 0.001$; $Q < 0.05$), and threefold induction] in CAT2HP2 plants after 1 h of HL exposure were retained. From the CATMA (v2.3, A-MEXP-120) experiment, we have chosen genes showing a significant induction [mixed model according to Wolfinger et al., (2001): interaction significance ($P < 0.001$)] in CAT2HP1 plants after 8 hours of HL irradiation. The assembly of genes differentially expressed in these transcript profiling experiments led to the formation of a database of 783 H_2O_2 induced genes (HIGs; Inzé et al., 2012). For detailed information on oxidative stress-triggered transcriptomic inducibility of these genes we refer to Inzé et al., (2012). In order to elucidate the function of identified HIGs we set out to analyze the performance of their T-DNA mutant lines under oxidative stress promoting conditions. For this we identified and up-scaled 198 T-DNA-insertion lines (corresponding to 197 genes; Table S1) obtained from the ABRC stock collection to fuel a reverse genetics-based phenomics screen. We did not investigate whether the T-DNA insertions present within each line lead to a loss-of-function of a respective gene/protein, therefore lines used in this study can be described as putative mutants.

A high throughput *in vitro* 96-well plate-based photorespiratory stress assay

The *in vitro* oxidative stress assay employed in this study was inspired by the existing RGCL assay (Vanderauwera et al., 2011; Kerchev et al., 2014) described in detail in Chapter 3. To obtain a higher throughput, the experimental format was tuned into a 96-well plate. Approximately 7 plants per well were grown in liquid half-strength Murashige and Skoog medium supplemented with 0.2 % sucrose. After 10 days of growth, plants were transferred to continuous light conditions. The exposure to continuous light combined with restriction of gas exchange were shown earlier to induce photorespiration (Kerchev et al., 2014; Chapter 3). After the treatment, PSII maximum efficiency (Fv'/Fm') was monitored on a daily basis and served as a proxy for stress sensitivity (see materials and methods for detailed experimental procedure). Figure 1A illustrates the progressive decrease of the Fv'/Fm' in both wild-type (Col-0) and a CATALASE2-deficient mutant (*cat2-2*; Queval et al., 2007). Significantly lower (t-test p-value = 0.0044) PSII maximum efficiency in the *cat2-2* plants (95 % of control value) was observed already under control conditions. Following the treatment, the decline of the Fv'/Fm' parameter was much more pronounced in *cat2-2* than in wild-type plants, reaching respectively 73% and 85% of initial values after 2 days (Fig. 1A). After 3-4 days of treatment progressive chlorosis of leaves was observed in *cat2-2* plants while the Col-0 control line retained its chlorophyll content (Fig. 1B).

The optimization of RGCL assay for the 96-well plate format created the necessity for the use of liquid medium. We therefore closely followed the growth of wild-type and *cat2* plants in the assay conditions with no shift to CL to investigate the long-term effects of such conditions. Interestingly, we observed that after 13 days of growth in liquid medium under long-day (LD) conditions *cat2* mutants develop phenotypes similar to that of plants shifted to continuous light (Fig. 1 C, D). In *cat2* plants, the long-term growth in liquid medium is associated with a decrease in PSII maximum efficiency (Fig. 1C) and formation of chlorosis (Fig. 1 D). Submergence is often associated with limited oxygen availability leading to hypoxia/anoxia (Crawford and Braendle, 1996; Fukao and Bailey-Serres, 2004). Paradoxically, anoxic conditions promote formation of ROS (Blokhina et al., 2001; Baxter-Burrell et al., 2002; Vergara et al., 2012) that are important signaling molecules controlling adaptation to low oxygen concentration (Baxter-Burrell et al., 2002; Gibbs et al., 2011; Licausi et al., 2011; Chang et al., 2012). Therefore, we can not exclude the possibility that phenotypes of *cat2* plants exhibited in liquid-based RGCL assay are partially related to hypoxia/anoxia-induced ROS production.

Plants develop a number of adaptations that allow efficient photosynthesis in submergence conditions i.e. epidermal orientation of chloroplasts, reduced cell wall and cuticle thickness (Mommer et al., 2005; Mommer and Visser, 2005). However, *Arabidopsis* plants grown in a sucrose-free medium under LD conditions applied for the screening purposes in this work, failed to develop beyond

the cotyledon stage (Fig. 1 E) indicating that exogenous sucrose supplementation is necessary for seedling establishment in tested conditions. The availability of nutrients is a key factor controlling the post-embryonic meristem activities (Xiong et al., 2013). The requirement for exogenous sucrose supplementation indicates that the photosynthesis efficiency in underwater grown *Arabidopsis* seedlings described herein is not sufficient to sustain the proper growth. Consequently, our data indicate that plants subjected to the assay conditions applied in this study rely at least to a certain extent on the growth medium as nutrient (sugar) source.
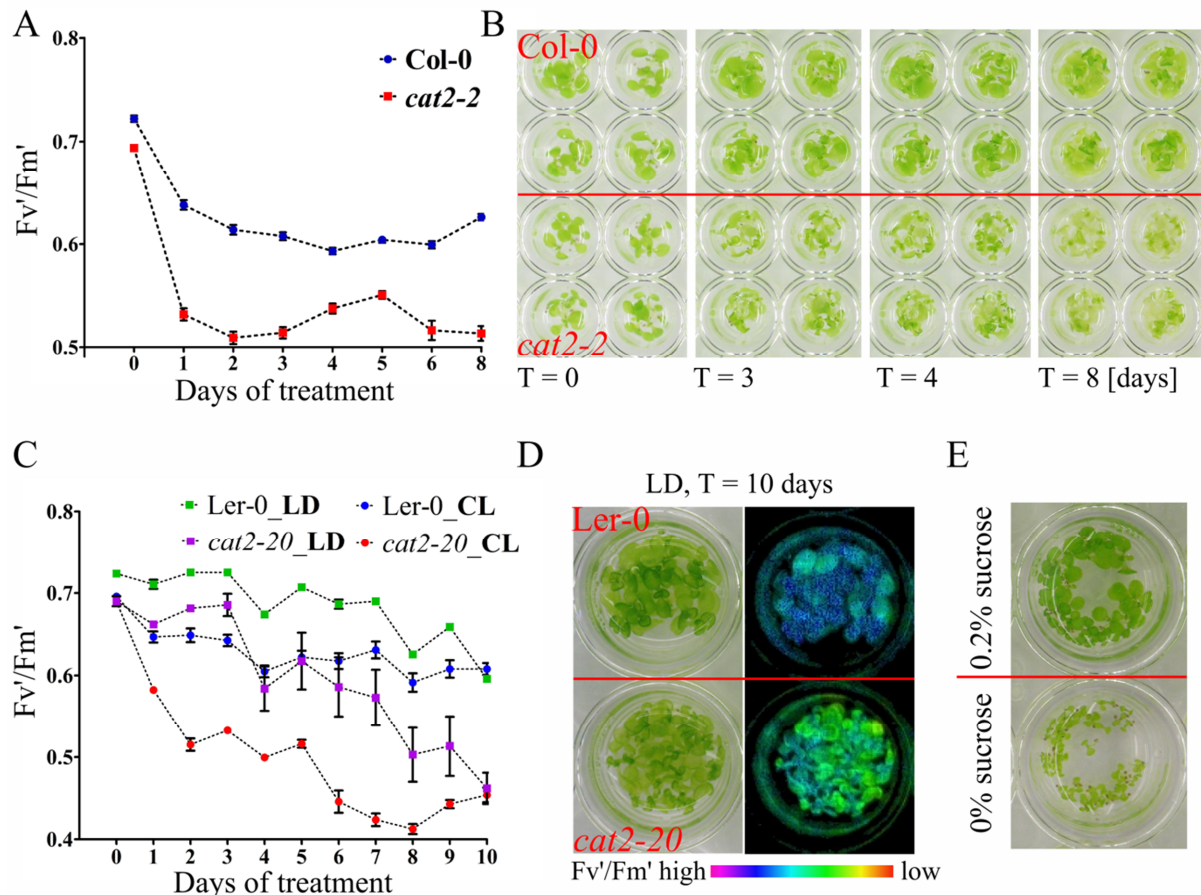
Fig. 1 Induction of oxidative stress in a 96-well plate-based RGCL assay. Ten-days old Col-0 and *cat2-2* plants grown in half-strength MS liquid medium (0.2 % sucrose) under LD conditions were subjected to oxidative stress by transfer to continuous light (CL). **A)** Changes of PSII maximum efficiency (Fv'/Fm') observed after transfer to CL conditions, data points represent means of 8 biological replicates (separate wells) ± SE. **B)** Progression of cell death observed after the onset of treatment **C)** Growth in liquid medium negatively influences PSII maximum efficiency of *cat2* plants. Ten-days-old liquid grown plants were transferred to CL or left in LD conditions. Data points represent means of 4 biological replicates (separate wells) ± SE. **D)** Phenotype and Fv'/Fm' of Ler-0 and *cat2-20* (see Chapter 3) plants grown in liquid medium for 20 days **E)** Phenotype of Col-0 plants grown for 10 days in liquid half-strength MS medium with/without sucrose supplementation

Lack of SUGAR TRANSPORT PROTEIN 13 leads to a decrease in PSII maximum efficiency and promotes survival in submerged conditions

A suite of 198 T-DNA insertion lines (putative mutants) was screened for altered PSII maximum efficiency (Fv'/Fm') curves and the occurrence of cell death following the exposure to 96-well RGCL

assay. Among the tested mutant lines, SALK_045494 (*stp13-1*) deficient in SUGAR TRANSPORT PROTEIN 13 (STP13; Norholm et al., 2006; Yamada et al., 2011) exhibited the most pronounced phenotype (Fig. 2). Upon stress treatment the values of Fv'/Fm' ratio observed in line *stp13-1* were lower when compared to Col-0 control but still higher than those of *cat2-2* line (Fig. 2 A, B). The typical progress of leaf chlorosis characteristic for *cat2-2* knockout was not observed (Fig. 2D).
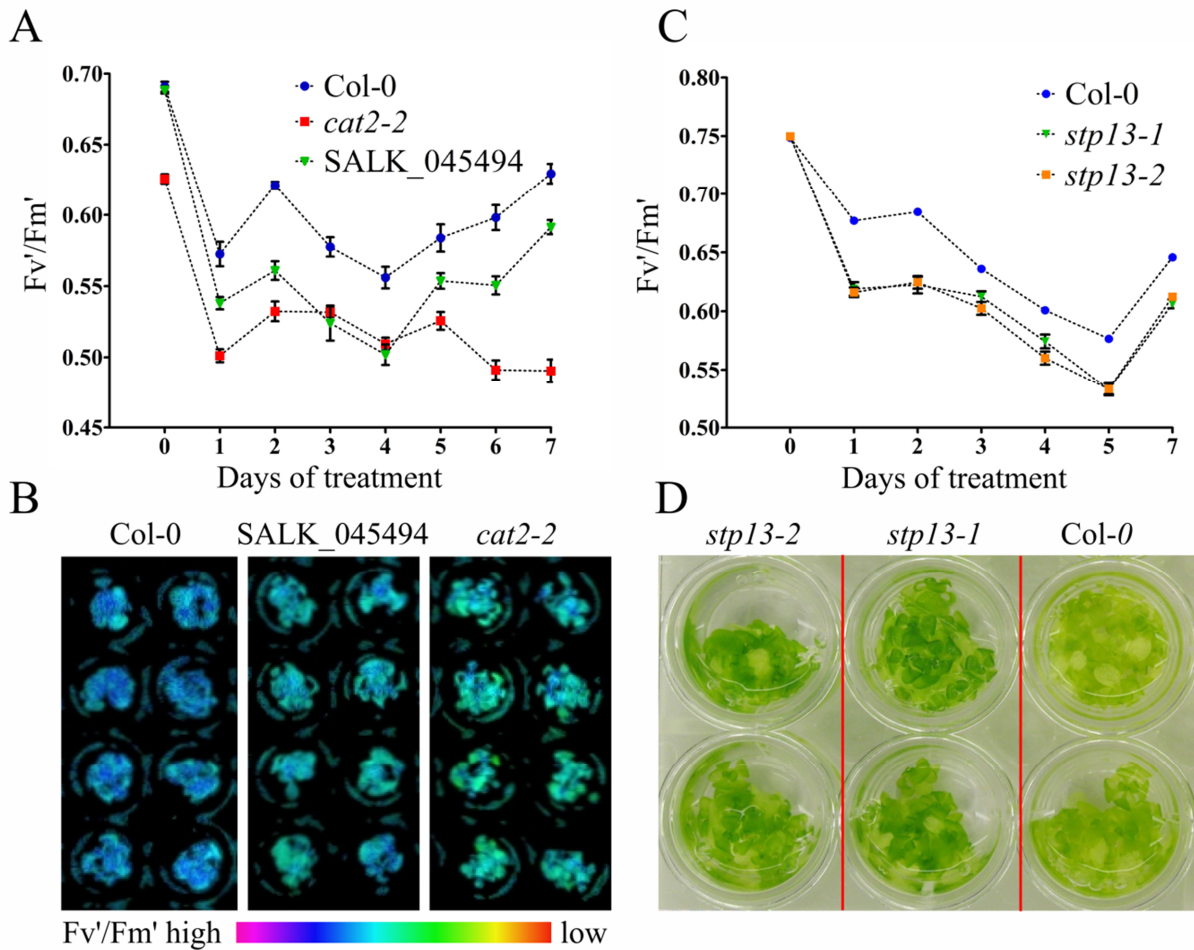

Fig. 2 Oxidative stress related phenotypes conferred by lack of STP13. Ten-days old plants grown in half-strength MS liquid medium (0.2 % sucrose) under LD conditions were subjected to photorespiratory stress by transfer to continuous light (CL). **A)** Changes of PSII maximum efficiency (Fv'/Fm') observed after transfer to CL conditions, data points represent means of 8 biological replicates (separate wells) ± SE. **B)** PSII maximum efficiency (Fv'/Fm') after 2 days of treatment. **C)** Both *stp13* mutants exhibit increased Fv'/Fm' drop when exposed to photorespiratory stress conditions **D)** Lack of STP13 promotes survival under submergence conditions. Plants were grown for 10 days in liquid half-strength MS medium in 24-well plate under LD light regime and subsequently transferred to CL. Photo taken 15 days after the transfer.

The *Agrobacterium* mediated T-DNA insertion mutagenesis often results in presence of multiple T-DNA insertion sites within a single mutant line (Feldmann, 1991; McElver et al., 2001). This creates the necessity for investigation of at least two independent mutant lines for the respective phenotype (Ulker et al., 2008). To verify whether the phenotype observed in line *stp13-1* is not caused by secondary T-DNA insertions we investigated the oxidative stress-related phenotype of independent

STP13 mutant line – *stp13-2* (SALK_021204; Norholm et al., 2006). Both T-DNA insertion lines i.e. SALK_045494 and SALK_021204 where shown before to be null *stp13* mutants (Norholm et al., 2006; Yamada et al., 2011) which is in agreement with gene expression analysis and insert localization studies performed in this work (data not shown). When tested in the assay conditions, both mutant lines exhibited similar stress sensitivity (Fig. 2C) which confirms that the lack of STP13 leads to the observed phenotypes. A close examination of the mutant lines carried out in 24-well plate format, revealed that despite the low Fv'/Fm' values observed in the early stages of the assay the lack of STP13 promotes long-term survival (Fig. 2 D). After 10-15 days of treatment both mutant lines retained higher chlorophyll content when compared to Col-0 control line that exhibited progressing chlorosis of leaves (Fig. 2 D).

STP13 belongs to a family of SUGAR TRANSPORT PROTEINS that has 14 members in *Arabidopsis thaliana* (STP1-STP14; Büttner, 2007). *At*STPs are plasma membrane transporters that mediate the uptake of hexoses from the apoplastic space into the cell. The expression profiles of *STP* genes suggest an important role during the establishment of source-sink relations (Büttner, 2007). STP13 was initially identified as a glucose transporter in a screen of cDNA library of *Arabidopsis* transporters in *Xenopus* oocytes with a ^{14}C-glucose uptake assay (Nour-Eldin et al., 2006). Further biochemical analysis indicated that alike other members of the family, STP13 acts as a high affinity H^+/D-hexose symporter with a broad substrate activity. Interestingly, the expression of *STP13* positively correlates with programmed cell death (Norholm et al., 2006) and is promoted by a variety of environmental stresses (Yamada et al., 2011).

The expression of *STP13* is strongly induced under oxidative stress conditions

Next, we performed an in-depth expression analysis of the all 14 members of the *Arabidopsis* STP family under oxidative stress conditions. For this, we assembled a portfolio of both publicly and in-house available oxidative stress-related microarray-based transcript profiling experiments in which stress conditions were triggered by genetic perturbations of particular components of the cellular antioxidant system [*cat2* (Vanderauwera et al., 2005; Queval et al., 2012; Chapter 3), *vte1, vte2* (Sattler et al., 2006), *vtc2* (Kerchev et al., 2011)], exposure to oxidative stress promoting conditions [low CO_2 (unpublished), UV-B radiation (AtGenExpress acc. no. ME00329), ozone fumigation (Short et al., 2012)] or chemical compounds such as antimycin A (Ng et al., 2013), rotenone and oligomycin (Clifton et al., 2005), lincomycin (GEO acc. no. GSE5770) and methyl viologen (AtGenExpres acc. no. ME00340; Scarpeci et al., 2008). For descriptions of the microarray experiments see Table S2. We found that among the STP family, *STP13* is the most responsive under a broad array of oxidative stress-promoting conditions (Fig. 3A). This is in agreement with previous study (Yamada et al., 2011) that described similar properties of STP13 in the context of multiple stress conditions. In order to gain insight into the spatiotemporal expression of *STP13* we have used the transgenic

Arabidopsis line expressing β-glucuronidase (GUS) under the control of *STP13* promoter (p*STP13*:GUS; Schofield et al., 2009). The activity of *STP13* promoter was observed in a time-scale experiment following the exposure to severe oxidative stress conditions. For this, p*STP13*:GUS plants were grown in soil under a long day photoperiod at elevated CO_2 concentration (3000 ppm).
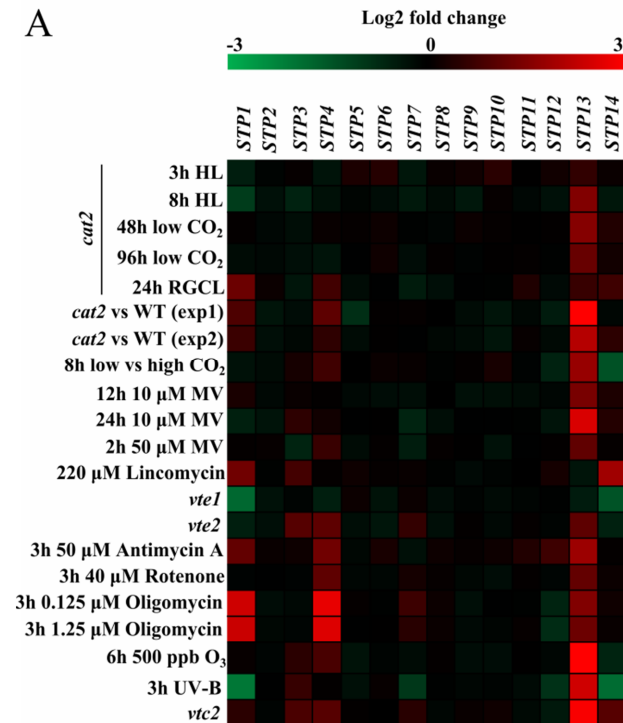

Fig. 3 Expression of STP13 is highly induced under oxidative stress conditions. **A)** Meta-analysis of *STP* family transcript profiles under conditions promoting oxidative stress (for description of experiments see Table S2) **B-G)** Spatiotemporal localization of *STP13* expression. p*STP13*:GUS plants were grown in soil for 21 days under a long day [16 h light ($100\mu mol \cdot m^{-2} \cdot s^{-1}$)/8 h dark] photoperiod at elevated CO_2 concentration (3000 ppm). After this period, plants were transferred to ambient air (300-400 ppm CO_2) and exposed to continuous excess light irradiation (1100-1200 $\mu mol \cdot m^{-2} \cdot s^{-1}$) for indicated time period. Detection of reporter β-glucuronidase activity was assayed as described in materials and methods.
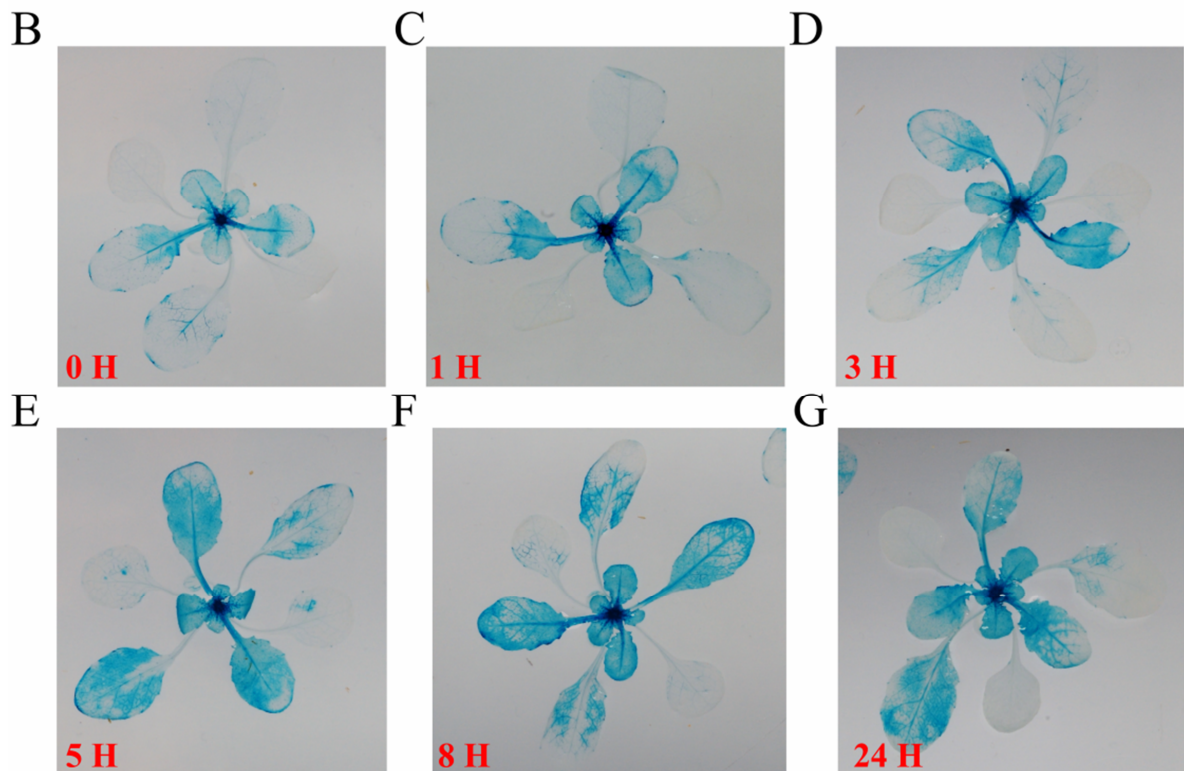
Next, plants were transferred to ambient air and exposed to continuous excess light irradiation for 24 hours. This treatment promotes production of photorespiratory hydrogen peroxide as demonstrated by a dramatic reduction of maximum efficiency of PSII and the formation of cell death lesions in the *cat2-2* line (described in Chapter 3). In order to observe the tissue specificity and dynamics of p*STP13* activity the whole rosettes were sampled after 0, 1, 3, 5, 8, and 24 hours of treatment. The p*STP13* driven expression of β-glucuronidase following the oxidative stress treatment as demonstrated by the histochemical detection of its activity (Fig. 3 B – G). Under control conditions the staining was limited to the shoot apical meristem, young developing leaves and enriched in vascular tissue and hydatodes (Fig. 3B). The photorespiratory stress treatment induced gradual spreading of the signal towards the middle-age leaves (Fig. 3 C-G) with a weak signal appearing in rosette leaves 1 and 2. However, even after the 24 h treatment time the staining was not observed in cotyledons (Fig. 3 G). Together our results suggest that under control conditions STP13 might be involved in establishing a sink force in the young developing tissue.

Overexpression of STP13 leads to sugar-dependent phenotypes

After finding that multiple oxidative stress promoting conditions greatly induce the activity of *STP13* promoter, we set out to investigate the effect of increased STP13 levels on oxidative stress tolerance. For this, we used two independent transgenic lines expressing *STP13* under constitutive CaMV 35S promoter (STP13OE-12 and OE-16; Schofield et al., 2009). The oxidative stress performance of both lines was tested in liquid medium-based RGCL assay adapted for 24-well plates to allow a closer examination of plant phenotypes. While the lack of STP13 leads to a rapid decrease in PSII maximum efficiency under stress conditions (Fig. 2) the STP13OE lines behaved in an opposite manner. Upon stress treatment both overexpressor lines retained higher maximum efficiency of PSII photochemistry when compared to Col-0 control line (Fig. 4A). Surprisingly, this was associated with the onset of chlorosis 6 days after start of the treatment (Fig. 4B). Next, we tested whether STP13 mutant and OE lines exhibit oxidative stress related phenotypes in solid medium-based RGCL assay (see Chapter 3). The overexpression of STP13 results in increased uptake of sugars from the growth media and sugar dependent growth promoting effects (Schofield et al., 2009), therefore the RGCL was conducted on sucrose supplemented (1%) and sucrose-free media. After RGCL treatment the STP13-deficient lines did not exhibit any visible phenotypes with no regard to the presence of sucrose in the growth media. In contrary, the phenotypes (described later in this paragraph) of STP13OE lines were linked with the availability of exogenous sucrose. In agreement with a previous report (Schofield et al., 2009), we observed for both OE lines exhibited a sucrose-dependent improvement of growth (Fig. 4C, data not shown). After two days of stress treatment on growth medium supplemented with 1% sucrose the decrease in Fv'/Fm' parameter was more pronounced for STP13OE lines when compared to Col-0 wild type plants (Fig. 4 C).
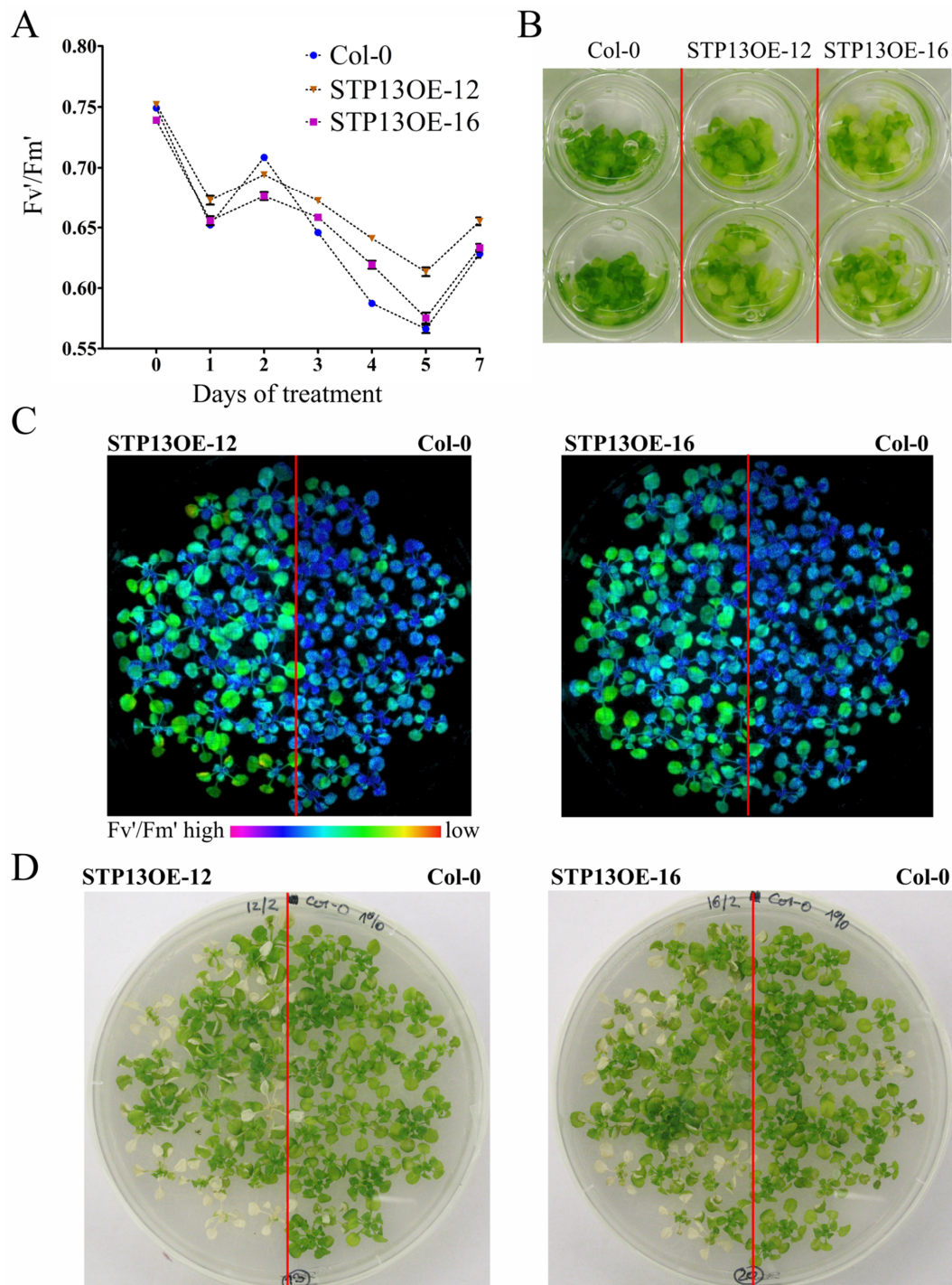
Fig. 4 The overexpression of STP13 leads to sugar-dependent phenotypes. Ten-days old plants grown in half-strength MS liquid medium (0.2 % sucrose) under LD conditions were subjected to photorespiratory stress by transfer to continuous light (CL). **A)** Changes of PSII maximum efficiency (Fv'/Fm') observed after transfer to CL conditions, data points represent means of 24 biological replicates (separate wells) ± SE. **B)** Overexpression of STP13 negatively influences survival under submergence conditions. Plants were grown for 10 days in liquid half-strength MS medium in 24-well plate under LD light regime and subsequently transferred to CL. Photo taken 9 days after the transfer. **C)** PSII maximum efficiency (Fv'/Fm') after two days of RGCL treatment. Three-week old Col-0 and *cat2-2* plants grown under control in vitro conditions on growth medium supplemented with 1% sucrose were subjected to photorespiratory stress by mechanical restriction of gas exchange and transfer to continuous light **D)** Phenotype of STP13OE and Col-0 control line after 11 days of RGCL treatment.

The progressive decrease in efficiency of PSII photochemistry was followed by the appearance of lesions after 9-11 days of treatment in contrast to Col-0 wild-type plants, which exhibited visible lesions at day 14 (Fig. 4 D). This phenotype might be related to an increased sugar concentration described earlier for STP13OE plants (Schofield et al., 2009) or the different developmental stage of STP13OE plants at the onset of the stress treatment. The growth improvement of STP13 OE lines, as well as early decrease in Fv'/Fm' and development of lesions were not observed on medium with no sucrose (data not shown). Next, we tested whether the level of STP13 influences oxidative stress tolerance in soil environment. For this, the STP13 mutant and OE lines were grown for three weeks in CO_2-enriched atmosphere and subjected to the excess light treatment combined with decrease in CO_2 availability as described before. Upon this stress treatment we did not observe any significant differences in decrease of PSII maximum efficiency and formation of lesions for the STP13OE and mutant lines when compared to Col-0 line. Similarly, Norholm et al., (2006) did not observe any effect of STP13 deficiency on cell death-progression in *accelerated cell death 11* (*acd11*) mutant. Furthermore, we did not observe any visual phenotypes conditioned by STP13 deficiency under standard growth conditions in soil which might indicate its functional redundancy with other sugar transporters. Together, our data demonstrate that exogenous sucrose supplementation is a crucial factor determining the phenotypes of STP13 transgenics.

Lack of STP13 delays the formation of oxidative stress-related lesions in CATALASE2-deficient plants grown in liquid medium

As a next step towards deciphering the role of STP13 under oxidative stress conditions we set out to investigate whether the lack of STP13 can revert the formation of cell death lesions observed under RGCL conditions in a CATALASE 2-deficient background. For this, the *stp13-2* null allele was introduced into *cat2-2* genetic background by means of crossing and double *stp13-2/cat2-2* plants were identified in F2 population by means of PCR genotyping. The resulting double mutant line exhibited a significant reduction in formation of cell death lesions when tested in 24-well liquid medium-based RGCL assay (Fig. 5) indicating that lack of STP13 has beneficial effects on oxidative stress tolerance of *cat2-2* line under submergence conditions. Conversely, the introduction of *stp13-2* allele into *cat2-2* background had no effect on its survival in solid medium-based RGCL assay or after high light treatment in soil (data not shown) suggesting that phenotypes exhibited by *stp13* mutants are related to survival in submergence conditions.

Exogenous sugar supplementation positively influences oxidative stress tolerance

In order to explore the link between exogenous sucrose supplementation and oxidative stress tolerance observed for *STP13* transgenics, and SHORT-ROOT-deficient plants (see Chapter 3) we performed the RGCL assay on plants grown on media supplemented with various concentrations

of sugars (Fig. 6). For this, Col-0 and *cat2-2* plants were grown in a liquid medium (0.2 % sucrose) in a 96-well plate format as described before. After 10 days, growth media were supplemented with sucrose to a final concentration ranging from 0.2 % (mock treatment) to 0.6 % (+0.4 %) and subjected to RGCL assay. Following the treatment, a positive correlation between sucrose concentration and PSII maximum efficiency was observed for both the Col-0 and *cat2-2* line (Fig. 6 A, B).
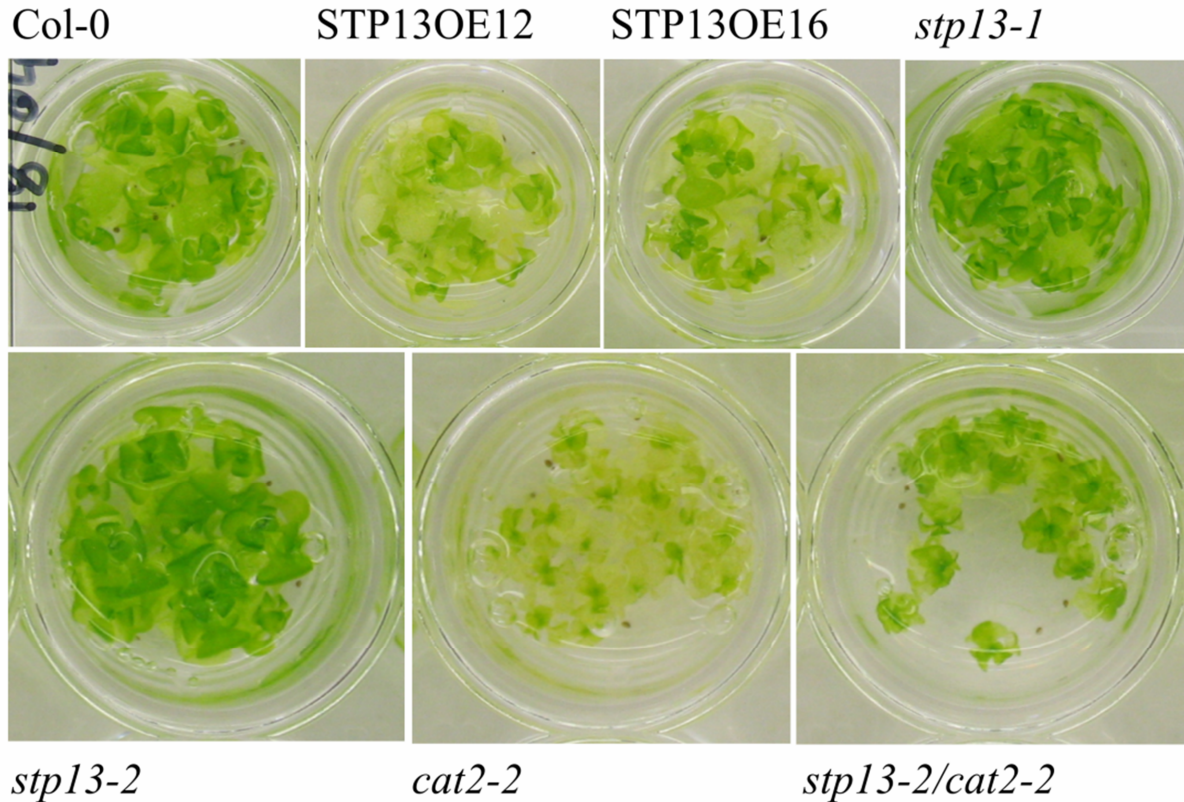

Fig. 5. Lack of STP13 confers delayed formation of cell death lesion in *cat2-2* plants. Plants were grown for 10 days in liquid half-strength MS medium (0.2% sucrose) in 24-well plate under LD light regime and subsequently transferred to CL. Photo taken 10 days after the stress treatment. The size of photos for *stp13-2*, *cat2-2* and *stp13-2/cat2-2* lines was enlarged for better visualization of the phenotypes.

Strikingly, the addition of sucrose at concentrations between 0.2 - 0.4 % completely attenuated the drop in Fv'/Fm' ratio observed in mock treated *cat2-2* line (Fig. 6 B). Moreover, this phenotype was associated with delayed progression of chlorosis (Fig. 6 A). Next, we investigated whether the same effect could be observed for plants grown on solid media. For this, the standard plate-based RGCL assay was performed on Col-0 and *cat2-2* plants grown on media supplemented with rising concentrations (25 – 150 mM) of sucrose, glucose, and mannitol as a control osmolite. As observed before for plants grown in liquid media, increasing concentration of sugars were positively correlated with Fv'/Fm' values in both Col-0 and *cat2-2* plants (Fig. 6C). Furthermore, *cat2-2* plants grown on medium supplemented with 150 mM glucose or sucrose did not exhibit any cell death lesions after 7 days of treatment. This was in contrast to plants grown on media with supplemented with

25 - 50 mM of these sugars (Fig. 6C). Plants grown on media supplemented with mannitol exhibited symptoms of osmotic stress as demonstrated by dramatic reduction in plant size (Fig. 6C) that were observed also for sugar fed plants albeit to a much lower extent. Together, in agreement with previous studies (Couée et al., 2006; Ramel et al., 2007; Sulmon et al., 2011), our results demonstrated a positive effect of exogenous sugars on plant oxidative stress tolerance. Notably, exogenous sugar supplementation strongly enhances tolerance to anoxia (Germain et al., 1997; Loreti et al., 2005). Therefore, phenotypes evoked by sucrose supplementation in liquid-based RGCL assay might be related to alleviated influence of hypoxia/anoxia.
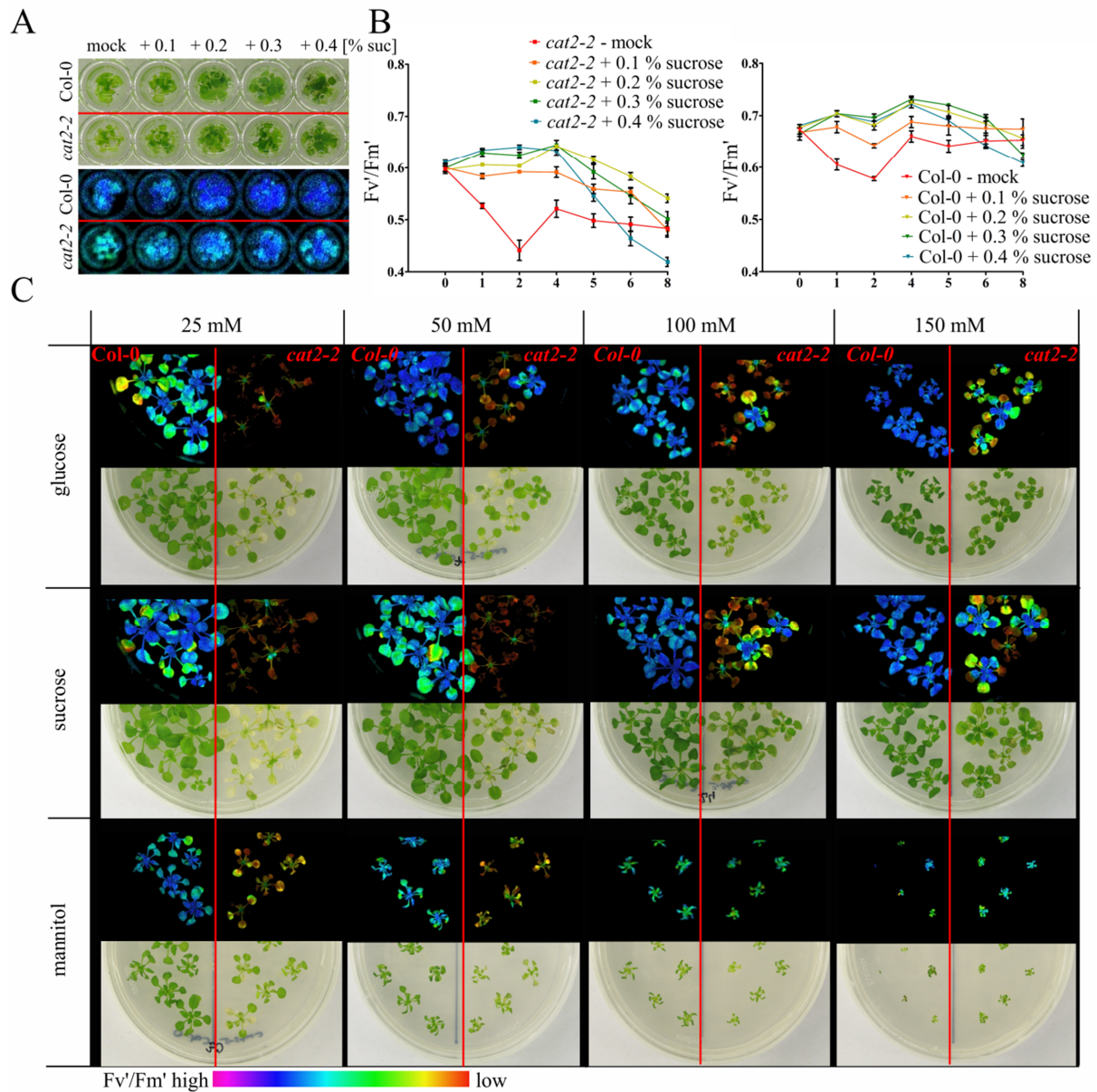

Fig. 6 The effect of exogenous sugar supplementation on oxidative stress tolerance. **A, B)** Exogenous sucrose supplementation positively influences survival in 96-well-based RGCL assay. Ten-days old Col-0 and *cat2-2* plants grown in half-strength MS liquid medium (0.2 % sucrose) under LD conditions were supplemented with additional sucrose dose of 0.1 – 0.4 % and subjected to photorespiratory stress by transfer to continuous light (continued on next page).

STP13 links photorespiratory stress with energy signaling

Multiple lines of evidence indicate that plant oxidative stress tolerance is related to energy signaling: i) exogenously applied sucrose leads to dose-dependent rescue of *cat2-2* plants in RGCL conditions; ii) the level of STP13 (presumably linked to endogenous sugar concentration) is positively correlated with the post-stress Fv'/Fm' values but inversely correlated with plant senescence; iii) previous studies correlate the positive effect of sucrose supplementation on resistance towards atrazine (induces generation of singlet oxygen ($^1O_2$) at PSII) treatment (Ramel et al., 2007; Ramel et al., 2009a) iv) and positively correlate pre-stress carbohydrate status with oxidative stress resistance (Ramel et al., 2009b).

Stress conditions often lead to inhibition of photosynthesis and result in sugar starvation responses that are largely regulated by SNF-1 RELATED KINASE1 (SnRK1; Baena-González et al., 2007). Under sugar starvation conditions, SnRK1 promotes autophagy and degradation of various cellular components and that are utilized as alternative sources of energy (Baena-González et al., 2007). Consequently, plants overexpressing the SnRK1 catalytic subunit SNF1 KINASE HOMOLOG 10 (KIN10) exhibit prolonged lifespan under starvation conditions (Baena-González et al., 2007). SnRK1 activity is controlled by cellular concentration of trehalose 6-phosphate (T6P; Zhang et al., 2009; Delatte et al., 2011). T6P is considered as a signaling molecule that indicates the intracellular carbohydrate availability status (Schluepmann et al., 2003; Lunn et al., 2006). The increase in intracellular sugar levels promotes accumulation of T6P (Lunn et al., 2006) which in turn inactivates SnRK1 (Zhang et al., 2009). Remarkably, the behavior of STP13OE plants [demonstrated before by Schofield et al., (2009) to have increased rates of sugar uptake from the growth media] in the liquid-based RGCL assay appeared opposite (accelerated chlorosis vs prolonged survival) to the phenotype exhibited by KIN10 overexpressors subjected to sugar starvation under similar submergence conditions (Baena-González et al., 2007). In contrast, the *stp13* lines exhibited prolonged survival which suggested elevated SnRK1 activity in these plants. To validate this hypothesis we investigated the oxidative stress performance of plants with altered SnRK1 activity and T6P levels. For this, we have utilized RNAi and OE lines of SnRK1 catalytic subunit (KIN10; Baena-González et al., 2007) and plants expressing *E. coli otsA* (osmoregulatory trehalose synthesis) gene encoding for trehalose-6-phosphate synthase (TPS, increased T6P levels) or *otsB* gene encoding for trehalose-6-phosphate phosphatase (TPP, decreased T6P levels) described before (Schluepmann et al., 2003; Wingler et al., 2012). In agreement with our hypothesis, when tested in 24-well RGCL assay plants

Fig. 6 (continued from previous page) **A)** PSII maximum efficiency (Fv'/Fm') and phenotype of Col-0 and *cat2-2* plants after 4 days in CL conditions. **B)** Changes in Fv'/Fm' observed in the course of experiment, data points represent means of 4 biological replicates (separate wells) ± SE. For clarity reasons, Col-0 and *cat2-2* line were visualized on separate graphs **C)** PSII maximum efficiency (Fv'/Fm') and phenotype of plants subjected to RGCL assay on solid media supplemented with various sugar concentrations. Pictures taken 7 days after the treatment.

overexpressing *otsA* exhibited phenotypes similar to those observed in STP13OE plants (Fig 7 A, B). Throughout the time of the treatment the PSII maximum efficiency was higher in *otsA* plants when compared to Col-0 control line (Fig. 7B), this was also associated with early progress of chlorosis (Fig. 7 B). Interestingly, we did not observe an opposite phenotype for plants overexpressing *otsB*. Next, we investigated the performance of KIN10 RNAi and OE plants in the same conditions. As expected, plants overexpressing KIN10 exhibited more pronounced initial decrease in PSII maximum efficiency and enhanced survival within the 24-well RGCL assay as compared to Col-0 line (Fig. 7 C, D). In contrast, the KIN10 RNAi line exhibited higher initial Fv'/Fm' values and faster progression of chlorosis (Fig. 7 C, D). Together, our results clearly demonstrate that modulation of SnRK1 activity either by altering the T6P levels or by overexpression/silencing of the KIN10 subunit influenced the survival of plants in our experimental conditions. This prompted us to test whether increase in SnRK1 activity could rescue the phenotype of CATALASE2-deficient plants as observed earlier for *stp13-2/cat2-2* knockouts. For this, KIN10 transgenic lines OE 5.7 and RNAi 7.8 (negative control) were crossed with cat*2-20* knockout line as both lines were in Ler-0 genetic background. Double homozygous KIN10RNAi-7.8/*cat2-20* and KIN10OE5.7/*cat2-20* were isolated in F3 generation by means of PCR genotyping and growth on selective media. The double mutant lines were tested in 24-well liquid medium based RGCL assay as described before. Following the stress treatment KIN10RNAi-7.8/*cat2-20* plants exhibited earlier onset of leaf chlorosis when compared to control *cat2-20* line (Fig. 7E), this is in contrast to KIN10OE-5.7/*cat2-20* plants which alike *stp13-2/cat2-2* line exhibited enhanced survival (Fig. 7E). Together, our results suggest that within our experimental conditions the lack of STP13 might lead to decreased sugar availability which promotes activation of SnRK1. In view of these results it would be very interesting to investigate the levels of sugars, T6P and the transcript levels of KIN10 marker genes in liquid grown STP13 transgenics.

T6P controls oxidative stress-induced anthocyanin accumulation

Among other processes, SnRK1 activity controls anthocyanin accumulation, with overexpression of KIN10, leading to inhibition of production of these pigments associated with growth on high sucrose media (Baena-González et al., 2007). Conversely, the overexpression of *otsA* (resulting in increased T6P levels and subsequent SnRK1 inactivation), promotes constitutive accumulation of these metabolites (Wingler et al., 2012). Interestingly, the overexpression of *otsB* inhibits accumulation of anthocyanins promoted by low nitrogen and high sugar availability (Wingler et al., 2012) while in a similar conditions STP13OE plants exhibit opposite behavior (Schofield et al., 2009) further strengthening the notion that the phenotypes of STP13 transgenics might be related to altered T6P levels. Accumulation of anthocyanins is one of the key adaptations towards oxidative stress conditions (Steyn et al., 2002; Hoch et al., 2003). Our previous results demonstrate that the high-light triggered up-regulation of a transcriptional cluster of genes [including transcription factors

PRODUCTION OF ANTHOCYANIN PIGMENT 1 (PAP1/MYB75) and PAP2/MYB90] involved in biosynthesis of these pigments is delayed in *cat2* plants (Vanderauwera et al., 2005).
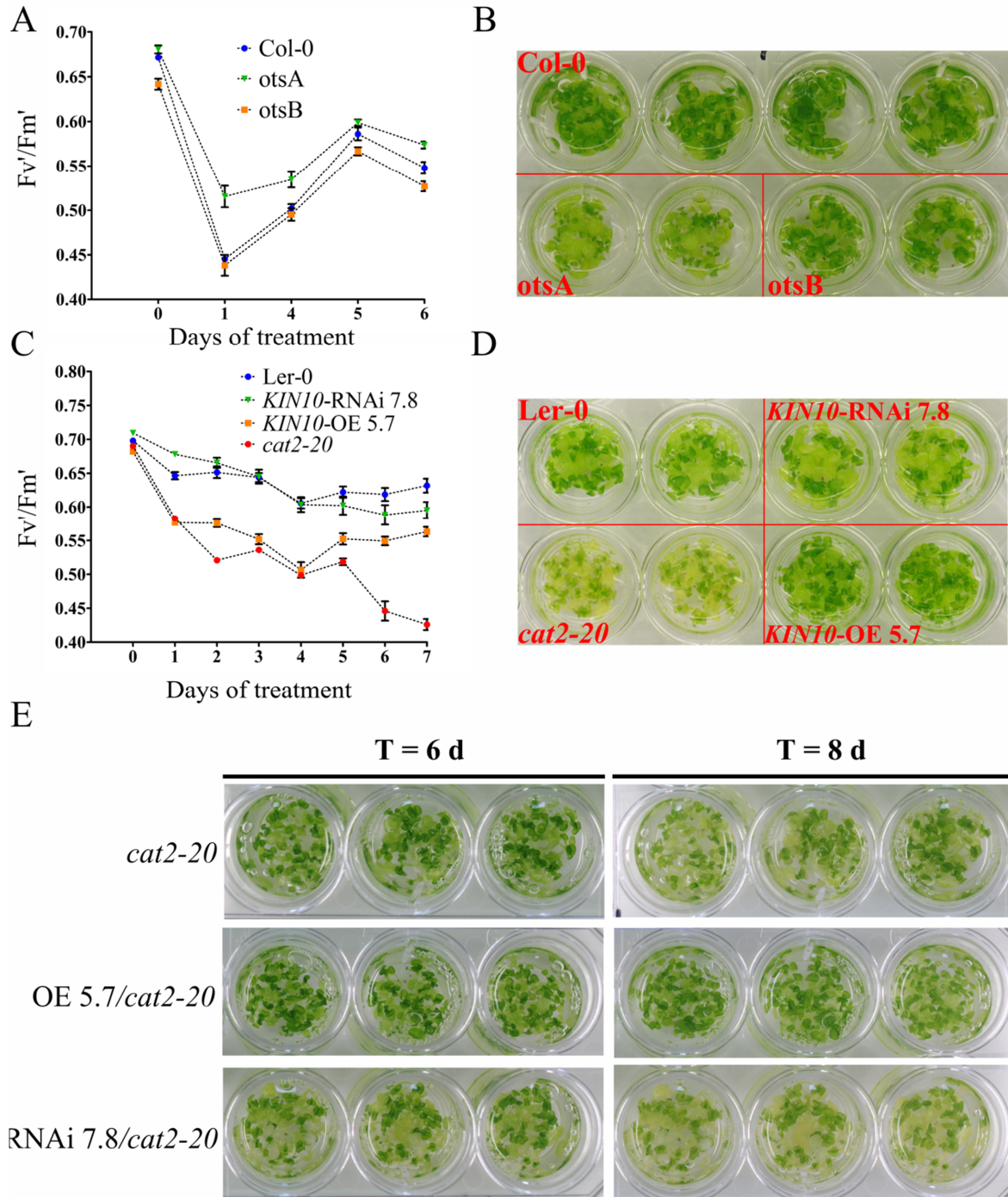

Fig. 7 Modulation of SnrK1 activity influences survival in liquid-based RGCL assay. Ten-days old plants grown in half-strength MS liquid medium (0.2 % sucrose) under LD conditions were exposed to continuous light for a specified time period. **A)** Changes in Fv'/Fm' observed for WT and plants with altered T6P levels in the course of experiment, data points represent means of 4 biological replicates (separate wells) ± SE. **B)** Progress of chlorosis observed 7 days after the treatment. **C)** Quantification of PSII maximum efficiency and (**D**) phenotype of plants with altered SnRK1 activity. Photo taken 8 days after the treatment. **E)** Progression of chlorosis observed for KIN10 OE/RNAi lines in *cat2-20* background.
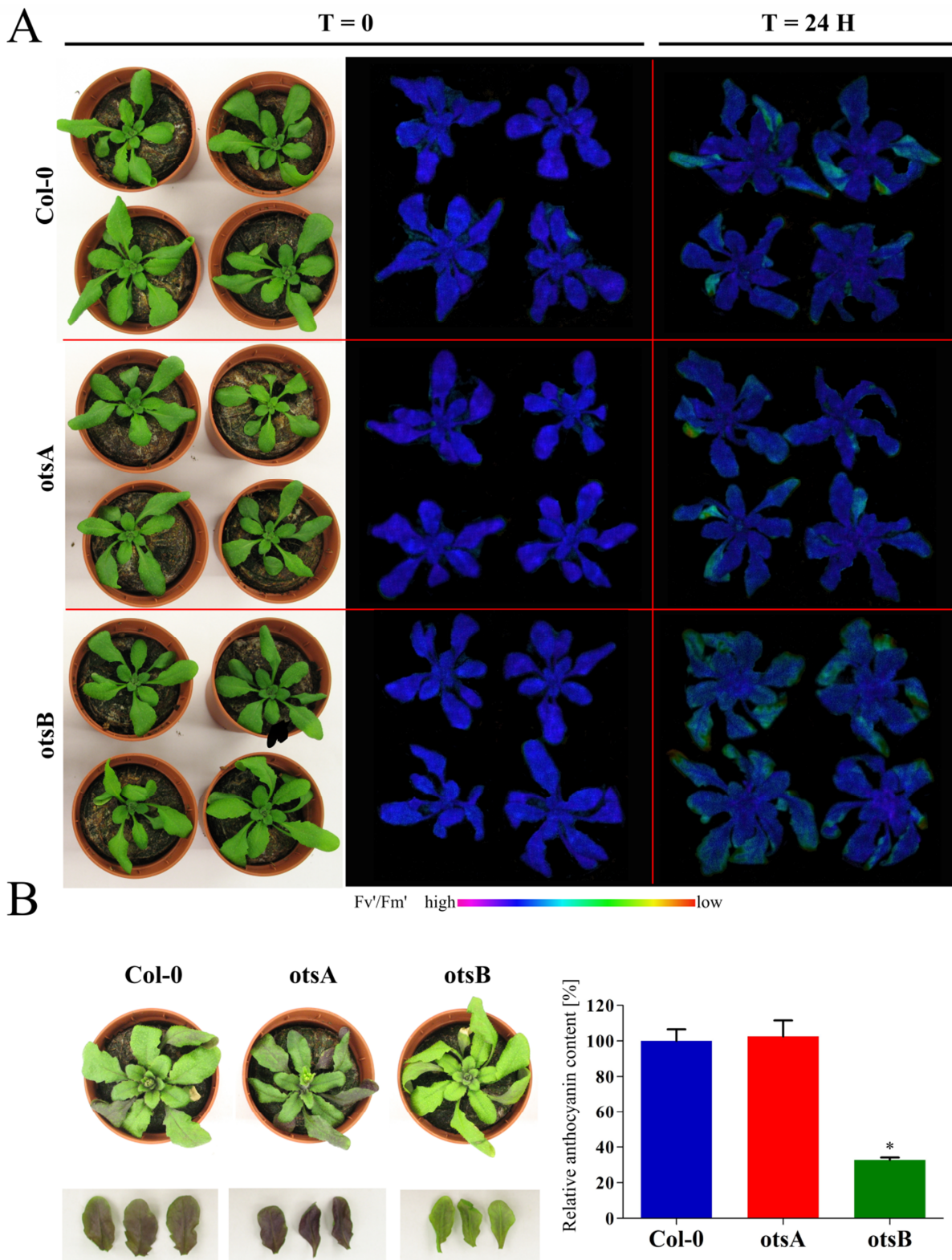
Fig. 8 The level of T6P determines oxidative stress-related accumulation of athocyanin pigments. Three-weeks-old plants grown in soil under a long day photoperiod at elevated CO_2 concentration (3000 ppm) were transferred to ambient air and exposed to continuous excess light irradiation for 48 hours. **A)** Phenotype and PSII maximum efficiency of Col-0, *otsA* and *otsB* plants before and after 24 hours of stress treatment. **B)** Phenotype and relative anthocyanin content after 48 hours of treatment. Bars indicate means of 10 biological replicates ±SE. Asterisk denotes significant difference to Col-0 control line (One-way ANOVA followed by Dunnett's multiple comparison test)

Consequently, *cat2* mutants fail to accumulate anthocyanins in response to HL treatment (Vanderauwera et al., 2005). To investigate whether the level of T6P might affect the oxidative stress induced anthocyanin accumulation we subjected plants expressing *otsA* (TPS), *otsB* (TPP) and Col-0 control line to HL treatment combined with transfer from high to ambient CO_2 atmosphere as described before. After 24 hours of HL plants overexpressing *otsB* exhibited a markedly higher decrease in PSII maximum efficiency than Col-0 and *otsA* plants (Fig. 8 A). Furthermore, after 48 hours of HL treatment, the accumulation of anthocyanin pigments was significantly lower in *otsB* plants reaching only 32% of Col-0 value while the anthocyanin content in *otsA* plants was comparable to that of wild-type (Fig. 8B). These results suggest that signaling pathway(s) that regulate the oxidative stress dependent accumulation of anthocyanin pigments are at least in part controlled by the abundance of T6P and presumably also the activity of SnRK1. In support of this notion, the expression of PAP1 transcription factor (which transcriptional up-regulation is delayed in *cat2* plants under photorespiratory conditions) was identified earlier to be negatively regulated by KIN10 overexpression (Baena-González et al., 2007) suggesting that photorespiratory hydrogen peroxide might directly or indirectly activate SnRK1 activity. We further suggest that SnRK1 is the previously hypothesized (Vanderauwera et al., 2005) oxidative stress-controlled master regulator of anthocyanin production. The working hypothesis drawn from publicly available data and results obtained in this chapter is schematically presented on Fig. 10.

Overexpression of KIN10 in *cat2* background is sublethal

To further investigate the relation between oxidative stress performance and SnRK1 activity we tested whether the modulation of KIN10 levels within WT and *cat2* background could have an influence on plant performance under low and moderate light intensities. In a pilot experiment, Ler-0, *cat2-20* and KIN10 transgenics (in Ler-0 and *cat2-20* background) were grown at light intensities of 100 and 300 $\mu mol \cdot m^{-2} \cdot s^{-1}$ under LD photoperiod for three weeks. Measurement of rosette fresh weight demonstrated that when grown at irradiance of 100 $\mu mol \cdot m^{-2} \cdot s^{-1}$ plants overexpressing KIN10 (OE-5.7) accumulated significantly less (One-way ANOVA followed by Bonferroni's post-hoc test p-value < 0.05) biomass (64%) compared to Ler-0 reference (Fig. 9A). Under higher irradiance (300 $\mu mol \cdot m^{-2} \cdot s^{-1}$), lines *cat2-20* and KIN10 OE-5.7 accumulated significantly less (One-way ANOVA followed by Bonferroni's post-hoc test p-value < 0.05) biomass that Ler-0, reaching 51%, and 25% of Ler-0 control value respectively. This data indicate that, in comparison to Ler-0 control, KIN10 OE5.7 line failed to utilize increased light intensity to intensify biomass production. Interestingly, the decreased biomass accumulation observed for KIN10 OE line was associated with the development of lesions on rosette leaves (Fig. 9 B). Moreover, the overexpression of KIN10 in *cat2-20* background resulted in 35% mortality (9 dead plants per 24) and a dramatic decrease in fresh weight (Fig. 9 A, B). At present, we are not able to provide a clear explanation for the phenotypes

observed in KIN10OE-5.7/*cat2-20* line grown under photorespiratory conditions. A plausible hypothesis might relate the oxidative stress induced inhibition of glycolate oxidase, accumulation of glycolate and reduction of CO_2 assimilation observed in *cat2* plants (see Chapter 3) with sugar starvation response and constitutive activation of SnRK1 kinase. Under these conditions, additional increase in SnRK1 activity provoked by KIN10 overexpression could lead to excessive autophagy/degradation of cell components and result in ~ 35% mortality observed within our experimental group of KIN10OE-5.7/*cat2-20* plants. An alternative hypothesis might link the decreased oxidative stress susceptibility of these plants to constitutive repression of anthocyanin accumulation that exhibit photoprotective functions. Future experiments will aim at investigating the level of anthocyanins in the soil-grown KIN10/*cat2-20* transgenics generated in this study.

ACKNOWLEDGEMENTS

MATERIALS AND METHODS

Plant material and growth conditions

STP13 T-DNA insertion mutant lines *stp13-1* (SALK_045494) and *stp13-2* (SALK_021204) were obtained from SALK T-DNA collection (Alonso et al., 2003) and PCR genotyped with respective gene specific primers (Table S3) according to T-DNA Express *Arabidopsis* Gene Mapping Tool (http://signal.salk.edu/cgi-bin/tdnaexpress). Independent STP13 overexpression lines 35S:STP13OE-12, 35S:STP13OE-16 and pSTP13:GUS reporter line (Col-0 background) were described before (Schofield et al., 2009). Line *stp13-2* was crossed with *cat2-2* line (Queval et al., 2007) and double mutant plants were identified in F2 population by means of PCR genotyping (Table S3). Lines with altered KIN10 levels (Ler-0 genetic background) 35S:KIN10-5.7 and KIN10 RNAi-7.8 were reported previously (Baena-González et al., 2007). Both lines were crossed with CATALASE2-deficient Ler-0 line (*cat2-20*, characterized in Chapter 3). Double mutant plants were identified in F2 population by means of PCR genotyping (Table S3) and growth on selective media containing 35 µg/ml kanamycin (selection for *cat2-20* alleles) and 6 µg/ml DL-phosphinotricin (for inserts altering KIN10 levels). Plants expressing the Escherichia coli TPS gene *otsA* or TPP gene *otsB* were described earlier (Schluepmann et al., 2003; Wingler et al., 2012). Plants were grown in Jiffy-7 soil pellets (Jiffy Products, Norway) in a controlled growth chamber at 21°C, 16 h light (80-90 µmol·m^{-2}·s^{-1})/8 h dark regime and 70% relative humidity or in vitro on full-strenght Murashige and Skoog agar solidified medium supplemented with 1% sucrose at 21°C and long day 16 h light (100 µmol·m^{-2}·s^{-1})/8 h dark conditions.
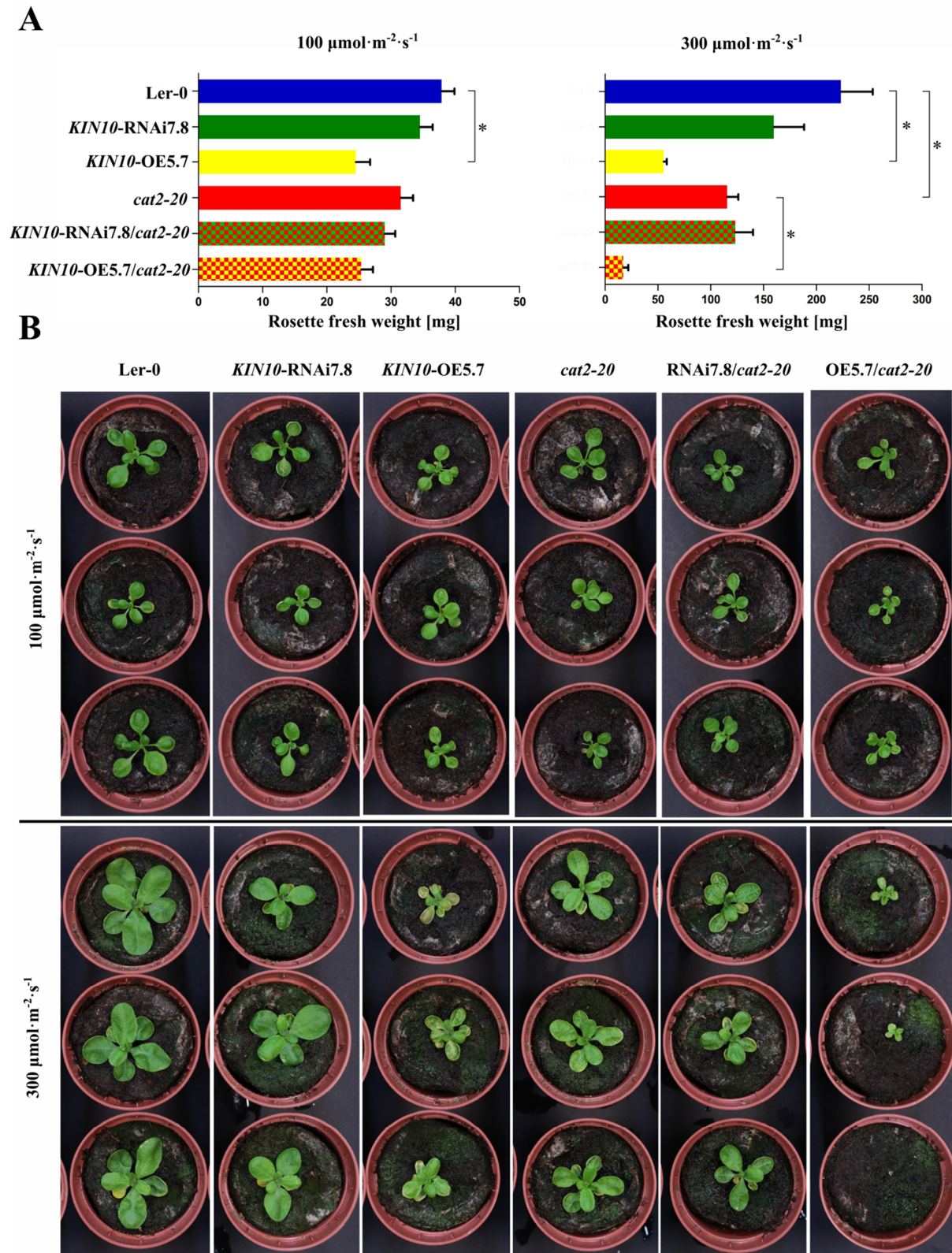
Fig. 9 Light intensity controls the influence of SnRK1 on biomass accumulation in soil. **A, B)** Plants were grown in soil in LD conditions at light intensity of 100 µmol·m^{-2}·s^{-1} and 300 µmol·m^{-2}·s^{-1} for four and three weeks respectively. Twenty three rosettes/line were collected for fresh weight determination. Bars represent means of 23 biological replicates ± SE. Asterisks indicate significant differences to respective control lines according to one-way ANOVA followed by Bonferroni's multiple comparison test (p < 0.05).
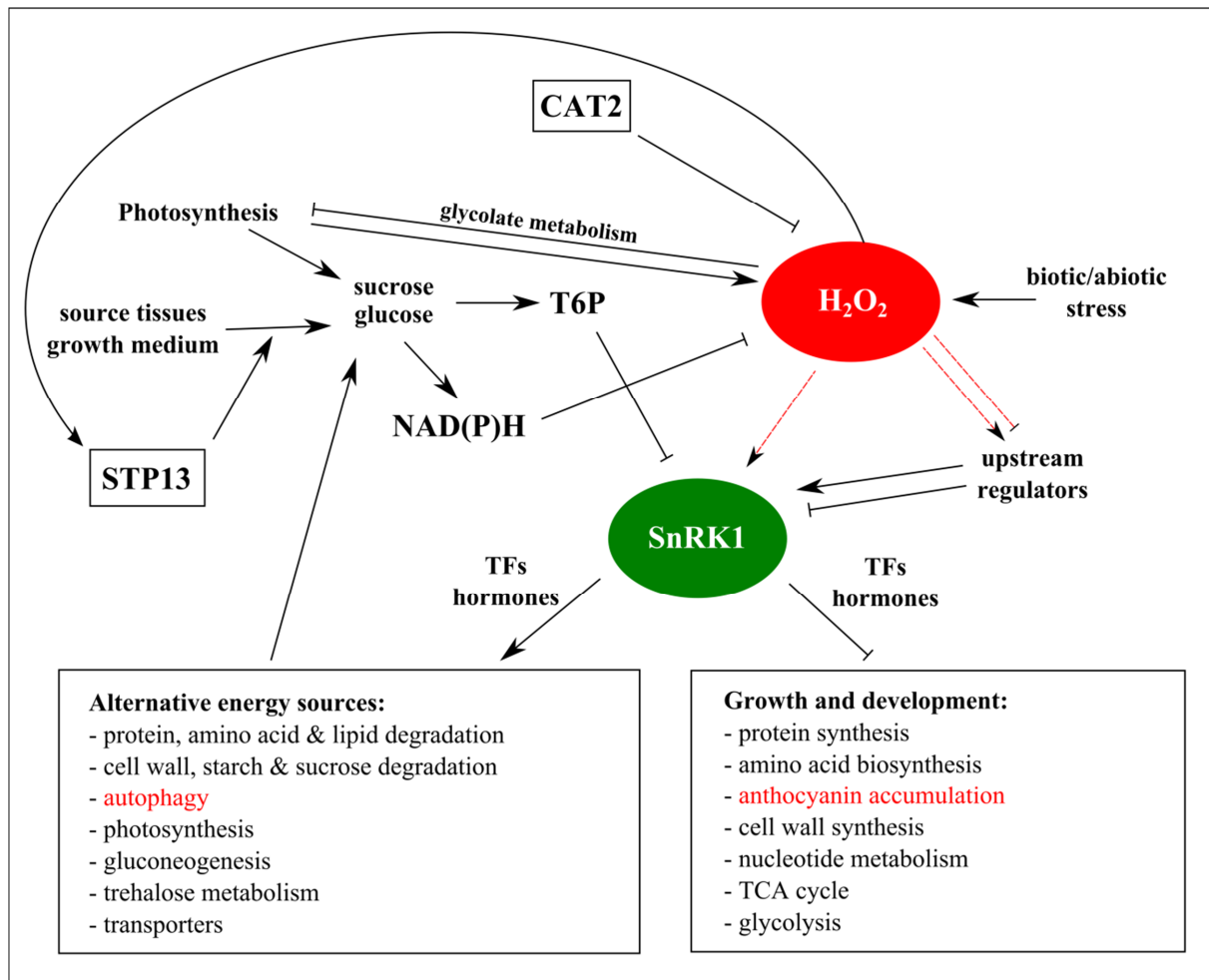
Fig. 10 Schematic representation of the working hypothesis linking photorespiratory hydrogen peroxide, STP13 and SnRK1, adapted from Baena-González et al., (2007). Stress induced expression of STP13 leads to increased sugar uptake by creating a sink force. Depending on the growth conditions sugars are transported from source organs or, when grown in vitro, the growth medium. Lack of CATALASE2 leads to accumulation of photorespiratory hydrogen peroxide that, most likely, via altered glycolate metabolism (see Chapter 3) leads to inhibition of photosynthesis. Low rate of photoassimilation leads to a drop in cellular energy level that via altered concentration of trehalose-6-phosphate (T6P) is perceived by SnRK1. We postulate (red arrows) that photorespiratory H_2O_2 activates SnRK1 directly, or via its upstream regulators. Upon oxidative stress-mediated activation, SnRK1 triggers defense mechanisms (including autophagy) aiming at mobilization of alternative energy sources necessary to restore the cellular redox balance. To increase the clarity of the figure multiple well established relationships e. g. photosynthetic production of NADPH, were not included. TFs, transcription factors.

Stress treatments

For a 96-well plate-based RGCL assay seeds were surface sterilized by means of chlorine gas sterilization and vernalized at 4°C for 72 hours; subsequently ~7 seeds per well were sowed into Microtest 3072 (Becton Dickinson) plates in 250 µl of liquid half strength Murashige and Skoog medium supplemented with 0.2% sucrose and 100 mg·L^{-1} myo-inositol. Each T-DNA insertion line was planted in four wells and each experimental plate contained Col-0 and *cat2-2* control lines and plates were sealed with parafilm (Parafilm M®, Bemis). After 10 days of growth at 21°C in 16 h light

(~100 μmol·m^{-2}·s^{-1})/8 h dark photoperiod, plants were transferred to continuous light (~100 μmol·m^{-2}·s^{-1}) conditions. PSII maximum efficiency (Fv'/Fm') was monitored at a daily basis. Changes in PSII maximum efficiency (Fv'/Fm') were followed with the use of PAM-2000 chlorophyll fluorometer and ImagingWin software (Walz, Germany). For a 24-well based RGCL assay plants were grown in parafilm sealed Falcon^{TM} 24-well tissue culture plates (BD Biosciences, USA) with approximately 20 seedlings per well filled with 2 ml of liquid medium. The composition of medium, growth conditions and stress treatment were the same as for 96-well assay.

The solid medium-based RGCL assay, high light treatments in soil and analysis of biomass accumulation under various light intensities were performed as described in Chapter 3.

Histochemical analysis and anthocyanin measurement

Detection of β-glucuronidase activity was performed on whole rosettes of pSTP13:GUS plants (Col-0 WT background) subjected to HL/ambient CO_2 treatment in soil for 0, 1, 3, 5, 8, 24 hours. Five rosettes per timepoint were analyzed. Immediately after harvesting tissue was de-stained for 8 hours in ice-cold 90% acetone, washed with assay solution (50 mM NaCl, 100 mM Tris pH 7.0, 0.1% v/v Triton X-100) and stored at 4°C. To avoid the influence of technical conditions precautions were taken to limit the destaining time to 8 h for samples from each time point. Samples from all time points were stained in parallel by incubating in assay solution supplemented with 2 mM X-Gluc for 3 h at 37°C in darkness and subsequently cleared in 80 % lactic acid.

Anthocyanin measurements were performed according to a procedure described previously (Vanderauwera et al., 2005, and references therein) adapted for the use of whole *Arabidopsis* rosettes. Ten rosettes per line were analyzed and the results were expressed as % of Col-0 value.

SUPPLEMENTARY METERIAL

Table S1. [Enclosed on a CD attached to this thesis] List of T-DNA insertion mutant lines screened with 96-well liquid-based RGCL assay.

Table S2. [Enclosed on a CD attached to this thesis] Description of microarray experiments used for meta-analysis of the STP family transcriptional regulation.

Table S3. List of primer sequences used for genotyping.

Primer	Sequence 5' → 3'
Genotyping - *stp13-1, stp13-2*	
SALK_045494_LP	CACGACTAGAATTGCGAAACC
SALK_045494_RP	AAAATTTTCTCCGGCATTGAC
SALK_021204_LP	TTATTGCAGGCAGGATATTGC
SALK_021204_RP	CTGAGGACGGTTTCTACGTTG
LBb1.3	ATTTTGCCGATTTCGGAAC
Genotyping - *cat2-2* Queval et al., 2007)	
sensCAT2	CCCAGAGGTACCTCTTCTTCTCCCATG
revbisCAT2	TCAGGGAACTTCATCCCATCGC
LB1_new	TGGACCGCTTGCTGCAACTCTC
Genotyping - *cat2-20*	
ET8347_LP	GTTCTCGGGAACCTAAATTCG
ET8347_RP	TCATGGAGGAGTTGTTGTTCC
DS3.2	CGATTACCGTATTTATCCCGTTC
DS5.1	GAAACGGTCGGGAAACTAGCTCTAC

REFERENCES

Alonso JM, Ecker JR (2006) Moving forward in reverse: genetic technologies to enable genome-wide phenomic screens in *Arabidopsis*. Nat Rev Genet **7**: 524–36

Alonso JM, Stepanova AN, Leisse TJ, Kim CJ, Chen H, Shinn P, Stevenson DK, Zimmerman J, Barajas P, Cheuk R, et al (2003) Genome-wide insertional mutagenesis of *Arabidopsis thaliana*. Science **301**: 653–7

Baena-González E, Rolland F, Thevelein JM, Sheen J (2007) A central integrator of transcription networks in plant stress and energy signalling. Nature **448**: 938–42

Baxter-Burrell A, Yang Z, Springer PS, Bailey-Serres J (2002) RopGAP4-dependent Rop GTPase rheostat control of *Arabidopsis* oxygen deprivation tolerance. Science (80-) **296**: 2026–2028

Blokhina OB, Chirkova T V, Fagerstedt K V (2001) Anoxic stress leads to hydrogen peroxide formation in plant cells. J Exp Bot **52**: 1179–90

Büttner M (2007) The monosaccharide transporter(-like) gene family in *Arabidopsis*. FEBS Lett **581**: 2318–24

Chang R, Jang CJ, Branco-Price C, Nghiem P, Bailey-Serres J (2012) Transient MPK6 activation in response to oxygen deprivation and reoxygenation is mediated by mitochondria and aids seedling survival in *Arabidopsis*. Plant Mol Biol **78**: 109–22

Clifton R, Lister R, Parker K, Sappl P, Elhafez D, Millar AH, Day DA, Whelan J (2005) Stress-induced co-expression of alternative respiratory chain components in *Arabidopsis thaliana*. Plant Mol Biol **58**: 193–212

Couée I, Sulmon C, Gouesbet G, El Amrani A (2006) Involvement of soluble sugars in reactive oxygen species balance and responses to oxidative stress in plants. J Exp Bot **57**: 449–59

Crawford RMM, Braendle R (1996) Oxygen deprivation stress in a changing environment. J Exp Bot **47**: 145–159

Delatte TL, Sedijani P, Kondou Y, Matsui M, de Jong GJ, Somsen GW, Wiese-Klinkenberg A, Primavesi LF, Paul MJ, Schluepmann H (2011) Growth arrest by trehalose-6-phosphate: an astonishing case of primary metabolite control over growth by way of the SnRK1 signaling pathway. Plant Physiol **157**: 160–74

Feldmann K A. (1991) T-DNA insertion mutagenesis in *Arabidopsis*: mutational spectrum. Plant J **1**: 71–82

Fukao T, Bailey-Serres J (2004) Plant responses to hypoxia--is survival a balancing act? Trends Plant Sci **9**: 449–56

Gadjev I, Vanderauwera S, Gechev T (2006) Transcriptomic footprints disclose specificity of reactive oxygen species signaling in *Arabidopsis*. Plant Physiol **141**: 436–445

Germain V, Ricard B, Raymond P, Saglio PH (1997) The role of sugars, hexokinase, and sucrose synthase in the determination of hypoxically induced tolerance to anoxia in tomato roots. Plant Physiol **114**: 167–175

Gibbs DJ, Lee SC, Isa NM, Gramuglia S, Fukao T, Bassel GW, Correia CS, Corbineau F, Theodoulou FL, Bailey-Serres J, et al (2011) Homeostatic response to hypoxia is regulated by the N-end rule pathway in plants. Nature **479**: 415–8

Hardie DG (2011) AMP-activated protein kinase: an energy sensor that regulates all aspects of cell function. Genes Dev **25**: 1895–908

Hoch WA, Singsaas EL, McCown BH (2003) Resorption protection . Anthocyanins facilitate nutrient recovery in autumn by shielding leaves from potentially damaging light levels. Plant Physiol **133**: 1296–1305

Inzé A, Vanderauwera S, Hoeberichts FA, Vandorpe M, Van Gaever T, Van Breusegem F (2012) A subcellular localization compendium of hydrogen peroxide-induced proteins. Plant Cell Environ **35**: 308–20

Jang JC, León P, Zhou L, Sheen J (1997) Hexokinase as a sugar sensor in higher plants. Plant Cell **9**: 5–19

Kerchev P, Mühlenbock P, Denecker J, Morreel K, Hoeberichts FA, Van Der Kelen K, Vandorpe M, Nguyen L, Audenaert D, Van Breusegem F (2014) Activation of auxin signaling counteracts photorespiratory H_2O_2 dependent cell death. Plant Cell Environ DOI: 10.1111/pce.12250

Kerchev PI, Pellny TK, Vivancos PD, Kiddle G, Hedden P, Driscoll S, Vanacker H, Verrier P, Hancock RD, Foyer CH (2011) The transcription factor ABI4 Is required for the ascorbic acid-dependent regulation of growth and regulation of jasmonate-dependent defense signaling pathways in *Arabidopsis*. Plant Cell **23**: 3319–34

Lemoine R, La Camera S, Atanassova R, Dédaldéchamp F, Allario T, Pourtau N, Bonnemain J-L, Laloi M, Coutos-Thévenot P, Maurousset L, et al (2013) Source-to-sink transport of sugar and regulation by environmental factors. Front Plant Sci **4**: 272

Licausi F, Kosmacz M, Weits DA, Giuntoli B, Giorgi FM, Voesenek L a CJ, Perata P, van Dongen JT (2011) Oxygen sensing in plants is mediated by an N-end rule pathway for protein destabilization. Nature **479**: 419–22

Loreti E, Poggi A, Novi G, Alpi A, Perata P (2005) A genome-wide analysis of the effects of sucrose on gene expression in *Arabidopsis* seedlings under anoxia. Plant Physiol **137**: 1130–1138

Lunn JE, Feil R, Hendriks JHM, Gibon Y, Morcuende R, Osuna D, Scheible W-R, Carillo P, Hajirezaei M-R, Stitt M (2006) Sugar-induced increases in trehalose 6-phosphate are correlated with redox activation of ADPglucose pyrophosphorylase and higher rates of starch synthesis in *Arabidopsis thaliana*. Biochem J **397**: 139–48

McElver J, Tzafrir I, Aux G, Rogers R, Ashby C, Smith K, Thomas C, Schetter a, Zhou Q, Cushman MA, et al (2001) Insertional mutagenesis of genes required for seed development in *Arabidopsis thaliana*. Genetics **159**: 1751–63

Mommer L, Pons TL, Wolters-Arts M, Venema JH, Visser EJW (2005) Biochemical responses in a terrestrial species affect gas diffusion resistance and photosynthetic performance. Plant Physiol **139**: 497–508

Mommer L, Visser EJW (2005) Underwater photosynthesis in flooded terrestrial plants: a matter of leaf plasticity. Ann Bot **96**: 581–9

Moore B, Zhou L, Rolland F, Hall Q, Cheng W-H, Liu Y-X, Hwang I, Jones T, Sheen J (2003) Role of the *Arabidopsis* glucose sensor HXK1 in nutrient, light, and hormonal signaling. Science **300**: 332–6

Ng S, Ivanova A, Duncan O, Law SR, Van Aken O, De Clercq I, Wang Y, Carrie C, Xu L, Kmiec B, et al (2013) A membrane-bound NAC transcription factor, ANAC017, mediates mitochondrial retrograde signaling in *Arabidopsis*. Plant Cell **25**: 3450–71

Norholm MHH, Nour-Eldin HH, Brodersen P, Mundy J, Halkier BA (2006) Expression of the *Arabidopsis* high-affinity hexose transporter STP13 correlates with programmed cell death. FEBS Lett **580**: 2381–7

Nour-Eldin HH, Nørholm MHH, Halkier BA (2006) Screening for plant transporter function by expressing a normalized *Arabidopsis* full-length cDNA library in *Xenopus* oocytes. Plant Methods **2**: 17

Petrov VD, Van Breusegem F (2012) Hydrogen peroxide-a central hub for information flow in plant cells. AoB Plants **2012**: pls014

Queval G, Issakidis-Bourguet E, Hoeberichts FA, Vandorpe M, Gakière B, Vanacker H, Miginiac-Maslow M, Van Breusegem F, Noctor G (2007) Conditional oxidative stress responses in the *Arabidopsis* photorespiratory mutant cat2 demonstrate that redox state is a key modulator of daylength-dependent gene expression, and define photoperiod as a crucial factor in the regulation of H2O2-induced cel. Plant J **52**: 640–57

Queval G, Neukermans J, Vanderauwera S, Van Breusegem F, Noctor G (2012) Day length is a key regulator of transcriptomic responses to both CO_2 and H_2O_2 in *Arabidopsis*. Plant cell Environ **35**: 374–87

Ramel F, Birtic S, Ginies C, Soubigou-Taconnat L, Triantaphylidès C, Havaux M (2012) Carotenoid oxidation products are stress signals that mediate gene responses to singlet oxygen in plants. Proc Natl Acad Sci U S A **109**: 5535–40

Ramel F, Sulmon C, Bogard M, Couée I, Gouesbet G (2009a) Differential patterns of reactive oxygen species and antioxidative mechanisms during atrazine injury and sucrose-induced tolerance in *Arabidopsis thaliana* plantlets. BMC Plant Biol **9**: 28

Ramel F, Sulmon C, Cabello-Hurtado F, Taconnat L, Martin-Magniette M-L, Renou J-P, El Amrani A, Couée I, Gouesbet G (2007) Genome-wide interacting effects of sucrose and herbicide-mediated stress in *Arabidopsis thaliana*: novel insights into atrazine toxicity and sucrose-induced tolerance. BMC Genomics **8**: 450

Ramel F, Sulmon C, Gouesbet G, Couée I (2009b) Natural variation reveals relationships between pre-stress carbohydrate nutritional status and subsequent responses to xenobiotic and oxidative stress in *Arabidopsis thaliana*. Ann Bot **104**: 1323–37

Sattler SE, Mène-Saffrané L, Farmer EE, Krischke M, Mueller MJ, DellaPenna D (2006) Nonenzymatic lipid peroxidation reprograms gene expression and activates defense markers in *Arabidopsis* tocopherol-deficient mutants. Plant Cell **18**: 3706–20

Scarpeci TE, Zanor MI, Carrillo N, Mueller-Roeber B, Valle EM (2008) Generation of superoxide anion in chloroplasts of *Arabidopsis thaliana* during active photosynthesis: a focus on rapidly induced genes. Plant Mol Biol **66**: 361–78

Schluepmann H, Pellny T, van Dijken A, Smeekens S, Paul M (2003) Trehalose 6-phosphate is indispensable for carbohydrate utilization and growth in *Arabidopsis thaliana*. Proc Natl Acad Sci U S A **100**: 6849–54

Schofield RA, Bi Y-M, Kant S, Rothstein SJ (2009) Over-expression of STP13, a hexose transporter, improves plant growth and nitrogen use in *Arabidopsis thaliana* seedlings. Plant Cell Environ **32**: 271–85

Short EF, North K a, Roberts MR, Hetherington AM, Shirras AD, McAinsh MR (2012) A stress-specific calcium signature regulating an ozone-responsive gene expression network in *Arabidopsis*. Plant J **71**: 948–61

Steyn WJ, Wand SJE, Holcroft DM, Jacobs G (2002) Anthocyanins in vegetative tissues: a proposed unified function in photoprotection. New Phytol **155**: 349–361

Sulmon C, Gouesbet G, Ramel F, Cabello-Hurtado F, Penno C, Bechtold N, Couée I, El Amrani A (2011) Carbon dynamics, development and stress responses in *Arabidopsis*: involvement of the APL4 subunit of ADP-glucose pyrophosphorylase (starch synthesis). PLoS One **6**: e26855

Tognetti VB, Van Aken O, Morreel K, Vandenbroucke K, van de Cotte B, De Clercq I, Chiwocha S, Fenske R, Prinsen E, Boerjan W, et al (2010) Perturbation of indole-3-butyric acid homeostasis by the UDP-glucosyltransferase UGT74E2 modulates *Arabidopsis* architecture and water stress tolerance. Plant Cell **22**: 2660–79

Tognetti VB, Mühlenbock P, Van Breusegem F (2012) Stress homeostasis - the redox and auxin perspective. Plant Cell Environ **35**: 321–33

Ulker B, Peiter E, Dixon DP, Moffat C, Capper R, Bouché N, Edwards R, Sanders D, Knight H, Knight MR (2008) Getting the most out of publicly available T-DNA insertion lines. Plant J **56**: 665–77

Vandenabeele S, Vanderauwera S, Vuylsteke M, Rombauts S, Langebartels C, Seidlitz HK, Zabeau M, Van Montagu M, Inzé D, Van Breusegem F (2004) Catalase deficiency drastically affects gene expression induced by high light in *Arabidopsis thaliana*. Plant J **39**: 45–58

Vanderauwera S, Suzuki N, Miller G, van de Cotte B, Morsa S, Ravanat J-L, Hegie A, Triantaphylidès C, Shulaev V, Van Montagu MCE, et al (2011) Extranuclear protection of chromosomal DNA from oxidative stress. Proc Natl Acad Sci U S A **108**: 1711–6

Vanderauwera S, Zimmermann P, Rombauts S, Vandenabeele S, Langebartels C, Gruissem W, Inze D, Van Breusegem F (2005) Genome-wide analysis of hydrogen peroxide-regulated gene expression in *Arabidopsis* reveals a high light-induced transcriptional cluster involved in anthocyanin biosynthesis. Plant Physiol **139**: 806–821

Vergara R, Parada F, Rubio S, Pérez FJ (2012) Hypoxia induces H_2O_2 production and activates antioxidant defence system in grapevine buds through mediation of H_2O_2 and ethylene. J Exp Bot **63**: 4123–31

Wardlaw IF (1990) Tansley Review No. 27 The control of carbon partitioning in plants. New Phytol **116**: 341–381

Wingler A, Delatte TL, O'Hara LE, Primavesi LF, Jhurreea D, Paul MJ, Schluepmann H (2012) Trehalose-6-phosphate is required for the onset of leaf senescence associated with high carbon availability. Plant Physiol **158**: 1241–51

Wolfinger RD, Gibson G, Wolfinger ED, Bennett L, Hamadeh H, Bushel P, Afshari C, Paules RS (2001) Assessing gene significance from cDNA microarray expression data via mixed models. J Comput Biol **8**: 625–637

Xiong Y, McCormack M, Li L, Hall Q, Xiang C, Sheen J (2013) Glucose-TOR signalling reprograms the transcriptome and activates meristems. Nature **496**: 181–6

Yamada K, Kanai M, Osakabe Y, Ohiraki H, Shinozaki K, Yamaguchi-Shinozaki K (2011) Monosaccharide absorption activity of *Arabidopsis* roots depends on expression profiles of transporter genes under high salinity conditions. J Biol Chem **286**: 43577–86

Zhang Y, Primavesi LF, Jhurreea D, Andralojc PJ, Mitchell R a C, Powers SJ, Schluepmann H, Delatte T, Wingler A, Paul MJ (2009) Inhibition of SNF1-related protein kinase1 activity and regulation of metabolic pathways by trehalose-6-phosphate. Plant Physiol **149**: 1860–71

CONCLUSIONS AND PERSPECTIVES

In this study we applied forward and reverse genetic approaches in order to gain better understanding of plant adaptation to adverse environmental conditions. Despite being relatively diverse in experimental techniques all three research chapters of this thesis are oriented towards exploration of mechanisms that are potentially able to alleviate the negative influence of oxidative stress on plant growth and productivity.

Mining of *A. thaliana* sulfenome

Ample evidence indicates that reactive oxygen species (ROS) accumulate under various stress conditions and are often used by plant cells as stress signaling molecules (Petrov and Van Breusegem, 2012). This signaling function largely depends on the ability of ROS to oxidize redox sensor proteins which result in oxidative modifications that are often associated with changes in conformation and activity of these proteins. Depending on the nature of the protein signal perception might lead to direct changes in enzymatic activity i.e. in case of metabolic enzymes, or trigger signaling pathways that deliver the signal to the nucleus. While the information on redox modifications of metabolic enzymes is abundant (Schürmann and Buchanan, 2008) relatively little is known about the perception of redox status by signal tranducers (reviewed in Chapter 1). Within Chapter 2 of this thesis we describe the novel strategy for identification of proteins (collectively termed as sulfenome) able to perceive changes in redox status by oxidation on specific cysteine residues. The pioneering character of this work was the combination of Cys-SOH trapping with tandem affinity purification (TAP) approach. Our efforts led to identification of 97 proteins that are potentially involved in redox regulated cellular processes.

The TAP technology used in this work serves to isolate protein complexes (Van Leene et al., 2007). Despite obvious advantages i.e. ability to express probes in defined subcellular compartments or tissues, the use of protein tags requires the use of native conditions for protein purification. This technical feature is of crucial importance for identification of protein complexes based on e.g. hydrophobic interactions, however in case of our study (aimed at identification of complexes based on covalent bonds) creates uncertainty about the order of interactions. Despite of multiple wash steps included in the protocol most likely not all of the YAP1GS interactors identified in this study are direct binders, e.g. some of them could co-purify with their non-redox active interacting partners. Future efforts including the use of TAPtag compatible with more stringent washes could facilitate enrichment of the YAP1 interactome with primary interactors. Consequently, this would facilitate the subsequent validation experiments by narrowing the list of pray proteins to disulfide bonded interactors. On the other hand, the information about the secondary interactors might be useful for further genetic analysis and therefore can not be underestimated.

Validation of results obtained in this study will be crucial for future exploration of ROS signaling pathways as multiple proteins identified herein as potentially undergoing oxidative post-translational modifications belong to protein families known to participate in signaling cascades e.g. mitogen-activated protein kinases. Next to *in vitro* validation of oxidative modification, among the most informative experiments is the complementation of plants lacking respective proteins with their mutant forms deprived of cysteine residues crucial for signal perception. Another piece of information could be obtained from analogical experiment using mutations that are able to mimic sulfenic acid residues. In this regard, mutation of redox-active cysteine(s) to aspartate that due to its charged side-chain is able to mimic –SOH group (Wang et al., 2012). Phenotypical observation of mutant lines could indicate whether and which cysteine residues are necessary for the redox properties of protein of choice.

As indicated earlier among the most important advantages associated with the use of genetically encoded protein probes is the ability to target the protein into various subcellular compartments. The YAP1GS probe used in this work was not equipped with any signal peptide, consequently a great majority of identified proteins are known to reside in cytosol which also confirms the cytosolic localization of the probe. Future experiments could aim at tagging the YAP1 probes with signal peptides targeting the protein to various subcellular compartments to complete the landscape of *A. thaliana* sulfenome.

Finally, we believe that this technology could be applied to plants growing in physiologically relevant conditions. Studies at the whole plant level enable application of multiple stress treatments and therefore open a possibility for identification of proteins responsive to particular set of treatments.

Early plant development and metabolism of photorespiratory glycolate

Efforts described in Chapter 3 of this work were devoted to identification of 2nd site mutations able to revert the cell death symptoms exhibited under photorespiratory conditions by plants lacking photorespiratory CATALASE2. We performed a broad forward genetic screen and identified 13 mutants that exhibited significantly better performance under photorespiration-promoting conditions. Two of these mutation were mapped in this thesis and found to localize within coding sequence of SHORT-ROOT (SHR) transcription factor known mostly for its role in determination of root radial patterning (Cui et al., 2007) and GLYCOLATE OXIDASE1 (GOX1) a photorespiratory enzyme involved in conversion of glycolate to glyoxylate. The molecular functions of two genes are highly different however both mutant lines share a common theme related to metabolism of glycolate. We shown that plants lacking SHR exhibit a broad range of phenotypes related to photorespiratory metabolism, including decreased levels of GOX and CAT activity and accumulation of glycolate. Intriguingly, we also found that *shr* plants are Pi-deficiency mutants which explains some of the phenotypes described earlier for this mutants such as anthocyanin accumulation or inability to mobilize starch. As levels of phosphate are of crucial importance for proper function of biological

membranes including the transmembrane transport particularly important for the proper photorespiratory fluxes it is tempting to relate the Pi deficiency with glycolate hyperaccumulation phenotype. Future experiments that could address this questions could investigate the ultrastructure of chloroplasts and composition of chloroplast membranes. It would be also interesting to check whether *cat2* plants grown on Pi deprived medium mimic the phenotypes exhibited by *shr/cat2* plants, a similar information could also be obtained by introduction of Pi transport mutants into *cat2* background e.g. *pho1* (Poirier et al., 1991). Finally, it would be of interest to investigate to which extent phenotypes exhibited by *shr* plants could be explained by Pi deficiency. Experiment that could help to answer this question could involve genetic introduction of *low phosphate resistant (lpr)* mutations into *shr* background (López-Bucio et al., 2005). Alternative approaches could explore the possibilites for Pi supplementation via alternative uptake channels e.i. leaves. Foliar phosphate fertilisation or growth in phosphate-enriched liquid medium could help to understand the consequences of Pi deficiency in shr mutant.

The discovery of GOX1 as enzyme controling the survival of *cat2* plants under photorespiratory conditions could be explained by its enzymatic activity. Reaction catalyzed by this enzyme is the major source of hydrogen peroxide in peroxisomes. Intriguingly, we also found that the activity of this enzyme is constitutively repressed in *cat2* plants most likely at the post-translational level. These observation raises a question about the metabolic fates of glycolate in *cat2* and *gox1/cat2* mutant lines. Numerous publications hypothesized the existence of alternative routes for glycolate scavenging, of which the most recent one indicates that this pathway might involve chloroplast pyruvate dehydrogenase complex (Blume et al., 2013). We anticipate that targeted metabolic analysis of *gox1/cat2* double knockouts could help to understand alternative routes in glycolate metabolism. Even more informative, would be the investigation of *gox1/gox2/cat2* triple mutant that according to our results should not exhibit any foliar GOX activity. However, the generation of such line by means of genetic crossing is practically impossible as GOX1 and GOX2 occupy adjacent positions on chromosome III. GOX1 and GOX2 exhibit 92 % sequence similarity (https://www.arabidopsis.org/Blast/), therefore an alternative strategy could implement the artificial microRNA (amiRNA) technology that enables silencing of closely related genes.

Notably, we observed a significant growth improvement for *gox1/cat2* double knockouts. However the potential of modification of GOX1 activity to increase plant productivity is questionable. This is largely caused by i) lack of beneficiary effects of decreased GOX activity in maize and rice – indicating that phenotypes observed for *Arabidopsis* might be species specific or delimited to e. g. *Brassicaceae* family ii) recent data indicate that hydrogen peroxide produced by GOXs is crucial for establishing efficient hypersensitive response (Rojas et al., 2012) and plants lacking any of the five isoforms of GOX are severely impaired in resistance towards pathogen infections.

The role of SnRK1 in oxidative stress responses.

In the last chapter of this thesis we describe the use of reverse genetic approach to identify genes important for oxidative stress response. We performed a meta-analysis of microarray-based transcript profiling experiments dealing with responses towards increased levels of photorespiratory hydrogen peroxide (Inzé et al., 2012). Analysis of mutant lines corresponding to genes highly responsive towards H_2O_2 accumulation revealed a function for SUGAR TRANSPORT PROTEIN 13 in oxidative stress response. Soon after the phenotype was discovered we realized that plants lacking/overexpressing STP13 exhibit altered sugar levels and therefore we shifted our attention to a major player controlling stress-related energy signaling SNF1-RELATED PROTEIN KINASE (SnRK1) (Baena-González et al., 2007). Our results suggest its major function in control of oxidative stress-triggered anthocyanin accumulation and energy deprivation. We expect that future efforts towards engineering oxidative stress tolerance will involve the aspect of energy (sugar) signaling.

REFERENCES

Baena-González E, Rolland F, Thevelein JM, Sheen J (2007) A central integrator of transcription networks in plant stress and energy signalling. Nature **448**: 938–42

Blume C, Behrens C, Eubel H, Braun H-P, Peterhansel C (2013) A possible role for the chloroplast pyruvate dehydrogenase complex in plant glycolate and glyoxylate metabolism. Phytochemistry **95**: 168–76

Cui H, Levesque MP, Vernoux T, Jung JW, Paquette AJ, Gallagher KL, Wang JY, Blilou I, Scheres B, Benfey PN (2007) An evolutionarily conserved mechanism delimiting SHR movement defines a single layer of endodermis in plants. Science **316**: 421–5

Inzé A, Vanderauwera S, Hoeberichts F a, Vandorpe M, Van Gaever T, Van Breusegem F (2012) A subcellular localization compendium of hydrogen peroxide-induced proteins. Plant Cell Environ **35**: 308–20

Van Leene J, Stals H, Eeckhout D, Persiau G, Van De Slijke E, Van Isterdael G, De Clercq A, Bonnet E, Laukens K, Remmerie N, et al (2007) A tandem affinity purification-based technology platform to study the cell cycle interactome in *Arabidopsis thaliana*. Mol Cell Proteomics **6**: 1226-38

López-Bucio J, Hernández-Abreu, Esmeralda Sánchez-Calderón, Lenin Pérez-Torres A, Rampey RA, Bartel B, Herrera-estrella L (2005) An auxin transport independent pathwayis involved in phosphate stress-induced root architectural alterations in *Arabidopsis*. Identification of BIG as a mediator of auxin in pericycle cell activation. Plant Physiol **137**: 681-691

Petrov VD, Van Breusegem F (2012) Hydrogen peroxide-a central hub for information flow in plant cells. AoB Plants **2012**: pls014

Poirier Y, Thoma S, Somerville C, Schiefelbein J (1991) Mutant of *Arabidopsis* deficient in xylem loading of phosphate. Plant Physiol **97**: 1087–93

Rojas CM, Senthil-Kumar M, Wang K, Ryu C-M, Kaundal A, Mysore KS (2012) Glycolate oxidase modulates reactive oxygen species-mediated signal transduction during nonhost resistance in *Nicotiana benthamiana* and *Arabidopsis*. Plant Cell **24**: 336–52

Schürmann P, Buchanan BB (2008) The ferredoxin/thioredoxin system of oxygenic photosynthesis. Antioxid Redox Signal **10**: 1235–74

Wang Y, Gibney PA, West JD, Morano KA (2012) The yeast Hsp70 Ssa1 is a sensor for activation of the heat shock response by thiol-reactive compounds. Mol Biol Cell **23**: 3290–8

Zhang Y, Primavesi LF, Jhurreea D, Andralojc PJ, Mitchell RAC, Powers SJ, Schluepmann H, Delatte T, Wingler A, Paul MJ (2009) Inhibition of SNF1-related protein kinase1 activity and regulation of metabolic pathways by trehalose-6-phosphate. Plant Physiol **149**: 1860–71

SUMMARY

Photosynthesis drives nearly all food webs on our planet. The importance of this process, largely associated with CO_2 incorporation into organic molecules as well as production of O_2 is difficult to overestimate. Therefore, the efficiency of photosynthesis is crucial for the survival of nearly all organisms. Adverse environmental conditions collectively termed as abiotic/biotic stresses are among the key factors limiting plant productivity. Consequently, research towards understanding and improving plant stress tolerance has become a major objective of plant biotechnology. The disequilibrium between production and scavenging of reactive oxygen species (ROS) is the common theme for nearly all environmental stresses. However, it is now clear that plants are able to sense the early fluctuations in ROS levels and utilize them as stress signals that ultimately trigger adequate responses at cellular and whole-organism level. This thesis aimed at i) exploration of signaling pathways that are able to sense and transduce the ROS information into the nucleus where it can be translated into fine-tuned transcriptomic responses and, ii) identification of genes that are able to alleviate the negative effects of oxidative stress on plant growth and productivity. While the scope and objectives for each of the three approaches undertaken in frames of this thesis were similar, strategies that were used in the respective parts of this work are largely unrelated.

In **Chapter 2** of this thesis we focused on discovery of proteins that are able to sense changes in cellular redox balance and therefore could potentially serve as sensors that initiate the ROS signaling cascades. Perception of ROS signal is largely achieved via oxidation of cysteine sulfhydryl groups (R-SH) to sulfenic acid, R-SOH (reviewed in Chapter 1). All proteins that undergo sulfenic acid modification constitute the cellular sulfenome. In order to identify members of *A. thaliana* sulfenome we joined the expertise of four research groups and devised a novel approach for discovery of sulfenic acid-forming proteins. Our strategy made use of natural R-SOH affinity of the C-terminal domain of the yeast (*Saccharomyces cerevisiae*) AP1 (YAP1) transcription factor and benefited from the use of tandem affinity purification (TAP) which is an excellent technique for identification of protein-protein interactions. Efforts described in this chapter led to identification of 97 proteins with potential redox sensing capabilities. As a proof-of-concept, within our subset we identified 30 proteins that had previously been reported to undergo oxidative modifications. To further confirm our results we investigated the redox properties of DEHYDROASCORBATE REDUCTASE 2 (DHAR2) present within the set of proteins undergoing early H_2O_2 dependent modification. Detailed biochemical analysis indicated that the DHAR2 active site cysteine (Cys20), is subjected to oxidation under oxidative stress conditions. The initial formation of sulfenic acid quickly results in reaction with reduced glutathione leading to S-glutathionylation, a PTM that protects the protein against oxidative damage. In the final stage of this project we generated a portfolio of *A. thaliana* plants expressing

YAP1 probes used in the proteomic studies. These transgenic lines will be used in the near future to *in vivo* mine the *A. thaliana* sulfenomes under various environmental stresses.

Chapter 3 describes the use of forward genetics approach, aiming at discovery of proteins able to modulate the photorespiratory metabolism which serves as the main source of hydrogen peroxide within photosynthetic plant cells. In this strategy we utilized CATALASE2-deficient plants as a model system for non-invasive regulation of hydrogen peroxide level. We used an EMS-mutagenesis approach and performed a broad screen for 2nd site mutations able to alleviate the negative effects of photorespiration in *cat2* plants (progression of cell death). The genetic screen covered approximately 113,000 M2 *cat2-2* seeds and yielded 13 second-site mutations, two of them were mapped in this thesis. Polymorphisms that could rescue the photorespiratory phenotype of *cat2* were localized within coding sequences of SHORT-ROOT (SHR) transcription factor that is involved in control of the developmental processes, and GLYCOLATE OXIDASE 1 (GOX1), a core photorespiratory enzyme catalyzing the oxidation of glycolate to glyoxylate with concomitant production of hydrogen peroxide. We demonstrate that reversion of cell death phenotype conditioned by SHR-deficiency depends on exogenous sucrose supplementation. We found that due to metabolic defects, already under control conditions, *shr* plants rely to a significant extent on growth media as the source of nutrients. This phenotype is most likely associated with early developmental defects observed in shr plants such as development of root endodermis and bundle sheath cells surrounding the leaf vasculature. In contrast, plants lacking GOX1 exhibit authentic tolerance towards oxidative stress conditions. Experiments performed in vitro and in natural growth conditions indicate the major role of GOX1 among the five GOX isoforms and provide potential for the manipulation of glycolate metabolism leading to growth improvements.

In the last part of this thesis (**Chapter 4**), we took a reverse genetic approach and screened the T-DNA insertion mutants of ~200 hydrogen peroxide responsive genes for altered oxidative stress tolerance. This screening effort implemented a new high-throughput oxidative stress test optimized in this work. Within the screened mutant lines we identified the most prominent phenotype for plants lacking *SUGAR TRANSPORT PROTEIN 13* (*stp13-1*) which encodes for a high affinity H^+/D-hexose symporter. Intriguingly, plants lacking STP13 exhibited early sensitivity towards applied stress conditions that was associated with enhanced survival in late stages of the test. Further characterization of gain- and loss-of-function STP13 transgenics provided a link between sucrose availability, levels of trehalose-6-phosphate and activity of SNF1-RELATED PROTEIN KINASE 1. Finally, we hypothesize that sugar signaling controls a significant part of metabolic adaptations towards oxidative stress conditions.

SAMENVATTING

Fotosynthese is de drijvende kracht van deze planeet en ligt aan de basis van alle voedselketens. Tijdens dit proces wordt CO_2 opgenomen en O_2 geproduceerd en vormt zo de cruciale basis van alle leven op aarde. De efficiëntie waarmee fotosynthese plaatsvindt, mede onder suboptimale condities, is dan ook alles bepalend. Zowel biotische als abiotische factoren kunnen een sterke invloed hebben op de productiviteit van de plant en worden aanzien als belangrijke limiterende stress condities. Bijgevolg vormt het ontwikkelen van verbeterde stress tolerante gewassen via onderzoek een belangrijk onderdeel van plantenbiotechnologie. De link tussen de verschillende stress condities is dat ze gepaard gaan met een stijging in reactieve zuurstofsoorten. Planten zijn echter zodanig geëvolueerd dat ze deze fluctuaties in reactieve zuurstofsoorten kunnen waarnemen, zodanig zelfs dat ze in een vroeg stadium in staat zijn om deze te benutten als signalisatie moleculen. Dit maakt dat planten een gepaste respons kunnen opwekken, gaande van bescherming van een cel tot de volledige plant, afhankelijk van de stress factor. Deze thesis had als doel om i) de signalisatie pathways te ontwarren die in staat zijn om een onbalans van reactieve zuurstofsoorten waar te nemen en deze te vertalen naar de kern van de cel waar het kan omgezet worden tot een precieze respons op transcriptieniveau. ii) Ook genen die in staat zijn om de negatieve gevolgen van oxidatieve stress op plantengroei te verminderen werden geïdentificeerd. De thesis is opgebouwd uit drie hoofdstukken die focussen op het verrichtte onderzoek en hoewel ze alle drie eenzelfde doel hadden zijn de gebruikte methodes toch grotendeels ongerelateerd.

In **hoofdstuk 2** lag de focus op eiwitten die als mogelijke stress sensoren een redox onbalans konden vertalen in een gepaste respons door het aanschakelen van signalisatie cascades. Oxidatie van de thiolgroep van cysteïne (R-SH) tot sulfeenzuur (R-SOH) is een belangrijke strategie om reactieve zuurstofsoorten waar te nemen (zoals besproken in Hoofdstuk 1). Alle eiwitten die deze modificatie ondergaan vormen samen het sulfenome van de cel. Om zulke eiwitten in *A. thaliana* te identificeren werd, dankzij de expertise van vier verschillende onderzoeksgroepen, een nieuwe methode ontwikkelt. Onze strategie maakte gebruik van een in de natuur voorkomend gist eiwit, namelijk YAP1, hetgeen een R-SOH groep bevat in zijn C-terminaal domein wat kon worden benut om te isoleren via tandem-affiniteits opzuivering (TAP). Deze laatste methode is bovendien een uitstekende techniek om eiwit-eiwit interacties op te pikken. Deze methode resulteerde in de identificatie van 97 eiwitten die als potentiële stress sensoren fungeerden. Bovendien werden 30 van deze eiwitten reeds in de literatuur gerapporteerd als zijnde eiwitten met oxidatieve modificaties. Om onze resultaten te bevestigen, onderzochten we het eiwit DEHYDROASCORBATE REDUCTASE 2 (DHAR2) verder in detail aangezien het in de dataset waterstofperoxide afhankelijke oxidatie onderging. Biochemische analyse wees uit dat het cysteïne van het actieve centrum (Cys20) oxidatie onderging bij blootstelling aan stress condities. Na oxidatie tot sulfeenzuur vindt er snel reactie plaats met gereduceerd glutathion wat

leidt tot glutathionylatie, hetgeen een gekende modificatie is ter bescherming van het eiwit tegen oxidatieve schade. Tot slot werd een portfolio gegenereerd van *A. thaliana* planten die YAP1 expresseren, welke opnieuw kunnen gebruikt worden om *in vivo* te vissen naar eiwitten behorende tot het sulfenome onder verschillende stress condities.

Hoofdstuk 3 beschrijft een forward genetics screen die als doel had om eiwitten te identificeren die het fotorespiratorisch metabolisme kunnen moduleren. Fotorespiratie is de belangrijkste bron van waterstofperoxide in fotosynthetisch plantenweefsel. Als model werd een CATALASE2-deficiente plantenlijn gebruikt waarin de concentratie van waterstofperoxide op een niet invasieve manier gereguleerd kan worden. Een EMS-mutagenese screen werd op deze plantenlijn uitgevoerd om secondaire mutaties te vinden die het fotorespiratorisch fenotype van de cat2 planten verbeterde (inductie van celdood). In deze screen werden 113000 EMS gemutageneerde planten getest waarin uiteindelijk 13 secundaire mutaties werden geidentificeerd die aanleiding gaven een verminderde progressie van celdood. In deze thesis werden twee van deze mutaties geïdentificeerd. Een mutatie werd gelokaliseerd in de coderende sequentie van de transcriptie factor SHORT-ROOT (SHR) welke een regulatorische functie heeft in de ontwikkeling. De tweede mutatie werd gevonden in de coderende sequentie van GLYCOLATE OXIDASE 1 (GOX1), een enzyme van de fotorespiratorische *pathway* die glycolaat oxideert tot glyoxylaat waarbij waterstofperoxide vrijkomt. We hebben aangetoond dat de verminderding van celdood door SHR deficientie afhankelijk is van een exogene toediening van sucrose. We toonden aan dat *shr* planten reeds onder standaard groeicondities sterk afhankelijk zijn van het groeimedium als bron van nutriënten. Dit fenotype is geassocieerd met ontwikkelingsproblemen van *shr* planten reeds vroeg in de ontwikkeling. Voorbeeld hiervan zijn de endodermis van de wortel en bundelschedecellen die de vaatbundels omgeven. GOX1 daarentegen vertoont een 'echte' tolerantie tegen oxidatieve stress. Zowel *in vitro* als *in vivo* experimenten wezen erop dat GOX1 de belangrijkste is van de vijf GOX isovormen. Verder werd het potentieel aangetoond om het glycolaat metabolisme te moduleren met het oog op verbeterde groei.

In het laatste deel van deze thesis (**hoofstuk 4**) wordt een reverse genetics strategie beschreven. In deze screen werden ~200 waterstof peroxide responsieve genen getest op hun tolerantie voor oxidatieve stress. Hiervoor werd een high-throughput oxidatieve stress assay toegepast die in dit werk werd geoptimaliseerd. Het meest opvallende fenotype werd gevonden bij planten die deficient zijn in *SUGAR TRANSPORT PROTEIN 13 (stp13-1)*. Dit eiwit is een H^+/D-hexose symporter met een hoge affiniteit. Opmerkelijk aan STP13 deficiënte planten was hun vroege sensitiviteit voor oxidatieve stress wat in latere fases leidde tot een verhoogde overleving onder dezelfde stresscondities. Verder karakterisatie van gain- en loss-of-function STP13 transgene planten toonde een verband tussen de beschikbaarheid van sucrose, de concentratie van trehalose-6-phosphate en de activiteit van SNF1-

RELATED PROTEIN KINASE 1. Tot slot werd de hypothese gesteld dat signalisatie door suikers een belangrijke rol heeft in de metabolische adaptatie aan oxidatieve stress condities.

Acknowledgements

With the completion of my Ph.D. studies it is time to thank all people that I met on my path during this 5,5 year period.

Firstly, I would like to acknowledge VIB for providing me with the predoctoral fellowship, excellent working conditions and plenty of training opportunities. VIB is the place to be!!!

I am especially grateful to my Ph.D. promoters, Prof. Dr Frank Van Breusegem and Prof. Dr Joris Messens for their continuous support throughout the last years. I really enjoyed the privilege of working in your labs and hope to extend our collaboration beyond the time frames of this Ph..D. studies. Thank you for reading and correcting my thesis.

I would like to thank all members of my Ph.D. examination and reading committee for accepting my invitation and valuable comments that greatly increased the quality of this thesis.

Pavel, thank you for all your contributions, especially the Łomża assay. I really enjoyed working and discussing with you. Thank you very much for reading and correcting my thesis – especially during the last hours before it was printed.

I would like to acknowledge valuable collaborations with Prof. Dr Geert De Jaeger, Prof. Dr Kris Gevaert, Prof. Dr Filip Rolland and Dr Didier Vertommen – thank you for sharing your excellent expertise.

Khadija, thank you for guiding me through the maze of FPLC tubings, the pitfalls of protein purification and the sea of knowledge on protein crystallization. Also, for your mental support in the difficult moments.

This Ph.D. work was based, and would not be possible without results obtained by former members of the Oxidative Stress Signaling Group – Sandy, Annelies, Pelle and Frank H., thank you very much for providing a solid ground for my research.

Silketje, Lianatje, Katrien, Salma, Brigitte, Debbie, Inge, Jenny, Barbara, Aurine, Jordi, Lorin, Simon, Valerie, Patrick, Davy, Vanesa, Iker, Wael, Koen, Elke, Karolien— thank you for your friendship, help throughput my stay at PSB and VUB, and a nice atmosphere in and outside the lab.

Very special thanks go to Michael and Renatatje — thank you for your friendship, continuous support, sharing your house with me, and making me feel like a member of your family.

I would like to acknowledge my previous supervisors, Dr Françoise Budar, Dr hab. Grzegorz Bartoszewski and Prof. Dr Luc Lens — thank you for introducing me to the world of science!

Oana, Łukasz, Marta, Tomek, Ula, Paweł, Joanna B., Joanna P. — dziękuję za polskie pogawędki i cenne wskazówki!

Serdecznie dziękuję moim nauczycielom z Zespołu Szkół w Seroczynie za trud i serce włożone w moje wykształcenie i wychowanie.

Bartku, Piotrku, Aniu i Amelio — dziękuję, że zawsze mogę na Was liczyć i za radość jaką przynosicie mi każdego dnia.

Kochani Rodzice, dziękuję za wsparcie w trudnych chwilach, Waszą miłość oraz ogromny trud i wysiłek włożony w moje wychowanie. Dziękuję Wam z całego serca!

Thank you / Dank U / Dziękuję,

Cersey

Cezary Waszczak

Date of birth: 20 Feb 1983

Nationality: Polish

Education

06/2007   Master of Science in Biotechnology, Warsaw University of Life Sciences.

Study profile - Biotechnology in Plant Production

Research experience

06/2014 - present   Researcher

Plant Stress Group, Department of Biosciences, University of Helsinki

09/2008 – 05/2014   Holder of VIB International Ph.D. Fellowship

Project title: **"Genetics screens to identify ROS signal transducers in *A. thaliana*"**

VIB Department of Plant Systems Biology - Ghent University

VIB Structural Biology Research Center - Vrije Universiteit Brussel

11/2007-06/2008   Holder of Marie Curie Fellowship for Early Stage Research Training.

Project title**: "Genetic characterization of cytoplasmic male sterility in *A. thaliana*".**

Organelles and Plant Reproduction Group, Genetics & Plant Breeding Station, The Jean-Pierre Bourgin Institute, INRA

07/2005-09/2007   Technician, master thesis research: **"Identification of molecular markers linked to male sterility gene *ms-8* in pepper (*Capsicum annuum* L.)".**

Department of Plant Genetics, Breeding and Biotechnology, Faculty of Horticulture and Landscape Architecture, Warsaw University of Life Sciences.

Academic experience

2009/2010   Student supervision

Silke Jacques, master thesis **"Toxicity and working mechanism of *A. thaliana* SERPIN 1 with pea aphid *A. pisum"***

Selected conferences and meetings

07/2013   11th International Conference on Reactive Oxygen and Nitrogen Species in Plants, Warsaw, Poland
Oral presentation: **Sensing thiol oxidation in *Arabidopsis thaliana* through a YAP1 genetically encoded probe.**

9/2011   ESF-EMBO Symposium on Glutathione and Related Thiols in Living Cells, Sant Feliu de Guixols, Spain.
Poster presentation: **Reverse genetic screens to identify ROS signal transducers in *Arabidopsis thaliana.***

7/2011   10th International Conference on Reactive Oxygen and Nitrogen Species in Plants, Budapest Hungary.
Poster presentation: **Reverse genetic screens to identify ROS signal transducers in *Arabidopsis thaliana.***

11/2009   EPSO Workshop on Plant Phenotyping, Jülich, Germany

11/2008   1st Brussels Center for Redox Biology Fall Symposium, Brussels, Belgium
Oral presentation: **ROS signal transduction in plants.**

Publications

- Waszczak C.*, Akter M.S.*, Jacques S., Gevaert K., Messens J., and Van Breusegem F., (2014) Oxidative post-translational modifications of cysteine residues in plant signal transduction. (in preparation)

- **Waszczak C.**, Kerchev P., Denecker J., Mühlenbock P., Hoeberichts, F. A., Van Der Kelen K., van de Cotte B., Vandorpe M., Messens J., Van Breusegem F. (2014) **SHORT-ROOT deficiency alleviates photorespiratory H_2O_2-dependent cell death in *Arabidopsis* leaves.** (in preparation)

- Kerchev PI.*, De Smet B.*, Waszczak C., Messens J., Van Breusegem F., (2014) **Redox solutions for crop improvement and food security.** (Submitted to ARS)

- Waszczak C.*, Akter M.S.*, Wahni K., Van Molle I., Vertommen D., Gevaert K., De Jaeger G., Van Montagu M., Messens J., Van Breusegem F., (2014) Sulfenome mining in Arabidopsis thaliana under oxidative stress. (Accepted for publication in PNAS)
  * equal contribution

- Gobron N., Waszczak C., Simon M., Hiard S., Boivin S., Charif D., Ducamp A., Wenes E., Budar F., (2013) **A** cryptic cytoplasmic male sterility unveils **a** possible gynodioecious past for *Arabidopsis thaliana.* PLoS ONE 8(4) : e62450

- Bartoszewski G., Waszczak C., Gawronski P., Stepien I, Bolibok-Bragoszewska H., Palloix A., Lefebvre V., Korzeniewska A., Niemirowicz-Szczytt K. (2012) Mapping of the *ms8* male sterility gene in sweet pepper (*Capsicum annuum* L.) on the chromosome P4 using PCR-based markers useful for breeding programmes. Euphytica 186:453-461
  * equal contribution